Planning Goal-Directed Actions: fMRI Correlates in Humans and Monkeys

Thesis by

Asha Iyer

In Partial Fulfillment of the Requirements

for the Degree of

Doctor of Philosophy

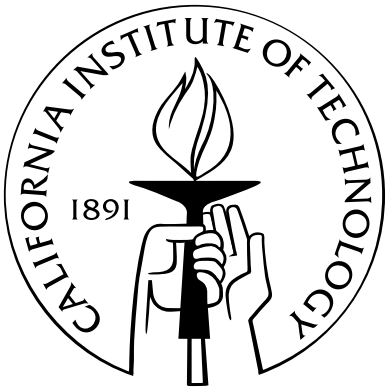

California Institute of Technology

Pasadena, California

2008

(Defended May 27, 2008)

For Hanuman, Florian, Redrik, and Gutalin

Acknowledgments

An ancestral proverb holds that we are little more than a product of all those who came before us and those who still shape us—of the lineage of mentors who teach us and the friends and family that encourage and support us. I believe this aphorism veritably captures the essence of any achievement, and accordingly, my gratitude extends to a plethora of people who have made this thesis possible. While I could never adequately do justice to them all, I would like to at least acknowledge a subset of individuals who have directly impacted my work and time at Caltech.

First, I would like to thank Dr. Richard Andersen, who took a chance on me midway through my academic journey at Caltech. He furnished me with an invaluable opportunity to learn and flourish in a scientific community of some of the most perspicacious and curious minds I have had the privilege to know.

The members of my committee have exceeded all expectation and obligation, by generously offering their time and constructive input at several points during the past few years. Dr. Shinuke Shimojo has continually provided incisive feedback and advice; Dr. Antonio Rangel has been fundamental in giving form to much of the work presented in this thesis. Dr. Marianne Bronner-Fraser has been an advocate and guide, personally and academically—indispensable in successfully navigating the unpredictable currents of the last few years' voyage.

Dr. Robert Sapolsky has served as an inspiring role model, whose tutelage and enthusiasm first forged my desire to unravel the mystery of the brain in the context of scientific research.

I would like thank my family for their abiding love and confidence: My parents, who always provided unconditional support; My sister, who has patiently listened to

the vicissitudes of graduate school, recounted in their every detail; My brother-in-law, whose curiosity and idealism constantly fueled my own; and Vijay, Anusha, and Anjali, who always embrace me with open arms.

My family at Caltech has been there at every step along the way: Hilary Glidden, for being my conjoined twin and sounding board, for dancing with Dagoba and for fake wedding receptions; Alex Holub, for countless moments of spontaneity and fun, for innumerable existential conversations, for rum-and-cokes and for McDonalds fries in China; Alan Hampton, for always smiling, even through stressful days, frightening tea houses, and caustic Indian food; Grant Mulliken, for breaking my stereotypes of pseudo-Republican wrestlers, and for almost getting me arrested by Caltech security; Allan Drummond, for embodying passion for knowledge, for dancing to LoneStar and for singing to O-town with me; Kai Shen, for his constant idealism and for far more coffee than any one person should drink. Also, my most profound gratitude to many other friends who have made my experiece here unforgettable and insuperable: Rajan Bhattacharya, Meghana Bhatt, Lisa Welp, Kerstin Preushcoff, Daniel Procissi, Robert Ward, Dan Busby, and Hilke Plassman. Leslie and Will have stood by me through more moments than I could possibly enumerate.

Finally, I would like to express my eternal gratitude and admiration for Igor Kagan and Axel Lindner, whom I facetiously call my 'doctor-father' and my 'doctor-mother'. They have been my co-workers and collaborators, my overprotective big brothers, and incredible scientific mentors. To them I largely owe the fruition of this work, my growth as a scientist, and the edification of my graduate school experience.

Abstract

In performing goal-directed actions, primates (humans and monkeys) flexibly select and plan appropriate behavioral responses. However, while a network of frontoparietal regions are traditionally implicated in the transformation of sensory input from the environment into these spatial, goal-directed movements, the type of information encoded in their activity remains nebulous.

This work first addresses the long-standing query as to whether this activity represents a prospective planning of the upcoming action, or a retrospective sensory representation of goals. In an fMRI experiment, subjects performed delayed-reach tasks, in which mnemonic and attentional demands were held constant. BOLD signals showed that the posterior parietal cortex (PPC) and premotor regions exhibit activity specifically related to the planning of upcoming actions.

Additionally, to select and plan the optimal action, the expected consequences of potential responses need to be assessed. To determine whether and how potential outcomes mold action planning activity, subjects were scanned while they performed a demanding motor task to obtain monetary gains or losses contingent on their performance. Monetary consequences modulated activity throughout the action-planning network, most significantly in PPC, as well as in reward structures. While reward areas reflected the expected value of a trial, frontoparietal activity was greatest for both high expected rewards and losses. Moreover, in frontoparietal areas, subjects beliefs about the likelihood of possible outcomes influenced BOLD signals, suggesting that cognitive biases may influence the planning of actions.

Finally, to compare human imaging findings to large body of related monkey electrophysiological experiments, humans and monkeys were scanned while performing

the same delayed-saccade tasks. Frontoparietal oculomotor-planning areas in monkeys and putative homologs in humans evinced coherent response patterns, though prominent differences in the degree of contralaterality and the hemodynamic responses between the two species emerged.

In sum, these findings help characterize fundamental aspects of goal-directed action planning in both species.

Contents

Acknowledgments **iv**

Abstract **vi**

List of Figures **xiii**

List of Tables **xiv**

1 Introduction **1**

1.1 Intentional Action 1

1.2 Delayed Response Tasks: Isolating and Studying Action Planning . . 3

1.3 Neural Regions Involved in Delay Period Activity 6

1.4 Information Encoded during Action Planning 9

1.4.1 Sensory versus Motor Representation 9

1.4.2 Action Outcomes and Consequences 13

1.5 Monkey fMRI—The Missing Link 16

1.6 Specific Aims 18

References 20

2 Roles of Human Posterior Parietal and Premotor Cortex in Action Planning **29**

2.1 Summary 29

2.2 Introduction 30

2.3 Results 32

2.4 Discussion 42

2.5 Experimental Procedures 48
2.S1 Supplemental Data 54
References 59

3 Dissociation of Objective Value and Subjective Absolute Value in Striatal and Cortical Representations of Expected Action Outcomes 65
3.1 Summary 65
3.2 Introduction 66
3.3 Results 69
3.4 Discussion 87
3.5 Experimental Procedures 94
3.S1 Supplemental Data 101
References 107

4 BOLD/fMRI Delay Period Signals in Monkeys and Humans: Spatial- and Non-Spatial Specific Signals 115
4.1 Summary 115
4.2 Introduction 116
4.3 Results 118
4.4 Discussion 141
4.5 Experimental Procedures 151
4.S1 Supplemental Data 158
References 179

5 Conclusion 192

Appendix 1—Expected Reward Modulation of Dorsal and Ventral Stream Activity in a Goal-Directed Oculomotor Task 197
A1.1 Summary 197
A1.2 Introduction 198
A1.3 Results 200
A1.4 Discussion 222

A1.5 Experimental Procedures 229
References 232

Appendix 2—Frontoparietal Timecourses Reflect Decision in a Free-Choice Oculomotor Task 240

A2.1 Summary 240
A2.2 Introduction 241
A2.3 Results 242
A2.4 Discussion 252
A2.5 Experimental Procedures 256
References 260

Appendix 3—Published Work 262

A3.1 Components of bottom-up gaze allocation in natural images 262
A3.2 What do we perceive in a glance of a real-world scene? 264

List of Figures

1.1 Delayed response task structure 3
1.2 Representative areas recruited during a delayed response task. 5

2.1 The behavioral tasks 33
2.2 Behavioral performance 36
2.3 fMRI activity related to motor planning and visual memory 39
2.S1 Representative examples of subjects' performance 54
2.S2 Individual ROIs in parietal and pre-motor cortex 55
2.S3 Target load-related fMRI activity 58

3.1 Trial structure and hypothetical responses 71
3.2 Subjects attitudes towards performance and contexts 75
3.3 Delay-period ROIs and representative timecourse and beta values . . . 78
3.4 SPL beta values and timecourses by performance. 80
3.5 Delay-period ROI BOLD timecourses by performance 81
3.6 Statistical maps for delay period and 'performance-weighted' absolute value 83
3.7 Dorsal striatal BOLD signal timecourses, objective performance 86
3.S1 Dorsal striatal BOLD signal timecourses, subjective performance . . . 101
3.S2 Orbitofrontal cortex BOLD signal timecourse 102

4.1 Oculomotor tasks, behavior and event-related design 119
4.2 Spatial distribution of cue, memory, and saccade activity 123
4.3 Maps for the memory delay rightward versus leftward contrast for memory trials 126

4.4 Event-related averaging (ERA) of trial timecourses and analysis of frontal ROIs . . . 129
4.5 ERA BOLD trial timecourses in selected frontal, posterior parietal, and parieto-temporal sts cortical areas . . . 131
4.6 Summary of contraversive selectivity, ramping indices, and response amplitude . . . 135
4.7 Human imaging results . . . 137
4.8 Summary of contraversive selectivity, ramping indices, and response amplitude for humans . . . 140
4.S1 Evaluation of EPI and data selection for event-related analysis . . . 159
4.S2 Comparison of BOLD response timing in monkeys and humans . . . 164
4.S3 Comparison of BOLD response timing in monkey data collected with TR 1 s and 2 s . . . 166
4.S4 Supplementary statistical maps for +cue and memory contrasts in humans 169
4.S5 Mean response amplitude and contraversive selectivity by hemisphere . 172
4.S6 Contralaterality by hemisphere in humans . . . 173

A1.1 Experimental task and timing . . . 201
A1.2 Experimental task and timing: Phase II and III . . . 203
A1.3 Behavioral findings for Phase I . . . 205
A1.4 Statistical map and timecourses: Target presentation/saccade execution epoch . . . 207
A1.5 Statistical map and timecourses: Expectation delay epoch . . . 209
A1.6 Statistical map and time-courses: Reward receipt epoch . . . 211
A1.7 Behavioral findings for Phase II . . . 213
A1.8 BOLD timecourses separated by day relative to reversal . . . 215
A1.9 Behavioral findings for Phase III . . . 219
A1.10 Phase I ROIs during Phase III . . . 221
A2.1 Task structure and timing . . . 243
A2.2 Choice behavior of both monkeys . . . 244

A2.3 Reaction times for Instructed and Choice trials 245
A2.4 BOLD timecourses from monkey R for delay-period ROIs exhibiting contralaterality 247
A2.5 BOLD timecourses from monkey G for delay-period ROIs exhibiting contralaterality 249
A2.6 BOLD timecourses from monkey R for ROIs exhibiting contralaterality during the cue period 251

List of Tables

3.1 Ordering of Gain-Loss Contexts for Parametric Modulation 100
3.S1 Cue and Delay Period ROIs with Significant Parametric Modulation due to Gain-Loss Contexts 103
3.S2 Regions significant for parametric modulation of the cue epoch 104
3.S3 Regions significant for parametric modulation of the delay epoch . . . 105
3.S4 Regions significant for parametric modulation of the outcomes epoch . 106

Chapter 1

Introduction

1.1 Intentional Action

> *Now thought alone moves nothing; only thought which is directed to some end and concerned with action can do so.*
>
> -Aristotle

Humans perform voluntary actions. Assuming most of these actions are not haphazardly and desultorily generated, they are done according to a purpose—to create or modify some event, or state of affairs, towards a desired end or goal. The performance of a goal-directed action presupposes that the agent has some knowledge about the goal, the means by which it can be achieved, and a corollary anticipation of the goal event (Hommel 2003). Implicit in this notion, then, is that he plans the action: with some comprehension of movement-effect relationships, he selects, specifies, and prepares an appropriate behavioral response before he executes it.

A distinction between the cognitive operations prior to action and those during action was first posited by Woodworth (1899), based on his seminal study examining the use of visual feedback in on-line control of movement. Since Woodworth's time, these separate stages have been the subject of much investigation (Beggs & Howarth 1970, 1972; Carlton 1981; Fitts 1954; Keele 1968; Meyer et al. 1988; Vince 1948; Elliott et al. 2001). Expectedly, a wealth of psychological and theoretical reports solidified the view that during execution of a movement, an action comes increasingly under the influence of a " 'control' system, which uses a limited but quickly updated

visual representation, coupled with visual and proprioceptive feedback, and an efference copy of the movement plan"(Glover 2004), in order to best ensure accuracy (Shadmehr 2008).

Strikingly, though, psychophysical findings established also that the *initial* selection and/or implementation of a motor behavior was influenced, even prior to a movement's initiation, by a broad range of sensory and cognitive variables. Experiments with human subjects demonstrated that with an increasing amount of pertinent information provided in advance, movement reaction times become faster, suggesting a period of time before movement initiation in which a certain set of parameters are specified (Rosenbaum 1980; Klapp 1977; Riehle et al. 1994). Similarly, the manner in which humans initially approach an object is typically influenced by their knowledge of what they intend to do with the object (Jeannerod 1981, 1984). For example, a waiter will usually reach for an inverted cup with his thumb facing downwards if he intends to pour water into it, but he will grab it with his thumb upwards if he is transferring it to a dishwasher. Psychologists call this the 'end-state comfort effect,' when we adopt initially unusual, and perhaps uncomfortable, postures to facilitate subsequent usage of an object according to our objective. Based on these examples and a plethora of other studies, psychologists broadly classified the factors relevant before the execution of an action—for the *planning* of the action—into a few categories: 1) the spatial characteristics of and relations between the actor and the target; 2) the non-spatial characteristics of the target influencing the manner in which it is interacted with or acquired (e.g., its function, weight, fragility, and the coefficient of friction of its surfaces); and 3) the overarching goal(s) of the action (Glover 2003; Jeannerod 1988; Rosenbaum 1991).

1.2 Delayed Response Tasks: Isolating and Studying Action Planning

The desire to unravel these cognitive operations before and leading up to movement, has spurred an interest in elucidating the neural substrates of action planning, and in characterizing the computations performed and the precise information encoded in involved brain regions. In order to isolate these planning processes, experimental tasks requiring delayed behavioral responses have been employed.

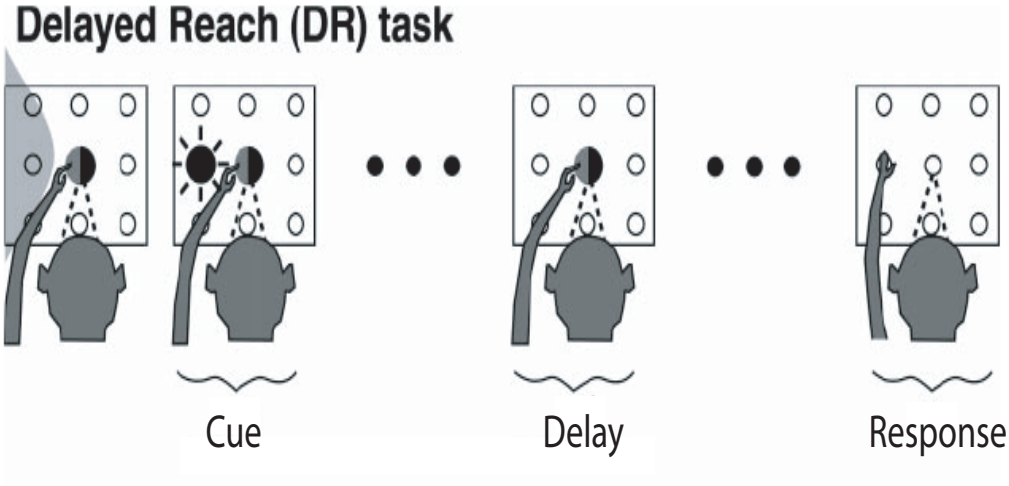

Figure 1.1:

Delayed response task. *The subject fixates. An instructive cue (Cue) indicates, in this example, where the subject should reach. At this time, the subject does not reach. After a Delay, a 'go' signal (here, extinction of central fixation point) tells the subject to execute the previously cued response.*

Generally, these tasks present a sensory cue, which provides information requisite for planning an action, but defers the execution of that action until some later-presented 'go' signal (Fig. 1.1). By imposing a temporal delay between instructive

cue and a contingent motor response, neural activity underlying either immediate processing of the sensory cue or action execution can be disambiguated from the intervening phase in which selection and planning of the action occurs. These tasks then are predicated on the notion that areas which subserve these planning processes will exhibit sustained activity during the delay until the movement is initiated (Hikosaka and Wurtz 1983), providing a temporal window during which to analyze these regions.

An example of this is illustrated in Fig. 1.2, showing typical functional MRI responses of representative sensory, motor, and 'delay-period' cortical areas. Two signals are shown, in dark gray and light gray, corresponding to a typical delayed-response task and a control task, respectively. In the delayed-response task, a set of visual cues are presented at time 0, fully specifying where the subject will reach after the delay period, which lasts 15 seconds; motor execution begins at time 15. In the control, a set of visual cues are again displayed at time 0; however, these cues bear no relation to the upcoming movement, the target locations of which will instead be explicitly specified after the delay at the time of movement. Thus these cues are behaviorally irrelevant, and no planning can occur during the control task delay period.

In an area primarily concerned with sensory/visual processing, such as V1 (visual cortex), there is an initial rise in activity due to the cue presentation, which significantly decays during the delay period before rising again due to the movement initiation (at which time the subjects sees targets and cursor motion on screen); this signal profile is similar in both conditions when the cues allow planning and when they do not (regions in red, mostly comprising areas in occipital cortex, exhibit this pattern of activity). In areas putatively involved with motor execution, such as M1 primary motor cortex, there may be a slight blood-oxygenation-level-dependent (BOLD) response to the cue presentation, but an expectedly much larger signal increase during the motor execution phase (after time 15 seconds); again, both the delayed-response task and the control task generate comparable patterns of fMRI activity (regions in blue). Finally, the presumptive action planning areas (in green), here exemplified by superior parietal lobule in posterior parietal cortex, yield a strikingly different signal:

while there is a response to the cue presentation and motor execution, activity is sustained throughout the delay period. Furthermore, this level of activity is significantly higher when planning can occur (delayed-response task) than when planning cannot occur (control task). These findings corroborate the proposition that these delay-period regions exhibit activity bridging cues with contingent motor responses, when these cues mold the future behavior.

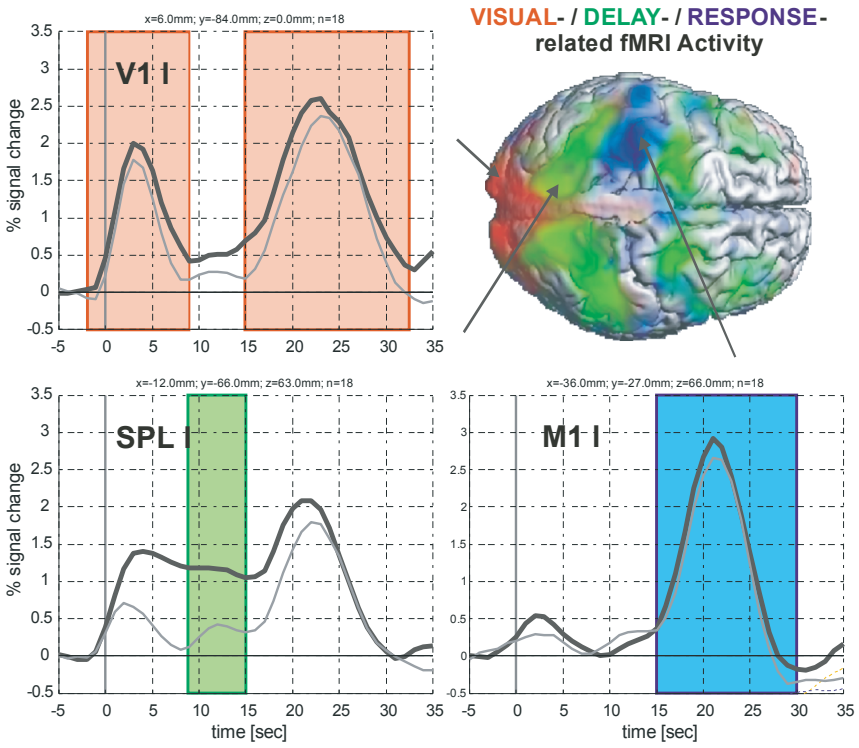

Figure 1.2:

Representative areas recruited during a delayed response task. *Upper left panel (red): primary visual cortex (V1). Bottom left (green): left superior parietal lobule. Bottom right: primary motor cortex (M1). Delay period between cue and response in all timecourses is between time 0 and 15. Dark gray curves: typical delayed response task. Light gray curves: control task. See text for further detail.*

1.3 Neural Regions Involved in Delay Period Activity

Sustained delay period activity typically recruits a network of cortical regions in the frontal and parietal lobes of the brain. Traditionally these cortical regions comprise three main areas: supplementary motor area (SMA), premotor cortex (PM), and posterior parietal cortex (PPC). This section briefly describes these areas—their anatomical connections and lesion pathology—to provide a cursory overview of their functional involvement in the generation of action.

Frontal Lobe Areas: Medial Wall (Supplementary and pre-Supplementary Motor Areas) and Pre-central Gyrus (dorsal and ventral Premotor)

In general, a variety of experiments indicate that these frontal areas use information from other cortical regions to select and/or prepare movements appropriate for the context of the action. The supplementary motor cortex and premotor cortex produce movements and contractions following stimulation, and are somatotopically organized. They project directly to both primary motor cortex and the spinal cord. However, they receive visual and proprioceptive inputs indirectly, via the parietal and prefrontal cortex.

Supplementary Motor Area. The removal of the SMA in a monkey reduces the number of self-initiated or 'spontaneous' movements the animal makes, whereas the ability to execute movements in response to external cues remains largely intact. Imaging studies suggest that this cortical region in humans functions in much the same way. For example, PET scans show that the medial wall of the premotor cortex is activated when the subjects perform motor sequences from memory (i.e., without relying on an external instruction). In accord with this evidence, single unit recordings in monkeys indicate that many neurons in SMA begin to discharge one or two seconds before the onset of a self-initiated movement. Also, this region may play a specific

role in programming motor sequences, as stimulation of the area produces complex movements, such as orienting the body or opening and closing the hand (Watts 2004)

The medial wall additionally encompasses the supplementary eye fields (SEF), which may play an analogous role for eye movements. Lesions in this regions, especially in the left hemisphere, impair the patient's ability to make a remembered sequence of saccades. Patients additionally may have difficulty altering the direction of saccades from a previously learned sequence (Miller et al. 2005).

Premotor Cortex. As with the medial wall, the precentral gyrus areas comprise regions with both skeletomuscular and oculomotor behavior functions. The premotor cortex (PM) subdivision is thought to play a role in the generation of goal-directed hand movements. Lesions in this region severely impair the ability of monkeys to perform visually cued conditional tasks, even though they can still respond to the visual stimulus and can perform the same movement in a different setting. Similarly, patients with premotor lesions experience problems with voluntary movements that require sensory guidance. Patients have specific impairments in using sensory (visual, auditory, tactile) cues to recall previously learned movements, though they have no problem retrieving the same movements based on spatial cues (Halsband and Freund 1990). Premotor cortex may also be involved in specifying task contingencies for planning an appropriate response, but from a more arbitrary stimulus-response mapping (Watts 2004). The premotor area itself contains subregions (ventral and dorsal), receiving segregated inputs from parietal regions. Selective inactivations reveal differential contributions of these subregions to hand movements, for example, temporary inactivation of monkey PMv causes severe deficits in the grasping component of hand movements, leaving unaffected the hand transport (Fogassi et al. 2001), whereas PMd inactivations may impair appropriate sequencing, amplitude, or direction of reaching movements (Davare et al. 2006).

The frontal eye fields (FEF) are generally considered a part of the premotor area. As the name implies, the FEF is concerned with eye movements, and may3 program the corresponding primary areas so as to guide gaze shifts (Braun et al. 1996; MacAvoy et al. 1991), in conjunction with the superior colliculus and lower brain-

stem. It receives projections from the primary and association visual cortices in the occipital lobe, the auditory association and multimodal visual association areas in the temporal lobe, and the somatosensory association area, and hence is multimodally responsive. Damage to the FEF can cause abnormalities in fixation, decreased sensitivity to stimuli throughout the visual field, slowed visual scanning and searching, inattention and neglect, as well as mislocalization of sounds (Joseph 2000).

Parietal Lobe Areas: Posterior Parietal Cortex

Anatomically, PPC is positioned along the dorsal visual pathway of the brain, also known as the vision-for-action pathway (Ungerleider and Mishkin 1982; Goodale 1998), located between the visual cortex on the one end and motor cortices on the other. PPC receives converging sensory inputs from a variety of sources, including visual, somatosensory, proprioceptive information. As such, this region is ideally situated to represent targets or goals in the environment, independent of modality. Lesions of parietal posterior cortex (PPC) do not lead to primary motor or sensory deficits, but often produce a deficit known as optic ataxia, or impairment of the visual control of pointing and grasping (Blint 1909). Furthermore, lesions of the left parietal lobe have been shown to lead fairly consistently to apraxia, a condition in which the affected person's ability to voluntarily produce motor actions is altered (Liepmann 1905; Sirigu et al. 1999). These impairments range from an inability to produce a movement upon instruction to the incapacity to perform complicated sequences of movements. Unilateral parietal lesions particularly of the right hemisphere generally produce contralateral neglect, in which the patients appear unable to perceive and attend to objects, or even one's own body, in a part of space, despite the fact that visual acuity, somatic sensation, and motor ability remain intact. Affected individuals fail to report, respond to, or even orient to stimuli presented to the side of the body (or visual space) opposite the lesion.

To summarize the involvement of frontoparietal network, this profile of lesion symptomatology and anatomical connectivity attests to the fact that all of these cor-

tical regions are clearly necessary for the voluntary generation of action. Regions in the PPC appear explicitly involved in the perception, processing, and/or transformation of sensory and spatial information to guide action. The frontal areas play a fairly direct role in generating movements, though they are more removed from sensory inputs. Moreover, they appear to function as motor associative areas involved in more arbitrary stimulus-response mapping or internal generation of movement.

1.4 Information Encoded during Action Planning

In forming a plan for a goal-directed action, the goal or intended effects of that action may be hierarchically defined. At a relatively incipient and abstract level, an action plan, in following with the traditional formulation of an action 'intention' (Kalaska and Crammond 1995; Snyder et al. 1997, 2000), specifies the interaction with the environment, essentially stipulating the target of the movement and the type of movement. At this level, the intention can be independent from action execution, specifying potential movements without actually being acted upon (Calton et al. 2002; Snyder et al. 2000). Progressively more concrete levels expound upon this plan, providing information about the details of a movement, i.e., precise movement trajectories and the particulars of the joint angles, and finally the exact set of muscle activations required to make the movement. For example, my goal may be to imbibe a cup of highly concentrated coffee, and hence the movement plan would be to reach, with either my hand or my mouth, for the goblet of chemical energy. Such an objective requires the transformation of spatiotemporal cues into directed behavior, involving the extraction of spatial and sensory characteristics of the target, and the spatial relationship between my body (and hand or mouth) and the target, in order to shape the motor commands that will best achieve the desired interaction with that target.

1.4.1 Sensory versus Motor Representation

For the accurate implementation of sensorimotor tasks, such as reaching or moving the eyes towards a spatial target/goal, imaging and electrophysiology explorations

have irrefutably implicated a network of frontal and posterior parietal regions in delay period activity representation. However, the function and potentially differential contributions of these regions to sensorimotor transformation remain nebulous. In particular, the specific role the posterior parietal cortex may play in visuomotor processes has been stridently debated. While Mountcastle et al. first demonstrated over two decades ago that PPC neurons fire during movement of the eyes and limbs to an illuminated target, the interpretation of that firing activity has been alternatively conceived to reflect higher-order sensory or attentional processes, or to largely reflect movement-related function (Mountcastle et al. 1975; Robinson 1978; Eskandar and Assad 1999). In other words, activity elicited during a 'sensorimotor transformation' may signify a retrospective sensory encoding of behaviorally relevant targets, or a prospective encoding of the movement intentions with respect to those targets.

Single-unit recordings in the lateral bank of the intraparietal sulcus of the macaque (LIP) spawned the notion that the posterior parietal cortex integrates or selects sensory information, which can then be conveyed to frontal areas when anticipating a movement (Robinson et al. 1978; Gottlieb et al. 1998). Parietal neurons respond when a target is placed in its receptive field. This response becomes enhanced when the target becomes behaviorally relevant, with this enhancement occurring whether or not a movement to the behaviorally relevant stimulus is generated (Bushnell et al. 1981; Goldberg et al. 1990). Also, these neurons fire less when a movement is made towards no target as compared to when the exact same movement acquires a target (Colby et al. 1996). Drawing on these characteristics in LIP, posterior parietal areas have been postulated to represent behaviorally salient locations in space, rather than underlie movement-related activity (Colby et al. 1996). An alternative hypothesis contends that posterior parietal cortex is more directly involved in the formation of early movement plans. This dispute has been waged on the intricate terrain of coordinate transformations, and heterogeneous subpopulations specific for different types of movements. At least in some areas in posterior parietal cortex, sensory input from the environment is construed in forms useful for preparing coordinated movements. The representation of target locations is in spatial reference frames based on

visual/retinal coordinates, but also incorporates signals about eye, head, and limb positions (Buneo and Andersen 2002)—information required for an abstract movement plan specifying where to look or reach. In addition, anatomically segregated subregions are specialized for the type of movement to be performed, i.e., neurons in LIP respond when a saccade is being planned to a stimulus, whereas cells in parietal reach region (PRR) preferentially respond to reaches planned to the same stimulus (Snyder et al. 2000). Moreover, in conditions where the spatial configuration of the visual stimulus is held constant, a change in upcoming motor plans can elicit a robust increase in response (Snyder et al. 1998). Finally, in paradigms in which the target cue direction is dissociated from the movement direction, neural activity is correlated more strongly with the motor goal, and not the visual cue (Gail and Andersen 2006). Taken together, these findings suggest that action plans rather than sensory encoding may be the jurisdiction of PPC (Mountcastle et al. 1975; Lynch et al. 1977; Snyder et al. 1997, 2000; Buneo and Andersen 2002).

In contrast, neurons in premotor areas demonstrate a more consistent pattern. PMd cells also transform the spatial reference frame in which target locations are represented. Though in PPC subregions reference frames are in visual/eye coordinates, PMd neurons may also encode targets in hand-centered coordinates or by the relative position of the target, hand, and eye (Batista et al. 2007; Pesaran et al. 2006). In so doing, these cells represent targets in space at a level even 'closer' to the motor output. Like parietal neurons, neural activity reflects the motor goal more strongly than the visual cue in paradigms when they are dissociated (Cisek and Kalaska 2002). However, unlike parietal neurons, when a movement is inhibited, i.e., an instruction is provided to cancel an impending action plan, neurons cease firing (Cisek and Kalaska 2002). Thus, from results obtained from single-cell investigations, it is possible that either parietal cortices generate a sensory representation of salient spatial locations based on which frontal areas create action plans, or that parietal regions represent all potential action plans and premotor regions more fully elaborate the most probable or selected plan.

More recently, functional imaging studies have tackled a similar question regard-

ing alleged human action-planning areas. While PPC and frontal areas both exhibit prolonged activation during a delay period between an instructive cue and contingent motor responses, this activation could represent either sustained motor intention, or sustained visuospatial attention or working memory for the cued location. Studies which note PPC activation to co-vary with attentional/memory load (Simon et al. 2002), or remain the same whether or not a saccade is generated to the same target (Brown et al. 2006), have prompted some authors to conclude that PPC is primarily involved in retrospective visuospatial processes. Recently, Curtis et al. directly addressed the question of whether sustained activity during a delay period between cue and response reflected retrospective coding of sensory information or prospective coding of motor intentions, utilizing delay periods long enough to rule out confounds of cue or motor responses. Curtis et al. (2004) compared delay-period activity in which a cue indicated either where an upcoming memory-guided saccade should be directed or where it should not be directed. When metrics were known before the delay, FEF activation was slightly increased and IPS activity decreased, as compared to when such information of the upcoming movement was not known. Similarly, after one response was selected from several pre-cued options, FEF activity sustained until response execution, while PPC activity diminished (Curtis and D'Esposito 2006). They thus argued for a retrospective, sensory representation in PPC, and for one more biased towards motor encoding and response preparation in FEF.

With a rationale similar to monkey electrophysiologists, other authors suggest that effector information is integrated with spatial information in PPC, and thus this area carries intention-related signals in addition to sensory-related activity (Medendorp et al. 2005; see discussion of chapter 2 for a full exposition of these studies). Finally, in a variable delay task, when a cue indicating the probability of upcoming movement is presented, frontal areas exhibited greater activity the more likely the movement, whereas parietal regions demonstrated similar activation irrespective of movement probability. Based on these findings, the authors speculated that parietal activity may cover a range of potential responses defined by the task settings whereas frontal activity may focus on a probable movement (Thoenissen et al. 2002). Thus, despite

the body of both monkey and human studies, the question of whether these brain areas subserve a retrospective, sensory encoding of salient locations versus a prospective motor encoding in the preparation of action remains unresolved.

1.4.2 Action Outcomes and Consequences

So far, the action plan was considered at the level of how and where to move to acquire a goal. However, equally important is the issue of selecting or determining the most appropriate action plan in a particular context. Ultimately, we select and plan an action in order to attain or maximize a rewarding state. In reaching for the earlier chalice of caffeine, I did so to attain some consequence I value: to enjoy the flavor, or to stay awake long enough to write just one more sentence. However, in a natural environment, a plan of action seldom promises to successfully achieve the desired outcome, but rather furnishes a possibility of failure and undesired outcomes. Thus all the outcomes or consequences of an action need to be evaluated, and these anticipations should be used to discern the optimal action plan in a given circumstance. And as the rewards of tasks are not constant, the solution cannot be hardwired. Accordingly, action planning cannot solely rely on sensorimotor processes that are merely more intricate versions of stimulus-response reflexes (Jeannerod 1998), but rather must utilize expectations and contextual information through cortical top-down or subcortical-cortical interactions to bias their computations (Frith 2000; Passingham et al. 2000).

On a slightly tangential note, while the evaluation of an action plan, in terms of its potential consequences, is a prerequisite for optimal response selection, the processes of selecting the plan and the actual planning do not obligatorily occur jointly. By one hypothesis, they may transpire separately, in a modular fashion, where certain regions underlie valuation of objects and possible goals, and then the action-planning machinery is steered towards the attainment of the selected goal. Copious studies in humans and monkeys have speculated that regions such as the orbitofrontal cortex and striatum (Schultz et al. 2000; Hollerman et al. 2000; Knutson et al. 2000;

O'Doherty 2004) attach a value to various goods and actions, representing a large domain of possible stimuli and responses with one internal measure of utility. These areas, for example, may guide the frontoparietal network towards a certain end, and thus action-planning regions need only be concerned with preparing the one behavioral response provided them.

Alternatively, the action-planning substrates may subserve both processes. At any given time, many possible actions exist; and in a natural, unpredictable environment, many of them may be relevant and tenable options. Regions engaged in encoding action plans then may represent this range of options and weight them according to their value or expected outcomes, essentially permitting a competition among intentions to ensue until one eventually is selected. Indeed, many current models of response choice propose that for each competing response, evidence accumulates until a decision threshold is reached (Cisek 2007; Glimcher 2003; Rorie and Newsome 2005). On a single-cell level, recent neurophysiological findings demonstrated that when there are two potential movement choices, activity within PPC neurons initially represents both potential targets, before one diminishes and the other eventually dominates (Scherberger and Andersen 2007), consonant with a mutual competition model of selection (Cisek 2006). From this perspective, competition between conflicting responses is a crucial process for action selection, analogous to models that propose competition to be an underlying principle of selection for sensory attention (Desimone and Duncan 1995; Duncan et al. 1997; Itti and Koch 2000). Such competition would require that these action planning areas bias response representations based on 'many different aspects of an animal's state, e.g., prior probabilities or reward contingencies, as well as changes in the environment (e.g., new information that alters the weight given to a particular stimulus)' (Coulthard 2008), in order to derive the eventual response from the outcome of competition.

Finally, there is no reason to believe these two approaches are mutually exclusive. Canonical reward circuitry may valuate stimuli and actions, and additionally, the action-planning network may exploit this information, and incorporate other relevant information, in order to bias the selection and preparation of the courses of action

present at a given time.

Monkey electrophysiological studies that examined neural activity throughout many structures involved in generating movement supported the proposition that action-planning areas do encode information pertaining to the value or consequences tied to actions, consistent with the latter two models. These investigations reveal modulations of neural activity which generally correlate with the likely selection, or factors affecting the selection, of an action. Specifically, when a movement was paired with a fluid reward, posterior parietal areas reflected the sensory information indicating a particular eye movement will generate a reward (positive outcome), as well as the probability and magnitude of the associated reward (Glimcher 2003; Shadlen and Newsome 2001). In addition, premotor regions, prefrontal areas, and the superior colliculus—all nodes in the oculomotor network—revealed activity that correlated with the expected value (probability times magnitude) of the fluid reward associated with the eye movement (Roesch and Olson 2003, 2004; Tanji et al. 2002; Shima et al. 1998; Basso and Wurtz 1997, 1998; Dorris et al. 1997). Presumably these signals serve to bias eye movement selection towards maximization of reward. In addition, behavioral measures indicate that expected value systematically influences not only selection of eye movements, but also modulates saccade metrics, including amplitude, velocity, and reaction time (Leon and Shadlen 1999; Takikawa et al. 2002; McCoy et al. 2003), suggesting further an influence on formation of action plans.

However, in all these studies, both monkey and human, the movements required a trivial amount of action planning and preparation. For the most part, eye movements and (in humans) key presses were utilized in these studies. Key presses, while corresponding to the general notion of a stimulus-response mapping, do not necessarily require the conversion of spatial information about the target into a motor plan. While eye movements do constitute spatial-target directed behaviors, they may not demand complex reference frame transformations from visual to other effector-centered coordinates. Therefore, the action planning machinery may not be recruited heavily. In addition, the simplicity of the responses engendered a negligible probability of failure, and even for the failures that occurred, no costs and punishments

were generally imposed. Conversely, many real-life goal-directed behaviors are more complex. And with increasing complexity comes a significant probability of failure, which likely leads to some cost or punishment. For example, I might reach for the grail of bitterly divine *C. arabica* intoxication, miss, and tip its ascorbic contents onto my laptop, where currently the only version of my thesis is stored—a potential penalty that clearly influences whether and how I choose to grab it. Thus, both the possible rewards and punishments to be incurred impinge upon the evaluation of actions and the determination of the optimal action plan; yet previous studies of the rewards associated with action shed no light on this process. Whether and how rewards and punishments related to complex actions modulate neural representations in the human frontoparietal network has yet to be established.

In this vein, elucidating those areas specifically recruited in motor encoding, beyond mere sensory or spatial representations, and determining whether they additionally incorporate information as to the expected consequences of the actions they represent, are both essential for understanding the neural underpinnings of action planning. However, previous experiments, while delineating these neural substrates, have not conclusively addressed these issues, leaving amorphous the nature of action-planning representations.

1.5 Monkey fMRI—The Missing Link

To probe neural activity in humans during the selection, preparation, and monitoring of action, the techniques used most often include EEG and MEG, and imaging techniques such as PET and fMRI. Each of these methods have their advantages and disadvantages. However, given its better spatial resolution compared to EEG/MEG and use of endogenous, nonradioactive contrast as opposed to PET, fMRI is often employed to delineate the specific subcortical and cortical regions involved with these processes. In fact, fMRI is currently the most widely used method to map brain areas and study the neural basis of human cognition (Logothetis 2002).

Nevertheless, while functional imaging can provide indirect measurements of the

distributed activities of frontoparietal structures engaged in planning motor responses, it faces certain limitations in its ability to elucidate the neural computations underlying these processes. It is therefore important to assess how fMRI responses compare with those reported in the much larger body of monkey electrophysiology literature. Direct comparisons between human imaging and monkey electrophysiological studies, however, are hampered for several reasons. First, the relationship of the hemodynamic response to neural activity is still ambiguous. While electrophysiology experiments generally assay firing rates of populations of neurons, recent reports suggest that BOLD hemodynamic signals may better correlate with local field potentials than firing patterns (Logothetis 2002). In addition, the manner in which neural inhibition may translate into BOLD signals is still debated (Shmuel et al. 2006). Second, different time-scales are often used, with considerably longer experiments employed in imaging paradigms to allow for the lag and sluggishness of the hemodynamic response. Thus, these dissimilar task durations could promote different signal dynamics, as well as disparate behavioral strategies. The poorer temporal resolution of BOLD fMRI, as compared to electrophysiological recording, additionally impedes appraisal of the relationship between signal profiles reported across the two bodies of literature. Third, interspecies discrepancies may exist, confounding interpretation of incongruent findings reported by human imaging versus macaque electrophysiological studies.

Reconciling findings is further hampered by the inhomogeneity of frontal and particularly parietal regions. Distinct subpopulations demonstrate varying response profiles; and given its coarser spatial resolution, imaging studies may conflate effects from these different subpopulations. Characteristics of subregions are better defined in monkeys, but mappings between monkey and human subregions have not been conclusively established. Thus, even when implications from monkey electrophysiology and human imaging are taken together, incontrovertible descriptions about human neuronal response properties cannot be made. Two strategies exist to address this chasm. One possibility is to directly assess neural firing patterns in humans, through iEEG or intraoperative single-neuron recording, for example. However, these ap-

proaches are constrained, as areas of investigation are limited by medical necessity. Hence, the only remaining and tenable means by which to make veridical assertions as to the neural activity generating patterns of fMRI activation observed in the previous experiments is by comparing fMRI findings of humans and of monkeys performing the same task, and then in turn relating monkey fMRI results to neurophysiological data.

1.6 Specific Aims

The focus of this thesis is on action planning activity in the human and the macaque. In both species, variants of delayed response task and time-resolved event-related fMRI are employed to answer specific questions. In humans, the primary aim is to characterize the neural representations of action planning at different epochs during delayed response tasks. In monkeys, the impetus is to develop a new technique that allows direct comparison of monkey and human studies of action planning, and to apply this technique to investigations of oculomotor goal-directed actions.

The work presented in Chapter 2 ripostes to a debate that has long raged about the differential functional contributions of cortical areas engaged in action planning (see Section 1.4.1). In controlling for attentional and mnemonic demands, we show that PPC activity carries specific signals reflecting planning and preparation for goal-directed actions.

In Chapter 3, the question of whether an action's predicted outcomes are incorporated in human action planning areas is addressed. Specifically, we required subjects to perform complex motor responses similar to those used in Chapter 2, with monetary gains and losses imposed as consequences for successful or unsuccessful task performance. fMRI findings indicate that action planning areas were modulated by expected gain-loss consequences of actions, reflecting the importance of behaviorally relevant reward/punishment context in shaping neural activity. In addition, these data show that subjective beliefs influence the reward context representations in cortical, but not in certain subcortical areas involved in the task, emphasizing distinct

functional contributions within reward and action-processing circuitry.

To link together large bodies of information on action planning representations accumulated through monkey electrophysiology and human imaging, a fMRI study in awake behaving monkeys was conducted, in which event-related analysis of activity was developed and employed to characterize activation patterns in cortical oculomotor network. Analogous experiments were conducted on humans, to enable direct cross-species comparisons. These results, depicted in Chapter 4, demonstrate consistency between the monkey single-unit physiology and imaging, on one hand, and activity in monkey areas and human putative homologs, on the other. Importantly, these data also revealed apparent interspecies differences, with respect to their hemodynamic responses and the contralateral organization of action planning representations.

In the future, we wish to continue studying reward-modulated action planning and decision-making in both the human and the macaque. To do so, areas involved in encoding reward associations, including the putative reward circuitry, need to be mapped in the monkey. In addition, the ability to detect the temporal evolution of spatial decisions in different areas needs to be assessed. Therefore, preliminary macaque fMRI results investigating these issues have been obtained. Appendix 5 describes recent data mapping brain areas which incorporate and learn the rewarding consequences associated with stimuli. Appendix A1.5 illustrates the time-course of oculomotor decision-related activity in the saccade-planning network in free-choice spatial task.

In summary, these findings have helped to characterize human and monkey cerebral areas specifically involved in the planning and the evaluation of behavioral responses, making it an important contribution to the study of response selection, decision-making, and goal-directed action.

References

R. Balint. Seelenlahmung des schauens, optische ataxie, raumliche storung der aufmerksamkeit. *Monatsschrift fur Psychiatrie und Neurologie*, 25:51–81, 1909.

M. A. Basso and R. H. Wurtz. Modulation of neuronal activity by target uncertainty. *Nature*, 389(6646):66–9, 1997.

M. A. Basso and R. H. Wurtz. Modulation of neuronal activity in superior colliculus by changes in target probability. *J Neurosci*, 18(18):7519–34, 1998.

A. P. Batista, G. Santhanam, B. M. Yu, S. I. Ryu, A. Afshar, and K. V. Shenoy. Reference frames for reach planning in macaque dorsal premotor cortex. *J Neurophysiol*, 98(2):966–83, 2007.

W. D. Beggs and C. I. Howarth. Movement control in a repetitive motor task. *Nature*, 225(5234):752–3, 1970.

W. D. Beggs and C. I. Howarth. The movement of the hand towards a target. *Q J Exp Psychol*, 24(4):448–53, 1972a.

W. D. Beggs and C. I. Howarth. The accuracy of aiming at a target. some further evidence for a theory of intermittent control. *Acta Psychol (Amst)*, 36(3):171–7, 1972b.

D. I. Braun, D. K. Boman, and J. R. Hotson. Anticipatory smooth eye movements and predictive pursuit after unilateral lesions in human brain. *Exp Brain Res*, 110 (1):111–6, 1996.

M. R. Brown, J. F. DeSouza, H. C. Goltz, K. Ford, R. S. Menon, M. A. Goodale, and S. Everling. Comparison of memory- and visually guided saccades using event-related fmri. *J Neurophysiol*, 91(2):873–89, 2004.

M. R. Brown, H. C. Goltz, T. Vilis, K. A. Ford, and S. Everling. Inhibition and generation of saccades: rapid event-related fmri of prosaccades, antisaccades, and nogo trials. *Neuroimage*, 33(2):644–59, 2006.

C. A. Buneo, M. R. Jarvis, A. P. Batista, and R. A. Andersen. Direct visuomotor transformations for reaching. *Nature*, 416(6881):632–6, 2002.

M. C. Bushnell, M. E. Goldberg, and D. L. Robinson. Behavioral enhancement of visual responses in monkey cerebral cortex. i. modulation in posterior parietal cortex related to selective visual attention. *J Neurophysiol*, 46(4):755–72, 1981.

J. L. Calton, A. R. Dickinson, and L. H. Snyder. Non-spatial, motor-specific activation in posterior parietal cortex. *Nat Neurosci*, 5(6):580–8, 2002.

L. G. Carlton. Processing visual feedback information for movement control. *J Exp Psychol Hum Percept Perform*, 7(5):1019–30, 1981.

P. Cisek. Integrated neural processes for defining potential actions and deciding between them: a computational model. *J Neurosci*, 26(38):9761–70, 2006.

P. Cisek. Cortical mechanisms of action selection: the affordance competition hypothesis. *Philos Trans R Soc Lond B Biol Sci*, 362(1485):1585–99, 2007.

P. Cisek and J. F. Kalaska. Simultaneous encoding of multiple potential reach directions in dorsal premotor cortex. *J Neurophysiol*, 87(2):1149–54, 2002.

C. L. Colby and J. R. Duhamel. Spatial representations for action in parietal cortex. *Brain Res Cogn Brain Res*, 5(1-2):105–15, 1996.

C. L. Colby, J. R. Duhamel, and M. E. Goldberg. Visual, presaccadic, and cognitive activation of single neurons in monkey lateral intraparietal area. *J Neurophysiol*, 76(5):2841–52, 1996.

E. J. Coulthard, P. Nachev, and M. Husain. Control over conflict during movement preparation: role of posterior parietal cortex. *Neuron*, 58(1):144–57, 2008.

C. E. Curtis and M. D'Esposito. Selection and maintenance of saccade goals in the human frontal eye fields. *J Neurophysiol*, 95(6):3923–7, 2006.

C. E. Curtis, V. Y. Rao, and M. D'Esposito. Maintenance of spatial and motor codes during oculomotor delayed response tasks. *J Neurosci*, 24(16):3944–52, 2004.

M. Davare, M. Andres, G. Cosnard, J. L. Thonnard, and E. Olivier. Dissociating the role of ventral and dorsal premotor cortex in precision grasping. *J Neurosci*, 26(8): 2260–8, 2006.

R. Desimone and J. Duncan. Neural mechanisms of selective visual attention. *Annu Rev Neurosci*, 18:193–222, 1995.

M. C. Dorris, M. Pare, and D. P. Munoz. Neuronal activity in monkey superior colliculus related to the initiation of saccadic eye movements. *J Neurosci*, 17(21): 8566–79, 1997.

J. Duncan, G. Humphreys, and R. Ward. Competitive brain activity in visual attention. *Curr Opin Neurobiol*, 7(2):255–61, 1997.

D. Elliott, W. F. Helsen, and R. Chua. A century later: Woodworth's (1899) two-component model of goal-directed aiming. *Psychol Bull*, 127(3):342–57, 2001.

E. N. Eskandar and J. A. Assad. Dissociation of visual, motor and predictive signals in parietal cortex during visual guidance. *Nat Neurosci*, 2(1):88–93, 1999.

P. M. Fitts. The information capacity of the human motor system in controlling the amplitude of movement. *J Exp Psychol*, 47(6):381–91, 1954.

L. Fogassi, V. Gallese, G. Buccino, L. Craighero, L. Fadiga, and G. Rizzolatti. Cortical mechanism for the visual guidance of hand grasping movements in the monkey: A reversible inactivation study. *Brain*, 124(Pt 3):571–86, 2001.

C. D. Frith, S. J. Blakemore, and D. M. Wolpert. Abnormalities in the awareness and control of action. *Philos Trans R Soc Lond B Biol Sci*, 355(1404):1771–88, 2000.

A. Gail and R. A. Andersen. Neural dynamics in monkey parietal reach region reflect context-specific sensorimotor transformations. *J Neurosci*, 26(37):9376–84, 2006.

P. W. Glimcher. The neurobiology of visual-saccadic decision making. *Annu Rev Neurosci*, 26:133–79, 2003.

S. Glover. Separate visual representations in the planning and control of action. *Behav Brain Sci*, 27(1):3–24; discussion 24–78, 2004.

M. E. Goldberg, C. L. Colby, and J. R. Duhamel. Representation of visuomotor space in the parietal lobe of the monkey. *Cold Spring Harb Symp Quant Biol*, 55:729–39, 1990.

M. A. Goodale and A. Haffenden. Frames of reference for perception and action in the human visual system. *Neurosci Biobehav Rev*, 22(2):161–72, 1998.

J. P. Gottlieb, M. Kusunoki, and M. E. Goldberg. The representation of visual salience in monkey parietal cortex. *Nature*, 391(6666):481–4, 1998.

U. Halsband and H. J. Freund. Premotor cortex and conditional motor learning in man. *Brain*, 113 (Pt 1):207–22, 1990.

O. Hikosaka and R. H. Wurtz. Visual and oculomotor functions of monkey substantia nigra pars reticulata. iii. memory-contingent visual and saccade responses. *J Neurophysiol*, 49(5):1268–84, 1983.

J. R. Hollerman, L. Tremblay, and W. Schultz. Involvement of basal ganglia and orbitofrontal cortex in goal-directed behavior. *Prog Brain Res*, 126:193–215, 2000.

B. Hommel. Planning and representing intentional action. *ScientificWorldJournal*, 3: 593–608, 2003.

L. Itti and C. Koch. A saliency-based search mechanism for overt and covert shifts of visual attention. *Vision Res*, 40(10-12):1489–506, 2000.

M. Jeannerod. Intersegmental coordination during reaching at natural visual objects. In J. Long and A. Baddeley, editors, *Attention and Performance IX*, pages 153–168. Erlbaum, Hillsdale, NJ, 1981.

M. Jeannerod. The timing of natural prehension movements. *J Mot Behav*, 16(3): 235–54, 1984.

M. Jeannerod. *The neural and behavioural organization of goal-directed movements*. Oxford University Press, New York, 1988.

M. Jeannerod, Y. Paulignan, and P. Weiss. Grasping an object: one movement, several components. *Novartis Found Symp*, 218:5–16; discussion 16–20, 1998.

R. Joseph. *Neuropsychiatry, Neuropsychology, Clinical Neuroscience*. Academic Press, New York, 2000.

J. F. Kalaska and D. J. Crammond. Deciding not to go: neuronal correlates of response selection in a go/nogo task in primate premotor and parietal cortex. *Cereb Cortex*, 5(5):410–28, 1995.

S. W. Keele and M. I. Posner. Processing of visual feedback in rapid movements. *J Exp Psychol*, 77(1):155–8, 1968.

S. T. Klapp. Reaction time analysis of programmed control. *Exerc Sport Sci Rev*, 5: 231–53, 1977.

B. Knutson, A. Westdorp, E. Kaiser, and D. Hommer. Fmri visualization of brain activity during a monetary incentive delay task. *Neuroimage*, 12(1):20–7, 2000.

M. I. Leon and M. N. Shadlen. Effect of expected reward magnitude on the response of neurons in the dorsolateral prefrontal cortex of the macaque. *Neuron*, 24(2): 415–25, 1999.

H. Liepmann. Die linke hemisphare und das handeln. In *Reprinted in Drei Aufsatze aus dem Apraxiegebiet (neu durchgesehen und mit Zusatzen versehen). 1908.*, pages 17–50. Von Karger, Berlin, 1905.

N. K. Logothetis. The neural basis of the blood-oxygen-level-dependent functional magnetic resonance imaging signal. *Philos Trans R Soc Lond B Biol Sci*, 357(1424): 1003–37, 2002.

J. C. Lynch, V. B. Mountcastle, W. H. Talbot, and T. C. Yin. Parietal lobe mechanisms for directed visual attention. *J Neurophysiol*, 40(2):362–89, 1977.

M. G. MacAvoy, J. P. Gottlieb, and C. J. Bruce. Smooth-pursuit eye movement representation in the primate frontal eye field. *Cereb Cortex*, 1(1):95–102, 1991.

A. N. McCoy, J. C. Crowley, G. Haghighian, H. L. Dean, and M. L. Platt. Saccade reward signals in posterior cingulate cortex. *Neuron*, 40(5):1031–40, 2003.

W. P. Medendorp, H. C. Goltz, J. D. Crawford, and T. Vilis. Integration of target and effector information in human posterior parietal cortex for the planning of action. *J Neurophysiol*, 93(2):954–62, 2005.

D. E. Meyer, R. A. Abrams, S. Kornblum, C. E. Wright, and J. E. Smith. Optimality in human motor performance: ideal control of rapid aimed movements. *Psychol Rev*, 95(3):340–70, 1988.

N. Miller and N. Newman. *Walsh and Hoyt's Clinical Neuro-Ophthalmology*. Lippincott Williams & Wilkins, Baltimore, 2005.

V. B. Mountcastle, J. C. Lynch, A. Georgopoulos, H. Sakata, and C. Acuna. Posterior parietal association cortex of the monkey: command functions for operations within extrapersonal space. *J Neurophysiol*, 38(4):871–908, 1975.

J. P. O'Doherty. Reward representations and reward-related learning in the human brain: insights from neuroimaging. *Curr Opin Neurobiol*, 14(6):769–76, 2004.

R. E. Passingham, I. Toni, and M. F. Rushworth. Specialisation within the prefrontal cortex: the ventral prefrontal cortex and associative learning. *Exp Brain Res*, 133 (1):103–13, 2000.

B. Pesaran, M. J. Nelson, and R. A. Andersen. Dorsal premotor neurons encode the relative position of the hand, eye, and goal during reach planning. *Neuron*, 51(1): 125–34, 2006.

A. Riehle, W. A. MacKay, and J. Requin. Are extent and force independent movement parameters? preparation- and movement-related neuronal activity in the monkey cortex. *Exp Brain Res*, 99(1):56–74, 1994.

D. L. Robinson and M. E. Goldberg. Sensory and behavioral properties of neurons in posterior parietal cortex of the awake, trained monkey. *Fed Proc*, 37(9):2258–61, 1978.

M. R. Roesch and C. R. Olson. Impact of expected reward on neuronal activity in prefrontal cortex, frontal and supplementary eye fields and premotor cortex. *J Neurophysiol*, 90(3):1766–89, 2003.

M. R. Roesch and C. R. Olson. Neuronal activity related to reward value and motivation in primate frontal cortex. *Science*, 304(5668):307–10, 2004.

A. E. Rorie and W. T. Newsome. A general mechanism for decision-making in the human brain? *Trends Cogn Sci*, 9(2):41–3, 2005.

D. A. Rosenbaum. Human movement initiation: specification of arm, direction, and extent. *J Exp Psychol Gen*, 109(4):444–74, 1980.

D. A. Rosenbaum. *Human motor control*. Academic Press, New York, 1991.

H. Scherberger and R. A. Andersen. Target selection signals for arm reaching in the posterior parietal cortex. *J Neurosci*, 27(8):2001–12, 2007.

W. Schultz, L. Tremblay, and J. R. Hollerman. Reward processing in primate orbitofrontal cortex and basal ganglia. *Cereb Cortex*, 10(3):272–84, 2000.

M. N. Shadlen and W. T. Newsome. Neural basis of a perceptual decision in the parietal cortex (area lip) of the rhesus monkey. *J Neurophysiol*, 86(4):1916–36, 2001.

R. Shadmehr and J. W. Krakauer. A computational neuroanatomy for motor control. *Exp Brain Res*, 185(3):359–81, 2008.

K. Shima and J. Tanji. Role for cingulate motor area cells in voluntary movement selection based on reward. *Science*, 282(5392):1335–8, 1998.

A. Shmuel, M. Augath, A. Oeltermann, and N. K. Logothetis. Negative functional mri response correlates with decreases in neuronal activity in monkey visual area v1. *Nat Neurosci*, 9(4):569–77, 2006.

S. R. Simon, M. Meunier, L. Piettre, A. M. Berardi, C. M. Segebarth, and D. Boussaoud. Spatial attention and memory versus motor preparation: premotor cortex involvement as revealed by fmri. *J Neurophysiol*, 88(4):2047–57, 2002.

A. Sirigu, E. Daprati, P. Pradat-Diehl, N. Franck, and M. Jeannerod. Perception of self-generated movement following left parietal lesion. *Brain*, 122 (Pt 10):1867–74, 1999.

L. H. Snyder, A. P. Batista, and R. A. Andersen. Coding of intention in the posterior parietal cortex. *Nature*, 386(6621):167–70, 1997.

L. H. Snyder, A. P. Batista, and R. A. Andersen. Change in motor plan, without a change in the spatial locus of attention, modulates activity in posterior parietal cortex. *J Neurophysiol*, 79(5):2814–9, 1998.

L. H. Snyder, A. P. Batista, and R. A. Andersen. Intention-related activity in the posterior parietal cortex: a review. *Vision Res*, 40(10-12):1433–41, 2000.

Y. Takikawa, R. Kawagoe, H. Itoh, H. Nakahara, and O. Hikosaka. Modulation of saccadic eye movements by predicted reward outcome. *Exp Brain Res*, 142(2): 284–91, 2002.

J. Tanji, K. Shima, and Y. Matsuzaka. Reward-based planning of motor selection in the rostral cingulate motor area. *Adv Exp Med Biol*, 508:417–23, 2002.

D. Thoenissen, K. Zilles, and I. Toni. Differential involvement of parietal and precentral regions in movement preparation and motor intention. *J Neurosci*, 22(20): 9024–34, 2002.

L. Ungerleider and M. Mishkin. Two cortical visual systems. In D. J. Ingle, M. A. Goodale, and R. J. W Mansfield, editors, *Analysis of visual behavior*. MIT Press, Cambridge, MA, 1982.

M. A. Vince. Corrective movements in a pursuit task. *Q J Exp Physiol Cogn Med Sci*, 1(Pt. 2):85–103, 1948.

R. Watts. *Movement Disorders: Neurologic Principles & Practice*. McGraw-Hill Professional, New York, 2004.

R. S. Woodworth. The accuracy of voluntary movement. *Psychological Review*, 3 (monograph supplement):1–119, 1899.

Chapter 2

Roles of Human Posterior Parietal and Premotor Cortex in Action Planning

2.1 Summary

The advance planning and preparation of actions is of the highest ecological relevance, as it permits rapid and flexible behavioral responses to environmental stimuli. To access the neuronal processes underlying planning without being confounded by action execution or sensory processing, tasks which temporally separate instructive information from the execution of the contingent motor responses are often used. However, putative planning activity prior to the response may likewise reflect attention or a sensory memory of the contextual information previously cued. We thus devised a time-resolved fMRI experiment that allowed delineating preparatory fMRI activity specifically related to the planning and the inhibition of right index finger reaches towards memorized target locations while directly controlling for mnemonic and attentional demands. Preparatory fMRI activity was most pronounced in the left superior parietal lobule, but also present in other regions within the posterior parietal and premotor cortices. Remarkably, parietal and premotor planning thereby considered both types of targets relevant for reaching—those to be acquired and those to be avoided.

2.2 Introduction

The prospective planning of future action is composed of various interacting processes that range from the specification of a behavioral goal (intention) to the orchestration of dynamic muscular activity. Intuitively, one might think that the latter specification of movement dynamics is at the core of motor planning. However, movements are initially programmed in an extrinsic (visual) rather than an intrinsic (effector-specific) reference frame (Morasso 1981; Wolpert et al. 1995), making it difficult to extract the earliest precursors of our behavior from the neuronal representation of the sensory context in which they are embedded. In order to come up with such a distinction, experimenters engaged so-called pre-cuing paradigms with delayed behavioral responses (Rosenbaum 1980). These paradigms enable the separation of planning processes from both (i) the sensory representations they depend on and (ii) the motor acts they produce. This is realized by briefly providing the sensory 'context/spatial cue(s)', relevant for the planning of an upcoming behavior, while interdicting the actual execution of this behavior until the later presentation of a 'go signal', thereby temporally isolating planning processes within the intervening 'delay period'. Thus, sustained neuronal activity recorded during this delay period would neither refer to the immediate processing of the sensory input nor to the actual movement performance. Rather, sustained activity would reflect isolated processes related to the planning of an upcoming movement (Hikosaka and Wurtz 1983). Following this rationale, various groups employed delayed response tasks to expose these otherwise 'covert' mental processes attributed to human action planning (e.g., Astafiev et al. 2003; Brown et al. 2004; Connolly et al. 2002, 2007; Medendorp et al. 2005, 2006; Schluppeck et al. 2006; Thoenissen et al. 2002). Amongst the areas that were reported to exhibit sustained activity throughout the preparatory delay period of such tasks, the human posterior parietal cortex (PPC) seemed to play a dominant role. Situated between the visual and somatosensory cortex, and with connections to motor cortex, pre-motor cortex, and the aforementioned sensory areas, PPC has the anatomical prerequisites that qualify it as a candidate structure for visual action

planning. Moreover, both the properties of neurons within PPC (for review see Andersen and Buneo 2002) as well as the symptoms of patients with lesions of this part of the brain (Karnath and Perenin 2005; Perenin and Vighetto 1988; Rushworth et al. 2003; Trillenberg et al. 2007) further support this notion.

However, the idea that PPC would primarily contribute to behavior is in sharp contrast with a long-espoused interpretation of its function in subserving processing of visuo-spatial sensory information (Robinson et al. 1978; Gottlieb et al. 1998). Following these dichotomous views the analogous question naturally arises as to whether sustained PPC activity in delayed-response tasks already underlies a prospective plan for an upcoming movement or, alternatively, merely reflects the processing of retrospective sensory information. According to the latter, sustained activity in the PPC might specifically be explicated by: (*i*) a sensory memory of contextual cues (e.g., Curtis et al. 2004; Curtis and D'Esposito 2006; Mars et al. 2008; Rowe et al. 2000; Simon et al. 2002; Volle et al. 2005), (*ii*) a manipulation of such sensory information within working memory (e.g., Champod & Petrides 2007) or (*iii*) a reactive shift of covert attention that is triggered by the contextual cues (e.g., Kastner et al. 1999; Corbetta and Shulman 2002). In fact, to date there is no conclusive evidence in favor of prospective action planning in human PPC that would allow an unequivocal distinction from the various mnemonic and attentional processes mentioned above. Towards this end, we devised an experiment that enabled the separation of movement planning from these latter processes, while monitoring brain activity using time-resolved, event-related fMRI. Using this approach, we demonstrated that preparatory processes related to both movement planning and movement inhibition are already realized at the level of the posterior parietal cortex. Moreover, planning activity was also present in regions within the pre-motor cortex, while the dorsolateral pre-frontal cortex (DLPFC) seemed rather to be engaged in the maintenance of retrospective visual memory.

2.3 Results

Eight human subjects were scanned over three consecutive runs while performing variants of a delayed-response task. In these tasks, sequences of finger reaches had to be performed using an fMRI-compatible trackball. While in one of the randomly interleaved tasks subjects were only required to memorize target locations, in other tasks the same targets either instructed the goals for an upcoming movement sequence or, alternatively, they instructed movements that should be inhibited. Hence, by varying the planning demands across tasks while keeping both the mnemonic and the attentional requirements constant, we aimed to isolate delay-related fMRI activity recruited by the preparation of upcoming behavior.

In order to engage movement planning in a subset of trials, subjects performed a 'classical' version of the delayed-response task (DRT). In this task movements were instructed by either two or four cues that were presented before the delay period (Fig. 2.1A). After the delay, subjects were required to move a trackball-controlled cursor as fast as possible to each of the remembered cue locations in order to successfully complete the trial. Importantly, in this (and each other) experimental condition, response times were limited in order to encourage advance planning of the required behavioral response. Furthermore, central fixation was required throughout all trials.

In the second trial type, the 'non-match to sample task' (NM2ST), sample cues signified undesired target locations, and the required motor response was only later defined by a second set of randomly selected cues that were presented immediately after the delay period. Subjects were instructed to perform movements towards all the new targets within the second set, i.e., those targets that were not previously presented in the first set of sample cues (Fig. 2.1B). This procedure ensured that subjects could not predict the required sequence of finger reaches during the preparatory delay. However, subjects could actively inhibit movements to the pre-cued target locations in order to limit the number of possible movement alternatives in the response phase.

In order to control for retrospective visual spatial memory of the target cues as well as covert shifts of attention towards these cues, we devised a 'match to sample

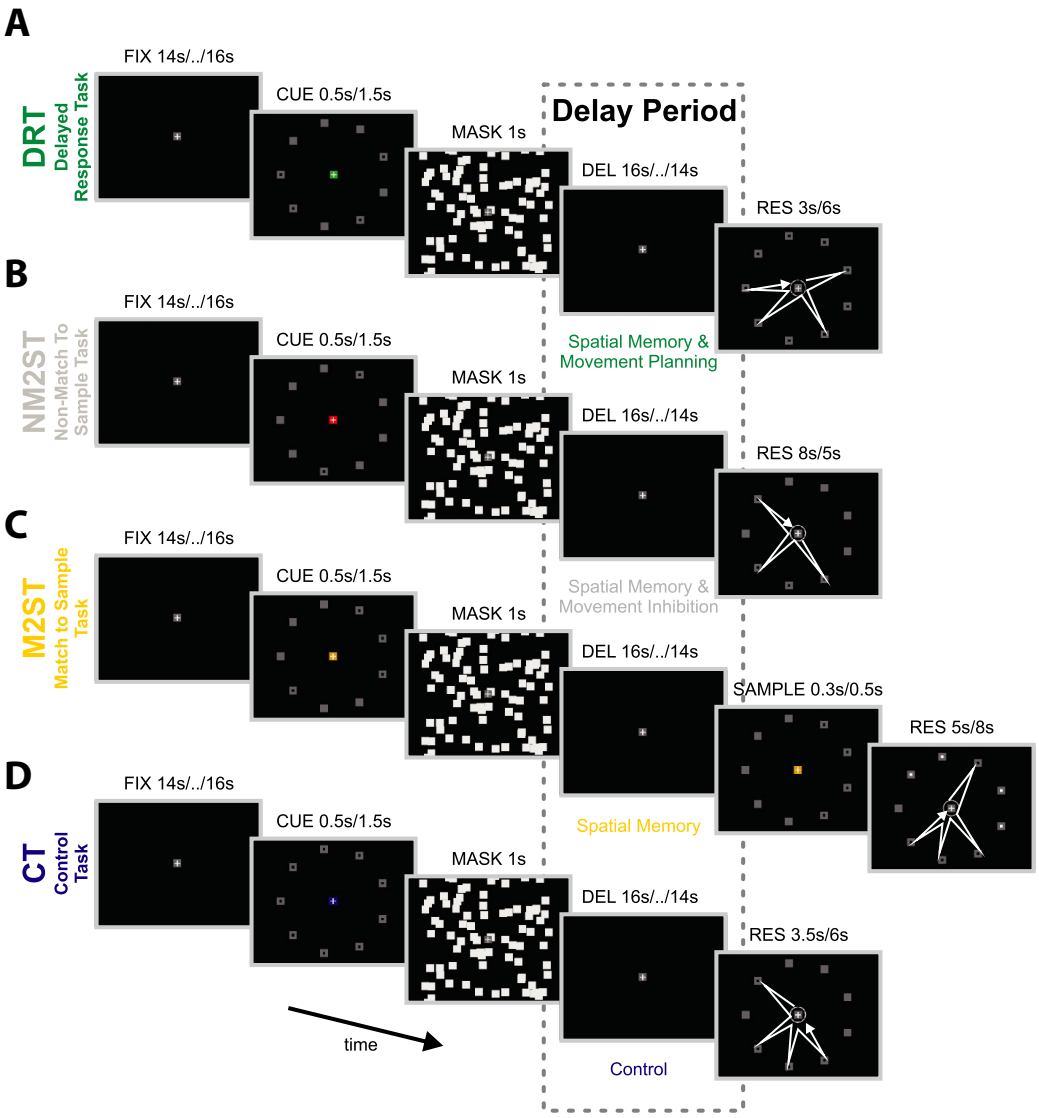
A
DRT
Delayed
Response Task
FIX 14s/../16s
CUE 0.5s/1.5s
MASK 1s
Delay Period
DEL 16s/../14s
RES 3s/6s
B
NM2ST
Non-Match To
Sample Task
FIX 14s/../16s
CUE 0.5s/1.5s
MASK 1s
Spatial Memory &
Movement Planning
DEL 16s/../14s
RES 8s/5s
C
M2ST
Match to Sample
Task
FIX 14s/../16s
CUE 0.5s/1.5s
MASK 1s
Spatial Memory &
Movement Inhibition
DEL 16s/../14s
SAMPLE 0.3s/0.5s
RES 5s/8s
D
CT
Control
Task
FIX 14s/../16s
CUE 0.5s/1.5s
MASK 1s
Spatial Memory
DEL 16s/../14s
RES 3.5s/6s
time
Control

Figure 2.1:

The behavioral tasks. *Each task started with a fixation period of random duration (FIX) which served as a baseline epoch for our fMRI-analysis. In the following cue period (CUE, durations refer to the 2/4-target condition, respectively) varying numbers of peripheral targets (empty squares) were presented. Depending on the task, these targets reflected goals for an upcoming movement (A), signified undesired locations (B), marked spatial positions that had to be memorized (C) or served as irrelevant distracters (D). Note that the color of the central fixation spot in the cue period indicated subjects which of the aforementioned strategies they should pursue in the randomly interleaved trials. The cue-period was followed by a brief random dot pattern (MASK) which masked putative after-images of the cue. During the delay period (DEL) subjects were asked to prepare for the upcoming response (RES): (A) In the DRT movements had to be planned to all remembered target locations. (B) In the NM2ST subjects should inhibit movements to all pre-cued locations while performing reaches towards all those targets in the response period that had not been shown before. (C) In the M2ST subjects just needed to memorize the initial cues in order to perform a delayed match to sample comparison (MATCH). Importantly, in this task subjects were not able to prepare or to inhibit specific movements during the delay period since the manual response was ultimately determined by a randomly generated response screen at the very end of the trial: subjects were asked to indicate a match/mismatch by reaching towards the white/black targets, respectively. (D) In an additional condition which controlled for unspecific preparatory activity during the delay (CT) the initial cues were irrelevant and could be simply ignored. Subjects' task was to reach towards all targets that were shown during the response phase. Note that all responses should be performed as quickly as possible and that the respective time limit for trial completion varied depending on both the number of targets (2/4) and the planning demands of the task.*

task' (M2ST). In this trial type, the initial sample cues could neither predict the required motor response nor could they limit the number of response alternatives. Instead, subjects simply needed to memorize cue locations in order to compare them to a second set of cues which was presented after the delay: If both sets were identical (50% of the M2ST trials), subjects moved the cursor towards the white targets of a randomly generated third set of response cues. If the two sets differed (50% of trials), subjects were instructed to move the cursor towards the black targets of the response set (Fig. 2.1C). Hence, both the memory load and the attentional demands in the NM2ST were identical to those in the two movement planning conditions. However, only in the 'movement planning' conditions could reaches be either prepared (DRT) or inhibited (NM2ST). Thus, any brain area that would exhibit greater delay-related fMRI activity in these conditions would be deemed to participate in movement planning.

Finally, a 'control task' (CT) served as an additional baseline control. In this task the initial cues were irrelevant for the later motor response. Subjects simply moved the cursor towards the targets that were presented immediately after the delay period (Fig. 2.1D). This task controlled for unspecific visual responses and unspecific motor preparation common to all tasks.

Behavioral Performance

In order to guarantee that fMRI activity during the delay period would solely reflect the differential contributions of the preparatory, attentional, and mnemonic processes under investigation, we carefully looked for any task-related differences in subjects' behavioral performance, which was monitored throughout the scanning sessions. Representative examples of subjects' reach- and oculomotor-performance are given in Supplemental Fig. 2.S1 for each experimental task condition. Importantly, the number of fixational saccades (Fig. 2.2A), as well as the frequency of eye blinks (Fig. 2.2B), did not significantly differ for the delay period across task conditions (2-way ANOVA—task $p>0.05$ [n.s.]; #cues n.s.; interaction n.s.). Furthermore, while

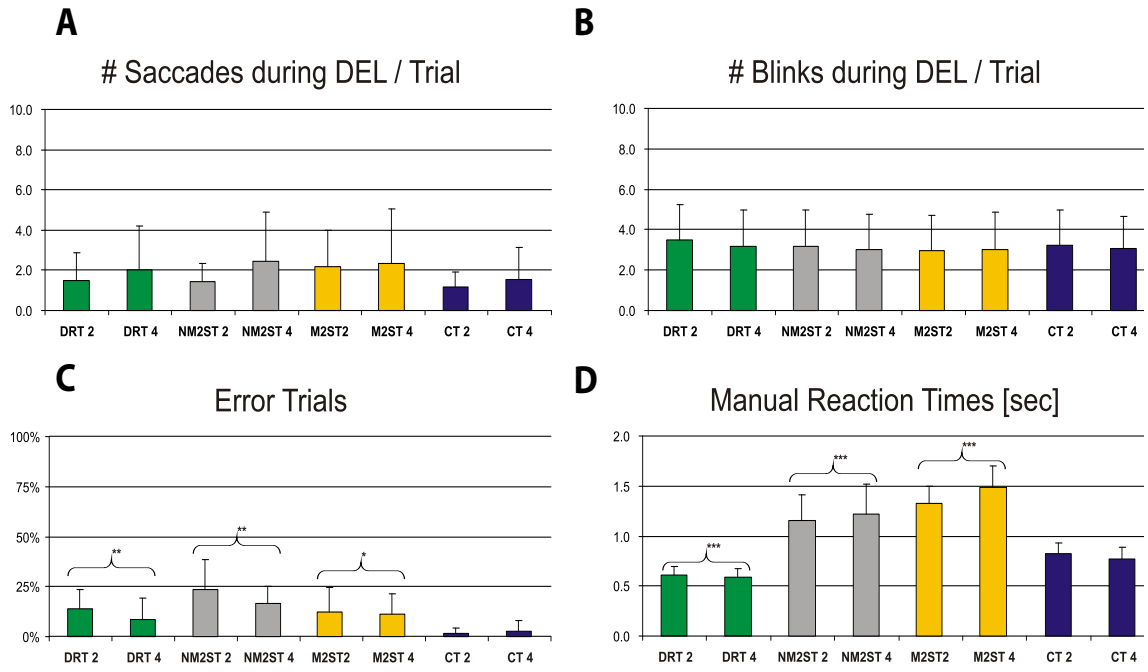

Figure 2.2:

Behavioral performance. *Estimating the behavioral performance during scanning allowed us to guarantee that delay-related fMRI activity would not be biased by any systematic differences in the number of fixational saccades (A) or in the frequency of eye blinks (B). Moreover, performance levels did not differ between the DRT, NM2ST, and M2ST as indicated by the share of error trials (C). However, error rates in these conditions were significantly increased as compared to the control task, as was expected due to the additional mnemonic demands (CT; post-hoc tests: * $p<0.05$, ** $p<0.01$, *** $p<0.001$). Finally, the reaction times for the manual responses are shown in (D). Importantly, reaction times in the DRT were significantly shorter as compared to the CT. This signifies that subjects had used the delay period to pre-prepare the required sequence of finger reaches. Longer reaction times were detected in the NM2ST and the M2ST since both tasks involved additional match-to-sample comparisons.*

there was an overall significant effect of the experimental conditions on performance levels (2-way ANOVA: task $p<0.01$; #cues n.s.; interaction n.s.; Fig. 2.2C), error rates were statistically indistinguishable for the memory- and the movement-planning conditions (post-hoc test, n.s.), with a significant decrease only in the control task as compared to all other conditions (post-hoc test, $p<0.05$). Finally, and most importantly, reaction times significantly varied across experimental conditions (2-way ANOVA: task $p<0.001$; #cues n.s.; interaction n.s.; Fig. 2.2D): as compared to the control condition (CT), reaction times in the DRT were significantly decreased by about 200ms (post-hoc test, $p<0.001$), signifying that subjects had prepared the upcoming movement sequence during the delay phase. In contrast, manual reaction times were significantly higher in the NM2ST and the M2ST (post-hoc test, $p<0.001$). However, this was expected, as movement performance in both conditions critically depended on an additional match-to-sample comparison. In summary, the analysis of the various behavioral measures asserted that (*i*) subjects had prepared the pre-cued movement sequence in the DRT, and (*ii*) apart from such planning, there was no difference either in subjects' behavior during the delay or in their overall performance levels (except for the control task), indicating a comparable degree of task-difficulty in the DRT, the NM2ST, and M2ST.

Correlates of Retrospective Visual Memory and Prospective Motor Planning

Brain activity was analyzed using a region of interest (ROI)-based approach, which was chosen in order to best account for the anatomical variability across subjects. By contrasting a linear combination of delay-period fMRI activity across all memory- and planning-conditions against the corresponding period of the control task, we were able to functionally define ROIs that showed significant sustained activity in each individual subject ($p(FWE)<0.05$). This procedure ensured that the selection of ROIs was not biased by any particular task's main component, for instance working memory in the M2ST or motor planning in the DRT. Across all subjects, the most

significant delay-related activity was mapped bilaterally in PPC, namely the medial aspects of superior parietal lobule (SPL) next to the intra-parietal sulcus (IPS). This activation further spread along the IPS and formed another pronounced cluster of significantly activated voxels in its most anterior portion (antIPS). Furthermore, there was a consistent activation in both left and right dorsal premotor cortex (dPM), as well as the supplementary motor area (SMA). Finally, delayed fMRI-responses were also present in the dorsolateral prefrontal cortex (DLPFC), mainly associated with an activation of the left middle frontal gyrus (MFG). While some subjects also appeared to recruit their right MFG, significant delay activity was not observed in this region in all of our subjects. Fig. 2.3 illustrates these functionally defined ROIs. The activity pattern rendered on a canonical brain surface depicts the statistical map obtained from a second-level group analysis that was calculated across the aforementioned 'delay contrasts'; this group map is in good spatial correspondence with individual subjects' activation patterns (refer to Supplemental Fig. 2.S2).

In order to compare the relative contributions of the various task components to the sustained fMRI responses within these functionally defined ROIs, we took two approaches. In a first approach the fMRI-signal timecourse within each ROI for each individual subject was extracted. For each of these regions and for each experimental condition an average event-related average (ERA) BOLD timecourse was calculated across subjects. The resulting ERAs are depicted in Fig. 2.3, all aligned to the onset of the delay period. Importantly, we did not account for the hemodynamic delay of the fMRI-signal (about 5–6s time to peak). As expected from the statistical maps, all ROIs showed an increased level of fMRI activity in the memory- (M2ST, yellow traces) and the planning-conditions (DRT, green traces; NM2ST, grey traces) as compared to the control condition (CT, blue traces). This increase occurred immediately after the cue presentation and continued throughout the delay period, indicating a putative involvement of these regions in motor planning, retrospective memory, or attention. Importantly, in most of the ROIs the level of sustained activity systematically varied across conditions: delay activities were the strongest in the motor planning condition DRT, response amplitudes were the lowest in the memory condition M2ST, while

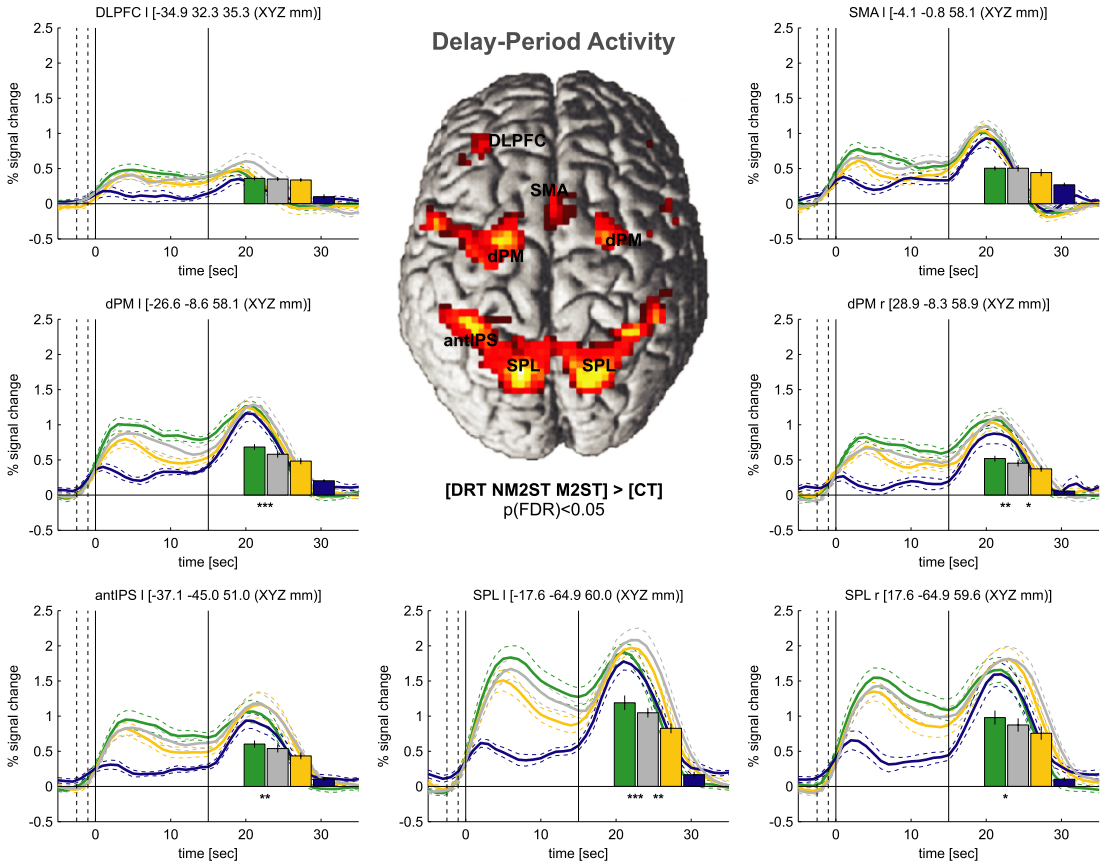
Delay-Period Activity
DLPFC
SMA
dPM
dPM
antIPS
SPL
SPL
[DRT NM2ST M2ST] > [CT]
p(FDR)<0.05
DLPFC l [-34.9 32.3 35.3 (XYZ mm)]
SMA l [-4.1 -0.8 58.1 (XYZ mm)]
dPM l [-26.6 -8.6 58.1 (XYZ mm)]
dPM r [28.9 -8.3 58.9 (XYZ mm)]
antIPS l [-37.1 -45.0 51.0 (XYZ mm)]
SPL l [-17.6 -64.9 60.0 (XYZ mm)]
SPL r [17.6 -64.9 59.6 (XYZ mm)]
% signal change
time [sec]

Figure 2.3:

fMRI activity related to motor planning and visual memory. *Significant sustained fMRI activity related motor preparation, memory, and/or attention was consistently mapped in each subject's posterior parietal cortex (SPL, antIPS), premotor cortex (dPM, SMA), and dorsolateral pre-frontal cortex (DLPFC). This is illustrated by the respective 2nd-level activation-map which is overlaid on a canonical brain surface. For each of the aforementioned regions of interest (ROIs) that were separately mapped in each individual subject (MNI coordinates refer to average XYZ location across subjects, also refer to Supplemental Figs. 2.S2 and 2.S3 for individual maps) as well as for each experimental condition, the respective fMRI-signal timecourses are depicted (average across individual subjects' mean +/- SE): DRT in green, NM2ST in grey, M2ST in yellow, CT in blue. Timecourses are aligned to the onset of the memory delay, while the solid vertical lines indicate the average duration of this delay epoch. Broken vertical lines denote the onset of the cues in the 4/2-target condition at -2.5s/-1.5s, respectively. Subjects' average %-signal change during the delay period (+/- SE) is further illustrated by the bars. Asterisks denote a significantly increased signal-change as compared to the memory-control task (M2ST; * $p<0.05$, ** $p<0.01$, *** $p<0.001$; corrected for multiple comparisons). Note that significant sustained fMRI-activity related to both movement planning and inhibition was mapped in parietal and premotor cortex. The pattern of activity in DLPFC rather seems to reflect its putative role in maintaining visual memory.*

intermediate levels of activity were obtained in the NM2ST. Importantly, this pattern of activity was most pronounced in the left SPL, the left anterior IPS and the left dPM. Similar but less robust patterns emerged for the corresponding cortical areas in the right hemisphere (ipsilateral to the effector) and for the SMA. Interestingly, only the fMRI responses in the DLPFC did not show any variation across conditions, indicating a probable involvement of DLPFC in the maintenance of retrospective visual memory but not in motor planning.

In a second analysis, the beta values were obtained for each of the delay-related regressors in our single subject analyses and for each ROI. Beta values were normalized to represent estimates of the percent signal change of the fMRI signal. As with the ERA timecourses, normalized beta values were then averaged across subjects. Furthermore, since beta values provided a single estimate of the 'strength' of the delay-related fMRI signal, they were used to perform ROI-based group statistics. Normalized beta values for each of the experimental conditions and for each ROI are shown as bars in Fig. 2.3. Note that the beta estimates mirror the relative order of the BOLD signal amplitudes during the delay period. However, the apparent amount of signal change captured by the delay period predictors somewhat underestimated the actual level of fMRI activity during the delay. Presumably, this underestimation stems from the fact that this activity was already partly captured by the regressors for the cue response. More importantly, the normalized beta values further support the previously described patterns of planning-related fMRI activity: Beta values for the DRT were significantly greater compared to those for the memory condition in the SPL, antIPS, and dPM, and higher levels of significance were yielded for brain regions contralateral to the effector (compare asterisks in Fig. 2.3). Furthermore, in these ROIs the normalized beta values for the NM2ST lay intermediate to those obtained for the DRT and for the M2ST. Significant differences emerged between the NM2ST and the M2ST, but only in the left SPL and the right dPM, implying a contribution of these areas to the inhibition of movements to undesired target locations. Similar patterns were revealed for the SMA, approaching statistical significance. In contrast, beta values for the DLPFC were indistinguishable and thus denote fMRI activity

solely related to visual memory or attention.

2.4 Discussion

The patterns of fMRI activity in the posterior parietal and premotor cortex cannot be solely explained by factors related to retrospective memory or visual attention, which were identical across conditions. Instead, they indicate an additional involvement of these regions in the planning of upcoming goal-directed movements while encoding both types of targets relevant for action, those to be acquired (DRT) and those to be avoided (NM2ST). In contrast, fMRI activity within DLPFC was rather consistent with its putative role in maintaining visual memory (Petrides 2000; Constantinides 2001).

Evidence for Prospective Planning in Posterior Parietal Cortex

The role of the PPC in motor planning is a matter of ongoing debate (Colby and Goldberg 1999; Andersen and Buneo 2002; Goodale and Milner 1992; Ungerleider and Mishkin 1982). The idea that this part of the brain may contribute to the generation of overt behavior originally stems from the pioneering electrophysiological experiments by Mountcastle and coworkers, who demonstrated that the PPC encompassed diverse sets of neurons concerned with various aspects of goal-directed arm- and eye-movements. However, Robinson and coworkers later noted that the described PPC activity could be accounted for by task-related sensory or attentional processes rather than the generation of behavior itself. To date, the most convincing electrophysiological evidence in favor of a role of PPC in prospective motor planning stems from studies that could demonstrate effector-specific 'movement intentions': in fact, sustained neuronal firing in certain sub-regions of the PPC distinguishes between the planning of an eye- (area LIP) vsersus a reach- movement (PRR = parietal reach region) to one and the same remembered target location (Snyder et al. 1997). In

the latter experiment the attentional and mnemonic demands were identical, while the only difference in planning related to the way the memorized target had to be acquired. Following this approach, various research groups performed human imaging experiments demonstrating effector-specific planning within regions of both posterior parietal and premotor cortex (Astafiev et al. 2003; Beurze et al 2007; Conolly et al. 2007; Glidden et al. 2008; Medendorp et al. 2005). However there were confounding factors remaining which may vary for different effectors and could thus explain the differential patterns of activity described in these latter studies: task difficulty, the sensory consequences of movement, the spatial transformations necessary for the effector being used, and the sensory information relevant when planning an upcoming behavior (e.g., proprioceptive information about the effector) may largely differ when using eyes, arms, hands, or fingers. Moreover, imaging effector-specific movement preparation cannot resolve cases in which planning occurs simultaneously for multiple effectors (Snyder et al. 1997) or in which planning refers to more abstract aspects of behavior that are effector-independent (global trajectories, sequential order, etc.).

In order to fully access these various levels of movement preparation we chose an alternative experimental approach. We designed a time-resolved fMRI-experiment that allowed us to temporally isolate planning processes from both cue- and movement-related fMRI responses, while carefully controlling for subjects' behavior, task difficulty, visual memory load and attention. Towards this end, we deployed variants of a delayed-response task that involved the same effector—speeded finger reaches. Importantly, the average number of movements required to complete a trial was kept constant across conditions. Thereby we could rule out any unspecific movement preparation that could bias our results. Indeed, unspecific preparatory activity was present in the PPC and in premotor cortex, as these regions displayed delay-related activity in the CT that differed from baseline (Fig. 2.3). In order to additionally control for retrospective visual memory and attention we used a match-to-sample task (M2ST). Most importantly, this task did not allow subjects to predict the later response based on the pre-cued target locations while it was equally demanding with respect to the number of targets that had to be attended to and maintained in visual

working memory (compare Fig. 2.2C). A randomized and asymmetric arrangement of the potential target cues further prevented subjects from merely exploiting verbal memory strategies. The M2ST was presented randomly interleaved with two planning conditions: while in the DRT a specific sequence of finger-movements was instructed by the same initial cues, the NM2ST specified undesired target locations towards which movements should be avoided. In these and all other experimental conditions subjects were instructed to perform out-and-back movements in either a clockwise or counterclockwise fashion. This strategy should minimize any need for spatial updating and serial-order processing during sequential movement preparation. This is of importance since we did not want to bias our results by prompting preparatory processes specifically required for movement sequences. On the other hand, requiring multiple out-and-back finger reaches should guarantee a highly demanding and long-lasting movement preparation in order to justify the rather lengthy delay epochs. That such a preparation actually took place could be demonstrated by significantly reduced reaction times in DRTs as compared to the CTs. Accordingly, all areas that showed significantly increased levels of fMRI activity in the DRT were considered regions engaged in motor planning.

Such preparatory fMRI activity in the DRTs was most pronounced in the PPC (SPL, antIPS) but also present in premotor cortex (dPM, SMA). Moreover, in both SPL and dPM this activity was more strongly represented in corresponding regions of the left hemisphere (i.e., contralateral to the effector). The localization of these movement-planning areas is in good spatial correspondence with previously described parietal and pre-motor foci that are attributed to goal-directed reaching and pointing (Astafiev et al. 2003; Beurze et al 2007; Conolly et al. 2007; DeSouza et al. 2000; Glidden et al. 2008; Medendorp et al. 2005; Rowe et al. 2000; Volle et al. 2005). Moreover, the region within the left SPL which showed the most robust planning-related fMRI activity overlaps with a prevailing locus of lesion in optic ataxia patients (Karnath and Perenin 2005; Trillenberg et al. 2007). These patients have severe difficulties in reaching towards peripheral visual targets, i.e., in performing the same behavior that was required by our task.

Yet, SPL and all other parietal and pre-motor 'planning areas' also exhibited sustained fMRI activity in the M2ST which cannot be directly explained by movement planning. Moreover, except in the SMA, the level of this sustained BOLD response was significantly higher in the 4-targets as compared to the 2-targets condition (compare supplemental Fig. 2.S3). The nature of this residual fMRI-activity remains to be revealed. This residual may be related to covert shifts of attention (e.g., Kastner et al. 1999; Corbetta and Shulman 2002). It also could relate to the maintenance or manipulation of visual information within working memory (Curtis, Rao and D'Esposito 2004; Curtis and D'Esposito 2006; Mars et al. 2008; Rowe, Toni et al. 2000; Simon et al. 2002; Volle et al. 2005). Moreover, it may reflect a preparatory set for action (Cavina-Pratesi et al. 2006) or other forms of motor attention (Rushworth et al. 1997). Finally, the elevated levels of fMRI activity in the M2ST might simply reflect subjects' arousal due to higher task demands as compared to the baseline condition (CT; compare Fig. 2.2C). While we cannot distinguish between these possibilities, we can highlight a significant contribution of both premotor cortex and PPC to the preparation of upcoming behavior.

Default Planning versus Retrospective Visual Memory in PPC

Our experimental approach is not without predecessors. Several groups have previously tried distinguishing movement intentions from mnemonic and attentional processes. However, with respect to PPC function they often arrived at different conclusions. Most studies ascribed to PPC the maintenance of visual memory rather than the planning of upcoming movement, while the latter function was commonly attributed to the pre-motor cortex. This view was predominantly based on pre-cuing experiments, in which the actual movement goal was not explicitly specified before the preparatory delay period. Rather, subjects had to hold various potential cues in memory, while only later a second cue would specify towards which of the pre-cued targets a movement should be performed (Curtis and D'Esposito 2006; Mars et al. 2008; Rowe et al. 2000; Volle et al. 2005). Unfortunately, this approach

harbors the possibility that subjects prepare all movements that are potentially required by default (Snyder et al. 1997). The fact that in SPL (as well as in dPM and SMA) sustained activity was most strongly modulated by the number of targets in the DRT (compare Supplemental Fig. 2.S3) provides support for this notion (also compare Medendorp et al. 2006). In addition, we have preliminary evidence that both PPC and premotor cortex represent alternative movement plans throughout the delay-phase, even in situations in which only one of these plans ultimately needs to be executed (Lindner A., Kagan I., Iyer A. and Andersen, R.A. 2008 Prospective coding of alternative actions in human Parietal and Premotor cortex. 6th FENS Forum of European Neuroscience). Given these findings, it seems highly likely that, in the aforementioned studies, sustained PPC activity related to such 'default plans' rather than solely to the maintenance of retrospective visual memory. Interestingly, in two of these studies (Curtis and Esposito 2006; Volle et al. 2005) the specification of the final movement goal was followed by a second delay phase, during which fMRI activity related to preparation of the instructed movement could be assessed. In line with the idea of default planning, sustained levels of PPC activity decreased in the second as compared to the first delay period (Curtis and D'Esposito 2006; Volle et al. 2005), which, accordingly, would be simply due to the fact that a lower number of movement plans was represented after the required response was specified.

Finally, in an alternative experimental approach, Curtis and coworkers tried to distinguish prospective planning and retrospective visual memory by comparing delay activity in a delayed-saccade task with a non-match-to-sample task (NM2ST) comparable to the one used in this study. As will be pointed out in the following paragraph, the latter condition cannot control for memory-related processes since it does not rule out the possibility that subjects actively inhibited saccades to the pre-cued target location(s) in order to limit the number of response alternatives.

Inhibition as a Constituent Part of Motor Planning

Increased levels of sustained fMRI activity in the NM2ST as compared to the M2ST point towards a putative contribution of posterior parietal and pre-motor cortex to the planning of movement even in cases when a specific behavior could no longer be prepared. Such planning in the absence of immediate movement goals may seem surprising; however non-match-to-sample tasks like the one used in this study allow subjects to potentially inhibit movements to undesired, pre-cued target locations. Within the context of our experiment, preparatory inhibition must be considered a constituent part of motor planning despite the fact that it cannot elicit an overt behavior: movement inhibition actively reduces the number of response alternatives. Since behavioral reaction times increase with the number of available behavioral alternatives (refer to Hicks law), inhibition is necessary for tractable and rapid management of response options. Following this consideration it may not be surprising that regions exhibiting prospective planning fMRI activity also showed significantly increased levels of sustained fMRI activity in the delay period of the NM2ST. Yet, there might be alternative interpretations: First, the increased level of sustained fMRI activity could simply refer to a 'default-planning' of movements to all remaining potential target locations (Snyder et al. 1997; Cisek and Kalaska 2002, 2005). Second, activity could reflect covert shifts of attention to these default locations. However, both these interpretations can be dispelled since the level of fMRI activity in the NM2ST significantly increased with the number of undesired target locations, and thus was anti-correlated with both the default-planning load and the related attentional demands (please refer to supplemental Fig. 2.S3.).

In fact, recent evidence from primate electrophysiology suggests that pre-motor neurons in both FEF and pre-FEF show sustained activity that may specify whether or not a monkey should look at a pre-cued target location (Hasegawa et al. 2004). Our results are consistent with this finding and further indicate that not only the pre-motor but also the parietal cortex contributes to such putative preparatory processes related to movement inhibition. Human imaging studies on the cancellation of pre-

planned motor responses may further support this notion (e.g., Brown et al. 2006; Casey et al. 1997; Cavina-Pratesi et al. 2006; Curtis et al. 2005; Garavan et al. 1999; Watanabe et al. 2002). Note however, that in the aforementioned studies there was an obvious confound of a planned, pre-potent behavior and its subsequent cancellation, while in the present study the inhibition of a goal-directed motor behavior can be demonstrated in isolation (for further discussion see Hasegawa et al. 2004; Snyder and Lawrence 2004).

Taken together, our results clearly demonstrate that the human PPC is critically involved in the preparation of upcoming movements while coding for both types of targets relevant for action—those to be acquired and those to be avoided. Similar to the manner in which PPC highlights the utility of a planned behavior on the basis of expected reward (Platt and Glimcher 1999, Musallam et al. 2004) it may likewise signify the level of action rejection in case of undesired behavioral outcomes.

2.5 Experimental Procedures

Subjects

Eight subjects (5 males, 3 females) participated in the experiment. All of them had normal or corrected-to-normal visual acuity and all except one subject were right-handed. The latter subject performed equally well with both her left and right hand. Participants provided informed consent in accordance with the declaration of Helsinki and the Caltech Institutional Review Board guidelines. Subjects were reimbursed for participating in this experiment and received $10 per hour.

Stimulus presentation

All visual stimuli were back-projected onto a translucent screen ($22^o \times 16^o$ visual angle) by using a video projector (800×600 pixels, 60 Hz). Subjects viewed the visual stimuli via a mirror that was mounted on the head coil of the MRI scanner (viewing distance 1150mm). Stimuli were generated on a windows PC using Cogent Graphics

developed by John Romaya at the LON at the Wellcome Department of Imaging Neuroscience. For a comprehensive description of the different task instructions please refer to both the results section as well as Fig. 2.1. The following description will focus exclusively on common task epochs, their duration, and temporal order, as well as the geometric aspects of the visual stimuli. In short, each trial started with a random fixation period (14000ms, 15000ms or 16000ms) during which a white fixation cross in front of a background square (size $0.8^o \times 0.8^o$) was presented on the otherwise dark screen. This fixation cross always remained visible throughout the whole trial. The initial fixation period was followed by cue presentation (500ms or 1500ms). The length of cue presentation was determined by the number of targets being presented—it was longer for 4 targets than for 2 target trials in order to guarantee comparable performance rates (compare Fig. 2.2C.). All potential target locations were shown as equally spaced grey squares (size $0.8^o \times 0.8^o$, distance 40^o angle) that were arranged on a circle around the fixation spot (5.5^o radius). Across trials this overall circular arrangement was randomly rotated between -10 and 10^o. Both the asymmetric arrangement of the 9 targets as well as their additional rotation prevented subjects from forming verbal memory strategies. Actual targets were defined as empty squares (inner black square $0.3^o \times 0.3\ ^o$). Cue presentation was followed by a 1000ms mask to prevent specific after-images of the cues. This mask consisted of 80 randomly placed white squares that densely covered the relevant central part of the screen (7^o x 7^o). Afterwards, there was a delay period of random duration (14000ms, 15000ms or 16000ms) in which subjects should maintain central fixation on the otherwise dark screen while preparing for the upcoming response. The comparably long durations of the cue and delay period were required to allow a time-resolved analysis of preparatory fMRI activity without being confounded by preceding visual cues. In all conditions, except the M2ST, the delay period was immediately followed by the response period. In the response period subjects had to perform the instructed movements as quickly as possible. Specifically, subjects performed out-and-back finger reaches with their right index finger. Finger movements were recorded online using an MRI-compatible trackball (Current Designs, Philadelphia) which was placed in a comfortable reaching

distance on subjects' belly. Movements were fed-back visually by a circle (1.65^o diameter). This cursor was only visible during the response phase and thus served as a start signal for the response. However, subjects' finger movements were continuously monitored throughout the trial and with a sampling frequency of 60Hz. Importantly subjects were not allowed to lift their finger from the trackball. The sensitivity of this interface was thereby adjusted in a way that subjects could easily perform out-and-back 'finger-saccades', i.e., straight, quasi-ballistic finger movements, without the need for a re-adjustment of the trackball or any related compensatory movements (also compare supplemental Fig. 2.1). The (invisible) starting position of the cursor was always re-centered at the beginning of each trial. Finally, subjects were instructed to perform the instructed sequence of movements as fast as possible in either a clockwise or a counter-clockwise order, while the time for completing the instructed response was highly limited. The time remaining was indicated by the cursor itself, which simply faded until it became invisible at the end of the response period. The length of this period varied across conditions: the more movements required and the more cognitive processes presumably being performed, the longer the duration of the response phase. The respective times were chosen based on average reaction times and movement time measures obtained in a pilot study. In the M2ST the response period was preceded by a MATCH stimulus which had to be compared with the earlier cues which served as the sample. During the response period of this particular task, two different sets of randomly selected targets (a set of black and a set of white targets) served to indicate the outcome of the later match-to-sample comparison: movements towards white targets would indicate a match whereas movements to black targets would signify a mismatch. The response period of this and all other tasks was followed by another 1000ms random-dot mask and a 2000ms inter-trial interval. During the latter epoch subjects were allowed to blink or to look anywhere on the otherwise dark screen. All trials were randomly interleaved. Each subject performed a total of 18 trials per condition; one half of the trials showed only 2 targets while the other half presented 4 targets (i.e., 9 trials/target number/condition).

Performance Monitoring and Behavioral Analysis

Our experimental paradigms required subjects to perform finger reaches while maintaining central fixation. Behavior was registered using an fMRI-compatible trackball (see above) as well as an fMRI-compatible eye-camera (Resonance Technology Inc., USA). Eye movement recordings were realized with the ViewPoint Eye Tracker (Arrington Research Inc., Scottsdale, USA). Eye position was sampled at a frequency of 60Hz. Further processing of the behavior was performed off-line using Matlab 7.1 (The MathWorks, Natick, USA). In short, eye position samples were filtered using a 10Hz low-pass filter. Saccades were detected using an absolute velocity threshold (20^o/sec), while blinks were identified as gaps in the eye position records due to lid closure. As with eye movements, finger movement recordings were expressed in degrees of visual angle in order to allow direct comparison. Representative examples of 2D-finger and eye movement recordings are provided in supplemental Fig. 2.S1A. Finger movements were low-pass filtered at 24Hz. For reaction time estimates, we calculated the absolute finger velocity, while the onset of the response was defined by the time when this velocity exceeded a threshold of 8.1^o/sec (compare supplemental Fig. 2.S1C). Importantly, in no subject was movement detected during the delay phase (compare supplemental Fig. 2.S1B). Finally, performance was expressed by error rates: if the average direction of any individual out-and-back reach within the sequence would not be located within a 40^o arc of the target (20^o to either side), this would result in an error trial. As there were no systematic differences in error rates across the conditions of interest (DRT, NM2ST, and M2ST—compare results section), and even in error trials 50% or 75% of the reaches were made into the correct target bin, we did not treat these trials differently in our fMRI analysis.

Image Acquisition and fMRI Analysis

MRI images were acquired on a 3 Tesla Siemens TRIO scanner using an 8-channel head coil (Siemens, Erlangen, Germany). For each subject we obtained a T1-weighted MP-rage anatomical scan of the whole brain (176 slices, slice thickness=1 mm, gap=0

mm, in-plane voxel size=1×1 mm, TR=1500ms, TE=3.05ms, FOV=256×256, resolution= 256×256) as well as T2*-weighted gradient-echo planar imaging scans (EPIs: slice thickness=3.5 mm, gap=0 mm, in-plane voxel size=3×3 mm, TR=2000ms, TE=30ms, flip angle=90^o, FOV=192×192, resolution=64×64, 32 axial slices) for our fMRI time-series analysis. Overall we obtained 1458 EPIs per subject, which were collected during three consecutive runs of about 16min length, each. The EPI-volume completely covered the cerebral cortex as well as most subcortical structures. Only the more posterior aspects of the cerebellum were truncated in several of our subjects.

Functional image processing was performed using SPM2 (Wellcome Department of Cognitive Neurology, London). Images of each subject were realigned by using the first scan as a reference. T1 anatomical images were co-registered to the mean image of the functional scans and then aligned to the SPM T1-template in MNI space (Montreal Neurological Institute, mean brain). The resulting non-linear 3D transformation was applied to all images for spatial normalization. Finally the functional images were spatially smoothed with a Gaussian filter (7×7×7 mm^3 full-width at half-maximum) and high-pass filtered (cut-off period 128 ms). Functional images were analyzed both on individual-subject and group levels. In the subject-specific analysis (first level) we specified a general linear model (GLM) including regressors for each of our 8 different experimental conditions (4 tasks × 2 target amounts) and for each task epoch (cue presentation and mask, delay period, response-period). All regressors were convolved with the default canonical haemodynamic response function. The inter-trial interval and the initial fixation period were not explicitly modeled and served as the baseline epoch. On the group-level (second level), contrast images illustrating delay period activity (compare Fig. 2.3) and target-load effects (compare Supplemental Fig. 2.S3) were analyzed using a t-test. For all these GLM analyses, a statistical threshold of $p<0.05$ adjusted for multiple comparisons was imposed as the criterion for significance. In addition, we performed an ROI analysis. Towards this end, normalized beta weights of the delay-period regressors were extracted for a 3mm-radius sphere around the maxima of local clusters in individuals (i.e., based on the first level statistics) that (*i*) overlapped in different subjects, and (*ii*) showed

the most significant delay-related fMRI activity across subjects. All ROIs that were functionally defined by these criteria are depicted in both Fig. 2.3 and Supplemental Fig. 2.S3. Furthermore, the timecourses of the raw fMRI-signals in each of these individually mapped ROIs were extracted using the SPM2 Volumes Toolbox by Volkmar Glauche (Brain Imaging Lab, Freiburg, Germany). As with the GLM analyses, image timecourses were high-pass filtered (cut-off period 128 ms) and normalized by an estimate of baseline activity. This estimate was based on the mean image intensity 5–2sec before delay-period onset, averaged across all experimental conditions, i.e., the overall level of fMRI activity at the end of the fixation period. In order to come up with individual event-related averages (ERAs) of trial-related BOLD activity, timecourses were aligned to the onset of the delay period as specified by the GLMs. Due to an additional temporal jitter in our design we were able to express the resulting timecourses at a 1sec temporal resolution. The respective ERAs in Fig. 2.3 and Supplemental Fig. 2.S3 thereby represent an average calculated across the mean ERAs of each individual subject.

2.S1 Supplemental Data

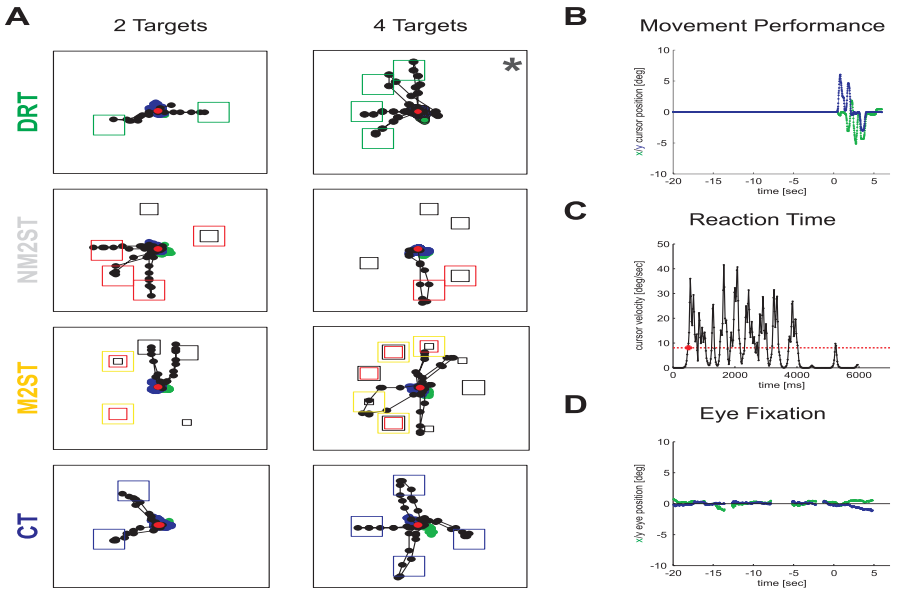

Figure 2.S1:

Representative examples of subjects' performance. *Eight examples of the different experimental conditions (4 tasks x 2 sets of target numbers, i.e. 2 or 4) are shown in (A). The position of the finger-guided cursor (in black) as well as gaze direction are overlaid (blue samples acquired during the delay phase, green samples were recorded during the response period). Note that in all conditions, this subject perfectly maintained central fixation throughout the trial. Green squares in the DRT indicate pre-cued movement goals. Black small squares in the NM2ST indicate undesired target locations. Red squares show a second set of targets that were presented during the response period. In the response period subjects should perform movements to those targets of the second set that did not correspond to the previous cues (i.e. only towards the empty red squares). In the match-to-sample task (M2ST), small red squares represent the initial cues (sample) while the yellow squares represent the match stimulus. In case of a match, subjects had to go to the white targets of the response screen (large black squares). In case of a mismatch, they were required to reach at the black targets (small black squares). Note that the location of the response targets and the location of the match-to-sample targets were completely uncorrelated. In the CT subjects had to reach towards the targets presented in the response period. These targets are indicated as blue squares. (B) depicts horizontal (green) and vertical (blue) cursor position for the example in (A), which is marked with an asterisk (DRT, 4 targets). This subject correctly performed a counter-clockwise sequence of finger reaches to all the four specified targets. (C) shows the absolute velocity trace of the same movement aligned to the onset of the response period. The red broken line indicates the velocity threshold used to determine response onset (red dot). The horizontal (green) and vertical (blue) eye position traces are shown in (D). Gaps in the eye records result from the rather frequent eye blinks of this particular subject.*

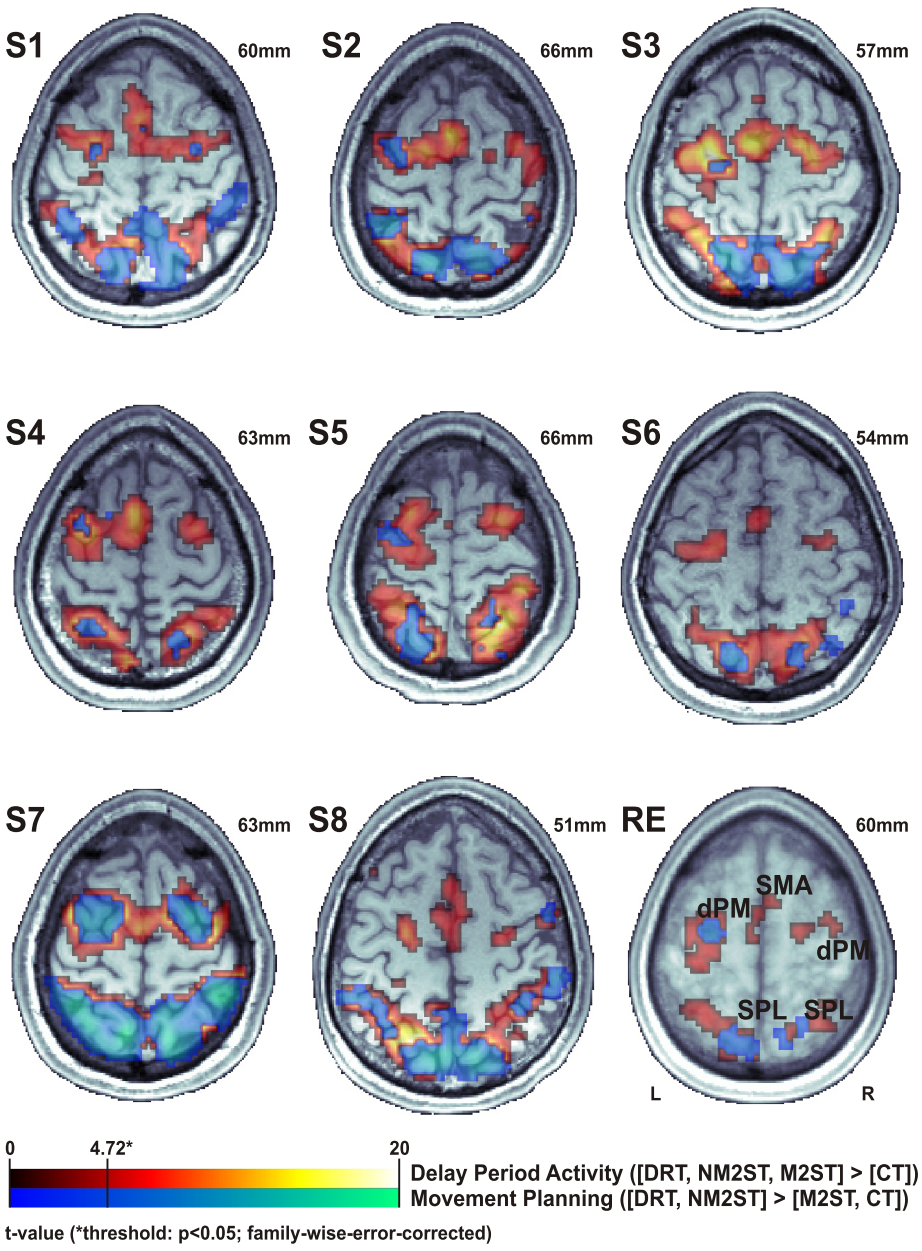
S1
60mm
S2
66mm
S3
57mm
S4
63mm
S5
66mm
S6
54mm
S7
63mm
S8
51mm
RE
60mm
SMA
dPM
dPM
SPL
SPL
L
R
0
4.72*
20
Delay Period Activity ([DRT, NM2ST, M2ST] > [CT])
Movement Planning ([DRT, NM2ST] > [M2ST, CT])
t-value (*threshold: p<0.05; family-wise-error-corrected)

Figure 2.S2:

Individual ROIs in parietal and pre-motor cortex. *Horizontal slices show subjects' activation maps (S1-8) that were used to specify functionally defined ROIs in each individual (reddish regions, delay-activity contrast, p(FWE)<0.05). The corresponding statistical map of the random effects analysis across subjects is shown as RE. In addition the bluish regions indicate areas stronger activated in the motor preparation conditions (DRT and NM2ST) as compared to the conditions in which such specific preparation was not possible (M2ST and CT). There is an obvious overlap with the reddish regions mapped using the delay-activity criterion. Note that the z-levels (mm) of the horizontal sections were selected based on the average level of the bilateral SPL activation peaks. Despite being centered on these PPC-ROIs the horizontal sections also show large parts of the task-related pre-motor areas (dPM and SMA).*

Target load-related fMRI-activity. *Significant fMRI-activity related to target-load was most pronounced in subject's posterior parietal cortex (SPL, antIPS) but also premotor cortex (dPM, SMA) and dorsolateral pre-frontal cortex (DLPFC) showed significant effects. This is resembled by the respective 2nd-level activation-map which is overlaid on a canonical brain surface. For all ROIs within these aforementioned regions as well as for each experimental condition the respective fMRI-signal time courses are depicted: DRT in green, NM2ST in grey, M2ST in yellow, CT in blue, solid lines indicate 4-target conditions, broken lines indicate 2-target conditions. Note that the ROIs correspond to the ones presented in figure 3 of the main article. Time-courses are aligned to the onset of the memory delay, while the solid vertical lines indicate the average duration of this delay-epoch. Broken vertical lines denote the onset of the cues in the 4/2-target condition at -2.5s/-1.5s, respectively. The difference in %-signal change between the 2-target and the 4-target conditions during the delay period (+/- SE) is additionally shown by the bars. Asterisks denote a significant differences (* $p<0.05$, ** $p<0.01$, *** $p<0.001$; corrected for multiple comparisons). Note that the most pronounced differences in target load were obtained in the SPL, notably for the motor planning conditions. The latter trend was similarly exhibited by pre-motor cortex, especially by the SMA. Yet, due to the rather limited number of trials per subject and per condition (9 trials), this distinction between planning- and memory-load awaits further investigation.*

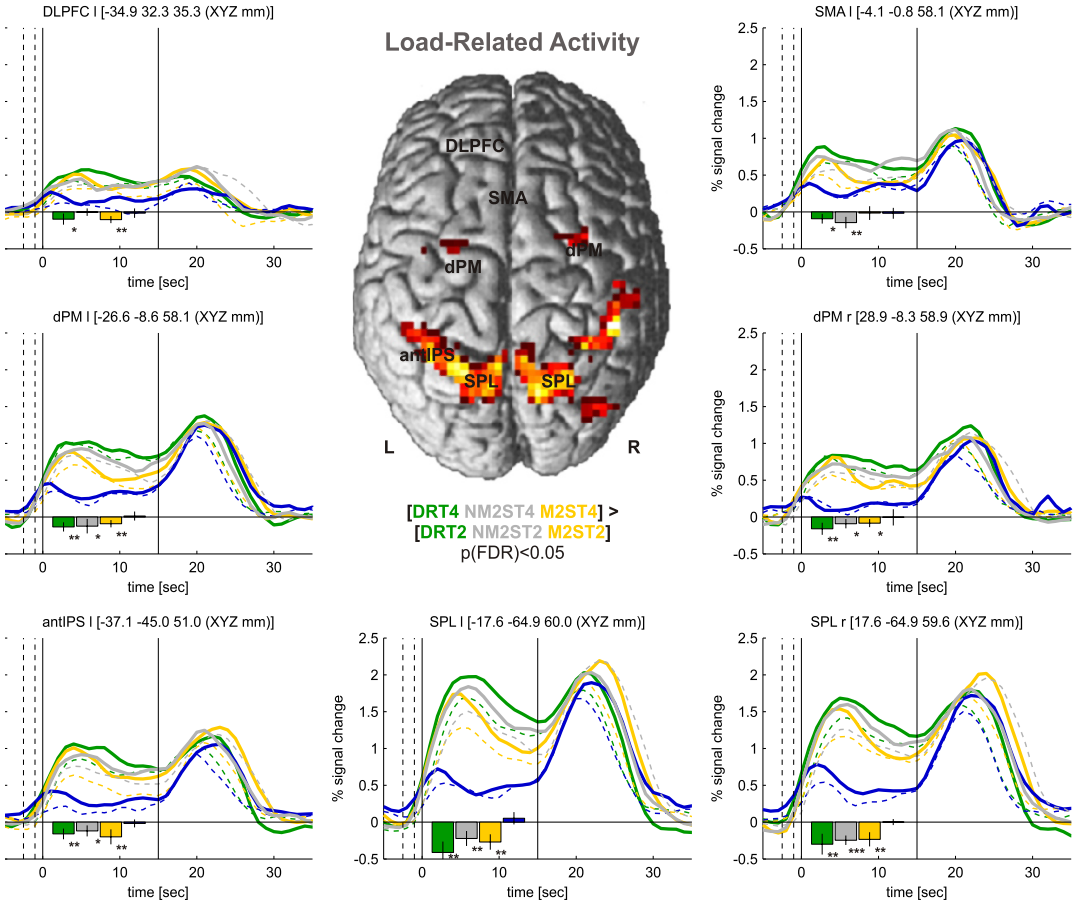
DLPFC l [-34.9 32.3 35.3 (XYZ mm)]
Load-Related Activity
SMA l [-4.1 -0.8 58.1 (XYZ mm)]
DLPFC
SMA
dPM
dPM
antIPS
SPL
SPL
L
R
dPM l [-26.6 -8.6 58.1 (XYZ mm)]
dPM r [28.9 -8.3 58.9 (XYZ mm)]
[DRT4 NM2ST4 M2ST4] >
[DRT2 NM2ST2 M2ST2]
p(FDR)<0.05
antIPS l [-37.1 -45.0 51.0 (XYZ mm)]
SPL l [-17.6 -64.9 60.0 (XYZ mm)]
SPL r [17.6 -64.9 59.6 (XYZ mm)]
% signal change
time [sec]

Figure 2.S3:

References

R. A. Andersen and C. A. Buneo. Intentional maps in posterior parietal cortex. *Annu Rev Neurosci*, 25:189–220, 2002.

S. V. Astafiev, G. L. Shulman, C. M. Stanley, A. Z. Snyder, D. C. Van Essen, and M. Corbetta. Functional organization of human intraparietal and frontal cortex for attending, looking, and pointing. *J Neurosci*, 23(11):4689–99, 2003.

S. M. Beurze, F. P. de Lange, I. Toni, and W. P. Medendorp. Integration of target and effector information in the human brain during reach planning. *J Neurophysiol*, 97(1):188–99, 2007.

M. R. Brown, J. F. DeSouza, H. C. Goltz, K. Ford, R. S. Menon, M. A. Goodale, and S. Everling. Comparison of memory- and visually guided saccades using event-related fmri. *J Neurophysiol*, 91(2):873–89, 2004.

M. R. Brown, H. C. Goltz, T. Vilis, K. A. Ford, and S. Everling. Inhibition and generation of saccades: rapid event-related fmri of prosaccades, antisaccades, and nogo trials. *Neuroimage*, 33(2):644–59, 2006.

B. J. Casey, F. X. Castellanos, J. N. Giedd, W. L. Marsh, S. D. Hamburger, A. B. Schubert, Y. C. Vauss, A. C. Vaituzis, D. P. Dickstein, S. E. Sarfatti, and J. L. Rapoport. Implication of right frontostriatal circuitry in response inhibition and attention-deficit/hyperactivity disorder. *J Am Acad Child Adolesc Psychiatry*, 36 (3):374–83, 1997.

C. Cavina-Pratesi, K. F. Valyear, J. C. Culham, S. Kohler, S. S. Obhi, C. A. Marzi, and M. A. Goodale. Dissociating arbitrary stimulus-response mapping from move-

ment planning during preparatory period: evidence from event-related functional magnetic resonance imaging. *J Neurosci*, 26(10):2704–13, 2006.

A. S. Champod and M. Petrides. Dissociable roles of the posterior parietal and the prefrontal cortex in manipulation and monitoring processes. *Proc Natl Acad Sci U S A*, 104(37):14837–42, 2007.

P. Cisek and J. F. Kalaska. Simultaneous encoding of multiple potential reach directions in dorsal premotor cortex. *J Neurophysiol*, 87(2):1149–54, 2002.

P. Cisek and J. F. Kalaska. Neural correlates of reaching decisions in dorsal premotor cortex: specification of multiple direction choices and final selection of action. *Neuron*, 45(5):801–14, 2005.

C. L. Colby and M. E. Goldberg. Space and attention in parietal cortex. *Annu Rev Neurosci*, 22:319–49, 1999.

J. D. Connolly, M. A. Goodale, R. S. Menon, and D. P. Munoz. Human fmri evidence for the neural correlates of preparatory set. *Nat Neurosci*, 5(12):1345–52, 2002.

J. D. Connolly, M. A. Goodale, J. S. Cant, and D. P. Munoz. Effector-specific fields for motor preparation in the human frontal cortex. *Neuroimage*, 34(3):1209–19, 2007.

C. Constantinidis, M. N. Franowicz, and P. S. Goldman-Rakic. The sensory nature of mnemonic representation in the primate prefrontal cortex. *Nat Neurosci*, 4(3): 311–6, 2001.

M. Corbetta and G. L. Shulman. Control of goal-directed and stimulus-driven attention in the brain. *Nat Rev Neurosci*, 3(3):201–15, 2002.

C. E. Curtis and M. D'Esposito. Selection and maintenance of saccade goals in the human frontal eye fields. *J Neurophysiol*, 95(6):3923–7, 2006.

C. E. Curtis, V. Y. Rao, and M. D'Esposito. Maintenance of spatial and motor codes during oculomotor delayed response tasks. *J Neurosci*, 24(16):3944–52, 2004.

C. E. Curtis, M. W. Cole, V. Y. Rao, and M. D'Esposito. Canceling planned action: an fmri study of countermanding saccades. *Cereb Cortex*, 15(9):1281–9, 2005.

J. F. DeSouza, S. P. Dukelow, J. S. Gati, R. S. Menon, R. A. Andersen, and T. Vilis. Eye position signal modulates a human parietal pointing region during memory-guided movements. *J Neurosci*, 20(15):5835–40, 2000.

S. Funahashi, C. J. Bruce, and P. S. Goldman-Rakic. Mnemonic coding of visual space in the monkey's dorsolateral prefrontal cortex. *J Neurophysiol*, 61(2):331–49, 1989.

H. Garavan, T. J. Ross, and E. A. Stein. Right hemispheric dominance of inhibitory control: an event-related functional mri study. *Proc Natl Acad Sci U S A*, 96(14): 8301–6, 1999.

M. A. Goodale and A. D. Milner. Separate visual pathways for perception and action. *Trends Neurosci*, 15(1):20–5, 1992.

R. P. Hasegawa, B. W. Peterson, and M. E. Goldberg. Prefrontal neurons coding suppression of specific saccades. *Neuron*, 43(3):415–25, 2004.

W. E. Hick. On the rate of gain of information. *Quarterly Journal of Experimental Psychology*, 4:11–26, 1952.

O. Hikosaka and R. H. Wurtz. Visual and oculomotor functions of monkey substantia nigra pars reticulata. iii. memory-contingent visual and saccade responses. *J Neurophysiol*, 49(5):1268–84, 1983.

H. O. Karnath and M. T. Perenin. Cortical control of visually guided reaching: evidence from patients with optic ataxia. *Cereb Cortex*, 15(10):1561–9, 2005.

S. Kastner, M. A. Pinsk, P. De Weerd, R. Desimone, and L. G. Ungerleider. Increased activity in human visual cortex during directed attention in the absence of visual stimulation. *Neuron*, 22(4):751–61, 1999.

R. B. Mars, M. G. Coles, W. Hulstijn, and I. Toni. Delay-related cerebral activity and motor preparation. *Cortex*, 44(5):507–20, 2008.

W. P. Medendorp, H. C. Goltz, J. D. Crawford, and T. Vilis. Integration of target and effector information in human posterior parietal cortex for the planning of action. *J Neurophysiol*, 93(2):954–62, 2005.

W. P. Medendorp, H. C. Goltz, and T. Vilis. Directional selectivity of bold activity in human posterior parietal cortex for memory-guided double-step saccades. *J Neurophysiol*, 95(3):1645–55, 2006.

M. Mishkin and L. G. Ungerleider. Contribution of striate inputs to the visuospatial functions of parieto-preoccipital cortex in monkeys. *Behav Brain Res*, 6(1):57–77, 1982.

P. Morasso. Spatial control of arm movements. *Exp Brain Res*, 42(2):223–7, 1981.

V. B. Mountcastle, J. C. Lynch, A. Georgopoulos, H. Sakata, and C. Acuna. Posterior parietal association cortex of the monkey: command functions for operations within extrapersonal space. *J Neurophysiol*, 38(4):871–908, 1975.

S. Musallam, B. D. Corneil, B. Greger, H. Scherberger, and R. A. Andersen. Cognitive control signals for neural prosthetics. *Science*, 305(5681):258–62, 2004.

M. T. Perenin and A. Vighetto. Optic ataxia: a specific disruption in visuomotor mechanisms. i. different aspects of the deficit in reaching for objects. *Brain*, 111 (Pt 3):643–74, 1988.

M. Petrides. The role of the mid-dorsolateral prefrontal cortex in working memory. *Exp Brain Res*, 133(1):44–54, 2000.

M. L. Platt and P. W. Glimcher. Neural correlates of decision variables in parietal cortex. *Nature*, 400(6741):233–8, 1999.

D. L. Robinson, M. E. Goldberg, and G. B. Stanton. Parietal association cortex in the primate: sensory mechanisms and behavioral modulations. *J Neurophysiol*, 41 (4):910–32, 1978.

D. A. Rosenbaum. Human movement initiation: specification of arm, direction, and extent. *J Exp Psychol Gen*, 109(4):444–74, 1980.

J. B. Rowe, I. Toni, O. Josephs, R. S. Frackowiak, and R. E. Passingham. The prefrontal cortex: response selection or maintenance within working memory? *Science*, 288(5471):1656–60, 2000.

M. F. Rushworth, P. D. Nixon, S. Renowden, D. T. Wade, and R. E. Passingham. The left parietal cortex and motor attention. *Neuropsychologia*, 35(9):1261–73, 1997.

M. F. Rushworth, H. Johansen-Berg, S. M. Gobel, and J. T. Devlin. The left parietal and premotor cortices: motor attention and selection. *Neuroimage*, 20 Suppl 1: S89–100, 2003.

D. Schluppeck, C. E. Curtis, P. W. Glimcher, and D. J. Heeger. Sustained activity in topographic areas of human posterior parietal cortex during memory-guided saccades. *J Neurosci*, 26(19):5098–108, 2006.

S. R. Simon, M. Meunier, L. Piettre, A. M. Berardi, C. M. Segebarth, and D. Boussaoud. Spatial attention and memory versus motor preparation: premotor cortex involvement as revealed by fmri. *J Neurophysiol*, 88(4):2047–57, 2002.

L. H. Snyder and B. M. Lawrence. Don't go there. *Neuron*, 43(3):297–9, 2004.

L. H. Snyder, A. P. Batista, and R. A. Andersen. Coding of intention in the posterior parietal cortex. *Nature*, 386(6621):167–70, 1997.

D. Thoenissen, K. Zilles, and I. Toni. Differential involvement of parietal and precentral regions in movement preparation and motor intention. *J Neurosci*, 22(20): 9024–34, 2002.

P. Trillenberg, A. Sprenger, D. Petersen, D. Kompf, W. Heide, and C. Helmchen. Functional dissociation of saccade and hand reaching control with bilateral lesions of the medial wall of the intraparietal sulcus: implications for optic ataxia. *Neuroimage*, 36 Suppl 2:T69–76, 2007.

E. Volle, J. B. Pochon, S. Lehericy, B. Pillon, B. Dubois, and R. Levy. Specific cerebral networks for maintenance and response organization within working memory as evidenced by the 'double delay/double response' paradigm. *Cereb Cortex*, 15(7): 1064–74, 2005.

J. Watanabe, M. Sugiura, K. Sato, Y. Sato, Y. Maeda, Y. Matsue, H. Fukuda, and R. Kawashima. The human prefrontal and parietal association cortices are involved in no-go performances: an event-related fmri study. *Neuroimage*, 17(3):1207–16, 2002.

D. M. Wolpert, Z. Ghahramani, and M. I. Jordan. Are arm trajectories planned in kinematic or dynamic coordinates? an adaptation study. *Exp Brain Res*, 103(3): 460–70, 1995.

Chapter 3

Dissociation of Objective Value and Subjective Absolute Value in Striatal and Cortical Representations of Expected Action Outcomes

3.1 Summary

For optimal response selection, the consequences associated with an action's potential success or failure must be appraised. To determine how these expected consequences influence the neural representation of action plans, human subjects were scanned while performing a complex motor planning task, with monetary gains and losses imposed for correct or incorrect trial completion. At the beginning of each trial, cues specified required movements and indicated the gains and losses for that trial. Reward structures reflected the expected value of the action, based on subjects' actual performance. In contrast, frontoparietal motor planning regions were more active in high-absolute value (high expected gains or losses) conditions. Furthermore, this activity depended on subjects' beliefs about their performance, being highest for high-gain contexts in subjects who believed they performed well; and highest for high-loss conditions in those who believed they performed poorly. These findings suggest that neural representations of action plans incorporate the subjective absolute value tied to action outcomes.

3.2 Introduction

The selection of one amongst a repertoire of potential behavioral responses entails the articulation of both an appropriate goal and the appropriate means to achieve that goal. In a natural context, however, a plan of action rarely guarantees a specific outcome. Most actions carry with them a certain probability of success or failure, and these successes and failures engender certain consequences. Thus to discern an optimal course of action, the expected consequences of actions—their possible outcomes and contingencies—must be assessed.

Functional imaging studies in humans have extensively investigated areas differentially responsive to various aspects of choice (Daw et al. 2006; Ernst et al. 2004; Kable and Glimcher 2007; Hampton et al. 2007), anticipation (Knutson et al 2000, 2001; Cooper and Knutson 2008; Jensen et al. 2003), and receipt of monetary gains and losses (Delgado et al. 2000; O'Doherty et al. 2001; O'Doherty et al. 2003; Delgado et al. 2003; Delgado et al. 2004; Rolls et al. 2008). Predominantly, these inquiries have emphasized subcortical and prefrontal cortical regions, speculating on their role in an array of tasks, from facilitating appropriate approach or avoidance behavior to monitoring outcomes in order to adjust future strategies. From this wealth of findings, considerable knowledge has been gleaned as to how rewards associated with stimuli are processed and exploited to guide behavior. However, these studies shed less light on whether and how rewards consequent of response execution mold action-planning activity, in the areas engaged in transforming sensory inputs into preparatory signals preceding motor events. A number of previous experiments have passively presented cues and outcomes, demanding no instrumental response on the part of the subjects to obtain rewards (Berns et al. 2001; McClure et al. 2003; D'Ardenne et al. 2008; Jensen et al. 2007; O'Doherty et al. 2003). Even in paradigms mandating movements—either as tools to maintain vigilance, signal choice, (O'Doherty et al. 2006; Knutson et al. 2000, 2001; Bray et al. 2007; Breiter et al. 2001; Kable et al. 2007), or to specifically investigate instrumental action-reward contingencies, the required responses were unnaturally and trivially easy; thus not prompting any sub-

stantial motor preparation (Ramnani and Miall 2003; Tricomi et al. 2004; Zink et al. 2004; O'Doherty et al. 2004; Bjork and Hommer 2007).

In recent years, macaque electrophysiological experiments have begun dissecting the influence of reward contingencies on the process of action selection and planning. These investigations have identified reward-related factors that bias neural activity in motor planning frontal and posterior parietal areas, which may in turn dispose the animal's selection of which movement to execute. Firing rates in lateral intraparietal area (LIP), the region in the macaque posterior parietal cortex thought to be involved in processing/encoding oculomotor action plans, have been shown to signify the weight of sensory input indicating which saccade target is rewarded (Shadlen and Newsome 2001), the log likelihood that a given eye movement will result in a reward (Gold and Shadlen 2001), the magnitude and probability of reward associated with a saccade target (Platt and Glimcher 1999), and the relative desirability of a saccade with respect to other possible saccade options (Dorris and Glimcher 2004). Information about the preference and magnitude of rewards for reach targets has been decoded from a complementary parietal region involved in reaching (Musallam et al. 2004); and recordings from premotor cortex imply that the motivation to choose and acquire a saccade target may shape neural responses as well (Roesch and Olson 2004).

While these investigations proffer insight into reward-modulated action planning activity, the movements employed in these paradigms were still rather undemanding and simple, as in most human studies examining reward. Conversely, many real-life goal-directed actions necessitate greater cognitive exertion, demanding effort at mnemonic, preparatory, and/or execution stages. This complexity generates uncertainty and variability in outcomes. And while the prediction and evaluation of these potential outcomes clearly pertain to adept behavioral response, little is known about how related parameters influence the neural activity subserving action planning.

In addition, the corpus of these studies largely assigns absence of reward rather than explicit punishment as the cost of failure, impeding distinctions between factors associated with a given action (but see Roesch and Olson 2004). Without explicit penalties, variables such as value, incentive (i.e., aversion to punishment or the ex-

pectation of reward), and internal motivation would likely change in step. Finally, as simple movements render the likelihood of success high and the ability to gauge performance straightforward, the effects of subjects' appraisal of probability of outcomes as opposed to the actual probability of outcomes cannot easily be disentangled. Thus, it is difficult to infer from previous work how these parameters impinge upon the neural representations of complex behaviors required in everyday life.

The goals of this study were to ascertain whether and, if so, how expected consequences of complex actions, dependent on human subjects' performance, modulate activity of neural substrates engaged in action specification and preparation. Using fMRI, we investigated the effect of expected monetary reward or punishment in cerebral areas recruited in a challenging delayed-response motor planning task. Subjects were allowed a limited time in which to complete their motor responses, prompting them to prepare movements in advance. To impose consequences for success and failure, trials were associated with variable gain-loss contexts, stipulating at the beginning of the trial the amount the subject would gain if she/he performed the task correctly and lose otherwise. Every trial instructed one correct response, so subjects unequivocally understood the appropriate action to garner success and maximize reward. Therefore, unlike most prior studies, sizable uncertainty in anticipation of reward or punishment stemmed entirely from subject's ability to successfully prepare and implement the response.

This study reports that the profile of activity throughout several task-relevant regions manifested modulation due to the gain-loss contexts. However, these structures evinced divergent roles: Subregions of the striatum encoded the objective value of this reward context as dependent on both the gain-loss cue and subjects' actual performance. In contrast, signal timecourses of frontoparietal cortical regions reflected the absolute value associated with an action in the delay period preceding the response. Moreover, these areas revealed a cognitive, framing effect, responding to action salience as dictated by subjective estimates of success rather than subjects' objective performance.

3.3 Results

Delayed-response tasks are widely employed in electrophysiological and fMRI studies to elucidate the neural substrates of working memory and motor preparation. By imposing a delay between instructive visual cues and the contingent motor response, this task structure permits delineation between neuronal contributions due to sensory, motor, and intervening preparatory processes. Here, we investigated the influence of expected monetary consequences on action plans by utilizing a delayed-response task and imposing upon each trial potential gains and losses.

In this experimental task, subjects moved a trackball with their right index finger to guide a cursor sequentially to five remembered out of nine possible target locations, in the exact order in which they were previously cued. Brief cue presentation, high memory/planning load and constrained response time made successful trial completion difficult. Subjects thus trained extensively on the task before scanning. This training helped to minimize learning effects and to stabilize performance during the experimental session, promoting stable expectations of action outcomes throughout the task.

The principal events of interest in the task included: first, the presentation of the gain-loss context cue, followed by the spatial cues; second, the delay period interposed between visual cue presentation and the motor response; third, the execution of the motor response; fourth, feedback indicating the gains or losses acquired (Fig. 3.1A).

The gain-loss contexts comprised different combinations of high or low gains and losses: \$0/-\$0, \$1/-\$1, \$1/-\$5, \$5/-\$1, and \$5/-\$5. These combinations enabled predictions as to the modulation of motor planning signals due to various parameters of the expected outcome: (i) The possible gains and losses may be reflected in the prospective monetary return, or **'value'**, of an action. Value is calculated as the sum of two products 1) likelihood of success (performance) times gains and 2) likelihood of failure(1-performance) times losses:

$$value = (performance \times gains) + ((1 - performance) \times losses)$$

This parameter predicts the highest and lowest signal amplitudes for positively and negatively valued conditions, respectively, i.e., a larger signal in high gain/low loss trials ($5/-$1) than in low gain/high loss trials ($1/-$5) across all performance levels. (Fig. 3.1B) (ii) The possible gains and losses may be encoded in a manner that reflects the behavioral import of an action, either through its ability to acquire a reward or avoid a loss. Indeed, avoiding a loss may in itself be rewarding (Kim et al. 2006) By this rationale, each outcome (gains and losses) may separately contribute or add in the appraisal of the action, here captured by the 'stakes' associated with the action. The stakes can be expressed as the sum of the absolute value of each weighted outcome:

$$stakes = ((performance) \times |gains|) + ((1 - performance) \times |losses|)$$

Following the stakes parameter, the greatest modulation would be observed in the high gain/high loss contexts ($5/-$5); the smallest in the low gain/low loss contexts ($1/-$1; $0/-$0) at any level of performance (Fig. 3.1C) (iii) Thirdly, an action's import in terms of acquiring reward and avoiding loss may not be a function of the reward and loss independently, but instead reflect the expected gains or expected losses. Alternatively stated, the magnitude of deviation from a neutral baseline of positively- and negatively-valued actions may be more germane to action representations, reflecting the possibility to procure the expected outcome if it is positive or preclude it if it is negative (aversive) . This magnitude is the absolute value of the action's value:

$$absolutevalue = |(performance \times gains) + ((1 - performance) \times losses)|$$

This definition yields disparate predictions of context-dependent modulation for subjects who perform well (Fig. 3.1D) versus those who do not (Fig. 3.1E): the conditions with the highest expected gains (at performance levels ¿ 50%) or with the highest expected losses (at performance levels $< 50\%$) should result in the largest

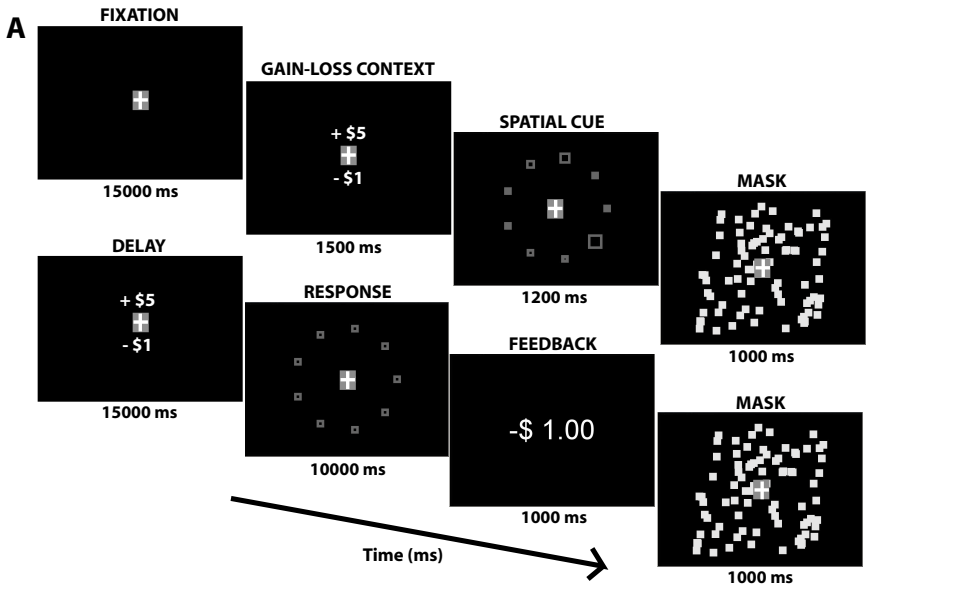
A
FIXATION
15000 ms
GAIN-LOSS CONTEXT
+ $5
- $1
1500 ms
SPATIAL CUE
1200 ms
MASK
1000 ms
DELAY
+ $5
- $1
15000 ms
RESPONSE
10000 ms
FEEDBACK
-$ 1.00
1000 ms
MASK
1000 ms
Time (ms)

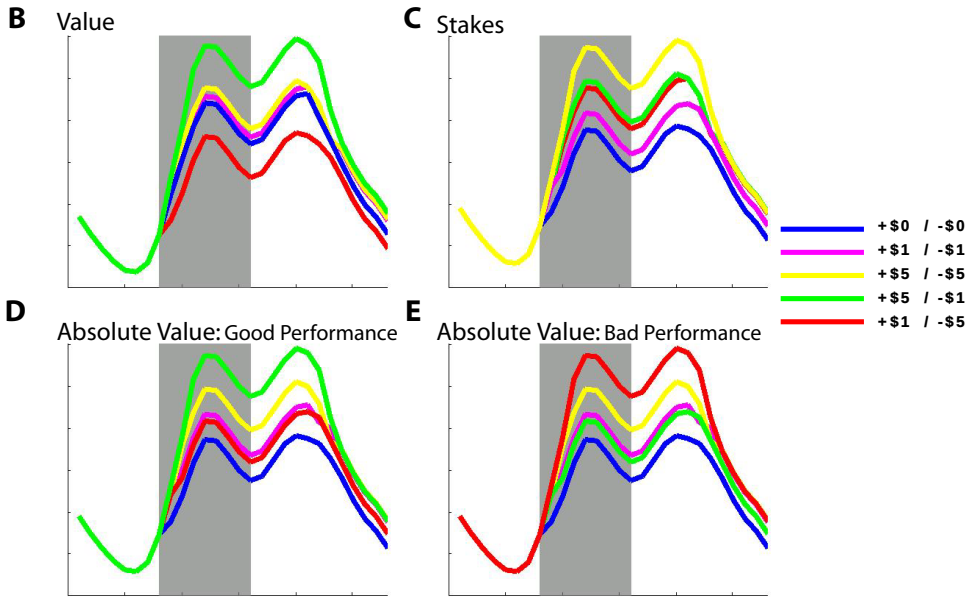
B
Value
C
Stakes
+$0 / -$0
+$1 / -$1
+$5 / -$5
+$5 / -$1
+$1 / -$5
D
Absolute Value: Good Performance
E
Absolute Value: Bad Performance

Figure 3.1:

Trial structure and hypothetical responses*(A) Trial timing and structure. The gain-loss contingencies for the trial were then displayed, follwed by spatial cues briefly specifying the required movement for the trial. After a delay, subjects performed the motor response, and received immediate feedback (gain or loss) based on their performance (successful or unsuccessful). (B) Hypothetical BOLD signals in motor-planning ROIs encoding value. Delay period (marked in gray) signal amplitudes are highest for +$5/-$1, lowest for +$1/-$5. The values associated with each gain-loss context, and hence the ordering of gain-loss contexts, depends on probability of success (here, performance). For the purpose of illustration, the ordering depicted here is averaged across all performance levels. (C) Hypothetical BOLD signals in ROIs encoding stakes. The +$5/-$5 produces the highest signal; the +$1/-$1 and +$0/-$0 produce the lowest at all performance levels. (D–E) Hypothetical BOLD signals in ROIs encoding absolute value. Again, the ordering varies dependant on performance level. For simplicity, the left plot (D) shows the predicted ordering at good performance levels, averaged over 50–100%. Under a high probability of success, conditions yielding higher gains generate the larger signal (+$5/-$1, +$5/-$5). On the right panel (E), ordering for bad performance is averaged over 0–49%, predicting the greatest signal in condition yielding high losses (+$1/-$5, +$5/-$5).*

magnitude deviation from baseline. Therefore, in the context of the current experiment, it is defined here as the outcome-weighted **'action absolute value'** (hereafter referred to as absolute value).

Behavioral Results

The 17 subjects who participated in this study achieved drastically different levels of performance, ranging from 10% to 70% correct responses (see Fig. 3.2A). However, performance levels across gain-loss contexts were indistinguishable (2-way ANOVA—subject: $p<10e\text{-}16$; context: $p=0.78$). To assess if performance changed throughout the scanning session, trials were evenly divided into 6 successive blocks. No significant differences in success rates across blocks of trials emerged (2-way ANOVA—subject: $p<10e\text{-}16$; block: $p=0.90$), indicating that no learning occurred during the course of the fMRI experiment.

Across gain-loss contexts, reaction time latencies were indistinguishable (2-way ANOVA—subject: $p<0.001$; context: $p>0.05$[n.s].; Friedmans ANOVA p=n.s). Total movement time to complete responses showed a slight trend, being shortest for the \$5/-\$1 condition. This trend did not reach significance (2-way ANOVA—subject: $p<0.001$; context: n.s.; Friedmans ANOVA p=n.s). From these observations, individual subjects' behavioral measures admit no significant disparities, yielding a relatively fixed probability of success for each subject during the experimental session.

Subjective Reports

Upon completion of the scanning session, but prior to receiving any feedback about overall performance and net winnings, all subjects completed a questionnaire. First, 16 of 17 subjects claimed to pay attention to the presented gain-loss contexts; all subjects reported investing maximal effort on all trials, independent of the gain-loss context, as instructed (see Experimental Procedures). Based on feedback received at the end of each trial as to the outcome of that trial, subjects also estimated their total winnings: whether they had net won money, net lost money, or broken even.

Given the task structure, net winning required greater than 50% performance on trials resulting in increments/decrements of total earnings; net losing required less than 50% performance on these trials. Fig. 3.2A portrays the relationship between perceived task winnings and subject's average performance across all trials. The 'good' group claimed a net gain based on their performance during the task (n=11); the 'bad' group claimed net losses (n=6). For comparison, subjects denoted by 'x' actually net won money (n=6) during the scanning session, and those by 'o' net lost (n=11). To our surprise, the objective and the perceived performances were completely uncorrelated. (Behrens-Fisher two-sampled t-test comparing actual performance of the subjective good versus subjective bad groups: p=0.70[n.s.]).

Additionally, subjects rated the gain-loss contexts in terms of both subjective motivation and preference. As the subjects' likelihood of obtaining gains or losses likely impacts how they perceive the gain-loss contexts, both their motivation and preference rankings are presented as a function of their objective and subjective performances. Fig. 3.2B depicts the mean preference rankings: on the left, the rankings for the objective good versus objective bad subjects; and on the right, subjective good versus subjective bad subjects. Intuitively, these rankings should parallel the value associated with the gain-loss contexts. Accordingly, subjects in all groups most preferred the high-gain/low-loss context ($5/-$1), and least preferred the converse, low-gain/high-loss context ($1/-$5). Between the objective good and bad groups, no significant differences existed in the rankings of the remaining contexts (2-way ANOVA—context: $F(4,75)=44.4$, $p<0.05$; group: $F(1,75)=0$, p=1.0[n.s.]; group×context: $F(4,75)=0.35$, p=0.85[n.s.]). However, different trends surfaced for the subjective good and bad groups; the subjective bad group preferred the low-gain/low-loss context over the high-gain/high-loss context, consistent with the values of these contexts at poor performance (2-way ANOVA—context: $F(4,75)=45.5$, $p<0.05$; group: $F(1,75)=0$, p=1.0; group×context: $F(4,75)=0.80$, p=0.50[n.s.]).

Subjects' motivation rankings (Fig. 3.2C) display an analogous but more striking trend. Objective good and bad groups show no dissimilarity in ratings (2-way ANOVA—context: $F(4,75)=42.3$, $p<0.05$; group: $F(1,75)=0$, p=1.0[n.s.]; group×context:

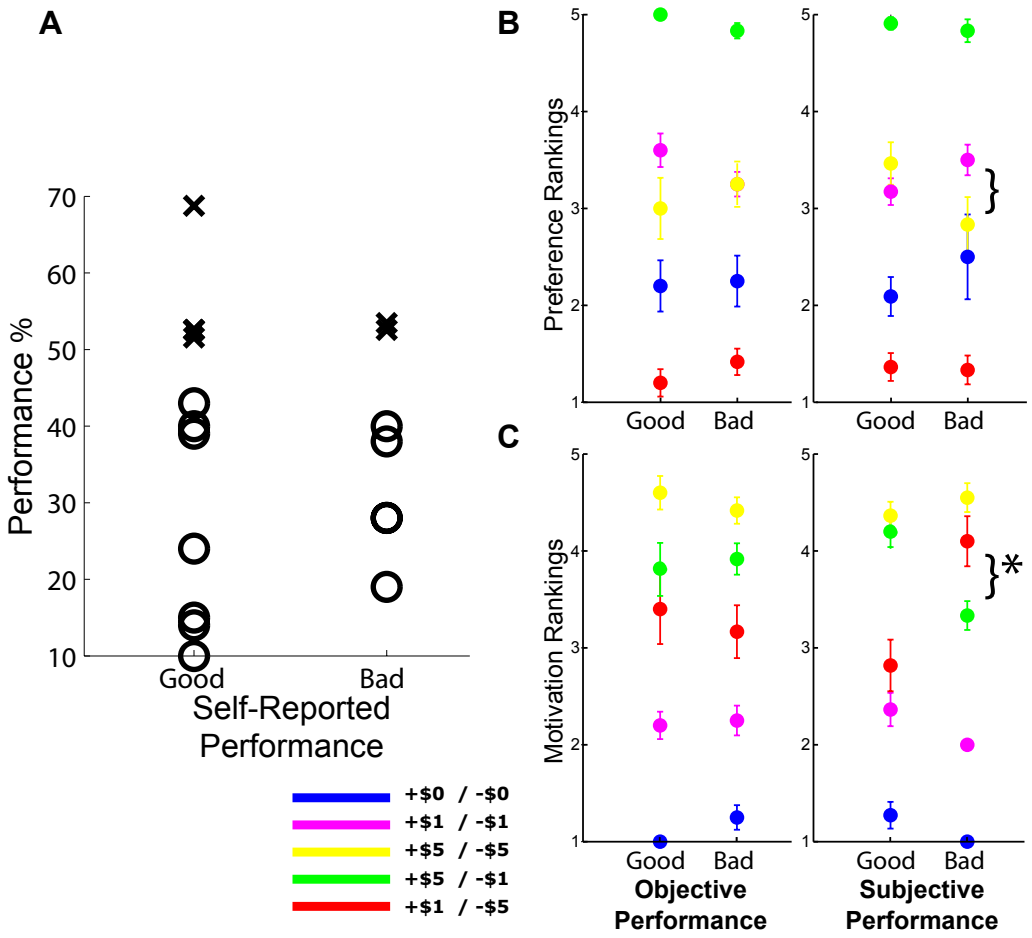

Figure 3.2:

Subjects Attitudes towards Performance and Contexts.*(A) Actual Performance vs Self-Reported Performance. 'Good' subjects reported net winning money; 'Bad' subjects reported the converse. For comparison, 'x' s are subjects who actually net won money; in 'o' s, subjects who net lost money. (B) Subjects' preference rankings of gain-loss contexts, divided by Objective(left panel) and Subjective (right panel) Performance. (C) Subjects' motivation rankings of gain-loss contexts, divided by Objective (left panel) and Subjective (right panel) Performance.*

$F(4,75)=0.21$, $p=0.94$). Groups divided on the basis of subjective performance however diverge significantly (2-way ANOVA—context: $F(4,75)=51.0$, $p<10e\text{-}16$; group: $F(1,75)=0$, $p=1.0$[n.s]; group×context: $F(4,75)=4.1$, $p=0.005$). Subjective good subjects rated the high-gain contexts (\$5/-\$1, \$5/-\$5) equivalently, followed by the low-gain contexts, indicating they viewed contexts in terms of gains. The subjectively bad group provided the reverse ranking, i.e., contexts involving high losses were more motivating than high-gain contexts, congruent with the notion that they believed themselves more likely to perform a trial incorrectly than correctly. As the ANOVA statistics indicate, grouping subjects by subjective as compared to objective performance—specifically through the interaction of gain-loss context and performance group—accounts for a greater proportion of the variance in both preference and motivation rankings.

Neuroimaging Findings

As this study chiefly concerns modulation of motor preparatory/planning activity, the focus lies primarily upon related BOLD activity during the delay period. Neural responses to the cue and the feedback are briefly summarized (see supplementary tables for more detail).

Motor Preparation/Planning ROIs

The primary analysis identified motor planning ROIs as those clusters with the strongest main effect of the delay period, irrespective of gain-loss context modulation.

By this approach, a group analysis ($p(FWE)<0.01$, corrected for spatial extent $p<0.05$) revealed significant delay period activity in a frontoparietal network putatively engaged in motor preparation/planning. Specifically, this network comprised bilaterally: multiple peaks in superior parietal lobule (SPL), and along the medial bank and fundus of the intraparietal sulcus (IPS); precuneus; dorsal premotor cortex; and pre-supplementary motor area/supplementary motor area (hereafter referred to

as SMA) (Fig. 3.3a).

Expressed in % signal change relative to the last 4 s of the initial fixation period, BOLD timecourses of these regions demonstrated four main components, exemplified in Fig. 3.3b. Temporal alignment in the figure occurs with respect to the delay period. Vertical lines demarcate delay onset at 0 sec and movement onset at 15 sec; cue presentation commences 3.7 sec (gain-loss context cue, spatial cue, and mask) prior to start of the delay period. Event-related BOLD modulations include: (1) a transient (high-amplitude) signal increase time-locked to the instructive cue, peaking approximately 6 sec after presentation; (2) a sustained level of activity during the delay period, but of a smaller magnitude than the earlier cue and the later movement peak amplitudes; (3) a transient (high-amplitude) signal increase time-locked to the initiation of movement, again peaking approximately 6 sec after movement onset; and (4) a (smaller) transient (small-amplitude) increase time-locked to the feedback (receipt of reward/punishment), sometimes obscured by the larger movement-related signal.

Of motor-planning ROIs, the left superior parietal lobule (SPL) demonstrated the most significant delay period activity; SPL BOLD timecourses, sorted by gain-loss context, are illustrated in Fig. 3.3B. To better isolate delay period modulations consequent of gain-loss contexts (without residual contributions from the cue epoch, for example), the corresponding beta values are depicted in Fig. 3.3C. As these beta values are regression coefficients that represent the 'weight' of each predictor in order to best fit the observed signal, they constitute an isolated estimate of the % signal change due to each predicted factor, i.e., in this figure, the delay periods under each gain-loss context. Averaged over all subjects, the preferred high-gain/low-loss (+$5/-$1) context produced the largest increase in signal. While this tentatively suggests that the BOLD response may reflect the value associated with the trial, the remaining gain-loss contexts do not generate levels of activity proportional to their value—most notably, the beta value associated with the strongly negative context (+$1/-$5) exceeds those associated with the relatively neutral gain-loss contexts (+$1/-$1 and +$0/-$0). That both positive- and negative-value contexts engender

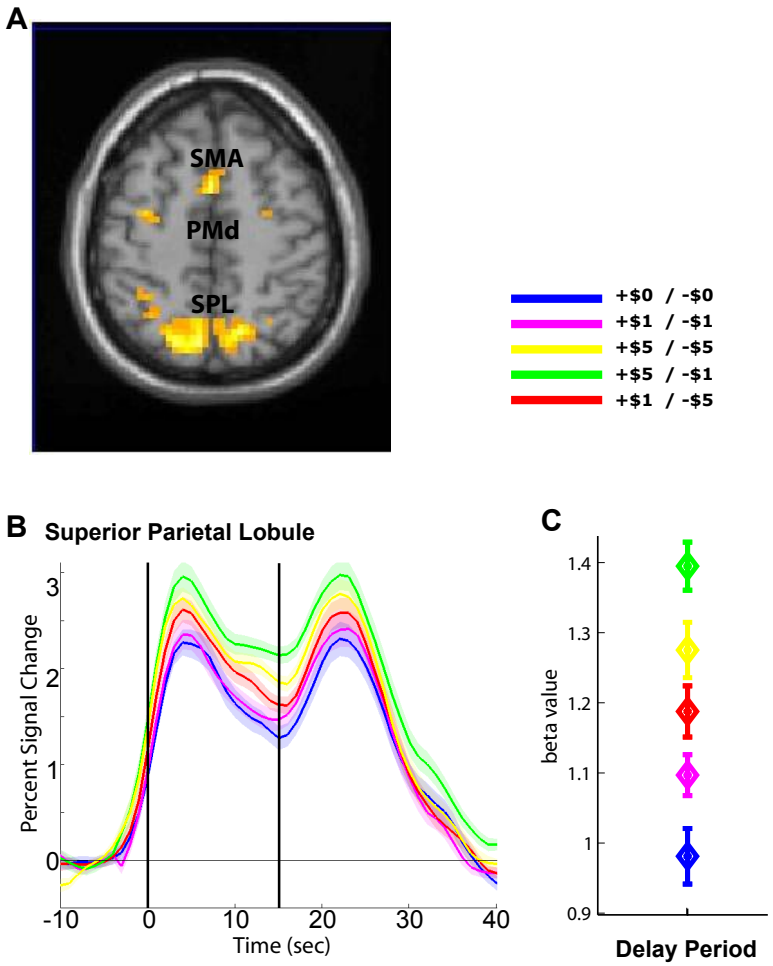

Figure 3.3:

Delay period ROIs and representative timecourse and beta values.*(A) Regions exhibiting significant delay-period activity, across all gain-loss conditions. (p(FWE)<0.01) (B) BOLD signal timecourses averaged over all subjects, extracted from left superior parietal lobule (SPL), sorted by gain-loss context. Black lines indicate onset and offset of delay period. (C) Delay period beta values averaged over all subjects, extracted from left superior parietal lobule (SPL), sorted by gain-loss context.*

greater activity compared to neutral contexts suggests that the absolute value associated with successful trial completion may play an explicative role in parietal delay-period responses.

In order to elucidate any relationship between task performance and delay-period activity, subjects were segregated on the basis of their earnings: those who net won money ('objective good') and those who did not ('objective bad') (see Fig. 3.2A. The 'objective good' group of subjects yielded no clear order of delay period beta values. The 'objective bad' group exhibited a pattern similar to that of the whole group result, with the positive-value context (+$1/-$1) highest, and the negative-value context (+$1/-$5) greater than the neutral contexts (Fig. 3.4A. This partition on the basis of objective performance explains no more of the variance in delay period beta values than does considering gain-loss contexts alone (2-way ANOVA—context: $F(4,75)=4.0$, $p<0.05$; group: $F(1,75)=0.11$, $p>0.05$; group×context: $F(4,75)=0.10$, $p>0.05$).

Alternatively, subjects can be divided according to subjective estimates of their own performance. This criterion furnished a dichotomous classification: those who believed they had done well on the task and net won money ('subjective good') and those who believed they had not ('subjective bad') (see Fig. 3.2). Delay-period beta values (Fig. 3.4B) disclose a significant interaction between gain-loss context and subjective perfornance (2-way ANOVA—context: $F(4,75)=4.7$, $p=0.002$; group: $F(1,75)=1.0$, $p=0.4$, context×group: $F(4,75)=9.7$, $p=0.003$). For the 'subjective good' group, the beta values of +$5 contexts exceed those of the +$1 contexts, with the highest produced by the +$5/-$1. For the 'subjective bad' group, the negative-value context garners a larger hemodynamic response than the positive-value context, which in turn produces a larger response than more neutral contexts. Collectively considered, these findings concur with the absolute value predictions for both subjective good and bad performance (refer to Fig. 3.1). To better observe the task-dependent modulation of activity throughout the trial, Fig. 3.4C renders the BOLD timecourses for the subjective good and bad performance groups.

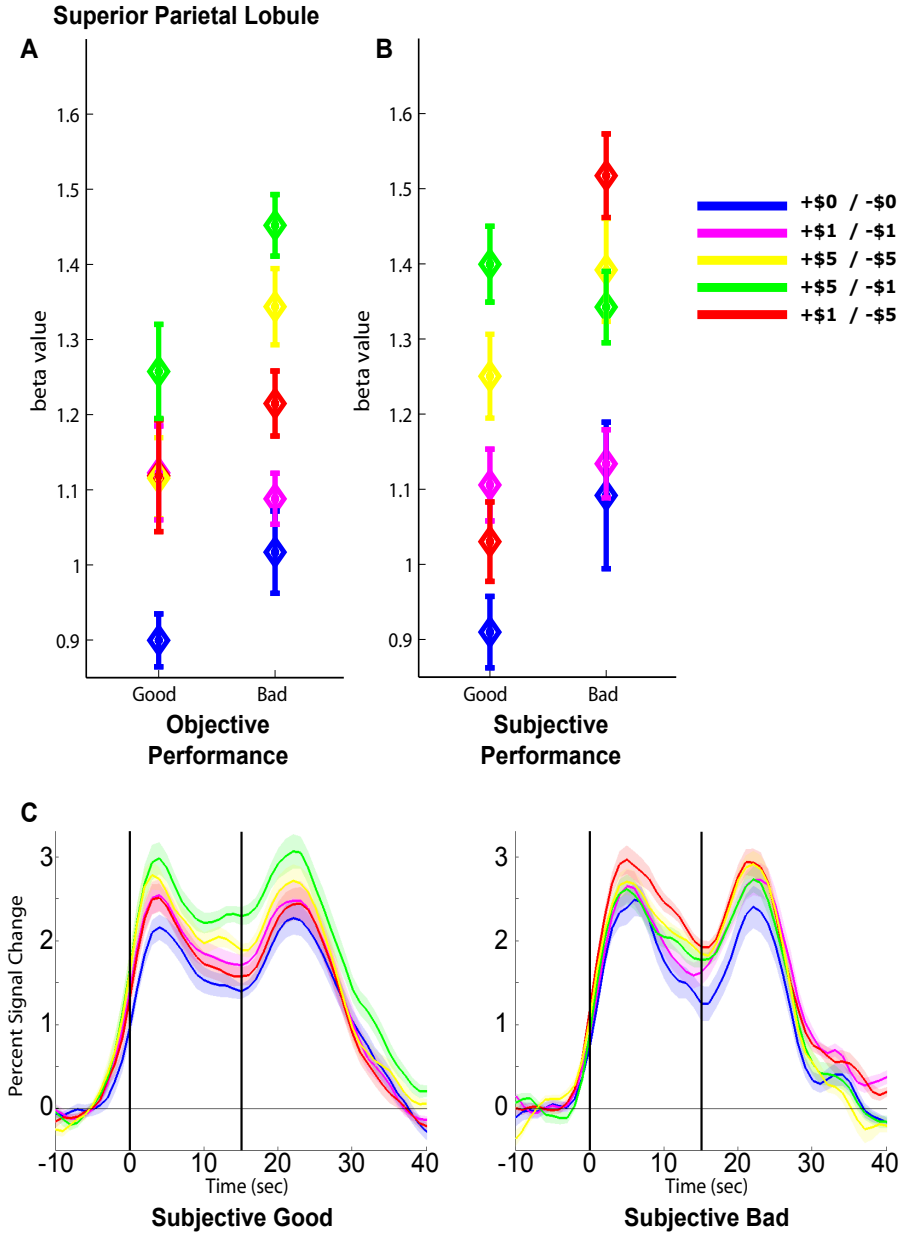

Figure 3.4:

SPL beta values and timecourses by performance. *Delay-period beta values for (A) Objective Good and Bad subjects, and (B) Subjective Good and Bad subjects, sorted by gain-loss context. (C) BOLD timecourses for Subjective Good (left panel) and Bad (right panel) subjects.*

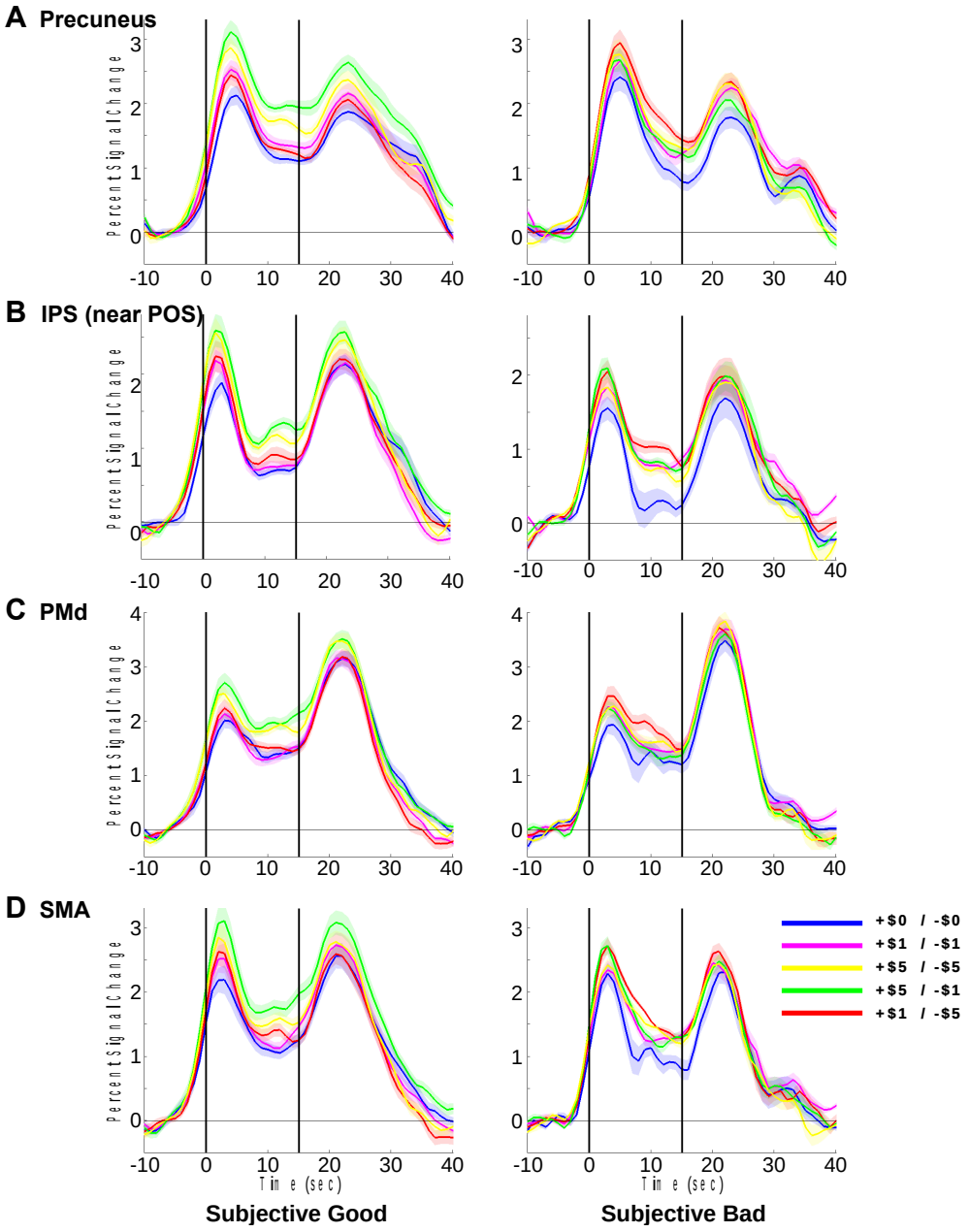

Figure 3.5:

Delay Period ROI BOLD timecourses *for Subjective Good subjects (left panel) and Subjective Bad subjects (right panel) for motor planning ROIs (A) Precuneus, (B) IPS, near its junction with POS, (C) PMd, and (D) SMA/pre-SMA. Black lines indicate onset and offset of delay period.*

The profile of BOLD activity in SPL echoed that in other motor planning ROIs. Fig. 3.5 portrays the analogous timecourses, for subjective good and bad subjects, for (Fig. 3.5A) left precuneus; (Fig. 3.5B) left intraparietal sulcus, close to parieto-occipital sulcus; (Fig. 3.5C) left dorsal premotor area; and (Fig. 3.5D) pre-SMA/SMA. Throughout this frontoparietal network, neural activity developed similarly, likely reflecting a modulation of BOLD responses by the absolute value tied to task completion; however, parietal areas revealed the most significant context-dependent responses.

To further corroborate these findings, a second set of group analyses were conducted to directly probe context-dependent modulations resonant with value, stakes, or absolute value. (Additional variables were tested; see Experimental Procedures.) These analyses further assessed the import of objective versus subjective performance estimates. On a first level, individual-subject general linear models (GLMs) employed a single regressor for each task epoch. For the cue, delay, and response epochs, an additional regressor captured the hypothesized parametric modulation of the signal due to gain-loss contexts. For the 'objective performance' models, these hypothesized modulations for each subject were determined by their objective performance (either good or poor); for 'subjective performance' models, by their subjective performance estimate (either good or poor). (See Experimental Procedures, table 1 for values used for these hypothesized modulations.) On the second level, a group analysis exclusively utilized contrast images from individual subjects which assessed this parametric modulation regressor.

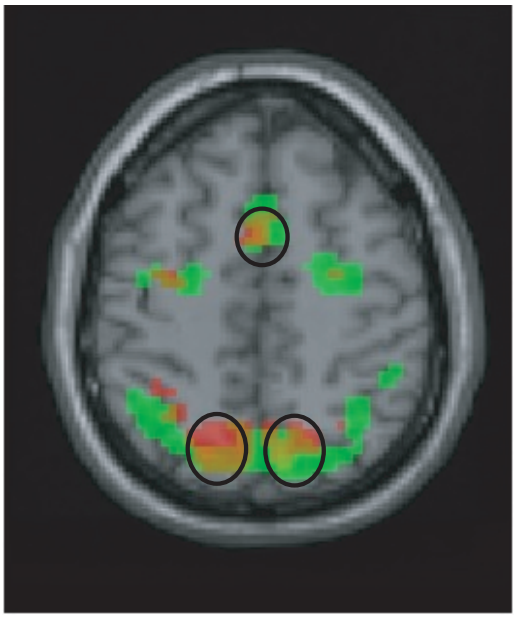

Figure 3.6:

Statistical maps for delay period and 'performance-weighted' absolute value. *Voxels revealing significant main effect of the delay period, in red (p(FWE)<0.01); and voxels revealing significant parametric modulation of absolute value, based on subjective performance, in green (p(FDR)<0.05). Voxels in orange are overlap for both contrasts, i.e., p(FWE)<0.05. Regions corrected for spatial extent, significant for both contrasts, are circled.*

By this approach, statistical analyses of the delay period elucidated all voxels with significant gain-loss modulation, independent of a main effect of the delay period. For (2nd-level) GLMs predicated upon stakes or value (either rooted in objective or subjective performance estimates), this contrast produced no significant voxels (up to a voxel level threshold of p(unc)<0.05). Conversely, absolute value models based on subjective performance (p(FDR)<0.05, corrected for spatial extent p(cor)<0.05) yielded significant clusters, rendered in green in Fig. 3.6. Models of absolute value based on objective performance also highlighted a subset of these clusters, but these

voxels did not survive the statistical threshold criteria. Confirming the results from our previous analysis, frontal and parietal areas show significant modulation dependant on subjective performance-related absolute value (see also Supplementary Table 3.S3). Superimposed on the related statistical map in Fig. 3.6 are the motor planning ROIs, which exhibited a significant main effect of the delay period (red). The overlap suggests that these main motor planning ROIs were also the regions most significantly encoding expected-outcome-related information.

Neural Responses to Spatial and Gain-Loss Contextual Cues

As the contextual cue supplies gain-loss information, areas engaged in processing the cue are potentially necessary for predicting the outcome of specific action plans. However, due to brief and contiguous viewing of spatial and contextual cues, BOLD responses to the individual cues could not readily be distinguished. Hence, they were modeled as one task epoch ('cue'). Regions exhibiting a significant response to the spatial and contextual (gain-loss) cue presentation ($p(FWE)<0.01$) encompassed subcortical structures including the thalamus and the striatum; and cortical clusters in bilateral precuneus, supplementary motor area, SPL, dorsal premotor cortex, middle occipital gyrus, posterior cingulate, and left lingual and fusiform gyri.

Of these cue-activated ROIs, a small subset—the thalamus, caudate, and precuneus—additionally revealed a significant parametric modulation due to the gain-loss context. Presumably, those areas not parametrically modulated are more involved in general sensory or mnemonic processing of the cue, rather than in encoding specific consequences or contingencies signified by the gain-loss context. (See Supplementary Table **??** for all cue ROIs showing modulation, and Supplementary Table **??** for all regions demonstrating a significant modulatory effect independent of a main cue effect.) Consistent with previous findings (Knutson et al. 2000, 2001), thalamic and caudate cue activity demonstrated similar modulatory trends, reflecting the value indicated by the gain-loss contexts. Furthermore, modulation of cue activity in these areas correlated best with the value based on objective performance of subjects (thalamus right [15 -27 12], $t = 3.94$ for objective value parametric modulation; caudate left [-3 15 0], t

= 4.36 for parametric and right [3 15 6], t = 4.40 for objective value parametric modulation). Caudate BOLD timecourses for objective good and bad groups are shown in Fig. 3.7.

In the timecourses presented on the left panel, the good performance 'weights' the gains of the gain-loss contexts, leading to high signal amplitudes in both the high-gain/high-loss (+$5/-$5) context (comparable to the high-gain/low-loss context), and in the low-gain/high-loss context (higher than $0/-0). Conversely, averaged over the objective bad subjects, where performance now weights the losses more, these contexts show relatively lower signal amplitudes. [For direct comparison with signals in motor planning ROIs, caudate timecourses for subjective good and bad groups are shown in Supplementary Fig. 3.S1.]

To discern other reward-related areas that may exhibit cue responses, the statistical threshold was eased (p(FDR)<0.01); additional voxels in the orbitofrontal cortex then showed similar objective-value-related modulation approaching significance (right [6 51 -6; 3 54 -12], t = 3.48, 3.50 for objective value parametric modulation).

Additional clusters in the caudate, while they did not reveal a main effect of the cue, did demonstrate robust modulation during the cue epoch. A subset of these clusters showed modulation consistent with objective value, as with the cue-activated caudate ROIs . However, the remaining clusters displayed BOLD patterns resonant with subjective absolute value. Voxels of peak absolute-value-related modulation in the caudate generally lay more dorsolaterally than voxels with value-modulated activity. [For a comprehensive list of clusters showing modulation of the cue epoch, see Supplementary Table 3.S2.]

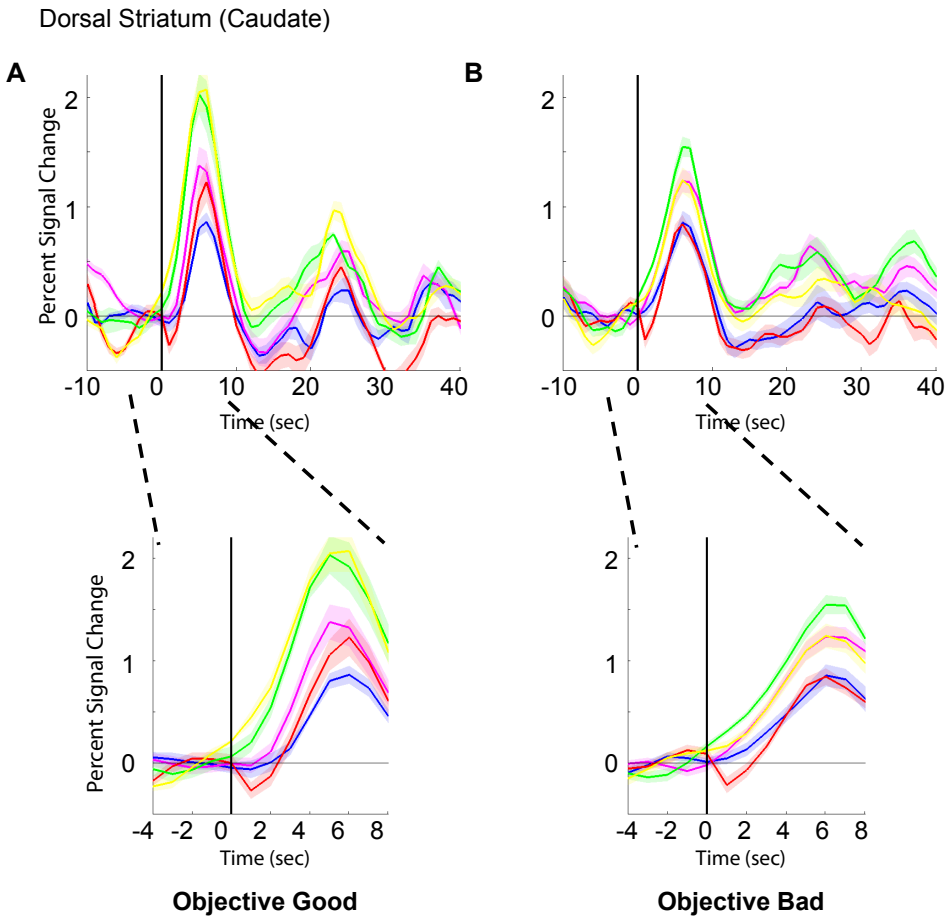

Figure 3.7:

Dorsal striatal BOLD signal timecourses *for Objective Good subjects (left panel) and Objective Bad subjects (right panel). The timecourse over the entire trial duration is presented on top; the cue epoch (from -4sec to +8sec, with 0sec denoting onset of cue gain-loss context cue) is depicted below. Black line indicates onset of cue presentation.*

Neural Responses to Outcome (Feedback)

Areas which process feedback/outcome of events offer information important for the comparison of actual versus predicted outcomes, and for the development of future expectations. In this experiment, feedback of monetary gains and losses at the end of each trial elicited significant cortical and subcortical activation (p(unc)¡0.001, corrected for spatial extent p<0.05). In accordance with prior studies, bilateral ventral striatum (left [-9 6 -3; -6 9 0], t = 6.10; right [6 6 -3], t = 5.16), bilateral putamen (left [-12 9 -6], t = 5.67; right [15 9 -6], t = 6.39), and caudate (left [-6 6 6], t = 5.27) showed a greater BOLD response to gain as compared to loss outcomes (Delgado et al. 2003; Wrase et al. 2007). Regions within the inferior frontal gyrus (right [36 27 27], t = 5.25), medial prefrontal and anterior cingulate (left [0 33 9], t = 5.50; right [12 39 21], t = 5.75), and inferior parietal (left [-51 -54 51], t = 6.33; right [51 -54 48], t = 5.65) displayed similar reward-related signals. Additionally, BOLD changes scaling both positively with the magnitude of the rewards and inversely with the magnitude of punishments on each trial were observed in medial orbitofrontal cortex (right [6 51 -6], t = 4.29) and caudate (right ([-3 18 0], t = 3.80) (O'Doherty et al. 2001; Delgado et al. 2003). Punishments produced greater BOLD responses than did rewarding outcomes in precentral (left [-27 -15 69], t = 4.15; right [24 -24 72], t = 3.80) and postcentral (right [33 -36 69], t = 4.50) gyri. No voxels demonstrated activity positively correlated with the magnitude of punishment.

3.4 Discussion

To determine which aspects of an action's reward contingencies appertain to action planning, human subjects were scanned while performing a motor planning task with monetary consequences, contingent on task performance. Importantly, task demands were of sufficient complexity to generate a range of performance levels and robustly recruit motor planning network, leading to several novel findings. First, we found that though subjects performed at a consistent success level throughout the experiment,

their perceived performance was poorly correlated with their actual performance; furthermore, subjective performance estimates better accounted for their attitudes towards gain-loss contingencies. Secondly, our findings show robust differential BOLD activity related to these gain-loss contingencies. As there was no evidence of behavioral differences between gain-loss contexts, BOLD modulation likely reflected subjects' evaluation of predicted monetary consequences of their actions. Specifically, our imaging findings demonstrated a dissociation within a widespread network recruited during the task: areas primarily responding to the contextual/spatial cues, such as subregions of the striatum, encoded the value as a function of subjects' actual performance. Conversely, cortical motor planning regions, most notably the posterior parietal cortex, assimilated the expected absolute value of a motor plan during the delay period. This absolute value was not predicated upon actual performance, but rather upon subjects' perceived performance, suggesting that subjective cognitive biases may play a significant role in the planning of action.

Involvement of Canonical Reward Structures in Encoding Reward Context

Frontostriatal reward circuitry demonstrated significant responses to the cue and outcome epochs of the task, but showed no sustained delay period/motor planning activity. Prior imaging studies investigating these regions do not generally employ delay periods long enough to unambiguously disentangle neural signals generated in these task epochs. However, the profile of orbitofrontal and striatal BOLD activity here corresponds to single-unit investigations (Schultz et al. 2000; Kobayishi et al. 2007; Samejima et al. 2005; Hikosaka et al. 2000). In addition, regions in the striatum and orbitofrontal cortex revealed similar reward-contingent modulation throughout the task. During cue presentation, signal modulation paralleled the value predicted by the cue. Both structures differentiated between rewarding and punishing outcomes, consonant with their purported role in utilizing feedback in the control of motivated behavior (Delgado et al. 2000; O'Doherty 2001). Our findings coherently contribute

to the idea that frontostriatal areas may process information relevant for guiding goal-directed action, but do not directly participate in planning and preparing movements.

Of frontostriatal structures, the caudate exhibited the most significant modulation in response to the reward-predicting/spatial cue. Comparable striatal evaluation of reward-predicting cues has been documented in human and nonhuman primates. (Schultz et al. 2000; Kawagoe et al.1998; Cromwell et al. 2003; Apicella et al. 1991; Gold 2003; Knutson et al. 2000; Delgado et al. 2003). The dorsal striatum, particularly the caudate, plays a critical role in establishing associations between an (goal-directed) action and its outcome, and the current value of the outcome (Dickinson and Balleine 1994; Balleine and Dickinson 1998; Tricomi et al., 2004; Haruno et al. 2004; O'Doherty et al. 2004; Hikosaka et al. 2006; Tremblay et al. 1998; Kawagoe et al. 2001; Shidara et al. 1998), underscoring its involvement with feedback-sensitive goal-directed actions (Haruno and Kawato 2006; Levy and Dubois 2006). However, previous experiments that sought to elucidate factors influencing the valuation of action have done so by manipulating predominantly stimulus-outcome associations; and factors, such as risk, uncertainty, probability, and mean (expected) value were all externally manipulated (e.g., varied by the experimenter). Extending these findings, reward structures also incorporate an estimation of response completion and outcome, the likelihood of which is governed by the subject's performance.

Interestingly, in this paradigm where objective and subjective estimates of performance diverged drastically, striatal computations of value mostly relied upon subjects' objective performance. The ventral and dorsal striatum receive dense dopaminergic innervation, which has been proposed to carry a prediction error signal (Montague et al. 1996; Schultz 1997; O'Doherty et al. 2003). This signal, which may veridically reflect the error between actual and predicted occurrences, might in turn be exploited by the striatum, underlying its role in the learning of selection preferences on the basis of obtained rewards and punishments (McClure et al. 2003, 2004; Tobler et al. 2006; Hollerman et al. 1998).

In addition to a value-encoding population, a subset of voxels in the dorsal striatum, though not exhibiting significant responses to the cue presentation irrespective

of reward context, showed significant absolute-value-related modulation during this cue period. Tonically active striatal neurons, which respond to both positive and negative predictive cues but not neutral stimuli (Ravel et al. 2003), could conceivably account for our observed BOLD signal reflecting absolute value modulation but no main cue effect. Furthermore, voxels demonstrating absolute-value-related BOLD activity tended to cluster more dorsolaterally in the caudate than those showing value modulation (see Supp Tables 3.S1 & 3.S2).

Anatomical examinations of basal ganglia connectivity expose several parallel corticostriatal subloops subserving different functions (Nakano 2000; Selemon and Goldman-Rakic 1988): Ventromedial striatal areas, to which more limbic roles have been ascribed, receive projections from orbitofrontal and anterior cingulate cortices (Selemon and Goldman-Rakic 1988); conversely, afferents from association cortices, including dorsolateral prefrontal and posterior parietal cortex, terminate in more dorsolateral regions of the striatum. In this study, orbitofrontal cortex activity resembled that of the ventromedial striatum, whereas more central and dorsolateral areas of the caudate displayed modulation similar to that of the motor-planning network. Our data thus poses the question of whether distinct basal ganglia-cortical loops differentially process and utilize reward context-related information in order to bias cortical action planning.

Role of Motor Planning Regions in Encoding Action Outcomes

Neural correlates of action planning that may be subject to reward modulation were recently delineated by us in separate studies (see Chapter 2). The delayed-response task variants employed in those studies elucidated a frontoparietal network, including SPL, SMA, and PMd, with substantial delay-period activity. Control conditions ensured that delay-period activity in these areas could not be explicated solely by concurrent processes such as visuospatial attention or working memory. These regions—most significantly SPL—showed greatest activity in conditions requiring that spatial

cues be encoded with respect to a motor plan: either as targets to be acquired or to be avoided.

In the current investigation, these neural substrates of action planning displayed modulation of delay-period activity due to gain-loss consequences. Cortical BOLD patterns insinuate cognitively modulated absolute value representations, speaking to differential involvement of this frontoparietal network in the representation of predicted action outcomes as compared to that of putative reward structures. Our results reveal that, throughout motor-planning regions of interest, signal amplitudes for trials in which actions could either endow high gains or high losses surpassed those in more neutral trials; the high-gain/low-loss (highest valued) context stimulated the most activity in subjects who believed themselves more likely to succeed, whereas the low-gain/high-loss (lowest valued) context produced the greatest response in subjects who believed themselves more likely to fail.

Action Planning in Posterior Parietal Cortex

Clusters throughout the superior parietal lobule exhibited the most significant delay period activity, consistent with our previous work, and also best exemplified context-dependent modulation of this activity. These clusters—in particular those most significantly demonstrating this modulation (independent of the main delay period)—closely correspond to areas in PPC localized as a putatiave human homolog of the parietal reach region (PRR) (Glidden et al., submitted). Similarly, recordings in the macaque have shown that, before the monkey performs a reach, PRR demonstrates activity related to expected value of the outcome (Musallam et al. 2004). These findings in PPR may speak to a general role of PPC in encoding expected outcomes of actions as a facet of action plans. Accordingly, a plethora of monkey electrophysiology studies have examined how expected reward influences neural activity in PPC, with a particular focus on visuo-oculomotor behavior. Firing rates in LIP, the region of PCC thought particularly devoted to the representation of eye movements, reflect behaviorally relevant information in saccadic paradigms probing target detection, expected value, relative utility, and internal choices (Shadlen and

Newsome 1996; Platt and Glimcher 1999; Coe et al. 2002). In demonstrating and characterizing outcome-related modulation in *human* PPC, our data augments these previous findings, and extends their interpretation by considering PPC responses to penalties in combination with rewards.

Dorsal Premotor Cortex Activity in Delayed-Response Tasks

Another region traditionally implicated in cognitive aspects of action planning and preparation is the dorsal premotor cortex (PMd). In the macaque premotor area, the question of value versus motivation encoding has been investigated through single-cell recordings (Roesch and Olson 2004). In this decision-making study, monkeys made saccades to indicate their choice between targets yielding either a punishment or a fluid reward. Neurons in premotor cortex fired robustly in anticipation of both large rewards and punishments, a finding deemed reflective of 'motivation.' The predictions of motivation as put forth by those authors would coincide with those of absolute value and stakes/risk as defined in our experimental framework. Given this correspondence, human dorsal premotor areas manifested the same trend (here, absolute value), albeit not significantly. In previous recordings of macaques performing multiple movements, premotor neurons fired less robustly when the monkey made memorized sequential button presses than when he made the same number of visually guided independent button presses (Tanji 2001). The task design used in this study, involving sequential memorized 'reaches', thus may not optimally drive premotor areas; given an alternative motor paradigm, greater activity and modulation may be revealed in PMd.

Action Planning: Attention versus Reward Modulation

As objects or events that carry rewarding and punitive consequences are behaviorally salient, the possibility that reward-related modulation may develop as an epiphenomenon of attention has been raised. As both high-gain and high-loss contexts induce activity in frontal and parietal regions, a possible explicative role of attention or arousal cannot be entirely ruled out (Maunsell 2004; Bendiksby and Platt

2006). Certain features of this experiment, however, argue against attention as solely accountable. Cognitive modulation, dependent on higher-order beliefs and expectations, render a simple form of attention linking objects or features to reward unlikely. Furthermore, all subjects received instructions to perform maximally on all trials. According to post-experimental surveys, subjects claimed to have followed directions, working to the best of their abilities irrespective of the gain-loss context. Supporting this claim, no subject showed significant differences in accuracy across context/trial types. Given the level of task difficulty, presumably subjects deployed full and comparable attentional resources in all trials, reaching a ceiling of performance. Outcome-related modulation therefore more likely corresponds to actual valuation of the action plan rather than attention or motor variables.

The Influence of Subjective Biases on Motor Planning Activity

An added dimension in the exposition of motor planning activity stems from the unexpected impact exerted by subjects' perceived performance upon delay-period BOLD signals. In this study, subjects' 'conception of acts, outcomes and contingencies' (Tversky and Kahneman 1981) deviated from objective likelihood of outcomes. The greater importance of perceived as opposed to actual performance, in explicating both subjective attitudes and neural data, attests to a strong framing effect. That attitudes and beliefs about the likelihood of outcomes affect behavior or decision-making is not surprising. Psychologists have long posited that humans exploit certain heuristics or simplifying beliefs under conditions when available information is incomplete or overly complex (Tversky and Kahneman 1974). However, in our experimental scenario, variability in outcomes stems from subjects' abilities and all information necessary to track performance is provided. Nonetheless, our results suggest that motor-planning regions seem more susceptible to subjective beliefs than areas primarily engaged with appraising reward-predicting cues or feedback.

Implications for Response Selection

Collectively taken, lesion, electrophysiology, and imaging studies highlight the function of PPC in integrating relevant, non-sensory information with sensory- and movement-specific representations, asserting its role in decision making related to action. Moreover, recent studies advocate PPC's capacity to simultaneously encode competing motor plans (Lindner A., Kagan I., Iyer A. & Andersen, R.A. 2008 Prospective coding of alternative actions in human Parietal and Premotor cortex. 6th FENS Forum of European Neuroscience). Incorporating expected consequences into these action representations renders PPC a suitable substrate for response selection. In this context, the absolute value linked to performing an action may constitute the most pertinent determinant when choosing among response options.

Expectations about outcomes, derived from generalizations of precedent predictive relationships, are especially relevant for resolving a current course of action. Cognitive biases can distort these expectations or generalizations; if they thereby also distort activity in those regions encoding action representations, they likely contribute to suboptimal response selection. It may form one of the ways in which people deviate from rationality in their goal-directed behaviors (Kahneman et al. 1982; Gilovich et al. 2002), taking action that is contrary to logic or self-interest.

3.5 Experimental Procedures

Subjects

Seventeen subjects (7 males, 10 females), ranging from 17–27 years old, participated in the experiment. All subjects were right-handed and exhibited normal or corrected-to-normal visual acuity. Participants provided informed consent in accordance with the Caltech Institutional Review Board guidelines. Subjects received a $15 recompense for completing all training and scanning, in addition to their earnings during the experiment.

Experimental Setup and Behavior

Subjects lay supine on the scanner bed and viewed the task backprojected onto a mirror, attached to the headcoil, subtending 21.6^o visual angle. Subjects positioned a fiber optic trackball (Current Designs, Pennsylvania) upon their stomach, holding the device in place with their right hand and adjusting exact placement for comfort. All subjects used their right index finger to make 'finger reaches', manipulating the trackball to correspondingly move the cursor on the screen. These trackball movements were recorded, and analyzed on-line in MATLAB.

The experimental task required subjects to dissociate arm and eye movements, demanding central visual fixation throughout each trial (subjects could make eye movements during the intertrial interval). An infrared eye camera (Resonance Technologies, California) placed inside the headcoil monitored eye movements during all scanning sessions. Recorded eye behavior (ViewPoint Software, Arrington Research, Arizona) was then analyzed offline in MATLAB.

Experimental Tasks

Fig. 3.1A depicts in detail the task structure and timing. Each trial began with an initial fixation period (approximately 15s, jittered between 14 and 16 seconds). The gains and the losses were then presented, above and below the fixation point, respectively, for 1500ms. Next, the spatial cues were presented (1200ms). Nine squares, radially equidistant from the fixation spot, were presented. To prevent subjects from memorizing a set number of locations, two configurations of squares, rotated 20^o with respect to one another, were interleaved across trials. Of these nine squares, five were 'hollow' (containing an inner black square), denoting them as targets for the upcoming finger reaches. In addition, these five square targets varied in size, specifying the order (from smallest to largest) in which the subjects should move to them. A visual mask (80 randomly placed white squares) displayed for 1000ms erased any iconic/visual memory of the targets. The ensuing delay period, during which subjects were reminded of the gains and losses for the trial, lasted approximately 15

seconds, again jittered between 14 and 16, complementary to the baseline fixation duration to ensure all trials were of equal length. Penultimately, the response screen appeared, serving as the 'go' signal, with nine identical squares in the same locations as the squares during presentation of the spatial cues/targets. A ring cursor was also shown, centered on the fixation point. At this time, subjects moved the cursor in a center-out fashion (from center to target, back to center, to next target, etc) sequentially to the five targets, in the order previously instructed, and were allowed 10 seconds in which to complete the task. Finally, subjects received feedback: the gain amount if they successfully acquired all targets; the loss amount otherwise.

This experiment utilized five gain-loss contexts: +$0/-$0, +$1/-$1, +$1/-$5, +$5/-$1, and +$5/-$5. Each gain-loss context trial type occurred 6 times per run, producing a total of 30 trials per run; the order of trial types was pseudorandomized and counterbalanced. Subjects trained extensively, performing 5 practice runs outside the scanner and 1 practice run within the scanner. They then completed 2 runs during scanning. To promote constant performance throughout the task, subjects were additionally instructed to 'do their best' on all trials, irrespective of the gain-loss context. Given this instruction and exhaustive practice, individual subjects' performance on the task during scanning remained stable (see Results). Each subject's mean performance is therefore taken as their fixed probability of success.

These contexts permitted predictions of neural activity in brain areas encoding parameters/statistics related to the action's expected consequences. An action's value, defined here as performance (likelihood of success) times the gains plus likelihood of failure (or 1-performance) multiplied by the losses—$value = (performance \times gains) + ((1 - performance) \times losses)$—stipulates a particular ordering of contexts. Across all levels of performance, the greatest modulation would be observed in the +$5/-$1 context, the lowest in the +$1/-$5 context, and the order of the remaining conditions dictated by the performance level (Fig. 3.1B). Action 'performance-weighted' absolute value, in the framework of this experiment,is tantamount to the absolute value of the action's value, thus yielding disparate context-dependent modulation depending on performance—$absolutevalue = |(performance \times gains) + ((1 - performance) \times$

$losses)|$. For good performance levels (above 50%), +\$5/-\$1 produces the largest signal amplitude; for poor performance levels (below 50%), +\$1/-\$5 generates the largest signal amplitude; at all performance levels, neutral contexts (+\$0/-\$0 and +\$1/-\$1) engender the smallest amplitude (Fig. 3.1D). Finally, the 'stakes' associated with an action could be expressed as the probability-weighted sum of the absolute value of each outcome. Across all performance levels, an area responsive to this parameter would show the largest signal increase under the +\$5/-\$5 context, and the smallest signal under the more neutral contexts +\$1/-\$1 and +\$0/-\$0 (Fig. 3.1c). $stakes = ((performance) \times |gains|) + ((1 - performance) \times |losses|)$.

Immediately after the scanning session and before ascertaining any information about their actual performance or net winnings, subjects answered a questionnaire: (1) whether they paid attention to the gain-loss contexts; (2) whether they had performed well on the task (net made money); performed poorly (net lost money); or roughly broke even (approximately 50% performance). Moreover, they ranked the five gain-loss contexts with respect to preference (under which context trial types they preferred working, from most to least) and motivation (under which context trial types they wanted to perform well, from most to least). Including all training and scanning sessions, subjects had viewed each of the gain-loss contexts 42 times. Thus, while meticulous calibration procedures were not utilized to determine subjects' attitudes (such as preference), we believe the subjects' extreme familiarity with the limited number of gain-loss scenarios was adequate for an ordinal ranking of those few contexts.

Functional and Anatomical Imaging

Echo-planar functional images were acquired in a Siemens 3 Tesla Trio scanner at Caltech's Brain Imaging Center, using an 8-channel head coil. The scan volume provided full coverage of cortical and (subcortical) structures in 32 axial slices, though it did not cover the cerebellum in its entirety (slice thickness=3.5mm, gap=0mm, in-plane voxel size=3×3mm, TR=2000ms, TE=30ms, flip angle=90^o, FOV=192×192, resolution=64×64). Subjects completed 2 runs, each 1487s in duration. Anatomical

images were acquired using a T1-weighted MP-RAGE sequence with the same head coil used for functional image collection. The whole brain volume was scanned in 176 slices (slice thickness=1mm, gap=0mm, in-plane voxel size=1×1mm, TR=1500ms, TE=3.05ms, FOV=256×256, resolution=256×256).

Data Preprocessing and Analysis

Functional data preprocessing, conducted through SPM5 (Wellcome Department of Imaging Neuroscience, Institute of Neurology, London, UK), included slice scan time correction, 3D motion correction, and linear trend removal. Mean EPI images were coregistered to whole-brain high resolution T1-weighted structural image (1×1×1mm) acquired for all subjects. Anatomical images were spatially normalized to a standard T1 template; the same normalization parameters were then applied to all functional images. All EPIs received additional intensity normalization, spatial smoothing (7mm Gaussian kernel), and temporal high-pass filtering (0.005Hz).

After data preprocessing, two whole-brain, across-subject analyses were performed: (1) 'ROI', delimiting brain regions of interest for each epoch of the task, allowing characterization of BOLD modulation due to gain-loss contexts in those regions; and (2) 'hypothesis-driven', exposing all regions that display a predicted modulation due to gain-loss contexts. The ROI-based approach defined motor planning areas on the basis of the linear combination of all delay period covariates, i.e., under all gain-loss contexts. Areas involved in cue processing were delineated similarly (significant positive beta value for all cue predictors). The 'ROI' analysis utilized a general linear model (GLM, Friston et al 1995) incorporating 21 total predictors of interest: the cue period for each gain-loss context (5 cue predictors); delay period for each gain-loss context (5 delay predictors); response period for each gain-loss context (5 response predictors); and outcome period for each magnitude of reward or punishment (6 outcome predictors: +$5, -$5, +$1, -$1, +$0, -$0). These boxcar predictors were convolved with the canonical hemodynamic response function. Statistical comparisons of the BOLD activations related to these different events, based on a group random effects with a statistic threshold at p(FWE) ¡ 0.001, determined the relevant regions

of interest (ROIs). From these ROIs, beta values and BOLD signal timecourses were extracted from each subject; for both measures, the means across subjects are presented. This method thus conservatively highlighted regions manifesting a consistent deviation from baseline during the delay (or cue) period without biases imposed by any predetermined hypothesis as to the modulation expected during this task epoch.

In contrast, the second, hypothesis-driven method is predicated upon explicit suppositions as to BOLD signal modulation. This analysis encompassed a distinct GLM for each relevant reward-related statistic or parameter (e.g., value, stakes, absolute value, etc.). These GLMs employed only four main predictors, one for each epoch of the task: cue, delay, response, and outcome. Additional predictors for the first three epochs modeled the modulation due to each trial's gain-loss context, orthogonalized with respect to the main epoch predictor. A final predictor also reflected modulation of the outcome epoch due to magnitude and valence of feedback. Table 3.1 contains the order across gain-loss contexts employed for each parameter of interest. For value, absolute value, and stakes, different orders for good and bad performance were utilized; these orderings were drawn from averaging over 50–100% performance (good) or 0–50% performance levels (poor). Thus, in 'objective performance' models, subjects were assigned 'good' parametric modulation orders if they net won money; and 'poor' otherwise. Similarly, in 'subjective performance' models, subjects were assigned 'good' parametric modulation orders if they believed they had net won money; and 'poor' otherwise. For objective performance, an additional GLM, using ordering of contexts determined by each subject's actual performance, was also run. However, since subjective estimates can most conservatively be grouped as 'above 50%' or 'below 50%', all results reported here use this binary grouping for both objective and subjective performance models, permitting better comparison between subjects' actual and perceived performances. Models for 'gains' and 'losses' were also conducted to capture valence-selective modulations, addressing the possibility that separate systems respond to rewards and punishments. Additional models reflected (1) subjects' motivation ratings, (2) subjects' preference ratings, and (3) 'variance' in the outcomes. Finally, pairwise interactions of all aforementioned fac-

	Value		Absolute Value		Stakes		Gains	Losses
	Good	Bad	Good	Bad	Good	Bad		
+$5/-$1	1	1	1	3	2	2	1	2
+$5/-$5	2	4	2	2	1	1	1	1
+$1/-$5	5	5	3	1	2	2	2	1
+$1/-$1	3	3	4	4	3	3	2	2
+$0/-$0	4	2	5	5	4	3	3	3

Table 3.1: Ordering of Gain-Loss Contexts for Parametric Modulation

tors were also modeled, to see if they better accounted for observed neural activity. All orders were mean-corrected for use as hypothesized parametric modulation. Only those models significantly accounting for BOLD activation patterns are discussed.

To account for observed BOLD modulations that may be ascribed to behavior, performance-related regressors were included in all models, capturing (1) success (1 for successful trial completion, 0 otherwise), (2) reaction time latencies for each trial, and (3) total time required for motor response on each trial.

These predictors were convolved with the canonical hemodynamic response function. A group random effects analysis, with a statistic threshold at $p(FDR)<0.05$, disclosed voxels whose BOLD activations during the cue and delay epochs significantly correlated with these parametric modulations, independent of a main effect (significant beta value) for the task epoch.

3.S1 Supplemental Data

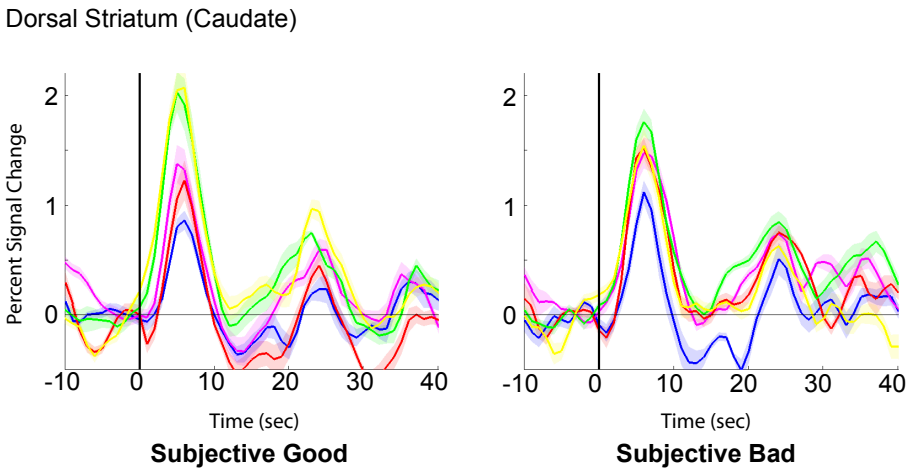

Figure 3.S1:

Dorsal striatal BOLD signal timecourses *for Subjective Good subjects (left panel) and Subjective Bad subjects (right panel). The timecourse over the entire trial duration is presented, with black line indicating onset of gain-loss contest cue presentation.*

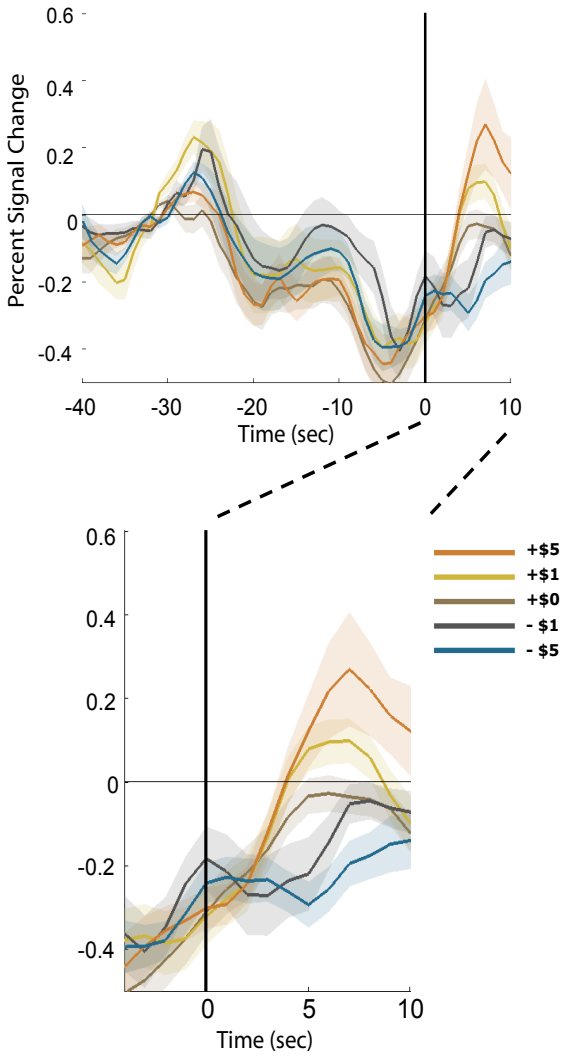

Figure 3.S2:

Orbitofrontal cortex (OFC) BOLD signal timecourse. *Upper graph depicts timecourse over the entire trial duration; below is the feedback epoch (from -4sec to +10sec). Black line at time 0 corresponds to onset of feedback epoch.*

Region Name		MNI Coordinates			Peak t-Stat
		x	y	z	
Cue ROIs, with significant parametric modulation:					
Value, Objective Performance					
Thalamus	L	-15	-12	18	4.36
	R	15	-27	12	3.94
Caudate	L	-3	15	0	4.70
	R	3	15	6	4.40
Gains					
Precuneus	L	0	-75	39	3.83
	R	15	-66	24	4.14
Delay ROIs, with significant parametric modulation:					
Absolute Value, Subjective Performance					
Supplementary Motor Area/Pre-SMA		0	6	54	3.93
Precuneus	L	-6	-69	54	3.85
	R	9	-69	54	5.40
Superior Parietal	L	-18	-72	54	4.82
Insula	R	33	21	3	4.47
Superior Occipital	L	-27	-75	36	3.77
	R	27	-78	43	4.05
Inferior Parietal	R	45	-45	45	4.81

Table 3.S1: All listed regions are significant (voxel p(FWE)<0.01, corrected for spatial extent p<0.05) for the main task epoch (either cue or delay period). In addition, they exhibit significant (voxel p(FDR)<0.05, corrected for spatial extent p<0.05) parametric modulation for that task epoch. Regions are listed under the model (parametric modulation regressor) for which they reach significance; t-statistics are for the parametric modulation regressor.

Region Name		MNI Coordinates			Peak t-Stat
		x	y	z	
Cue: Value, Objective Performance					
Caudate	L	-9	18	0	4.59
	R	6	15	0	5.20
Thalamus	L	-12	-18	18	6.12
	R	9	-6	18	5.38
Hippocampus	R	33	-39	6	5.36
Calcarine	L	-27	-63	18	6.07
	R	33	-60	12	5.99
Inferior Frontal gyrus	L	-45	15	33	5.63
Cue: Value, Subjective Performance					
No clusters show a significant modulation of the cue epoch consistent with value of gain-loss contexts, as derived from estimates of subjective performance.					
Cue: Absolute Value, Objective Performance					
No clusters show a significant modulation of the cue epoch consistent with absolute value of gain-loss contexts, as derived from estimates of objective performance.					
Cue: Absolute Value, Subjective Performance					
Caudate	L	-9	21	0	3.92
	R	18	21	12	5.03
		21	6	18	4.75
		21	9	21	4.70
		18	24	0	4.15
Thalamus	R	12	-15	18	5.61
Cuneus	L	-6	-90	24	6.63
Inferior Parietal	L	-27	-60	42	4.95
Middle Occipital	L	30	-72	24	4.93
Cue: Stakes					
Calcarine	L	-9	-72	15	4.88
Cue: Gains					
Precuneus	L	-9	-42	3	5.34
Cue: Losses					
No clusters show a significant modulation of the cue epoch consistent with potential losses of the gain-loss context.					

Table 3.S2: All listed regions are significant (voxel p(FDR)<0.05, corrected for spatial extent p<0.05) for parametric modulation regressor of the cue epoch.

Region Name		MNI Coordinates			Peak t-Stat
		x	y	z	
Delay: Value, Objective Performance					
No clusters show a significant modulation of the delay epoch consistent with value of gain-loss contexts, as derived from estimates of subjective performance.					
Delay: Value, Subjective Performance					
No clusters show a significant modulation of the delay epoch consistent with value of gain-loss contexts, as derived from estimates of subjective performance.					
Delay: Absolute Value, Objective Performance					
No clusters show a significant modulation of the delay epoch consistent with absolute value of gain-loss contexts, as derived from estimates of subjective performance.					
Delay: Absolute Value, Subjective Performance					
Superior Parietal	L	-15	-72	54	5.13
	R	12	-75	51	7.72
Precuneus	L	-3	-75	48	4.70
	R	12	-75	54	6.89
Insula	R	30	24	3	5.31
Inferior Parietal	R	45	-45	39	5.22
Supplementary Motor Area/Pre-SMA		6	6	54	4.99
Delay: Stakes					
No clusters show a significant modulation of the delay epoch consistent with stakes of gain-loss contexts, as derived					
Delay: Gains					
Frontal Operculum	R	48	6	24	5.02
Precentral	R	54	0	30	4.21
Delay: Losses					
No clusters show a significant modulation of the delay epoch consistent with potential loss of gain-loss contexts.					

Table 3.S3: All listed regions are significant (voxel p(FDR)<0.05, corrected for spatial extent p<0.05) for parametric modulation regressor of the delay epoch.

Region Name		MNI Coordinates			Peak t-Stat
		x	y	z	
Outcome: Reward > Punishment					
Ventral Striatum	L	-9	6	-3	6.10
		-6	9	0	5.75
	R	6	6	-3	5.16
Caudate	L	-6	6	6	5.27
Putamen	L	-12	9	-6	5.67
	R	15	9	-6	6.39
Insula-Caudal Orbitofrontal	L	-36	18	-15	7.22
Insula	L	-30	18	6	4.95
Inferior Parietal	L	-51	-54	51	6.33
	R	51	-54	48	5.65
Anterior Cingulate	L	0	33	9	5.50
	R	12	39	21	5.75
Inferior Frontal Gyrus	R	36	27	27	5.25
Orbitofrontal	L	0	48	-6	6.46
Outcome: Large Reward($5)> Small Reward($1)> Small Punishment(-$1)>Large Punishment(-$5)					
Middle Frontal Gyrus	L	-48	12	45	5.67
Inferior Frontal Gyrus	R	30	33	0	4.47
Orbitofrontal	R	6	51	-6	4.29
Caudate	R	-3	18	0	3.80
Outcome: Punishment>Reward					
Precentral Gyrus	L	-27	-15	69	4.16
	R	24	-24	72	3.80
Postcentral Gyrus	R	33	-36	69	4.50
Outcome: Large Punishment(-$5)>Small Punishment(-$1)> Small Reward($1)>Large Reward($5)					
No clusters show a significant modulation of the outcome epoch that scales positively with magnitude of punishment.					

Table 3.S4: All listed regions are significant (voxel p(unc)<0.001, corrected for spatial extent p<0.05) for parametric modulation regressor of the outcome epoch.

References

B. W. Balleine and A. Dickinson. Goal-directed instrumental action: contingency and incentive learning and their cortical substrates. *Neuropharmacology*, 37(4-5): 407–19, 1998.

M. S. Bendiksby and M. L. Platt. Neural correlates of reward and attention in macaque area lip. *Neuropsychologia*, 44(12):2411–20, 2006.

G. S. Berns, S. M. McClure, G. Pagnoni, and P. R. Montague. Predictability modulates human brain response to reward. *J Neurosci*, 21(8):2793–8, 2001.

J. M. Bjork and D. W. Hommer. Anticipating instrumentally obtained and passively-received rewards: a factorial fmri investigation. *Behav Brain Res*, 177(1):165–70, 2007.

H. C. Breiter, I. Aharon, D. Kahneman, A. Dale, and P. Shizgal. Functional imaging of neural responses to expectancy and experience of monetary gains and losses. *Neuron*, 30(2):619–39, 2001.

B. Coe, K. Tomihara, M. Matsuzawa, and O. Hikosaka. Visual and anticipatory bias in three cortical eye fields of the monkey during an adaptive decision-making task. *J Neurosci*, 22(12):5081–90, 2002.

J. C. Cooper and B. Knutson. Valence and salience contribute to nucleus accumbens activation. *Neuroimage*, 39(1):538–47, 2008.

K. D'Ardenne, S. M. McClure, L. E. Nystrom, and J. D. Cohen. Bold responses reflecting dopaminergic signals in the human ventral tegmental area. *Science*, 319 (5867):1264–7, 2008.

N. D. Daw, J. P. O'Doherty, P. Dayan, B. Seymour, and R. J. Dolan. Cortical substrates for exploratory decisions in humans. *Nature*, 441(7095):876–9, 2006.

M. R. Delgado, L. E. Nystrom, C. Fissell, D. C. Noll, and J. A. Fiez. Tracking the hemodynamic responses to reward and punishment in the striatum. *J Neurophysiol*, 84(6):3072–7, 2000.

M. R. Delgado, H. M. Locke, V. A. Stenger, and J. A. Fiez. Dorsal striatum responses to reward and punishment: effects of valence and magnitude manipulations. *Cogn Affect Behav Neurosci*, 3(1):27–38, 2003.

M. R. Delgado, V. A. Stenger, and J. A. Fiez. Motivation-dependent responses in the human caudate nucleus. *Cereb Cortex*, 14(9):1022–30, 2004.

M. R. Delgado, R. H. Frank, and E. A. Phelps. Perceptions of moral character modulate the neural systems of reward during the trust game. *Nat Neurosci*, 8(11): 1611–8, 2005a.

M. R. Delgado, M. M. Miller, S. Inati, and E. A. Phelps. An fmri study of reward-related probability learning. *Neuroimage*, 24(3):862–73, 2005b.

A. Dickinson and B. Balleine. Motivational control of instrumental performance following a shift from thirst to hunger. *Q J Exp Psychol B*, 42(4):413–31, 1990.

M. C. Dorris and P. W. Glimcher. Activity in posterior parietal cortex is correlated with the relative subjective desirability of action. *Neuron*, 44(2):365–78, 2004.

M. Ernst, E. E. Nelson, E. B. McClure, C. S. Monk, S. Munson, N. Eshel, E. Zarahn, E. Leibenluft, A. Zametkin, K. Towbin, J. Blair, D. Charney, and D. S. Pine. Choice selection and reward anticipation: an fmri study. *Neuropsychologia*, 42(12): 1585–97, 2004.

T. Gilovich, D. Griffin, and D. Kahneman. *Heuristics and biases: The psychology of intuitive judgment*. Cambridge University Press, New York, 2002.

P. W. Glimcher, M. C. Dorris, and H. M. Bayer. Physiological utility theory and the neuroeconomics of choice. *Games Econ Behav*, 52(2):213–256, 2005.

J. I. Gold. Linking reward expectation to behavior in the basal ganglia. *Trends Neurosci*, 26(1):12–4, 2003.

J. I. Gold and M. N. Shadlen. Neural computations that underlie decisions about sensory stimuli. *Trends Cogn Sci*, 5(1):10–16, 2001.

A. N. Hampton, R. Adolphs, M. J. Tyszka, and J. P. O'Doherty. Contributions of the amygdala to reward expectancy and choice signals in human prefrontal cortex. *Neuron*, 55(4):545–55, 2007.

M. Haruno and M. Kawato. Different neural correlates of reward expectation and reward expectation error in the putamen and caudate nucleus during stimulus-action-reward association learning. *J Neurophysiol*, 95(2):948–59, 2006.

M. Haruno, T. Kuroda, K. Doya, K. Toyama, M. Kimura, K. Samejima, H. Imamizu, and M. Kawato. A neural correlate of reward-based behavioral learning in caudate nucleus: a functional magnetic resonance imaging study of a stochastic decision task. *J Neurosci*, 24(7):1660–5, 2004.

O. Hikosaka, K. Nakamura, and H. Nakahara. Basal ganglia orient eyes to reward. *J Neurophysiol*, 95(2):567–84, 2006.

J. R. Hollerman and W. Schultz. Dopamine neurons report an error in the temporal prediction of reward during learning. *Nat Neurosci*, 1(4):304–9, 1998.

J. R. Hollerman, L. Tremblay, and W. Schultz. Influence of reward expectation on behavior-related neuronal activity in primate striatum. *J Neurophysiol*, 80(2):947–63, 1998.

J. R. Hollerman, L. Tremblay, and W. Schultz. Involvement of basal ganglia and orbitofrontal cortex in goal-directed behavior. *Prog Brain Res*, 126:193–215, 2000.

J. Jensen, A. R. McIntosh, A. P. Crawley, D. J. Mikulis, G. Remington, and S. Kapur. Direct activation of the ventral striatum in anticipation of aversive stimuli. *Neuron*, 40(6):1251–7, 2003.

J. Jensen, A. J. Smith, M. Willeit, A. P. Crawley, D. J. Mikulis, I. Vitcu, and S. Kapur. Separate brain regions code for salience vs. valence during reward prediction in humans. *Hum Brain Mapp*, 28(4):294–302, 2007.

J. W. Kable and P. W. Glimcher. The neural correlates of subjective value during intertemporal choice. *Nat Neurosci*, 10(12):1625–33, 2007.

D. Kahneman, P. Slovic, and A. Tversky. *Judgment under uncertainty: Heuristics and biases*. Cambridge University Press, New York, 1982.

R. Kawagoe, Y. Takikawa, and O. Hikosaka. Expectation of reward modulates cognitive signals in the basal ganglia. *Nat Neurosci*, 1(5):411–6, 1998.

B. Knutson, A. Westdorp, E. Kaiser, and D. Hommer. Fmri visualization of brain activity during a monetary incentive delay task. *Neuroimage*, 12(1):20–7, 2000.

B. Knutson, C. M. Adams, G. W. Fong, and D. Hommer. Anticipation of increasing monetary reward selectively recruits nucleus accumbens. *J Neurosci*, 21(16):RC159, 2001a.

B. Knutson, G. W. Fong, C. M. Adams, J. L. Varner, and D. Hommer. Dissociation of reward anticipation and outcome with event-related fmri. *Neuroreport*, 12(17): 3683–7, 2001b.

B. Knutson, G. W. Fong, S. M. Bennett, C. M. Adams, and D. Hommer. A region of mesial prefrontal cortex tracks monetarily rewarding outcomes: characterization with rapid event-related fmri. *Neuroimage*, 18(2):263–72, 2003.

S. Kobayashi, R. Kawagoe, Y. Takikawa, M. Koizumi, M. Sakagami, and O. Hikosaka. Functional differences between macaque prefrontal cortex and caudate nucleus during eye movements with and without reward. *Exp Brain Res*, 176(2):341–55, 2007.

R. Levy and B. Dubois. Apathy and the functional anatomy of the prefrontal cortex-basal ganglia circuits. *Cereb Cortex*, 16(7):916–28, 2006.

J. C. May, M. R. Delgado, R. E. Dahl, V. A. Stenger, N. D. Ryan, J. A. Fiez, and C. S. Carter. Event-related functional magnetic resonance imaging of reward-related brain circuitry in children and adolescents. *Biol Psychiatry*, 55(4):359–66, 2004.

S. M. McClure, G. S. Berns, and P. R. Montague. Temporal prediction errors in a passive learning task activate human striatum. *Neuron*, 38(2):339–46, 2003.

S. M. McClure, M. K. York, and P. R. Montague. The neural substrates of reward processing in humans: the modern role of fmri. *Neuroscientist*, 10(3):260–8, 2004.

P. R. Montague, P. Dayan, and T. J. Sejnowski. A framework for mesencephalic dopamine systems based on predictive hebbian learning. *J Neurosci*, 16(5):1936–47, 1996.

S. Musallam, B. D. Corneil, B. Greger, H. Scherberger, and R. A. Andersen. Cognitive control signals for neural prosthetics. *Science*, 305(5681):258–62, 2004.

K. Nakano. Neural circuits and topographic organization of the basal ganglia and related regions. *Brain Dev*, 22 Suppl 1:S5–16, 2000.

J. O'Doherty, M. L. Kringelbach, E. T. Rolls, J. Hornak, and C. Andrews. Abstract reward and punishment representations in the human orbitofrontal cortex. *Nat Neurosci*, 4(1):95–102, 2001.

J. O'Doherty, P. Dayan, J. Schultz, R. Deichmann, K. Friston, and R. J. Dolan. Dissociable roles of ventral and dorsal striatum in instrumental conditioning. *Science*, 304(5669):452–4, 2004.

J. P. O'Doherty, P. Dayan, K. Friston, H. Critchley, and R. J. Dolan. Temporal difference models and reward-related learning in the human brain. *Neuron*, 38(2): 329–37, 2003.

J. P. O'Doherty, T. W. Buchanan, B. Seymour, and R. J. Dolan. Predictive neural coding of reward preference involves dissociable responses in human ventral midbrain and ventral striatum. *Neuron*, 49(1):157–66, 2006.

M. L. Platt and P. W. Glimcher. Neural correlates of decision variables in parietal cortex. *Nature*, 400(6741):233–8, 1999.

N. Ramnani and R. C. Miall. Instructed delay activity in the human prefrontal cortex is modulated by monetary reward expectation. *Cereb Cortex*, 13(3):318–27, 2003.

S. Ravel, E. Legallet, and P. Apicella. Responses of tonically active neurons in the monkey striatum discriminate between motivationally opposing stimuli. *J Neurosci*, 23(24):8489–97, 2003.

M. R. Roesch and C. R. Olson. Neuronal activity related to reward value and motivation in primate frontal cortex. *Science*, 304(5668):307–10, 2004.

E. T. Rolls, C. McCabe, and J. Redoute. Expected value, reward outcome, and temporal difference error representations in a probabilistic decision task. *Cereb Cortex*, 18(3):652–63, 2008.

K. Samejima, Y. Ueda, K. Doya, and M. Kimura. Representation of action-specific reward values in the striatum. *Science*, 310(5752):1337–40, 2005.

W. Schultz. Dopamine neurons and their role in reward mechanisms. *Curr Opin Neurobiol*, 7(2):191–7, 1997.

W. Schultz. Predictive reward signal of dopamine neurons. *J Neurophysiol*, 80(1): 1–27, 1998.

W. Schultz, L. Tremblay, and J. R. Hollerman. Reward prediction in primate basal ganglia and frontal cortex. *Neuropharmacology*, 37(4-5):421–9, 1998.

W. Schultz, L. Tremblay, and J. R. Hollerman. Reward processing in primate orbitofrontal cortex and basal ganglia. *Cereb Cortex*, 10(3):272–84, 2000.

W. Schultz, L. Tremblay, and J. R. Hollerman. Changes in behavior-related neuronal activity in the striatum during learning. *Trends Neurosci*, 26(6):321–8, 2003.

L. D. Selemon and P. S. Goldman-Rakic. Common cortical and subcortical targets of the dorsolateral prefrontal and posterior parietal cortices in the rhesus monkey: evidence for a distributed neural network subserving spatially guided behavior. *J Neurosci*, 8(11):4049–68, 1988.

M. N. Shadlen and W. T. Newsome. Motion perception: seeing and deciding. *Proc Natl Acad Sci U S A*, 93(2):628–33, 1996.

M. N. Shadlen and W. T. Newsome. Neural basis of a perceptual decision in the parietal cortex (area lip) of the rhesus monkey. *J Neurophysiol*, 86(4):1916–36, 2001.

M. Shidara, T. G. Aigner, and B. J. Richmond. Neuronal signals in the monkey ventral striatum related to progress through a predictable series of trials. *J Neurosci*, 18 (7):2613–25, 1998.

J. Tanji. Sequential organization of multiple movements: involvement of cortical motor areas. *Annu Rev Neurosci*, 24:631–51, 2001.

P. N. Tobler, P. O'Doherty J, R. J. Dolan, and W. Schultz. Human neural learning depends on reward prediction errors in the blocking paradigm. *J Neurophysiol*, 95 (1):301–10, 2006.

L. Tremblay, J. R. Hollerman, and W. Schultz. Modifications of reward expectation-related neuronal activity during learning in primate striatum. *J Neurophysiol*, 80 (2):964–77, 1998.

E. M. Tricomi, M. R. Delgado, and J. A. Fiez. Modulation of caudate activity by action contingency. *Neuron*, 41(2):281–92, 2004.

A. Tversky and D. Kahneman. Judgment under uncertainty: Heuristics and biases. *Science*, 185(4157):1124–1131, 1974.

A. Tversky and D. Kahneman. The framing of decisions and the psychology of choice. *Science*, 211(4481):453–8, 1981.

M. Watanabe, H. C. Cromwell, L. Tremblay, J. R. Hollerman, K. Hikosaka, and W. Schultz. Behavioral reactions reflecting differential reward expectations in monkeys. *Exp Brain Res*, 140(4):511–8, 2001.

J. Wrase, T. Kahnt, F. Schlagenhauf, A. Beck, M. X. Cohen, B. Knutson, and A. Heinz. Different neural systems adjust motor behavior in response to reward and punishment. *Neuroimage*, 36(4):1253–62, 2007.

C. F. Zink, G. Pagnoni, M. E. Martin-Skurski, J. C. Chappelow, and G. S. Berns. Human striatal responses to monetary reward depend on saliency. *Neuron*, 42(3): 509–17, 2004.

Chapter 4

BOLD/fMRI Delay Period Signals in Monkeys and Humans: Spatial- and Non-Spatial Specific Signals

4.1 Summary

Delayed-response paradigms are used extensively in monkey electrophysiology and human fMRI studies to dissociate visual and motor events and to investigate working memory, attention, and movement planning. However the exact relationship between these studies is not clear due to differences in species, techniques, and trial durations. Here we directly compare fMRI activation in monkeys and humans with the same tasks: delayed visually and memory-guided saccades. Extending previous monkey fMRI studies that utilized block design, we developed event-related analysis of BOLD timecourses to delineate responses from different trial epochs. Delay-period activity in discrete frontal, parietal, and temporal areas revealed two types of cognitive signals: spatially-specific, strongly contralateral cue and memory/planning activity, and non-specific movement preparation. Consistent patterns were found in human functional homologs but contralaterality was less pronounced. These results elucidate BOLD activity distribution, temporal dynamics, and tuning differences in human and macaque cortical circuits subserving oculomotor goal-directed actions.

4.2 Introduction

The maintenance and processing of information no longer available from sensory input is important for a diverse array of activities involving the transformation of spatiotemporal cues into goal-directed actions. To investigate these processes, delayed or memory response paradigms have been used extensively in monkey electrophysiology(Bruce and Goldberg 1985; Gnadt and Andersen 1988; Hikosaka and Wurtz 1983; Funahashi et al. 1989; Mazzoni et al. 1996; Snyder et al. 1997), and more recently in human functional magnetic resonance imaging studies (Brown et al. 2004; Connolly et al. 2003, 2005; Curtis et al. 2004; Curtis and D'Esposito 2006; Courtney et al. 1998; Medendorp et al. 2005, 2006; Rowe et al. 2000; Schluppeck et al. 2006). In particular, memory-guided saccade or reach tasks were utilized to dissociate between visual, mnemonic, and motor response phases, and to investigate mechanisms of short-term memory, attention, and movement planning. Collectively taken, the results obtained from both bodies of studies concur: brain activations in human imaging studies correspond to putative homologs of monkey frontal and parietal fields, with timecourses typically consisting of relatively transient responses to the cue and motors events and persistent delay activity between them.

However, the exact relationship between human imaging and monkey electrophysiological studies of delayed responses is ambiguous due to differences in techniques and time-scales. First, the link between hemodynamic blood-oxygenation-level-dependent (BOLD) fMRI signals measured in human experiments and the firing of single neurons recorded in monkeys is far from being fully explicated, even in primary sensory areas of anaesthetized animals (Kayser et al. 2004; Logothetis et al. 2001). Second, most human imaging experiments utilize much longer trials (tens of seconds) than monkey electrophysiology experiments (usually less than 5 s). For example, a typical memory delay ranges between 10 and 15 s in human fMRI as compared to 0.5–2 s in monkey experiments. Therefore, the dynamics of underlying neural signals may vary between these conditions. Additionally, the difference in trial durations and possibly other cognitive factors may result in dissimilar mnemonic and preparatory strategies

employed by the two species. Third, different neuronal populations in monkey frontal and parietal areas exhibit disparate levels of cue, motor, and delay activity; how the net activity of these subpopulations would translate into BOLD 'activation' in monkey fMRI experiments similar to human fMRI studies is unknown. The comparison of fMRI activation patterns in monkeys and humans would greatly facilitate a search for functional homologies and corresponding network architecture. Finally, there seems to be a discrepancy between results obtained with human imaging and monkey electrophysiology. Recent human fMRI reports showed contralateral tuning of cue and memory, but not saccade, responses in the parietal and frontal cortex (Schluppeck et al. 2006; Srimal and Curtis 2007). Contralaterality in the human brain seems less profound than would be expected from monkey single-cell recordings, leaving open the question of whether this discrepancy owes more to inter-species or methodological differences. This is important because hemispheric contralaterality constitutes a major organizational principle of space representation. Hence, analagous monkey fMRI studies are necessary in order to provide a solid link between large bodies of data accumulated with the two methods, and to better interpret BOLD activity in terms of neuronal responses.

Several groups have recently applied fMRI in alert monkeys, predominantly focusing on various aspects of visual perception during passive fixation (e.g., Denys et al. 2004; Dubowitz et al. 1998, 2001; Nelissen et al. 2006; Pinsk et al. 2005; Sawamura et al. 2005; Tsao et al. 2003; 2006; Vanduffel et al. 2002). In addition, two previous monkey fMRI studies mapped saccade-related activation patterns using blocks of closely-spaced visually guided saccades (Baker et al. 2005; Koyama et al. 2004), demonstrating a distributed network of frontal-parietal-occipital cortical structures associated with saccadic eye movements. However, a monkey fMRI study of delayed-response tasks, potentially comparable to electrophysiological and human event-related imaging experiments and that hence addresses the aforementioned issues, has not yet been attempted.

We therefore sought to provide the first direct comparison between monkeys and humans performing the same delayed visually and memory-guided saccade response

tasks, using a high-field 4.7 T vertical MRI scanner for monkeys and a 3 T scanner for humans. Extending previous monkey fMRI studies that utilized block design, we developed and applied an event-related approach similar to human imaging and monkey electrophysiological studies. This approach enabled the extraction of BOLD signal timecourses and the delineation of responses from different epochs within the task sequence—initial fixation, visual cue, delay period, saccade execution, reward expectation, and acquisition. In this study, we focused upon activation patterns during delay/memory periods that precede visually and memory-guided eye movements, and systematically analyzed the spatial tuning and relative contribution of each response component across many cortical areas. In both species, we found spatially specific contralateral signals that reflect maintenance and retrieval of working memory and/or specific motor plan, as well as non-specific preparatory signals when no information about upcoming movement direction was available. In addition to frontal and parietal areas traditionally implicated in delayed oculomotor tasks, regions situated in superior temporal sulcus showed a similar signal profile. We show that contralaterality tuning is stronger in monkeys than in humans, and that dynamics of the BOLD response differs between species

4.3 Results

Two monkeys and 11 human subjects were scanned with BOLD-sensitive functional MRI sequences while they performed two oculomotor tasks under real-time behavioral control: the memory-guided saccade task (memory trials) and the deferred visually guided saccade task (direct trials, Fig. 4.1A, B). Memory and direct trials, and different saccade directions were randomly interleaved. A detailed account of the subjects' training, behavior and task performance is given in Supplemental Data. An event-related design with long and sometimes variable delays separated contributions from different intervals in the trial and distinguished between rightward and leftward saccade directions (Fig. 4.1C). Thus event-based spatial statistical activation maps and BOLD timecourses could be extracted from the actual EPI volume data.

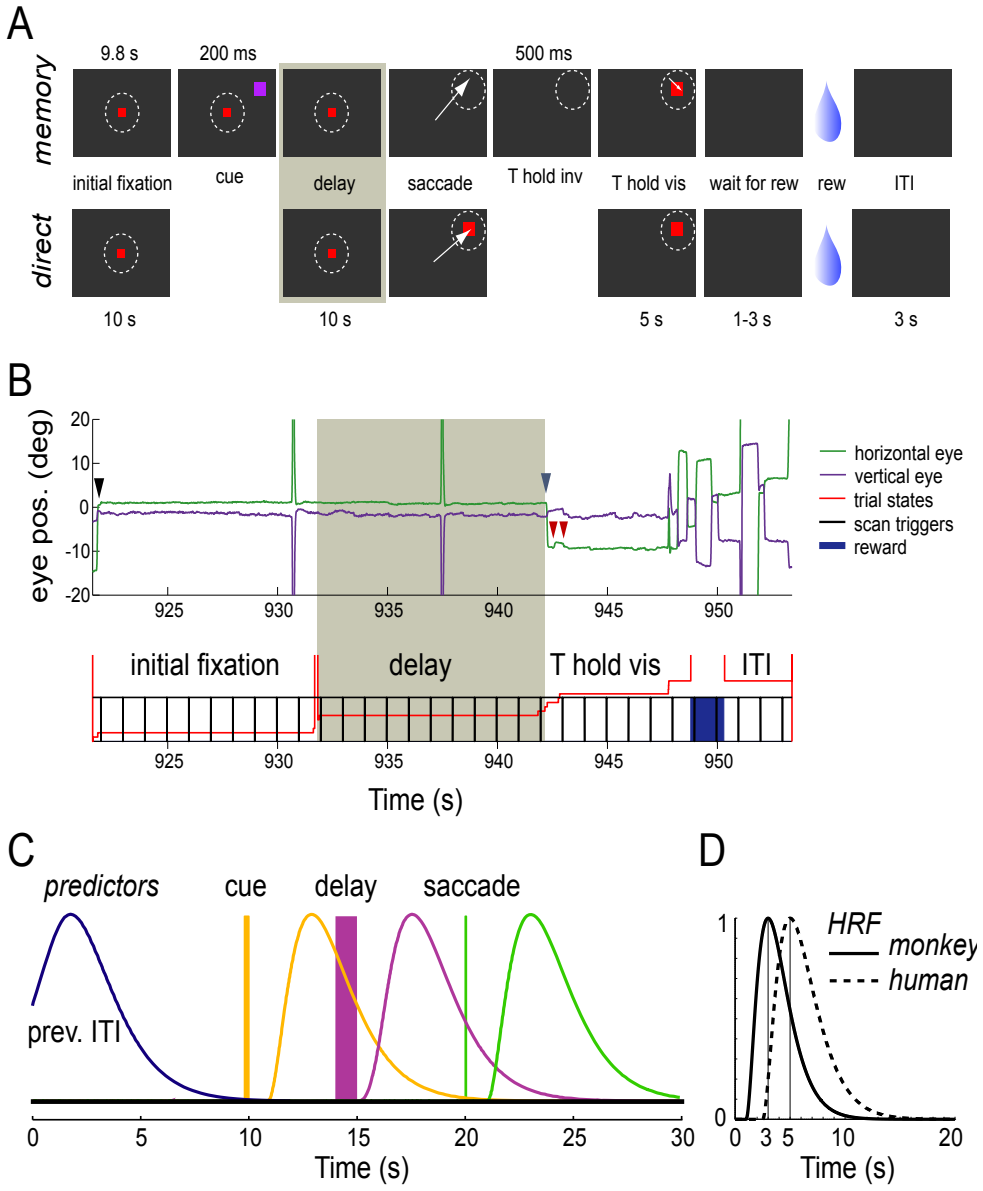
A
memory
direct
9.8 s
200 ms
500 ms
initial fixation
cue
delay
saccade
T hold inv
T hold vis
wait for rew
rew
ITI
10 s
10 s
5 s
1-3 s
3 s
B
eye pos. (deg)
horizontal eye
vertical eye
trial states
scan triggers
reward
initial fixation
delay
T hold vis
ITI
Time (s)
C
predictors
cue
delay
saccade
prev. ITI
Time (s)
D
HRF
monkey
human
Time (s)

Figure 4.1:

Oculomotor tasks, behavior, and event-related design. *(A) Timeline of events in memory-guided (memory) and deferred visually-guided (direct) saccade trials. Gray shaded area denotes memory delay period in memory trials and corresponding fixation delay period in direct trials. In memory trials, subjects remember the location of the cue and prepare a specific movement in advance. In direct trials, subjects can only mobilize non-specific readiness to make a saccade. Aside from visual effects of the cue, the difference between memory and direct trials would reflect these cognitive processes. Note that subjects were allowed to move their eyes during the wait for reward and intertrial interval (ITI) periods, causing strong activation in visual and oculomotor areas, evident in the first part of the baseline fixation (see Figs. 4.4, 4.5). (B) Example of eye position and trial event recordings in one (memory) trial in monkeys. Gray shaded area denotes the memory delay period. Upper panel: eye position. Saccades are denoted by inverted triangles above eye position traces. Note two corrective saccades that followed instructed the memory saccade, a characteristic behavior in both monkeys (see eye movement recordings and behavior). Lower panel: trial states, triggers from scanner (repetition time TR 1 s for each volume), and trigger for the liquid reward dispenser. Because of very long trials and thus a relatively small number of trials (∼200/session), each reward was large: ∼1 ml. (C) Model predictors for the GLM computation in monkeys after convolution with the monkey HRF (see D). Memory trial predictors are shown. Direct trials had fixation delay and saccade, but no cue, predictors. Different directions were modeled with separate predictors. Only predictors of interest for the current study are shown. Human predictors had the same structure, but were convolved with a standard Boynton HRF (see D). (D) Standard single gamma Boynton HRF function used for monkeys: δ=1, τ=1, n=3 (solid line), and for humans: δ=2.5, τ=1.25, n=3 (dashed line). The monkey HRF rises and returns to the baseline faster than the human HRF time to peak 3 and 5 s, respectively. Different HRFs (e.g., a difference of 2 gamma functions, that includes stimulus undershoot) were tried, which resulted in very similar activation maps.*

Hypothetically, these time-courses should approximate the dynamics of the underlying neuronal population activity. This study primarily concerns responses in cortical areas (Fig. 4.2A), first presenting results from monkey experiments and then from analogous human experiments.

Spatial Distribution of Cue, Delay, and Saccade Activity

Fig. 4.2B shows main cortical regions activated by the visual cue in memory trials (no cue was present in direct trials). To demonstrate the consistency between two monkeys, activation maps are separately illustrated for each subject. Cue activation maps overlapped significantly with a more extensive network of saccade-activated areas (Fig. 4.2C). Regions showing memory delay activation comprised a subset of cue and saccade responsive areas (Fig. 4.2D).

Saccade activation maps resembled those of earlier studies using block design experiments (which compared blocks of continuous fixation versus series of saccades; Baker et al. 2006; Koyama et al. 2004), confirming the ability to elicit robust activation patterns with the event-related approach of this study. These maps corroborated the activation of areas reported in the above fMRI studies during saccade execution—namely, dorsal and ventral premotor cortex. In addition, consistent saccade activation in the medial parietal area MP (7m) and in the posterior cingulate sulcus (area 23a) was revealed, in agreement with electrophysiological reports (Dean et al. 2004; Thier and Andersen 1998). Interestingly, areas 24b/a of the anterior cingulate sulcus showed significant activation as well. Neurons in anterior cingulate respond during oculomotor tasks in the context of performance monitoring, reinforcement learning, and reward processing (Ito et al. 2003); the observed activation during repetitive and well-learned tasks is surprising. Conceivably, after long demanding delays monkeys more actively monitored their responses, associating correctly performed saccades with the upcoming reward.

Many regions in FEF, SEF, anterior cingulate (preSMA/SMA/area 24c), LIP, caudal and mid sts (MT, MST, FST, TPO), PO, and in striate and extrastriate

visual areas were more strongly recruited by memory saccades than by direct saccades (Fig. 4.5). In frontal and parietal areas, stronger activation may reflect greater memory-related and/or performance-monitoring processing. However, in addition to oculomotor processes underlying saccade preparation and execution, 'saccade' activation includes visual activation elicited by the peripheral target appearance, visual 'motion' stimulation during saccadic eye movement, and acquisition of the target. Visual activation following memory saccades may differ from the direct saccade activation since in the former case: (1) the confirmation target became visible 500 ms after the acquisition of the remembered cue location, and (2) monkeys often made additional corrective saccades before and following target re-appearance. Consequently, many early visual areas showed increased activation for memory saccades. These consideration thus confound the interpretation of the differences between memory and direct saccade activation patterns.

To extract areas that differentially responded during memory as compared to fixation delay periods, delay-period activity in memory and direct trials was collapsed over all directions, similar to work done previously in humans (e.g., Brown et al. 2004). In order to separate the influence of the cue, delay predictors assayed for statistical maps (for memory>fixation delay contrast) encompassed only the second part of the delay period (see Fig. 4.1C). Using this approach, only a few small regions showed increased activity during memory trials (Fig. 4.2D): frontal—FEF, dlPFC, SEF, and area 24c in anterior cis; posterior parietal—LIP. In monkey R several areas in sts, including putative area TPO (or STP) located in the dorsal bank of mid sts, also displayed increased memory activation (in monkey G, whose brain was longer in the vertical dorsal-ventral dimension, the functional slice package did not extend ventrally enough to cover the comparable sts region, and neighboring areas did not show this effect, explained in more detail later).

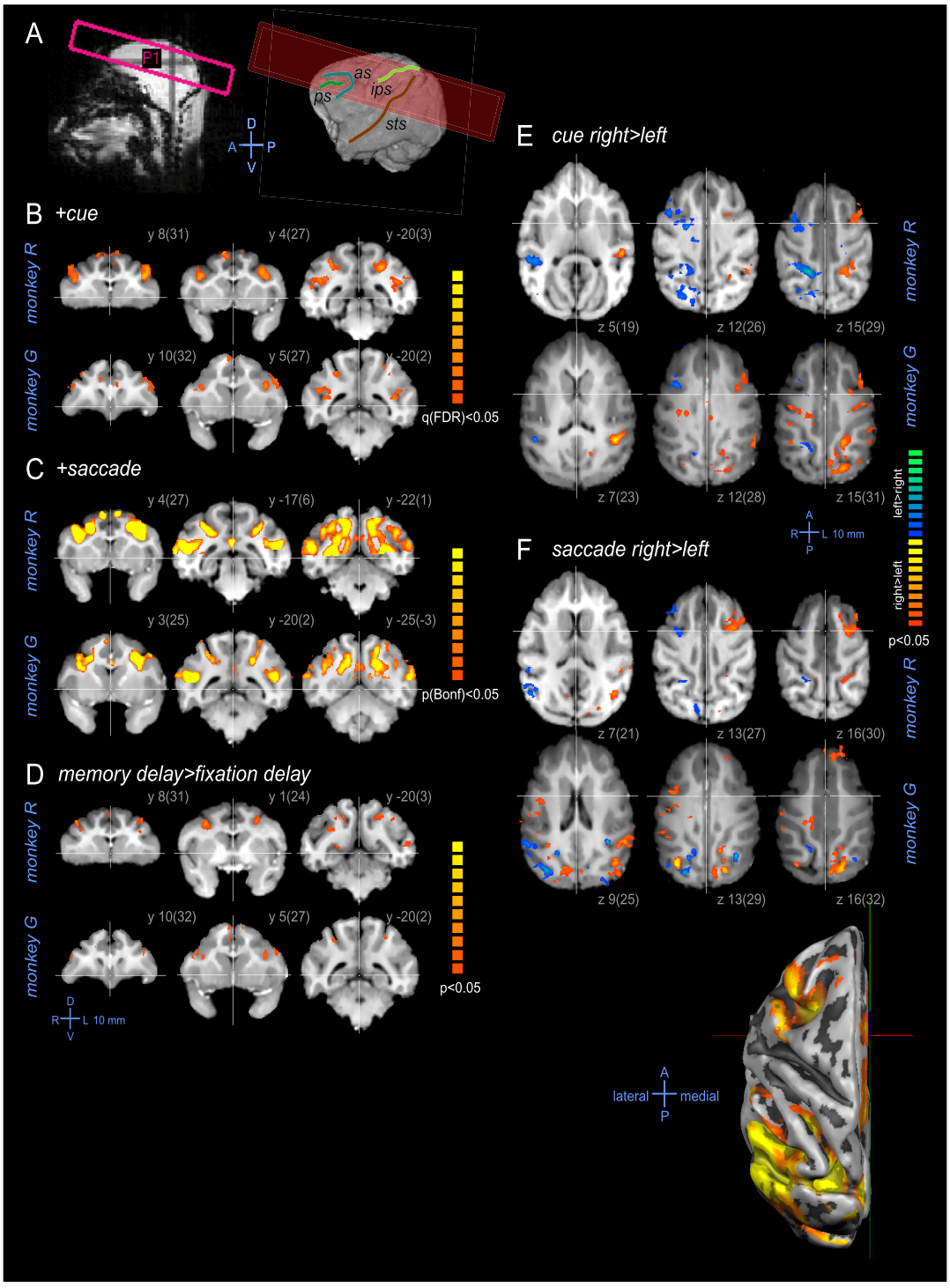
A
P1
as
ips
ps
sts
D
A
P
V
B +cue
monkey R
monkey G
y 8(31)
y 4(27)
y -20(3)
y 10(32)
y 5(27)
y -20(2)
q(FDR)<0.05
C +saccade
y 4(27)
y -17(6)
y -22(1)
y 3(25)
y -20(2)
y -25(-3)
p(Bonf)<0.05
D memory delay>fixation delay
y 8(31)
y 1(24)
y -20(3)
y 10(32)
y 5(27)
y -20(2)
p<0.05
R L 10 mm
E cue right>left
z 5(19)
z 12(26)
z 15(29)
z 7(23)
z 12(28)
z 15(31)
left>right
F saccade right>left
z 7(21)
z 13(27)
z 16(30)
z 9(25)
z 13(29)
z 16(32)
right>left
p<0.05
lateral
medial

Figure 4.2:

Spatial distribution of cue, memory, and saccade activity. *(A) Schematic of functional slice package positioning (20 mm, 10x2 mm adjacent slices, 15 angle) used in both monkeys, overlaid on the sagittal plane of the pilot localizer scan. The same slice package is shown on the 3D reconstruction of the brain surface (monkey G). Major sulci of interest for this study are depicted: ps—principle, as—arcuate, ips—intraparietal, sts—superior temporal. (B–D) Cortical areas that were significantly activated using +cue, +saccade, and memory>fixation delay contrasts, shown in 3 coronal sections. Activation sites for the cue (B) included frontal eye fields (FEF, areas 8 and 45) in as, dorsal lateral prefrontal cortex (dlPFC) in ps, dorsal and ventral premotor cortex (PMd, area F2 and PMv, posterior bank of lower as, areas 44 and F5), supplementary eye fields (SEF), lateral intraparietal area (LIP) in ips, and areas MT, MST, TPO (STP according to nomenclature of Felleman and Van Essen 1991), and Tpt in sts. Saccade activation (C), in addition to the areas listed above, also was detected in anterior and posterior cingulate (cis, acis, and pcis), ventral intraparietal area (VIP) and (weakly) in medial intraparietal area (MIP) in ips, area 7a in inferior parietal lobule (IPL), area 7m in medial parietal cortex (MP; Thier and Andersen 1998), areas V3/V3A, PO and LOP (parieto-occipital and lateral occipital parietal) located at the junction of ips and parieto-occipital sulcus (pos) and in the fundus of pos, dorsal parietal area (DP) at the junction of ips and lus and in extrastriate areas V2, V3/V3d, and V4 in the lunate sulcus (lus). EPI signal drop-out caused by headcap implants cancelled the activation in operculum V1 and in some V1/V2 areas located in the posterior bank of lus and calcarine sulcus (cas). Memory-related activation (D), without discrimination to leftward/rightward trials, was localized in FEF and in small clusters in SEF, acis, LIP, and TPO and Tpt in sts (sts ROIs not shown in the example slices). In monkey G this contrast did not reach a statistical significance with multiple comparison correction, therefore uncorrected maps are shown. (E) Map for the cue right versus left contrast for memory trials, shown on axial sections. (F) Map for the saccade right versus left contrast (direct and memory saccades combined). In this and all other figures, axial and coronal brain slices are shown using radiological convention (L=left hemisphere is on the right side). In sagittal slices, left corresponds to rostral/anterior (A). All monkey brain images are shown in AC-PC bicommissural plane coordinates (AC xyz 0,0,0: x—left to right, y—posterior to anterior, z—ventral to dorsal). The location of the origin is denoted by the cross-hair. The number next to each slice shows the coordinate of the section relative to the AC origin, the number in parentheses is the position in stereotaxic coordinates, relative to the interaural line. The color bars code significance t-value, the minimal statistical threshold is shown below. Either Bonferroni (p) or less conservative False Discovery Rate (FDR; Genovese et al. 2002, denoted by q) correction for multiple comparisons was employed. In (E) and (F), 'hot' (red-yellow) colors denote positive activation for the rightward>leftward contrast, and 'cold' (blue-green) colors - positive activation for the leftward>rightward contrast. **The reconstructed left hemisphere of monkey G shows cortical distribution of saccade responses*

Maps for the memory delay rightward versus leftward contrast for memory trials. *(A) Localization of ROIs in the frontal cortex in ps and as (lower limb asl, upper asu). Left sequence of coronal sections going from anterior (bottom) to posterior (top) show designated areas that had significant contralateral memory activation: dlPFC (area 46d/v), FEF (area 8A), and PMd in arcuate spur ('hot'/'cold', map as in Fig. 4.2E,F). To the right, several sections show areas that were active only during cue and/or saccade periods (magenta-brown map: +saccade contrast): areas 44 and 45 in asl, area 8B and PMd in asu. (B) Localization of ROIs in the posterior parietal cortex. Location of coronal slices across ips portion containing LIP is shown by yellow cross sections on the sagittal slice. Most posterior (caudal) LIP in the ips branches parallel to the midline was denoted pLIP and may correspond to area CIP or PIP. Note that anterior portion of LIP (aLIP) is distinct from AIP, which was not activated in our experiments. (C) Localization of ROIs in parieto-temporal cortex along superior temporal sulcus (sts). Location of coronal slices along sts is shown by yellow line sections on the sagittal slice. Areas and subdivisions (zones) are denoted according to Nelissen et al. (2006) and Saleem and Logothetis (2007). The exact partitioning of MST area is currently not clear (Van Essen 2004) and may depend on the functional tests used for parcellation (MSTd and MSTl, Komatsu and Wurtz 1988; MSTc and MSTp, Boussaoud et al. 1990; MSTdp, MSTm, and MSTl, Lewis and Van Essen 2000). MSTd occupies the anterior dorsal bank of sts. Ventral part of MSTv, located in the floor of sts, roughly corresponds to MSTl of Komatsu and Wurtz 1988 (Tanaka et al. 1993). MT is located in the posterior ventral bank of sts. More anterior along the sulcus, superior temporal polysensory (STP) cortex (area TPO) is situated in the dorsal bank of sts, and further down the sulcus, the temporal-parietal area Tpt is located. In the right ips and sts of monkey G, only a few voxels reached the minimal statistical significance ($p<0.05$) for the leftward>rightward memory delay contrast. Nevertheless, the contralateral delay activity in right LIP and TPO/Tpt was evident in ERA BOLD timecourses (Fig. 4.5).*

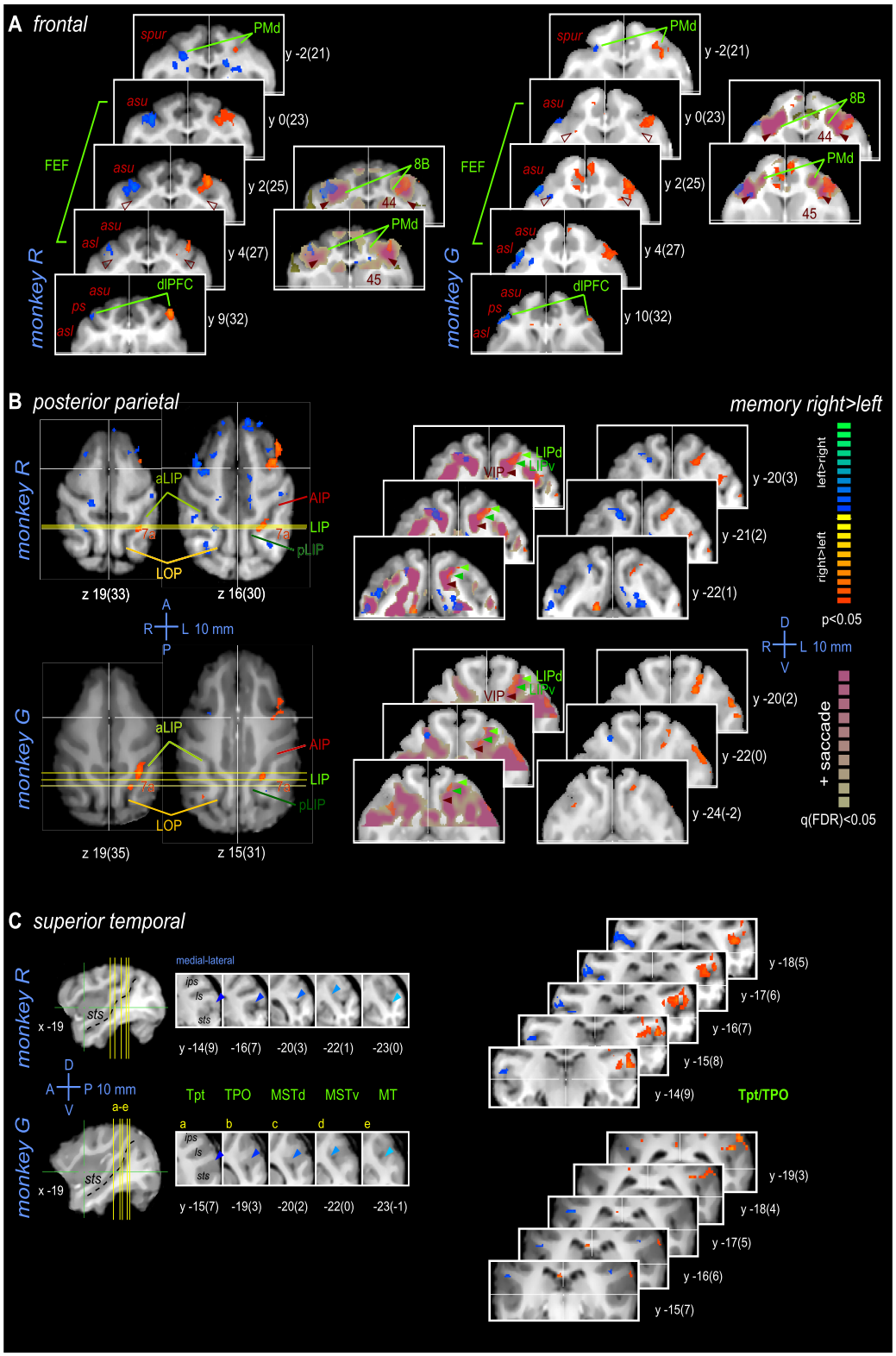
A frontal
spur
PMd
y -2(21)
asu
y 0(23)
FEF
y 2(25)
8B
44
asl
y 4(27)
45
ps
dlPFC
y 9(32)
monkey R
y 10(32)
monkey G
B posterior parietal
memory right>left
aLIP
AIP
LIP
pLIP
LOP
7a
z 19(33)
z 16(30)
A
R L 10 mm
P
VIP
LIPd
LIPv
y -20(3)
y -21(2)
y -22(1)
left>right
right>left
p<0.05
D
V
y -20(2)
y -22(0)
y -24(-2)
+ saccade
q(FDR)<0.05
z 19(35)
z 15(31)
C superior temporal
medial-lateral
ips
ts
sts
x -19
y -14(9)
-16(7)
-20(3)
-22(1)
-23(0)
P 10 mm
a-e
Tpt
TPO
MSTd
MSTv
MT
a
b
c
d
e
y -15(7)
-19(3)
-20(2)
-22(0)
-23(-1)
y -18(5)
y -17(6)
y -16(7)
y -15(8)
y -14(9)
Tpt/TPO
y -19(3)
y -18(4)
y -17(5)
y -16(6)
y -15(7)

Figure 4.3:

With all target directions pooled together, most activation patterns were bilaterally symmetric, suggesting no hemispheric lateralization of functions involved in these tasks. Yet, large proportions of neurons in multiple oculomotor areas exhibit contralateral directional tuning (e.g., Barash et al. 1991b; Funahashi et al. 1989). If the same is true for the BOLD responses representing a population effect, ipsilateral (i.e. in the left hemisphere for leftward and in the right hemisphere for rightward trials) activity would be expected to be less than contralateral activity. To assess the degree of spatial selectivity on a population level, we generated maps for right vs. left comparisons for each of the three time intervals of interest: cue, memory delay, and saccade response epochs. Most areas that exhibited cue and memory activity - dlPFC, FEF, LIP and several clusters in sts - also showed contralateral preference in these epochs (Fig. 4.2E - cue; Fig. 4.3 -memory). Selectivity for saccade directions (either ipsi- or contralateral) was prominent in retinotopically organized visual areas, and weak preference for contralateral saccades was observed in parietal and frontal areas (Fig. 4.2F). In the next section we present in-depth analysis of spatial specificity using time-courses extracted from these areas.

Timecourse of BOLD Activity

The activation maps for different response intervals, established in the preceding section, suggest that the temporal distribution of BOLD activity varies between different areas. To examine underlying BOLD signal timecourses, event-related averages (ERA) were computed for the two trial types and for rightward and leftward saccade directions, resulting in 4 different curves from each functionally and anatomically defined region of interest (ROI). This analysis is similar to constructing a peri-stimulus time-histogram of neuronal firing. A typical ERA example expressed in %BOLD change relative to the baseline (last 3 s of the initial fixation period) is shown in Fig. 4.4A and B for the ROIs localized to the left and right FEF in as, respectively.

The high signal magnitude in all 4 curves in the first few seconds of the initial fixation period is attributable to the activation caused by saccades and accompanying

visual stimulation in the preceding ITI. This component could be high or low, depending on area's response properties (Fig. 4.5). As the trial advances while central fixation is maintained, the BOLD signal gradually returns to the baseline. At the time 9.8 s, the 200 ms peripheral cue is flashed in memory trials, and subsequent memory delay (or a corresponding fixation delay in direct trials) continues for another 10 s (or variable time between 6 and 12 s). Transient time-locked cue responses typically lasted only up to 5 s, and were often separated by a trough from the rest of delay period activity, which manifested as a separate peak or as sustained activity in the late memory period. At time 20 s, the monkey makes an eye movement, and corresponding saccade response appears as another transient time-locked peak of high magnitude. This 3-component (cue-delay-saccade) response was characteristic across many oculomotor areas active in the task, though some areas had only a 2-component (cue-saccade) or only saccade response (Fig. 4.5). The activation peak subsequent to saccade response corresponds to the end of target fixation and free eye movements during reward expectation, delivery, and ITI.

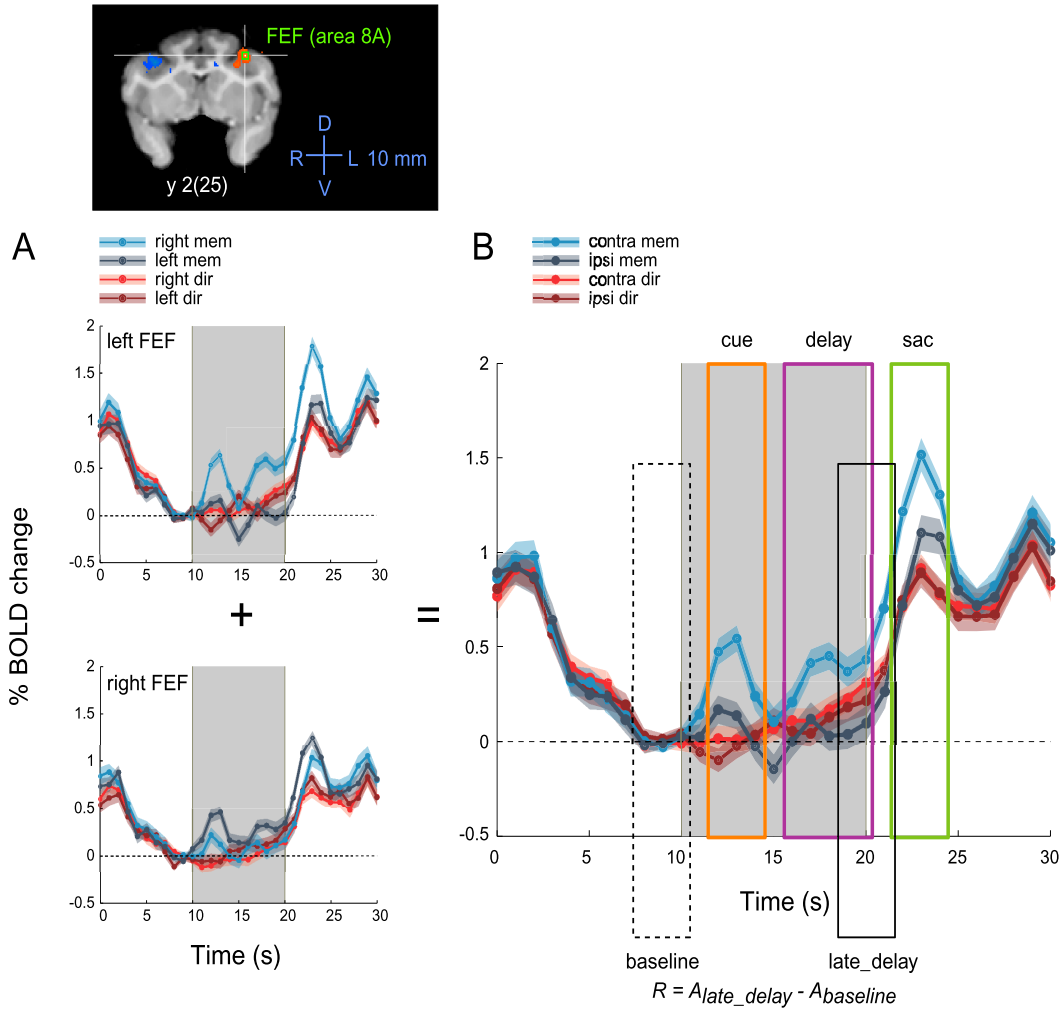

Figure 4.4:

Event-related averaging (ERA) of trial timecourses and analysis of frontal ROIs. *(A) ERA timecourses from left and right FEF and (B) combined contra-ipsilateral timecourses for bilateral, left and right ROIs. The bilateral combined arrangement is used through the rest of the paper. Colored rectangles denote corresponding intervals (cue, delay, and saccade) used for estimating mean response amplitudes and calculating the CS index. Black dashed and solid rectangles—baseline and late delay, respectively—denote intervals used for calculating the R index. The trough and subsequent peak after the saccade response correspond to the peripheral target fixation and free eye movement behavior during reward expectation, delivery, and ITI. Note that jaw movement and licking during reward cause significant field distortions and affect the shape of BOLD responses. However, this does not occur until 6 s after the instructed saccade and thus saccade responses were not contaminated by these artifacts. In this and other monkey ERA plots, shaded bands denote s.e.m across trials.*

In memory trials, contra- and ipsilateral BOLD signals diverge in the cue and especially in the memory intervals, the response amplitude being significantly higher for contralateral than ipsilateral conditions. The activation in the second half of the memory period reflects planning processes such as spatial working memory for the recent cue and saccade preparation. In contrast, there was no systematic difference between contra- and ipsilateral curves in direct trials, since no knowledge about the direction of upcoming response was available to subjects until the end of the fixation delay period. To quantify these patterns, timecourses from left and right ROIs (Fig. 4.4B) were combined, and the mean response strength was calculated to derive a contraversive selectivity index (CS, Experimental Procedures) for each of the three intervals of interest (cue, memory/fixation delay, saccade), and for each of the two trial types. The CS measures the normalized amplitude difference between contralateral and ipsilateral responses in specified intervals. In the example shown in Fig. 4.4, the memory trial CS is high for cue and memory intervals (0.64 and 0.81, respectively), low for the saccade interval (0.17), and near zero for corresponding periods in direct trials.

In addition to the activity increase during the memory periods preceding contralateral memory saccades, many areas exhibited a ramping of activity towards the end of fixation delay period in the direct saccade trials. In this condition subjects did not know the direction of the upcoming saccade (and could not reliably predict it because we used 8 or 18 randomized locations). Therefore we hypothesize that it may reflect a non-specific motor preparation/anticipation. To quantify this effect, a ramping index (R, Experimental Procedures) was calculated that estimates the activity prior to the saccade response relative to the fixation baseline, in %BOLD signal change. Note that in the example in Fig. 4.4, as in many other areas, there was almost no ramping for the ipsilateral memory trials.

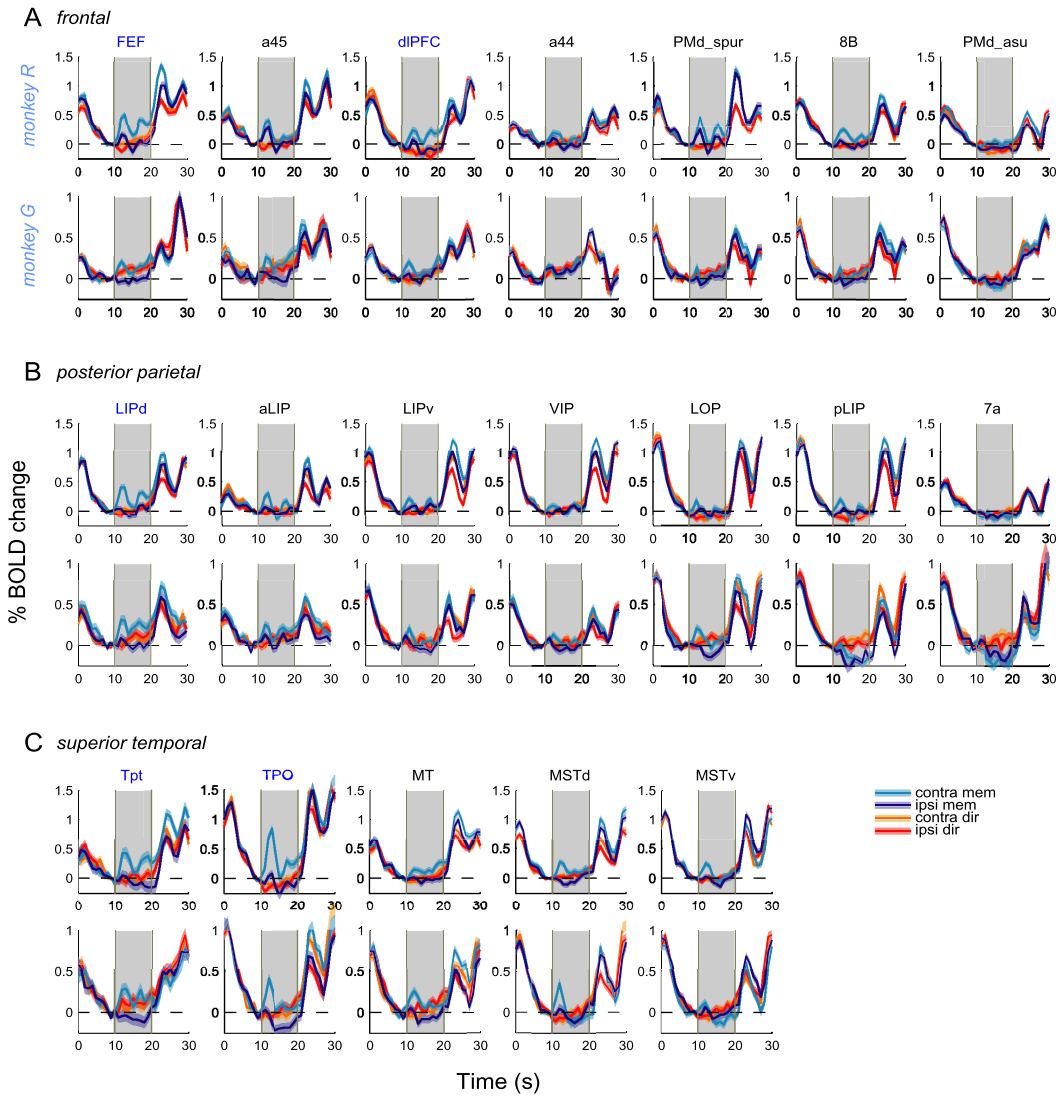

Figure 4.5:

ERA BOLD trial timecourses in selected frontal, posterior parietal, and parieto-temporal sts cortical areas. *Conventions are the same as in Fig. 4.4B. Blue-marked areas (FEF, dlPFC, LIPd, Tpt, and TPO) denote ROIs that exhibited the significant contralateral memory delay activity in both monkeys.*

To characterize the dynamics, relative contributions, and tuning of cue, delay, and saccade activity, a detailed region-of-interest analysis in the areas defined by the statistical mapping procedure, in combination with known anatomical landmarks, was performed (Figs. 4.2, 4.3). For each interval, the strength and the contralaterality of responses was assessed. In frontal cortex, dlPFC (area 46, along ps), and area 8A (FEF) in upper limb of as (asu) showed strongest contralateral cue and memory activation and high but weakly contralateral memory saccade responses (Fig. 4.5A; see Fig. 4.3A for localizations). Area 8B in asu had weaker cue and memory responses, but these responses exhibited contralaterality. Area 45 in the dorsal bank of asl had strong contralateral cue, but weaker memory activity, and area 44 in the ventral bank of asl showed weak cue and mostly saccade activity. Area 6 (F2) in PMd along asu showed only weak saccade response, but more posterior subdivision of PMd in the arcuate spur also had contralateral cue and memory responses. In all frontal areas, the direct saccade response was not spatially tuned, suggesting that weak contralaterality of memory saccade response could be residually carried over from the delay period. Non-specific ramping was present in both monkeys in areas FEF, 8B, 45, 44, and PMd spur. Non-specific ramping was more pronounced in monkey G, but spatially specific contralateral ramping was comparable between monkeys.

Activation in SEF and more ventrally in preSMA (area F6) was present in both monkeys, but the BOLD signal time-courses were noisier than in as and ps. This could be a consequence of lower SNR and partial signal dropouts caused by proximity to the surface beneath the headcap implant; and also because SEF may not be very active during simple highly overtrained tasks (Koyama et al. 2004). However, in both monkeys cue and robust saccade responses were present, and in monkey R both SEF and preSMA exhibited some contralateral memory delay activity.

In posterior parietal cortex (PPC, Fig. 4.5B; see Fig. 4.3B for localizations), the lower part of dorsal LIP (LIPd—Blatt et al. 1990; Lewis and Van Essen 2000) in the posterior third portion of ips exhibited strongest contralaterality in cue and delay intervals in memory trials. These activation loci correspond well to the histological verification of recording sites with sustained mnemonic/planning activity (e.g., Gnadt

and Andersen 1988). There was a systematic gradient of relative cue, memory, and saccade response amplitudes along the sulcus (i.e., in posterior-anterior direction) and dorsal-ventrally into the depth of the sulcus: the cue and delay activity progressively declined while the saccade response remained approximately at the same level (apart from a weaker saccade response in anterior LIP). Thus, ventrally from LIPd, LIPv showed weak contralateral cue and memory delay response, but the most ventral LIPv and/or area VIP in the fundus of ips showed a saccade response but no cue or memory components. While anterior LIP (aLIP) had weak cue and memory responses, areas caudal to LIP, such as posterior LIP (pLIP) and LOP, showed even weak cue, almost no memory, but equally strong saccade responses. In both monkeys, the non-specific ramping in direct trials was most pronounced in LIPd, but in monkey G it was also present in aLIP. In both trial types, an initial activation caused by uncontrolled eye movements/visual stimulation during the preceding ITI was strongest in posterior ips and diminished towards the anterior portions of the ips.

Since our functional slice package did not include the topmost part of the parietal lobule (Fig. 4.2A), the upper part of dorsal LIP and most of the surface area 7a was not covered. Regions in the area 7a located on the lateral surface of inferior parietal lobule and in the anterior bank of sts exhibited mostly saccade response and no cue or memory response, consistent with electrophysiological findings (Barash et al. 1991a; Andersen et al. 1990). In contrast to frontal cortex, all posterior parietal areas except 7a showed contralateral tuning for both memory and direct saccades. The most anterior portion of ips (area AIP) was not significantly activated in any of the three intervals, including saccades (cf. Durand et al. 2007).

In the superior temporal sulcus (sts, Fig. 4.3C, see Fig. 4.5C for localizations), areas MT and MST showed strong saccade responses and weaker cue responses, but no or little delay activity (see Constantinidis and Procyk 2004). Ventral MST (MSTv—Komatsu and Wurtz 1988; Nelissen et al. 2006; Tanaka and Saito 1989) had contralateral tuning for cue but weakly ipsilateral for saccade direction, while dorsal MST (MSTd) and MT showed contralateral tuning in both intervals. This distinction may be related to functional differences between two subdivisions of MST: MSTd is

thought to be specialized for optic flow analysis related to self-movement perception, while MSTv is involved in processing the motion of discrete objects passing through the visual field (Logan and Duffy 2005). Alternatively, it can be a consequence of the retinotopic organization: MSTv mainly represents the peripheral visual field, while the area adjacent to MSTd as defined by Nelissen et al. (2006) represents the central field and was included in our delineation of MSTd.

Further down sts, polysensory areas TPO (or STP) and Tpt, located in the anterior dorsal bank, also showed strong contralateral cue and weakly contralateral saccade responses and, unexpectedly, sustained delay activity for contralateral memory trials. All areas in sts showed some non-specific ramping in direct trials. Area FST, located in the fundus of sts, was only partially covered by our imaging slices and is not discussed here.

Response amplitude and contraversive selectivity (CS) in different trial intervals and the ramping index (R) are summarized across areas in Fig. 4.6. The CS and R plots should be considered together: since CS is a relative and normalized measure, it does not reflect the variations in response strength. The ramping index (in %BOLD change) and the difference between contralateral ramping in memory trials and average ramping in direct trials can serve as a reference. Although many areas show contralateral tuning of cue and memory responses, in both monkeys only LIPd, FEF, dlPFC, and TPO/Tpt displayed contralateral memory delay activity significantly higher than the non-specific ramping. Cue and memory tuning co-varied, and there was a correlation between cue and memory response amplitudes ($r=0.83$, $p<0.05$), but no significant correlation between memory and saccade response amplitudes ($r=0.42$, $p>0.05$).

Finally, several medial areas did not show any clear contralateral preference (or our spatial resolution was not fine enough to dissociate left and right hemisphere divisions of these midline structures). Therefore we combined corresponding time-courses with combined rightward, leftward, and additional up/down trials, to probe for non-specific ramping in anterior and posterior cingulate and in medial preSMA; however none of these areas exhibited any such trends in direct trials.

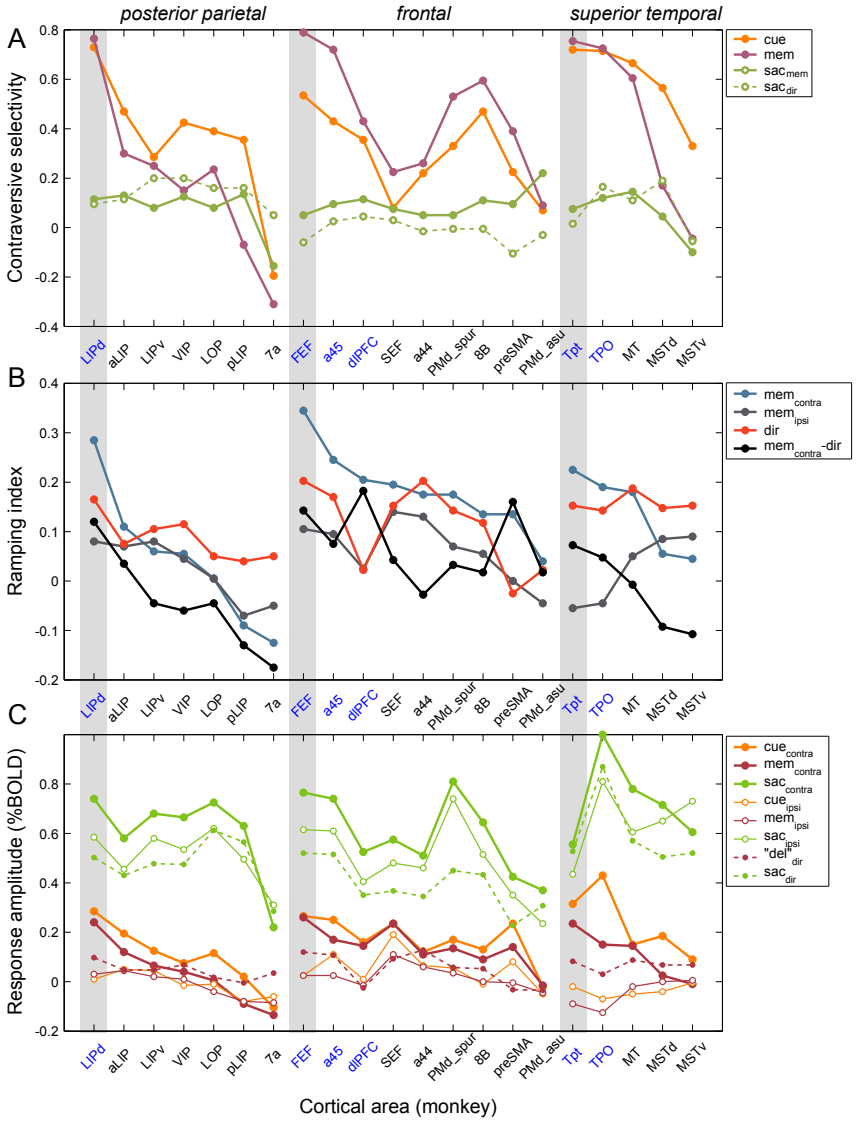

Figure 4.6:

Summary of contraversive selectivity *(A) and ramping indices (B) derived from the response amplitude estimates (C) averaged across two monkeys. Areas that exhibit strong contralateral memory delay activity are marked in blue.*

Comparison with Human Imaging Data

To directly compare results in monkeys to human imaging data, we conducted memory/direct saccade experiments in 11 human subjects: 8 subjects were tested with randomized variable delay periods of 6, 10, 14, and 18 s. Variable delays were employed to better separate initial cue response from subsequent memory delay activity (see Schluppeck et al. 2006). Additionally, 3 control subjects were tested with a fixed 14 s delay, to isolate potential behavioral effects of variable delay periods. The results from the fixed delay experiment corresponded to the results for the same delay in the variable delay experiment; therefore for brevity we present here only variable delay data from 8 subjects.

A plethora of areas reported in previous studies (e.g., Astafiev et al. 2003; Brown et al. 2004; Curtis and D'Esposito 2006) were activated during cue, memory delay and saccade response periods. Here we focus on several regions in PPC along ips and in superior parietal lobule (SPL), and human FEF complex, which are considered plausible candidates for functional homology to monkey areas LIP and FEF. These regions showed robust cue, saccade, and sustained memory delay activity (Fig. 4.7A,C). Several other prefrontal—SEF, dlPFC, pIFG—and inferior parietal and temporal areas—SMG, STG, and sts—exhibited robust cue and saccade activity and varying levels of memory activation.

We searched for evidence of contralateral organization in the cue and memory responses. However, we did not detect a comparable level of contralaterality as in monkeys using identical techniques (statistical mapping and ROI ERA timecourses, see Supplemental Results). Most subjects did show some spatial tuning of cue and memory responses, but the effect was weaker. Often, contralaterality was stronger in one hemisphere, but weaker, not existent, or even reversed (i.e. ipsi>contra) in the other. For example, across many task-relevant areas, right cue and memory responses were stronger than left cue and memory responses in the left hemisphere; while this still held true in the right hemisphere, less of a difference existed between left and right signals (Fig. 4.7A, the left dorsal frontoparietal network is more significantly

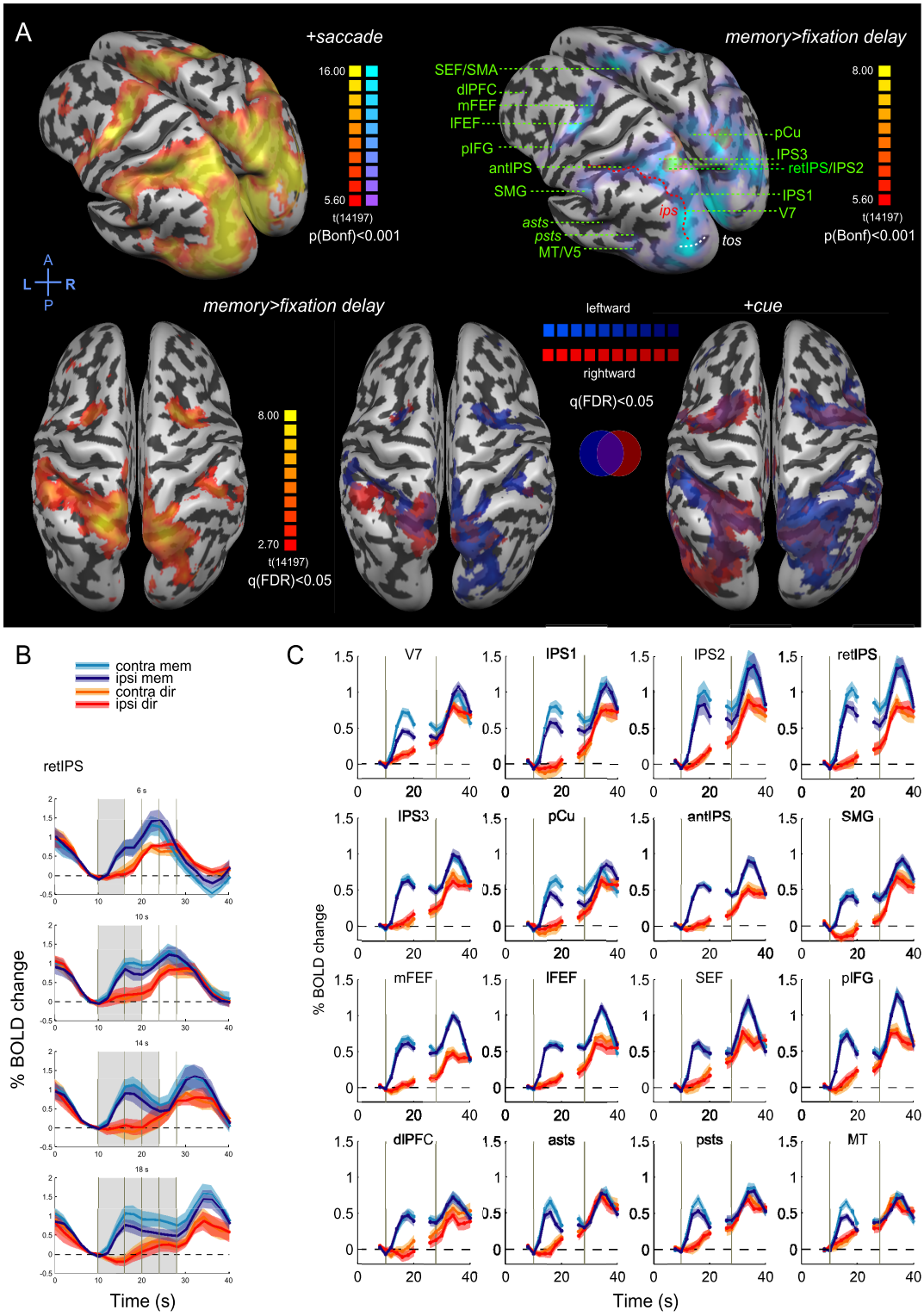
A
+saccade
16.00
5.60
t(14197)
p(Bonf)<0.001
memory>fixation delay
SEF/SMA
dlPFC
mFEF
lFEF
pIFG
antIPS
SMG
asts
psts
MT/V5
lps
tos
pCu
IPS3
retIPS/IPS2
IPS1
V7
8.00
5.60
t(14197)
p(Bonf)<0.001
A
L
R
P
memory>fixation delay
8.00
2.70
t(14197)
q(FDR)<0.05
leftward
rightward
q(FDR)<0.05
+cue
B
contra mem
ipsi mem
contra dir
ipsi dir
retIPS
6 s
10 s
14 s
18 s
% BOLD change
Time (s)
C
V7
IPS1
IPS2
retIPS
IPS3
pCu
antIPS
SMG
mFEF
lFEF
SEF
pIFG
dlPFC
asts
psts
MT
% BOLD change
Time (s)

Figure 4.7:

Human imaging results. *(A) Brain areas involved in the task. Statistical maps are superimposed on the inflated averaged brain of 8 subjects following cortex-based alignment. Top left: Saccade-activated network. Top right: cyan—+saccade contrast, transparency scales with significance of activation; yellow-red—memory>fixation delay most significant peaks. Bottom left: Memory>fixation delay contrast with lower (FDR) threshold. Bottom middle: Memory>fixation delay for leftward trials (shades of blue) and for rightward trials (shades of red). Purple signifies regions with overlap for leftward and rightward contrasts. Same representation is used for the +cue contrast (bottom right). 3D reconstructed partially inflated cortical surface is in neurological convention: left is left. (B) Example set of ERA contra-ipsi timecourses in 4 delay periods from bilateral ROI in retIPS (averaged across 8 subjects, shaded areas denote inter-subject s.e.m.). (C) ERA gap-plots for cortical areas involved in the task*

activated by maintaining rightward memory (red map); whereas the right hemisphere is activated by leftward and rightward trials (blue map)). This discrepancy between left and right hemisphere contralateral biases is consistent with the hypothesis that the left hemisphere codes predominately for right space, while the right hemisphere, for both hemi-fields (e.g., Mesulam 1999). But even when present, the tuning was modest—both hemispheres responded well in left and right trials. In PPC, the strongest contraversive selectivity was in medial SPL in anterior precuneus (pCu), putative "retinotopic IPS" (retIPS—Medendorp et al. 2006, Fig. 4.7B), IPS1 and IPS2 (Schluppeck et al. 2006), and higher visual area V7. Regions IPS3, anterior IPS, and IPL area SMG exhibited very little tuning.

Human frontal cortex showed even less contralaterality. Medial/superior FEF was more selective than lateral/inferior FEF. The dlPFC in superior frontal sulcus showed some residual tuning, and SMA/SEF and pIFG did not show any contralaterality, despite having some sustained memory responses. The temporal areas located in superior temporal sulcus and middle temporal gyrus (denoted anterior and posterior sts), and putative MT/V5 complex showed strong contralaterality for the cue but very little for the memory, and had minimal sustained memory activity.

As in monkeys, the human oculomotor network also showed the non-spatial specific ramping of activity towards the end of the fixation delay period in direct saccade trials. It is most clearly seen in long delay-trials (e.g., Fig. 4.7B) and in combined "gap" plots (Fig. 4.7C). This effect pervaded all parietal and frontal and some temporal areas that

were significantly activated in the task. In control regions not involved in the task, the timecourses did not show any consistent ramping pattern, signifying that this effect was indeed task related and not an extraneous global artifact (Supplemental Data). The timecourses in direct trials may also serve as a true baseline for spatially specific delay activation in memory trials. Figure 4.8 summarizes contraversive selectivity and ramping in human areas involved in the task, and compares contraversive selectivity in monkeys and humans in selected ROIs.

Finally, a difference in the timing of hemodynamic BOLD signals was apparent in the comparison of ERA timecourses between the two species: peak response latency to cue and saccade events was significantly longer in human than in monkey data, and the transition from cue to delay period activity was more gradual (Supplemental Results, Fig. 4.S2, see Discussion).

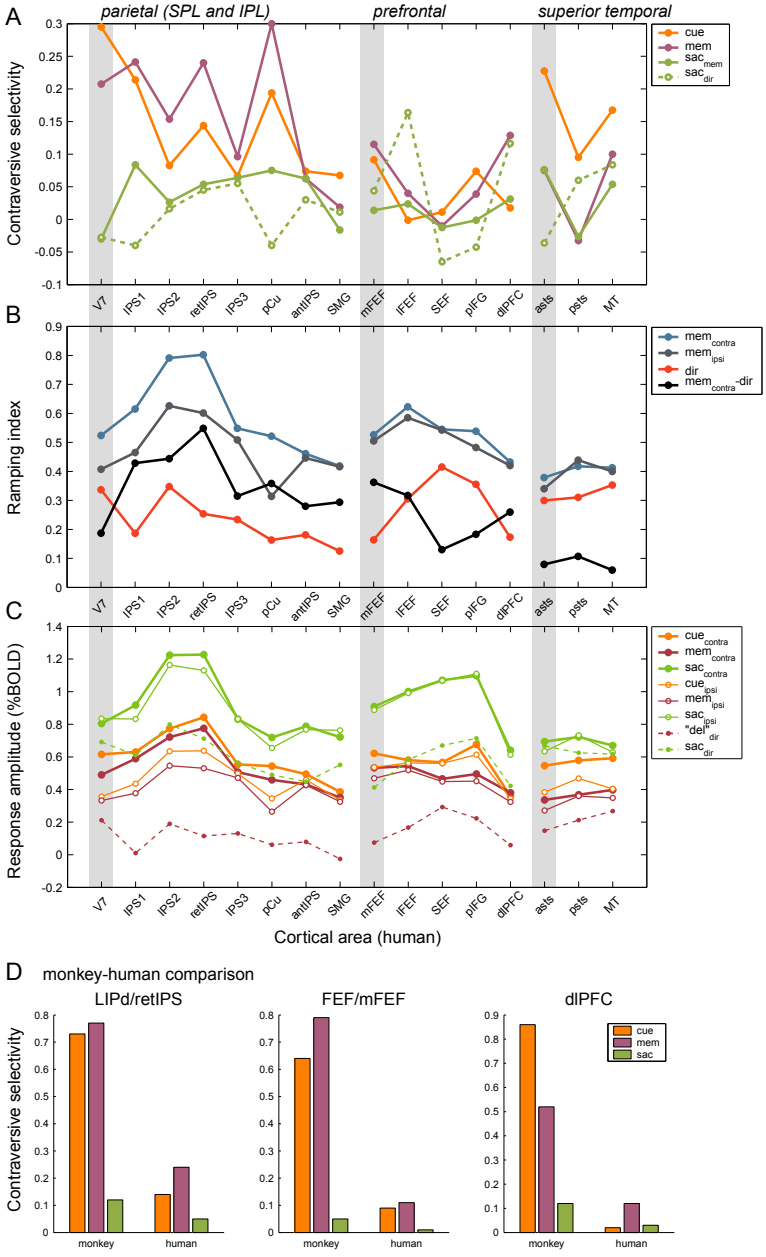

Figure 4.8:

Summary of contraversive selectivity *(A) and ramping indices (B) derived from the response amplitude estimates (C) averaged across 8 human subjects. For each subject, ERA timecourses were extracted using individual GLM ROIs, similarly to analysis in monkeys. (D) Monkey-human comparison of CS for memory trials in selected ROIs in parietal and frontal cortex (means of 2 monkeys and 8 humans)*

4.4 Discussion

We presented the first event-related fMRI study in monkeys that delineated timecourses from different epochs within the trial (see Supplemental Discussion for comparison with previous studies). This allowed us to quantify relative contributions of cue-, delay-, and saccade-related BOLD activity across different areas, in a manner similar to monkey electrophysiological studies and recent event-related imaging studies in humans. Using this approach, we detected delay period 'cognitive' signals that otherwise would be masked by stronger visual and motor events. Owing to this methodological innovation, our results contain several new findings. Both monkeys and humans exhibit two different types of delay activity. In memory-saccade trials, when the upcoming target position was known after the cue, spatial-specific, contralateral signals, which manifested as a separate peak or as sustained activation in the late part of memory delay period, were observed in areas dlPFC, FEF, LIP, TPO, and Tpt in monkeys and their putative functional homologs in humans. During fixation delay in deferred direct saccade trials, when no information about the direction of upcoming saccade was available but subjects anticipated a movement, non-specific build-up of activity towards the end of the delay was present in the same areas.

More specifically, our monkey data revealed: 1) stronger contralaterality of cue and delay period activity in monkeys as compared to humans; 2) a systematic gradient of cue, memory, saccade, and inter-trial activation along ips; 3) a separation of the initial cue response from the delay activity in the subsequent memory period; 4) strong cue response and presence of memory delay activity in sts; 5) contralateral tuning for memory saccades across most cortical areas, but only in parietal and parieto-temporal areas for direct saccades.

Finally, our results establish a link between sustained neuronal and BOLD signals that have been identified during delay periods in frontal and parietal areas of monkeys and humans. This link has been only assumed previously and had to be explicitly validated using time-resolved event-related fMRI in monkeys. The comparison of BOLD timecourses in monkeys and humans demonstrates differences in

the underlying hemodynamic response function and/or hemodynamic coupling to the neuronal activity. Below, these findings are discussed in the context of previous monkey electrophysiology and human imaging work.

Contralaterality in Monkeys and Humans

Our results in monkeys demonstrate strong contralateral specificity of cue and memory period responses, complementing pervasive (but often not systematic) electrophysiological evidence that a majority of neurons in areas dlPFC, FEF, and LIP have contralateral receptive fields (Barash et al. 1991b; Ben Hamed et al. 2001; Funahashi et al. 1989; Schall 1991). However, most human fMRI studies, including our dataset, show markedly less contralaterality. In phase-encoding (not event-resolved) experiments, the existence of spatial maps in frontal and parietal cortex has been shown (Hagler and Sereno 2006; Kastner et al. 2007, Schluppeck et al. 2005; Sereno et al. 2001; Silver et al. 2005), but these findings cannot be attributed to a specific epoch of a task, and provide no direct measure of tuning strength as compared to un-tuned activation. A few time-resolved event-related studies reported contralateral specificity of cue and memory responses in frontal but not parietal (Curtis and D' Esposito 2006) and in parietal (Schluppeck et al. 2006; Medendorp et al. 2006) areas, using different variants of delayed response tasks. Our data show weak contralaterality in several human parietal and frontal areas, agreeing with more recent investigations (Glidden et al. submitted; Srimal and Curtis 2007; see Supplemental Discussion). In all these human studies, the differential contra-ipsi signal modulates a larger un-tuned activation, in contrast to monkeys where the ipsilateral delay activity often stays near baseline level.

Except in early visual areas, the saccade response contralaterality was absent or very weak in humans (see Schluppeck et al. 2006); however, saccade contralaterality was present in monkeys, especially in posterior parietal and parieto-temporal areas, even in regions that were not tuned during the delay period. In monkey FEF and other frontal areas, direct saccades did not exhibit any contralaterality. Koyama et

al. (2004) reported statistically significant but weak contraversive tuning for visually guided saccades, most pronounced in dorsal LIP and FEF in monkeys and in posterior SPL and FEF in humans. While their task most closely resembled our direct saccade condition, Koyama et al. used two consecutive saccades in the same direction, so a possibly greater attentional modulation or movement preparation may have also contributed to the observed contralaterality. The analysis of saccade response periods is further complicated by potential effects of gain fields (Andersen et al. 1985), since we required peripheral target fixation (target hold period) for several seconds, in order to separate effects of the preceding instructed saccade from subsequent return/ITI saccades. Further experiments specifically designed to test for contralaterality of the saccade response in specifically adjusted visual conditions (e.g., memory saccade without target confirmation, dark background) will directly address the issue of saccade response tuning.

We emphasize that the issue of contralaterality is not a mere technical matter of correlation between neuronal and fMRI data. The contralateral tuning demonstrates a major organizational principle for perception and action in a primate visual world that is inherently separated into two hemi-fields by the current gaze axis. In both monkeys and humans, the two hemi-fields are initially represented in a strict contralateral manner by the opposite hemispheres. The gradual progression from finely topographically organized early visual areas to a coarser, mainly contralateral, topography of parietal and frontal areas (Felleman and Van Essen 1991) may reflect a transformation from the 'local' visual processing to a 'global' representation of action space. The difference in contralateral tuning between species might stem from a few causes. The macaque brain is mostly symmetrical (both anatomically and functionally), and lesions of left or right hemispheres cause comparable contralateral deficits (Gaffan and Hornak 1997). The human brain, however, exhibits strong lateralization of many cognitive functions, most notably verbal processing, but also related to memorizing, selecting, preparing, and executing actions. Right hemisphere lesions cause a more severe, frequent, and persistent spatial neglect than left hemisphere lesions (Mesulam 1999). Global (left and right) versus local (left or right) allocation of at-

tention was found to increase activation in right but not left inferior parietal lobule (Cicek et al. 2007), while Khonsari et al. (2007) found saccade preparatory signals only in the left PPC, but execution signals confined to the right PPC. The effects of TMS over human PPC during memory-guided pointing also revealed hemispheric asymmetry (Vesia et al. 2006). The leftward bias in the visuospatial attention network (which overlaps with visual-oculomotor areas) during passive fixation has been reported in both hemispheres (Siman-Tov et al. 2007). It appears that the human cortex, confronted with new complex tasks, has evolved to become more lateralized and specialized, losing the original functional symmetry. This may have led to a more uniform representation of both ipsi- and contralateral fields in frontoparietal areas, due to more developed inter-hemishperic transfer, or as a result of 'more abstract' (less visual, e.g. verbally mediated) representation of space. Therefore, most human frontoparietal areas respond almost equally to stimuli in either hemi-field, or even show a bilateral bias to one side of space during the delay period.

The foci of strongly contralateral memory delay activation in monkeys were limited to specific frontal and parietal sites, while in humans the weakly tuned delay activity was more widespread, reflecting a more extensive visual-oculomotor network. Aside from potential technical considerations (i.e., more prolonged response to the cue in humans), this may imply a training effect (overtrained monkeys versus almost naïve humans). However, it may also reflect the overall increase in complexity of the distributed network that evolved to solve difficult tasks, but is still recruited even in simple eye movement paradigms.

Functions of Spatial-Specific Activation

Within monkey electrophysiology and human imaging fields there is an ongoing debate on the functional significance of delay activity: retrospective storage of visual information versus prospective coding of a motor plan, as well as on the relative contribution of frontal and parietal areas to each function. In PPC, studies in monkeys provided evidence for both coding schemes (e.g., Andresen and Buneo 2002; Gold-

berg et al. 2002; Mazzoni et al. 1996; Snyder et al. 2000), while human imaging studies that tried to distinguish between the two possibilities mostly support sensory representation of potential targets (Curtis et al. 2004; Curtis and D'Esposito 2006; Srimal and Curtis 2007; but see Lindner et al. Society for Neurosciences 2006). The present study does not directly address this issue, since the delay activity in the memory saccade trials can be attributed both to retrospective coding of the cue and/or prospective movement preparation. The presence of non-specific preparatory signals in direct trials, however, can be interpreted as indirect evidence for a role in movement planning, as it is very unlikely that the same areas would only encode retrospectively a spatial location in one task but carry preparatory signals in another task.

One of the most intriguing questions in the current research on goal-directed behavior is identification of functional differences between parietal and frontal components of the frontal-parietal network involved in the control of visually-guided actions. More specifically, what are the differences between FEF and LIP in various oculomotor tasks (and PMd and PRR for reach tasks)? In the present study, we did not see pronounced differences between frontal and parietal representations of the delay activity (see Chafee and Goldman-Rakic 1998). In fact, FEF and LIP timecourse profiles in each monkey subject were quite similar, suggesting a high level of coherence between these areas (Curtis et al. 2005). More elaborate behavioral tasks are needed to elucidate possible dissociations between these areas.

Cue and Memory Activation in Monkey Superior Temporal Sulcus

The observed contralateral cue and especially delay-period activity in sts beyond MT/MST was perhaps initially unexpected. Neighboring areas in mid (and lower) sts are traditionally assigned to the ventral 'what' visual stream and have not been implicated in purely spatial memory saccade tasks. However, the inferior temporal cortex is reciprocally connected to the ventral aspect of the prefrontal cortex (area

45 and 12) and to FEF (reviewed in Constantinidis and Procyk 2004). In particular, area TPO receives projections from prefrontal areas 46/8 and PPC (Padberg et al. 2003), and from medial pulvinar (which in turn connects to FEF; Bos and Benevento 1975). Single-unit and lesion studies of superior temporal polysensory (STP) complex suggested that it is involved in the control of eye movements and visuospatial coordination (Bruce et al. 1981; Scalaidhe et al. 1995). On the basis of anatomical and physiological properties, STP and adjacent area PGa have been included in the spatial vision network (Ungerleider 1995). The activation of inferior sts regions during memory periods was reported previously for a range of tasks involving memorization of stimuli features and matching-to-sample (Miller et al. 1993). Recent work suggests that dorsal 'action' and ventral 'perception' streams interact in a highly cooperative manner by creating a distributed shared mechanism for perceptual and oculomotor decisions (Eckstein et al. 2007). There are also many indications that the temporal lobe in humans is involved in spatial awareness (Corbetta et al. 2005; Karnath et al. 2001; Watson et al. 1994). Similarly, the ablation of superior temporal gyrus (STG) in monkeys results in strong neglect (Luh et al. 1986; Watson et al. 1994). Thus, the collective evidence suggests that many areas along sts may indeed be involved in the processing and retention of spatial information.

Non-Specific Activation: Comparison with Other Studies

The spatially non-specific activation towards the end of the fixation delay period in direct saccade trials resembles spatially non-specific but effector-specific activation in single-unit recordings in monkey PRR and LIP (Calton et al. 2002; Dickinson et al. 2003), and in FEF (Lawrence and Snyder 2006). Connolly et al. (2002, 2005), using human fMRI, investigated motor preparation using gap saccade paradigm, in which location of the target was cued 0, 2, or 4 seconds after the end of the fixation period. They found a preparatory signal ("preparatory set") in FEF but not in ips, in apparent disagreement with our results on direct saccades and direct reaches in humans (Lindner et al., in preparation), and with single-unit recordings in PRR and

LIP. The absence of the gap in our task is unlikely to explain the discrepancy, as the build-up starts before the end of the fixation delay. Notably, Connolly et al. (2005) found contralateral build-up of activity preceding short-latency saccades, suggesting that it was not spatially non-specific but rather a predictive (anticipatory) directional signal. Conceivably, since Connolly et al. used only two (left or right) targets, subjects may have anticipated the upcoming direction with a high probability and formed a default motor plan. Since in our data the non-specific preparatory signal appears at least 6 seconds into the delay period (which incidentally was the duration of the fixation delay in Connolly et al. experiments), the nature of their FEF-only preparatory signal may indeed be different. In a more recent study Connolly et al. (2006) used a deferred saccade task with longer delay periods similar to our direct saccade condition, and in this context also observed some nonspecific build-up in FEF and PPC.

Several other human fMRI studies investigated preparatory activity for pro- and anti-saccades, but in all tasks, the contextual cue (i.e., pro- or anti-) was delivered in the beginning of the delay period and subjects had to retrieve (and retain) the memorized instruction (DeSouza et al. 2003; Curtis and D'Esposito 2003; Ford et al. 2005). Therefore, all these studies show strong cue response which may disguise the preparatory non-specific ramping. The speeded reaction time constraint and online control with immediate feedback may have also contributed to the strong preparatory activity in our task.

Dynamics of BOLD signals during memory delay period

One of the salient features of the activity in the delay period in monkeys was a separation of the initial cue response peak from the subsequent delay activity. This separation can possibly be explained by hemodynamics, in particular HRF undershoot (Buxton et al. 1998; Mandeville et al. 1998) after strong cue activation in the neuronal population. Many studies have demonstrated very strong cue response in frontal and parietal areas (e.g., Barash et al. 1991a; Pare and Wurtz 1997). Synchro-

nized co-activation of many neurons can drive the accompanying BOLD signal quickly (3 s time to peak in monkeys) and cause subsequent undershoot. Furthermore, many LIP cells respond with an initial burst of activity followed by a brief period of inactivity or lower firing rate, which separates cue responses from subsequent delay period activity (Bisley et al. 2004; Cui and Andersen 2007). Therefore, both actual neuronal dynamics and hemodynamic coupling may underlie the separation of the cue response. In contrast, the frequently observed separation between memory delay peak and following saccade response is harder to explain, as most electrophysiological data show a gradual increase of firing towards the end of the delay period.

Analogous separations did not surface in human BOLD time-courses. The cue response was not noticeably separated by a trough, and although human data for long memory periods sometimes show a decline of memory/preparation activity towards the end of memory period, there was no clear delay response peak (Fig. 4.7, see Schluppeck et al. 2006). However, at the longest (18 s) delays, IPS and FEF human timecourses provide a hint of separation after the cue. Slower hemodynamic responses in the human brain may account for these smoother, more gradual timecourses (Supplemental Data, Fig. 4.S2). The difference in scanning parameters (weaker field strength, slower TR and larger voxel size, see Experimental Procedures) may also contribute to this effect, although it is unlikely that the smearing effect caused by the lower sampling rate is alone responsible for the slower human BOLD time-courses. Our human data appears similar to data acquired with faster sampling rate (TR 1 s—Brown et al. 2004; Curtis and D'Esposito 2006; Medendorp et al. 2005; TR 1.5 s—Schluppeck et al. 2006). Monkey data collected with TR 2 s in control experiments showed time-to-peak of cue and saccade responses comparable with the data acquired using TR 1 s (Supplemental Fig. 4.S3), though the 2 s TR monkey timecourses were smoother and showed less separation between response components. Therefore, further investigation is needed to resolve whether the difference between monkey and human cue and delay period dynamics could be explained by imaging procedures, or if this phenomenon reflects actual hemodynamics and/or neurovascular coupling to the underlying neural activity due to disparities in brain size and vascularization.

Since no single-cell data are currently available for trials as long as those used here (see Supplemental Discussion), fMRI-targeted electrophysiological recordings in the same monkeys using the same tasks will help to address these alternatives.

Comparison between Techniques and Species

The apparent correspondence between activation patterns in monkeys and humans in previous studies (Koyama et al. 2004; Nakahara et al. 1999; Vanduffel et al. 2002) and partly in our work is encouraging, although it does not necessarily imply the same underlying behavioral strategies and neuronal activity. Nevertheless, monkey fMRI provides a crucial control for the interpretability of human imaging results in terms of monkey electrophysiology data. Several discrepancies between monkey electrophysiology and human imaging have been identified. For example, in double-step saccade tasks, human retIPS (a putative homolog of LIP) shows remapping and encodes both targets (Medendorp et al. 2006), but LIP neurons primarily encode the position of the first target (Mazzoni et al. 1996). Along the same lines, single neuron recordings in monkey FEF have demonstrated decreased activity for anti-saccade trials as compared with pro-saccade trials, while fMRI in humans has shown increased activation in FEF for anti-saccade trials (Everling and Munoz 2000). However, preliminary results from monkey fMRI are similar to fMRI studies in humans (Ford et al. Society for Neurosciences 2006). Similarly, perceptual visibility modulation in human fMRI data sharply contrasts with negative findings in monkey V1, but recent findings by Maier et al. (Society for Neurosciences 2006) detected the perceptual modulation in monkey fMRI experiments. These studies purport a complicated relationship between neuronal and BOLD activity and underscore possible difference between techniques. Our study presents an opposite example—the variation in level of contralateral tuning between human and macaque responses does not stem from the discrepancy between imaging and electrophysiology techniques, and may be attributed to actual species difference.

Until now, comparative studies on monkey and human functional topography that

utilized monkey fMRI have focused on spatial mapping and delineation of homologous areas using block-design tasks. Significant progress has been made using this approach (for review see Orban et al. 2004). The event-related approach would further facilitate the direct comparison between imaging studies, on the one hand, and between imaging and physiology, on the other, by introducing an additional temporal dimension.

Our data also have important implications for the block-design studies applying other imaging modalities such as positron-emission tomography (PET) and 14C-deoxyglucose methods (Bakola et al. 2006, 2007; Inoue et al. 2004). Since most activation would be derived from saccade responses and ITI periods, as compared to weaker cue and delay responses, the differential spatial activation patterns for memory-guided versus visually guided conditions may carry only partial information about the distribution of specific cue, delay, and saccade activity.

The elucidation of putative homologies, or functional correspondence, between human and monkey dlPFC, FEF, SEF, LIP, and PRR areas has been advanced by recent human event-related fMRI and TMS studies (Glidden et al. submitted, and references therein). Still, the direct comparison is difficult, in part because in humans, besides dlPFC, FEF, SMA/SEF and a host of posterior parietal areas denoted IPS1, IPS2, ISP3, antIPS, retIPS etc., several other cortical regions show sustained activation during memory periods and saccade responses (see Brown et al. 2004). Perhaps a simple one-to-one correspondence cannot be established—instead, several human (sub-)areas, possibly lateralized (Khonsari et al. 2007), may encapsulate the functionality of a single monkey area such as LIP. Although tempting, at the moment we cannot draw strong parallels between activation in monkey sts and specific loci of activation in humans, as functional homology in sts structures is far from resolved. Several human parieto-temporal (e.g., SMG, STG; temporo-parietal occipital junction) and sts areas showed cue and some sustained memory delay responses, but more research is needed to characterize the involvement of "non-classical" (i.e., not belonging to dorsal frontoparietal network) oculomotor areas in delay-period activity in both species.

In summary, we demonstrated that dynamics of visual, motor, and "cognitive"

signals can be studied in monkeys using event-related fMRI, making it a powerful link between human imaging and monkey electrophysiology. The development of this technique, and the identification of mnemonic and preparatory responses, are important prerequisites for our ongoing investigations of goal-directed decision-making. Combined with fMRI-guided electrophysiological recordings in the same monkeys (Logothetis et al. 2001; Sawamura et al. 2005, 2006; Tsao et al. 2006), and with human imaging using identical paradigms, these studies present a comprehensive approach to the investigation of various aspects of primate behavior.

4.5 Experimental Procedures

Monkeys

All surgical and animal care procedures were done in accordance with NIH guidelines and were approved by the California Institute of Technology Animal Care and Use Committee.

Experimental Preparation

Two male rhesus macaque monkeys (Macaca mulatta) weighing 4–5 kg were implanted with MR-compatible plastic (PEEK) headpost embedded in Palacos bone cement (BioMet) attached to the cranium with short ceramic screws (Thomas Recording), under general anesthesia. For training and scanning, monkeys sat in a specially designed vertical MR chair (Bruker), with the head rigidly attached to the chair with a plastic headholder. Convenient upright sitting position of the animals facilitated rigorous behavioral training and scanning procedures.

MR Imaging

Monkeys were scanned in a Bruker Biospec 4.7 T/60 cm vertical bore monkey scanner equipped with a Bruker BGA38S or (in later experiments) a Siemens Allegra AC44 gradient coil using a ParaVision 3.0.2/4.0 platform running on a Linux RedHat 6

kernel. We used a linear transmitter-receiver birdcage volume RF coil (Bruker) that allowed whole-head homogeneous coverage. The signal-to-noise ratio (SNR, mean signal/s.d. noise) was in the range of 80–130. First- and second-order shimming of the B0 field was performed with the FASTMAP algorithm along 6 projections through a 40 mm cubic volume inside the brain. Functional images were collected with BOLD-sensitive T2*-weighted GE-EPI single-shot sequence using TR 1 s, TE 20 ms, 60 flip angle, 200–250 kHz bandwidth, 128×128 matrix, 12.8 cm FoV, 1×1×2 mm voxel and 10 oblique (15^o) continuous slices. For registrations with EPI, in-plane structural images were obtained using T1-weighted IR-RARE or 2D MDEFT-RAGE during each session; a whole-head high-resolution (0.5/1 mm voxel) T1-weighted 3D-MDEFT or 2D MDEFT-RAGE scan was obtained in a separate session.

Humans

Human subjects (4 female, 7 male, 20–35 years old) were scanned in a Siemens Trio 3T scanner after giving informed consent in accordance with the Caltech Institutional Review Board guidelines. Similar to monkey experiments, the amount of reward (monetary for the humans) for successfully completed experiment depended on subjects' performance that was assessed online during scanning for each trial and reported to subjects after each run. MR images were acquired with Siemens 8-channel phased-array receiver head coil. Functional images were collected with GE-EPI sequences using TR 2 s, TE 30 ms, 90^o flip angle, 64×64 matrix, 192 mm FoV, 3×3×3 mm voxel and 30–32 oblique continuous slices. High-resolution T1-weighted MPRAGE structural scans (1×1×1 mm) were acquired for anatomical localization in the same session.

Stimulus presentation, task online behavioral control and data acquisitions

Visual stimuli were presented on 800×600@60Hz LCD goggles (Resonance Technology), subtending 30×24^o of visual angle using custom OpenGL software. Eye position

was monitored at 60Hz and 0.5–1^o accuracy with an MR-compatible mini-IR camera (Resonance Technology/Arrington Research) and recorded as an analog signal together with stimulus and timing information and TTL triggers from the scanner. Online behavioral control and feedback were implemented in a LabVIEW Real Time platform (National Instruments). Incorrect trials were aborted; successful trials were rewarded with 0.5–1 ml water drop (monkeys) or monetary reward (humans).

Initially, monkeys were trained on standard oculomotor tasks in regular electrophysiology isolated chambers (TDK) in actual MRI chairs. The direct (visually guided) saccade task involved central fixation, after which the fixation point (FP) was turned off and peripheral target (T), randomly chosen from 8 (11^o eccentricity) or 18 (10^o–16^o) locations was turned on (Fig. 4.1A). After the subject made a correct saccade to the T, it stayed on for another 5 s of peripheral fixation and then turned off. After an additional waiting period the monkey received liquid reward. In the memory saccade task, after the initial fixation period a peripheral cue appeared for 200 ms while the subject was required to maintain central fixation. The central fixation continued during the subsequent memory period, and following FP offset the subject was required to saccade to the remembered location of the cue. If the response was correct, a confirmation T appeared at the same place where the cue had been presented, and the trial continued as in the direct saccade task. After the monkeys learned the tasks, we gradually increased the duration of trials until the monkeys were able to perform trials up to 35 s long with at least 60% success rate. This was done in order to allow measurements of activity originating from different intervals of the task, which would not be possible otherwise due to temporal delay and dispersion of the hemodynamic response.

Prior to imaging experiments, monkeys were habituated to the acoustic noise, sound-attenuating cushions, and confined space during training sessions inside the scanner. A video-based motion detection system was used to train monkeys to minimize their body and limb motions, and to track their behavior during scanning. Trials compromised by motion were aborted and punished with a time-out, during training and scanning (see Supplemental Data for details). Inclusion of body and limb mo-

tion signals into behavioral paradigm was a crucial improvement for obtaining stable high-quality functional data.

During one daily session, monkeys typically completed 4 to 6 functional runs of 20 min each, resulting in a total time of up to 3–4 hours in the scanner (including shimming, adjustment, and anatomical scans). Human subjects performed a single 10 min training session inside the scanner prior to the start of data collection, followed by an anatomical scan and then 4 functional runs of 15 min each, resulting in total time of up to 1.5 hour in the scanner. Presentation of direct and memory trials as well as saccade directions was randomized. In monkeys, each daily session was analyzed separately, and as principal findings were consistent across sessions, all sessions fulfilling SNR, temporal stability, and behavioral performance criteria were combined. Altogether, 22 (14 and 8) sessions in two monkeys and 8 sessions in 8 human subjects were analyzed for the main experiment of this study.

Data analysis

Functional data were analyzed in BrainVoyager QX and MATLAB running on a Fedora Core 5 (64 bit) Linux platform. The first 5 EPI volumes were always excluded from functional analyses to remove transient effects of magnetic saturation, but were used for co-registration, since they provide better contrast for anatomical landmarks. Anatomical T1-weighted scans were processed in BrainVoyager QX and MIPAV. In monkey experiments, EPI sequences for each run were preprocessed using slice time correction, linear trend removal and a high-pass temporal filter with 3 cycles per 20 min run cut-off, and 6DOF 3D-aligned to a first volume of the last run in the session, which was always followed by the in-plane anatomical T1-weighted scan. The in-plane anatomical scan for each separate session was co-registered to the high-resolution structural scan in the AC-PC plane, and then EPI runs were aligned to the AC-PC-registered anatomical scan using rigid body transformations. Automated alignment procedures were followed by careful visual inspection and manual fine-tuning based on anatomical landmarks. Using these transformations, 3D volume

time-courses were computed in AC-PC space using 2×2×2 voxel size and 1000 unit image intensity threshold (mean image intensity within the brain ranged from 4000 to 6000 units). In human experiments, we used the same preprocessing steps, except that the high-resolution anatomical scans were also transformed from AC-PC into Talairach space. Human 3D volume timecourses were computed in Talairach space using 3×3×3 voxel size and 100 unit image intensity threshold (mean image intensity within the brain ranged from 500 to 700 units). No additional spatial smoothing was applied to the fMRI data.

All trial events (except baseline initial fixation period)—cue, fixation/memory delay, direct/memory saccades, target fixation, and reward delivery—were extracted and used as predictors for general linear model (GLM) after convolution with hemodynamic response function (HRF) (Fig. 4.1A–C). Events from all trials (successful and failed) were modeled to account for the overall variance. Fixational saccades and blinks were also detected, but not used as GLM predictors for final results, since their inclusion in the GLM did not bring about any significant effect. In monkeys, each session was analyzed separately to check the consistency of the results, and final statistical maps were generated using multi-session GLM. Human data were analyzed both separately using individual-subject GLM and together in across-subject GLMs (Talairach- and cortex-based aligned, see Supplemental Results).

For the BOLD timecourse event-related averaging (ERA), only successful trials were accumulated. Importantly, in humans and especially in monkeys, the epochs of the run affected by body or limb motions were automatically detected and eliminated from ERA analysis (Supplemental Data, Fig. 4.S1). ERA time-courses were constructed using individual baseline estimates for each single trial: mean activity in the last 3 or 4 s of the initial fixation period for monkeys and humans, respectively (epoch-based averaging in BrainVoyager). Following initial analyses, we decided to apply a faster HRF for monkeys as compared to the standard human HRF, because the difference in BOLD response timing was apparent in BOLD timecourses (Fig. 4.1D; see also Supplemental Data). It is important to emphasize that this manipulation only affects the resulting statistical contrast maps, but has no influence on

the ERA timecourses, since they were calculated from the actual EPI volume data without any prior assumptions about the shape of the HRF.

To quantify ERA timecourses, we estimated the mean response amplitude (A) in several intervals within each ERA timecourse and calculated contraversive selectivity (CS) and ramping (R) indices (Fig. 4.4B). For monkeys (sampling rate 1 s) the baseline interval was defined as the last 3 s of initial fixation, cue, and saccade as 3 s intervals starting 2 s after event onset, and memory/fixation delay as the last 5 seconds of the delay period, or the rest of the delay period for variable delay experiment. For humans (sampling rate 2 s, variable delay experiment) the baseline interval was defined as the last 4 s of initial fixation, cue, and saccade as the 6 s intervals starting 4 s after event onset, and memory/fixation delay as the remaining samples of the delay period (shortest delay 6 s was excluded from this calculation). Mean response amplitude in these intervals for contralateral and ipsilateral trials was used to calculate normalized CS index: CSnorm = (A_{contra} - A_{ipsi}) / (—A_{contra}— + —A_{ipsi}—) (see "lateralization index" L in Schluppeck et al. 2006). The normalization term, calculated as the sum of amplitudes across memory and direct trials within each interval, was chosen in order to facilitate the comparison of relative contraversive selectivity across different intervals. This (nonlinear) index ranges from -1 to 1, where positive values indicate contralateral tuning and negative, ipsilateral; CS 0.33 represents the case for contralateral amplitude being twice as large as ipsilateral response. The normalization may inflate sporadic differences when all response amplitudes in the interval are very small, e.g., in the delay period in the area that shows no significant delay activation.

Ramping index R for each of 4 trial types was calculated as the mean differential amplitude of the 3-sample intervals centered on the end of the delay period relative to the baseline. This measure is different from the mean response amplitude for the delay interval, since it was designed to capture the level of activation immediately preceding saccade response. R index was measured in %BOLD change. The statistical significance of the difference between contra- and ipsilateral, and between memory and direct, timecourses was calculated on sample-by-sample basis using a two-tailed

t-test ($p<0.05$).

The spatial extent of regions of interest (ROIs) used for the time-course extraction was 2.5×2.5×2.5 mm (15.62 mm^3) cubic volume for monkeys and 5×5×5 (125mm^3) mm for humans, or less if the span of the statistical activation map limited the amount of significantly activated voxels around the selected ROI center. Brain coordinates of ROI centers for monkeys are listed both in AC-PC (bicommissural) and stereotaxic frames of reference, for comparison with other studies. The angle between the AC-PC plane and the stereotaxic interaural-lower orbital plane was 0^o for monkey R, and $+4^o$ (clockwise) for monkey G. The nomenclature for monkey areas is based on the stereotaxic atlas by Saleem and Logothetis (2007), unless noted otherwise. Coordinates for human subjects are listed in Talairach space (Talairach and Tournoux 1988).

4.S1 Supplemental Data

Supplemental Methods

Body and Limb Motion Detection and Functional Data Selection

At the high magnetic 4.7 T field, and also to some extent at 3 T, the EPI signal is strongly affected by body, limb and jaw motions of the subject, even when movements occur far from imaging volume within RF coil (i.e., the head). This is a consequence of the "off-resonance" effect: body, limb, and jaw, and residual, movements introduce dynamic local B_0 field fluctuations, which lead to strong imaging artifacts such as changes in EPI intensity, geometric distortion, and signal mislocalization (Supplemental Data, Fig. 4.S1). These effects become especially pronounced in the Gradient Echo (GE) single-shot EPI sequence, which is very sensitive to B_0 field inhomogeneity.

To overcome these difficulties in alert monkey experiments, we developed a novel technique that combined careful monitoring of body, limb and jaw motions, rigorous training that encouraged monkeys to minimize these motions, and data selection and post-processing analysis that utilized information about these parameters (Kagan et al. Society for Neurosciences 2005, 2006, 2007; Lindner et al. Society for Neurosciences 2007). During both training and scanning, monkeys were monitored with IR-sensitive video cameras (regular security surveillance camera for training in the rig and miniature MR-compatible CMOS camera inside the scanner). Video feed was directed to an automatic motion-detection system (Pelco MD 2001, Pinsk et al. 2005) which allows adjustment of motion sensitivity threshold for TTL binary output. This signal was fed into LabVIEW-based real-time behavioral control system as one of behavioral parameters. The successful completion of the trial and subsequent reward delivery was contingent not only on the required oculomotor task performance but also on the absence of body and limb motions during the entire trial. Any time a noticeable motion occurred, the trial was aborted without reward, auditory and visual behavioral feedback was delivered and the monkey was punished with 5–10 s time-out. A new trial started only a few seconds after motion ceased, allowing for

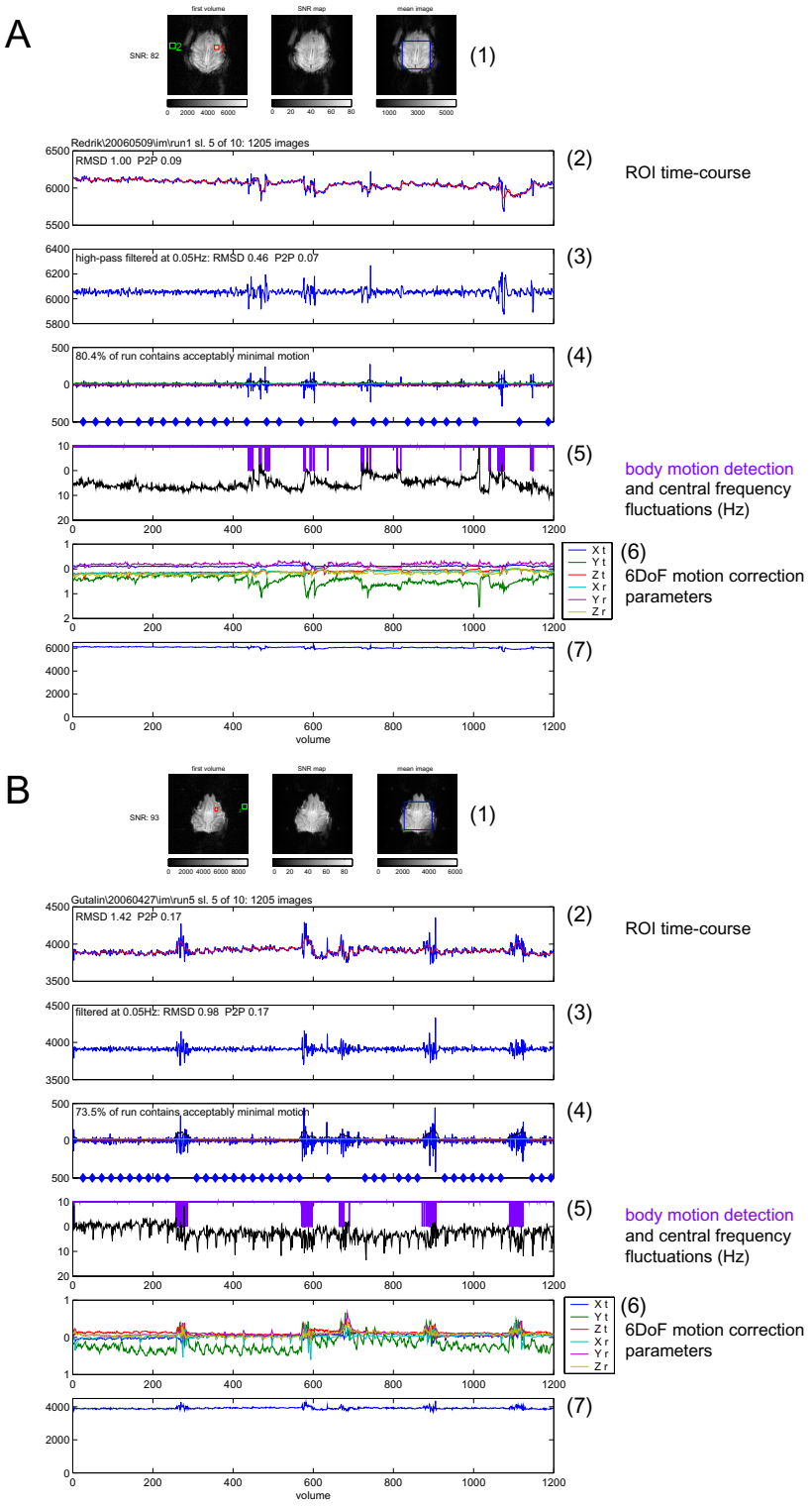
A
first volume
SNR map
mean image
SNR: 82
(1)
Redrik\20060509\im\run1 sl. 5 of 10: 1205 images
RMSD 1.00 P2P 0.09
(2)
ROI time-course
high-pass filtered at 0.05Hz: RMSD 0.46 P2P 0.07
(3)
80.4% of run contains acceptably minimal motion
(4)
(5)
body motion detection
and central frequency
fluctuations (Hz)
X t
Y t
Z t
X r
Y r
Z r
(6)
6DoF motion correction
parameters
(7)
volume
B
first volume
SNR map
mean image
SNR: 93
(1)
Gutalin\20060427\im\run5 sl. 5 of 10: 1205 images
RMSD 1.42 P2P 0.17
(2)
ROI time-course
filtered at 0.05Hz: RMSD 0.98 P2P 0.17
(3)
73.5% of run contains acceptably minimal motion
(4)
(5)
body motion detection
and central frequency
fluctuations (Hz)
X t
Y t
Z t
X r
Y r
Z r
(6)
6DoF motion correction
parameters
(7)
volume

Figure 4.S1:

Evaluation of EPI signal-to-noise (SNR) and temporal stability and data selection for event-related analysis. *Examples of 20 min runs (TR 1 s, 1200 volumes) in monkey R (A) and monkey G (B). Panel (1): single raw EPI slice (first volume), SNR map per voxel (calculated across the run), mean raw EPI image across the run, and ROIs used for SNR calculation (green—background noise, red—signal in arcuate sulcus) and temporal timecourse estimation (blue), shown below. Panel (2): Raw EPI timecourse extracted from the large blue ROI (blue curve) and corresponding low-pass filtered signal (cut-off 0.05 Hz, red curve). Two measures of the timecourse stability are RMSD (root mean square deviation) = std($ROI_{timecourse}$) / (mean($ROI_{timecourse}$)/100) and P2P (peak-to-peak) = (max($ROI_{timecourse}$) - min($ROIt_{timecourse}$)) / min($ROI_{timecourse}$); Panel (3): high-pass filtered signal calculated as original minus low-pass filtered signal. Panel (4): the derivative of the high-pass filtered signal, used as an input to an automatic adaptive algorithm that selected run epochs unaffected by monkey motion (marked by thick red lines). Blue diamonds denote times of liquid reward delivery. Panel (5): the purple curve shows the monkey body-motion detection signal, the black curve represents the fluctuations of the central frequency showing off-resonance changes due to jaw, head, and body motions (see Pfeuffer et al. 2002). Note that body motions and each reward delivery are accompanied by the central frequency changes (reward delivery effects are especially pronounced in the run shown for monkey G). The strength of the reward delivery effect depended on the placement of the reward tube. In the run shown, the tip of the reward tube was placed slightly away from the monkey mouth, which resulted in residual head shift and vigorous jaw/licking motions during the reward delivery. The data from this session was not included in the analysis and is presented here to illustrate detrimental effects of even small motions. Panel (6): BrainVoyager 3D motion correction parameters—translation and rotation. Jaw and body motions result in strong shift in phase-encoding (A-P direction), corresponding to the Y translation (Yt)—the green curve. Note that Yt curve mirrors the central frequency fluctuation timecourse. Panel (7): Raw-EPI timecourse re-plotted on a full scale.*

MR signal stabilization. Monkeys were trained to sit still during the entire EPI run (20 min) but were allowed to move in inter-run intervals (when no gradient noise was present), which typically lasted 1–3 min. Usually, there were no or very few movement bouts in the beginning of the session, when monkeys' motivation was high, and frequency of movements increased during the session, which typically consisted of 4–6 20-minute runs.

The combined information about change of the raw EPI signal intensity, motion detection triggers, and motion correction parameters was used to extract data from epochs that were not contaminated by body and limb movements. This significantly improved the resulting event-related average timecourses. Further details on effects of movements, training, behavioral control, and analysis will be presented in a future technical report (Kagan et al., in preparation).

Stimuli, Eye Movement Recordings, and Behavior

Horizontal and vertical eye position were sampled at 60 Hz, $\sim 0.15^o$ resolution and $0.5–1^o$ accuracy using ViewPoint with AnalogOut option (Arrington Research) for online control and recorded in the file at 1 KHz. For offline analyses, eye position was calibrated to degrees of visual angle and smoothed prior to computation of velocity and acceleration, which were used for automatic saccade and blink detection with a custom algorithm. Human eye data recorded in the scanner required additional removal of gradient and RF pulse interference noise, done with a custom filtering algorithm.

We were able to reliably detect saccades of $\sim 1^o$ amplitude, but not smaller fixational saccades. Two spatial configuration of the targets were used: 8 targets, placed equidistantly from the fixation point at 11^o eccentricity; or 18 targets, 9 right and 9 left of the fixation point, with 3×3 organization of targets placed between $10^o–16^o$) on either side of the fixation point. Targets (T) and central fixation point (FP) were 0.37^o squares. For contralaterality analysis, we sorted trials for the 8 target condition with saccades made to targets {1,2,3} as rightward and targets {5,6,7} as leftward. In a subset of experiments, we used a right-left array of 18 targets shown in the right

panel. The results in both experimental conditions were similar and thus were combined. The central fixation window radius was 3–5^o of visual angle, and peripheral target window radius was 5–7^o. Larger target windows were used to accommodate memory saccade end-point inaccuracy and systematic upward shift (Gnadt et al. 1991). We also allowed transient (<200 ms in monkeys; <400 in humans) deflections from the fixation window to accommodate blinks that were inevitable with such long fixation periods.

Timecourses of saccade and blink frequency in direct and memory trials demonstrate that the amount and distribution of these eye movements in the delay period (from -10 to 0 s) did not significantly differ between the two trial types($p>0.05$ for both saccades and blinks). The only difference between memory and direct trials is occurrence of small corrective saccades that followed instructed saccade to the remembered location. Interestingly, both monkeys tended to make two (rather then one) corrective saccades during the 500 ms period of fixating the remembered location before T became visible—one in the dark, prior to the appearance of the T, and one visually guided after T appearance. It is plausible that with first corrective saccade monkeys tried to use spatial cues such as edges of dimly-illuminated background, or alternatively, they may have utilized extraretinal (e.g., efference copy) signals.

Human subjects were instructed to make a corrective saccade, if necessary, to accurately acquire the T after its appearance. However, the frequency and distribution of corrective saccades in humans was less uniform and varied between subjects.

Human Cortex-Based Alignment

To improve anatomical correspondence beyond Talairach space matching by reducing human inter-subject variability of individual gyri/sulci patterns, we also applied cortex-based alignment (Fischl et al. 1999; van Atteveldt et al. 2004). Gray/white matter boundary of each individual hemisphere was segmented and borders of the two resulting segmented sub-volumes were tessellated to produce a surface reconstruction. The resultant surface was morphed into a spherical representation, and the hemispheres were aligned based on the curvature information regarding the gy-

ral/sulcal folding pattern. The target of the morphing procedure was a dynamical group average of all included hemispheres. The mapping between the individual hemispheres was used for the re-alignment of the functional data.

Supplemental Results

Variable Delay Experiment in Monkeys

In addition to the fixed (10 s) delay experiment in monkeys described in the main text, we also used randomized variable delays—6 s, 8 s, 10 s, and 12 s, similar to the human experiment. In both monkeys, variable delay data reproduced the main findings of the fixed delay experiment. In particular, the separation of the cue response from the later sustained memory delay activity was apparent. The unspecific ramping in the direct trials seems to be more pronounced in the variable delay data in monkey R, possibly because unpredictable GO signal timing facilitated motor "readiness"/attention (especially at the longest 12 s delay).

Timecourse of hemodynamic responses in monkeys and humans

Initial inspection of monkey ERA timecourses revealed that the cue response in memory trials rises and decays faster than would be expected from a typical (human) hemodynamic response. Fig. 4.S2 shows inter-species comparison of rightward memory trial ERAs extracted from left hemisphere ROIs in monkey areas FEF and LIPd, and two of presumptive functionally homologous human areas mFEF and IPS2. In monkeys, responses to clearly defined time-locked events (such as presentation of peripheral cues and saccade execution) reached maximum after approximately 2–3 s, while in humans the time-to-peak was about 5–6 seconds (corresponding to the typical BOLD signal latency in human imaging literature). Based on these findings, we used a faster HRF for the calculation of predictors in monkeys, in order to better capture the BOLD response dynamics in the GLM (Fig. 4.1D).

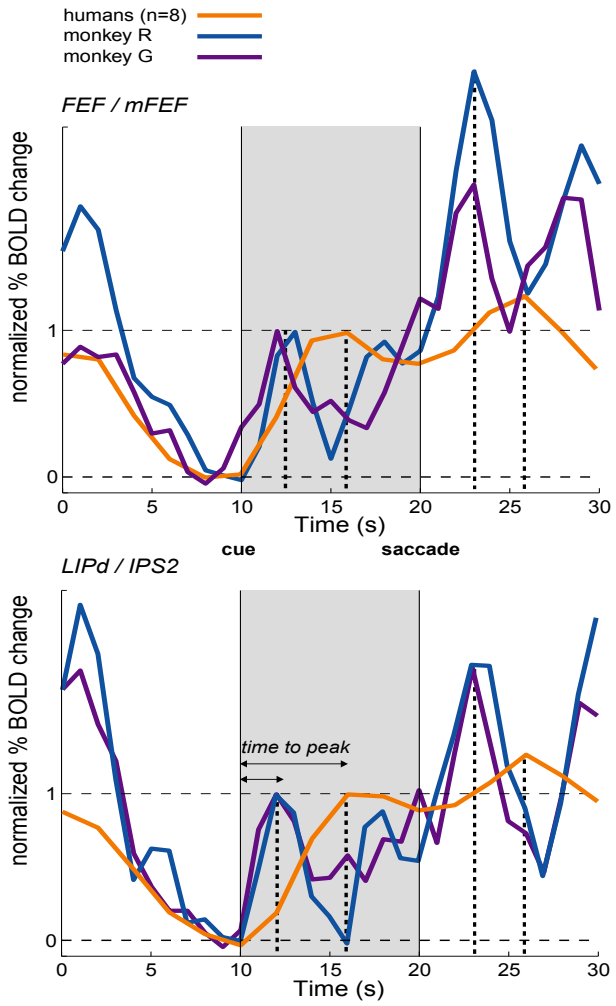

Figure 4.S2:

Comparison of BOLD response timing in monkeys and humans. *Upper panel—monkey FEF, human lFEF, lower panel—monkey LIPd / human IPS2. Contralateral memory trials from left ROIs are shown. Human data timecourses represent mean of ERAs extracted individually from each of 8 subjects. Timecourses for 2 monkeys are shown separately. For comparison purposes, to emphasize relative timing, timecourses from each monkey and the resulting average human timecourses were normalized so that the amplitude of cue response peak equals 1. Error bars are omitted for clarity. Cue was presented at time 10 s, 'Go' signal for saccade occurred at 20 s. Dashed vertical lines denote cue and saccade response peaks, horizontal arrows denote time-to-peak (shown only for LIPd / IPS2).*

Several methodological factors, besides real hemodynamics or neurovascular coupling, may account for the differences between human and monkey BOLD timecourses. The most conspicuous one is the TR, or sampling rate, of EPI volume acquisition—1 s for monkeys and 2 s for humans. The longer TR introduces more temporal smearing at the data acquisition stage. It also smoothes the timecourses during calculation of ERAs: since the trial events were not synchronized to the onset of volume acquisition, it results in a temporal jitter between event onset and corresponding volume sample. However, these effects are not expected to shift the time-to-peak estimate, since the offsets between event occurrences and data sampling times were completely randomized, so that positive and negative offsets average out. Fig. 4.S3 shows comparison of monkey ERAs extracted from the data acquired with TR 1 s and 2 s, in the same session. The timecourses acquired with TR 2 s were indeed smoother, but the time-to-peak of time-locked cue and saccade responses was between 2 and 4 s, similarly to the TR 1 s data.

Statistical Mapping, ROI definition, and Analysis in Humans

Human imaging data were analyzed in 3 different ways. First, we used individual subject GLM (similar to analysis of monkey data) and overlaid statistical maps for the +cue, memory>fixation delay, and +saccade contrasts on the subject's anatomical scan. The overlapping peaks for memory>fixation delay (or +memory when the memory>fixation delay contrast did not reach significance, in 3/8 subjects) and +saccade contrasts in anatomically defined locations using known landmarks were identified as centers of ROIs for the timecourse extraction (Srimal and Curtis 2007). The ERA timecourses were extracted separately for each subject and averaged (by calculating mean of means across trials). Second, an across-subject GLM for fixed effects analysis (i.e., calculating a combined GLM across all runs and all subjects: a multi-study, multi-subject GLM in BrainVoyager QX) was conducted, and the same statistical contrasts applied, in order to confirm the results of the individual ROI analysis and to compare the two approaches. The resulting timecourses were extracted by averaging all corresponding trials across all subjects (i.e., with equal weight). The

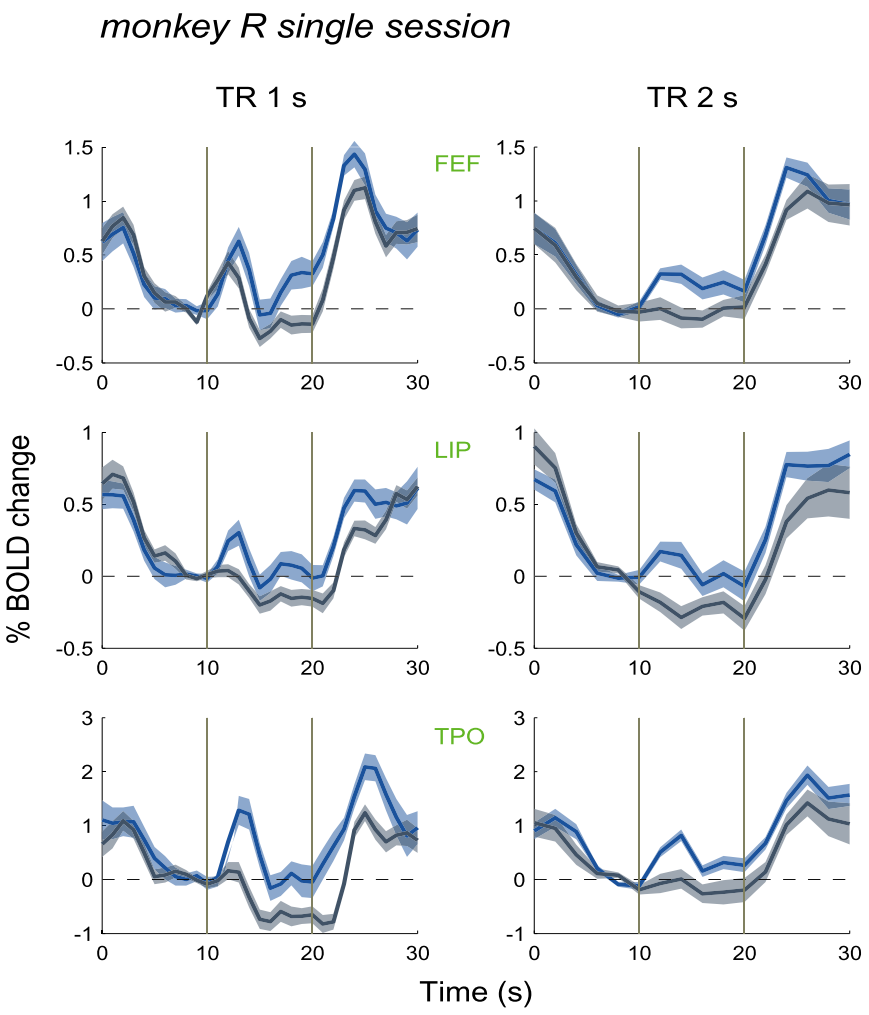

Figure 4.S3:

Comparison of BOLD response timing in monkey data *collected with TR 1 s (left column) and 2 s (right column), in areas FEF, LIP and TPO in the left hemisphere of monkey R. The cue was presented at time 10 s, and the "Go" signal for saccade occurred at 20 s. Data from one scanning session area are shown. Light blue traces - memory trials to the right, dark blue traces - memory trials to the left.*

results of both approaches generally agreed, but the across-subject GLM timecourses had slightly lower amplitudes. The correspondence between these two approaches demonstrates the consistency of activations among subjects and the robustness of our ROI extraction procedure. We also applied a random effects analysis to across-subject GLM calculation (RFX GLM option in BrainVoyager QX). Even though n=8 subjects is not enough for proper a random effects analysis, the resulting maps, although less extensive, corresponded well to the fixed effects GLM maps (not shown), further confirming that across-subject GLM results were not biased by activations originating only in few subjects (Fig. 4.S4 shows representative activations from the across-subject GLM.)

Finally, a cortex-based aligned GLM across subjects was also performed, to see if the improved co-registration, accounting for the cortical folding pattern variability, would yield more consistently contralateral maps and/or corresponding timecourses. However, tuning differences were less evident in the results of the cortex-based as compared to the Talairach alignment, presumably because of the weak effect on the individual subject level.

The nomenclature used for the posterior parietal areas is based on recent literature that delineated several large tentative regions tiling the medial SPL using phase-encoding topography (Schluppeck et al. 2005; Swisher et al. 2007), and on our own observation of multiple response peaks in PPC. The first areas that showed significant memory delay activity were V7 and, more anteriorly and dorsally, IPS1. In agreement with previous studies, most significant saccade and memory delay activation in posterior (or caudal) ips was found medially and in branches extending towards midline. The peak of memory activation was located in a small sulcus running medially and perpendicularly to ips, an area that encompassed IPS2 and retIPS. Originally, the "retinotopic" IPS (retIPS) was defined functionally in a left/right block design by Medendorp and colleagues (2006) as the site with the most pronounced contralateral tuning for memory saccades. Our dataset did not reveal robust bilateral contralateral regions in PPC in individual subjects, using memory delay right>left contrast. Therefore, in each subject we selected two ROIs in the vicinity of reported coordinates

for retIPS, one that showed the highest peak for memory>fixation delay or +memory contrast, and one corresponding to the peak of the relative contribution map for contralateral cue and memory (Fig. 4.S4E). The highest memory delay activation peak, regardless of contralaterality, was taken as IPS2. Usually, the slightly more lateral and ventral part of the activation was defined as retIPS; and an adjacent, or overlapping, region as IPS2. Even for the group data, the most straightforward cue and/or memory right>left contrast did not show significant peaks in this area (Fig. 4.S4D; the reason is a strong activation for rightward (ipsilateral) targets in right PPC, see below). Therefore, similar to individual datasets, in across-subject GLM the bilateral retIPS was defined as the highest activation for the memory>fixation delay contrast overlapping with contralateral predictor contribution (Fig. 4.S4F). More dorsally and anteriorly located was IPS3, and further down ips was the anterior IPS. On the medial wall of SPL, precuneus showed strong and contralateral cue and memory responses.

The detailed inspection of reported coordinates for different PPC regions from different labs, conducted by Glidden et al. (submitted), showed that retIPS is situated between, and partially overlaps with, IPS2 and IPS3. Putative human LIP (the notation is misleading because of its medial branch location), suggested by several studies (Astafiev et al. 2003; Sereno et al. 2001), also overlapped with IPS2 and retIPS. Interestingly, Glidden et al. demonstrated that this region (labeled "midIPS") shows preferential activation by saccades as compared to reaches, in agreement with our results showing most significant activation of IPS2 and retIPS in memory delay and saccade periods. This lends additional support to the analogy of retIPS/IPS2 with monkey LIPd.

However, the exact delineation and terminology of different PPC regions, while important, is not the main focus of the current study and does not affect our principal conclusions. By estimating the response amplitude and contralaterality across several parietal areas involved in the task, both on an individual level and across subjects, we attempted to present a full spectrum of responses and ensured we did not miss any significant (contralateral) activation.

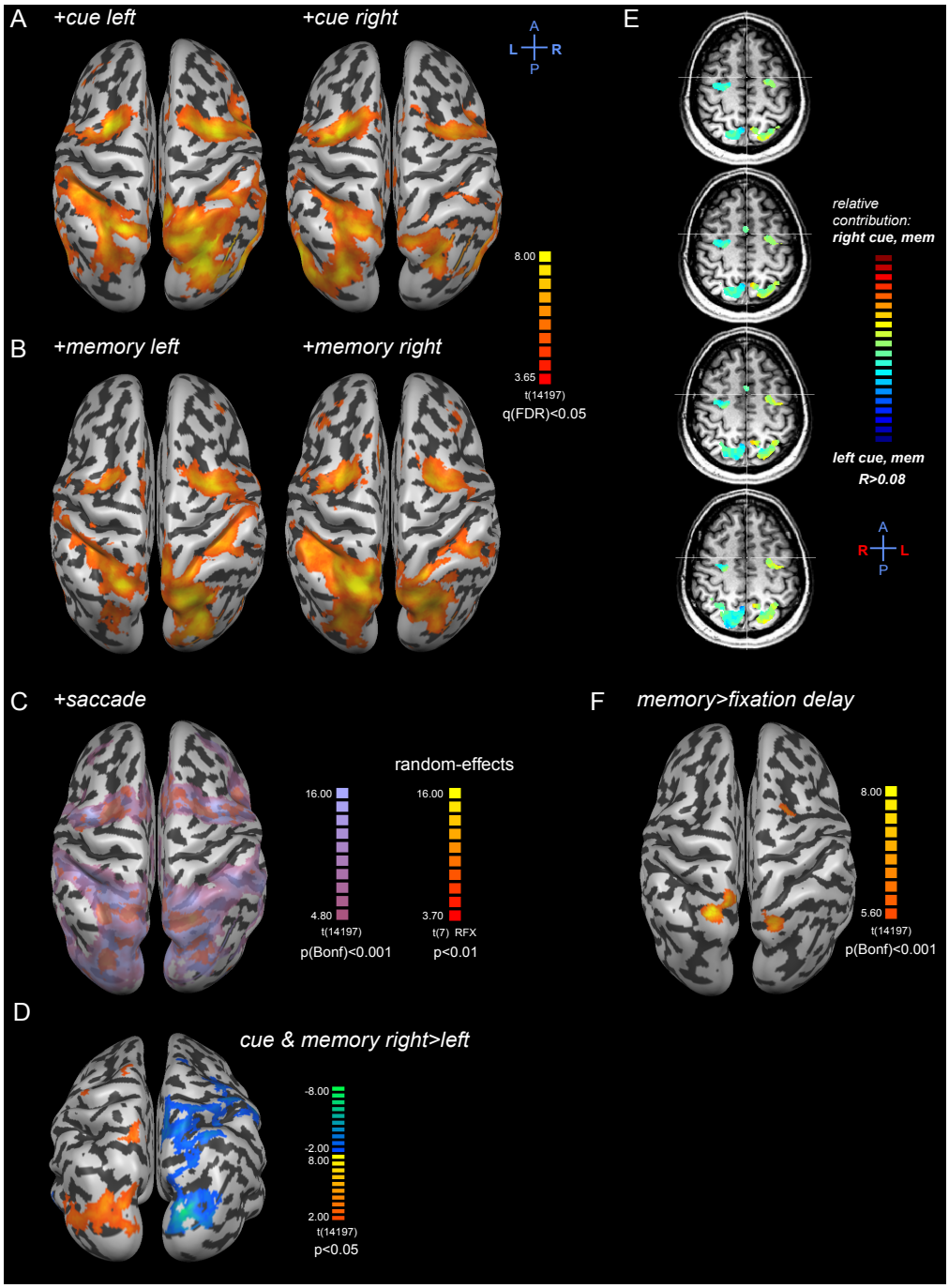
A
+cue left
+cue right
A
L
R
P
8.00
3.65
t(14197)
q(FDR)<0.05
B
+memory left
+memory right
E
relative
contribution:
right cue, mem
left cue, mem
R>0.08
A
R
L
P
C
+saccade
random-effects
16.00
4.80
t(14197)
p(Bonf)<0.001
16.00
3.70
t(7) RFX
p<0.01
F
memory>fixation delay
8.00
5.60
t(14197)
p(Bonf)<0.001
D
cue & memory right>left
-8.00
-2.00
8.00
2.00
t(14197)
p<0.05

Figure 4.S4:

Supplementary statistical maps *for (A) +cue left and +cue right contrasts; (B) +memory left and +memory right contrast. Note stronger and more extensive contralateral activation patterns. (C) +saccade (both left and right), with same random-effects map superimposed; note overlap of the two maps. (D) Cue and memory delay right>left contrast (p<0.05 uncorrected), significant differences are mostly localized to the occipital lobe, V7, and precuneus. (E) 4 axial slices showing relative contributions of left and right cue and memory delay predictors to variance, in significantly activated (p(Bonf)<0.001) voxels. Color map ranges from red–yellow—mostly right predictors contribute, to green—equal contribution, to cyan–blue—mostly left. On these images, left is right (radiological convention). These maps further demonstrate weak but extant contralaterality of frontoparietal areas. Note stronger contralaterality in pCu. (F) Memory>fixation delay peaks of activation (with stringent statistical threshold p(Bonf) <0.001), localized to retIPS, IPS2, and right mFEF ROIs with most significant spatially specific delay activity (as compared to non-specific ramping in direct trials).*

Hemispheric and Visual Field Asymmetry in Humans and Monkeys

An ideal contralateral organization assumes that both hemispheres respond in mirror-symmetrical fashion, manifesting comparable levels of contralateral tuning. We tested this assumption by separately calculating CS in left and right hemisphere ROIs. Interestingly, in both species the left hemisphere exhibited stronger contralaterality. However, this effect was modest in monkeys, but much more pronounced in humans (Fig. 4.S5B for monkeys, Fig. 4.S6 for humans). In monkey areas that showed strong consistent memory delay period activity (LIPd, FEF, dlPFC, Tpt, TPO), the difference between left and right brain CS for cue and delay (means.d.) was 2411% and 2413%, respectively, while in human parietal and frontal areas with strong delay activity (IPS1/2, retIPS, l/mFEF), the difference was 7955% and 11625%.

To quantify the asymmetry in contralateral tuning further, we calculated the correlation between %CSchange = (CS_{left_hemi}-CS_{right_hemi})/CS_{left_hemi}*100 for the left hemisphere, and the contralateral response amplitude for the right hemisphere, in corresponding trial epochs across cortical areas. Strong negative correlations in monkeys (Spearman r=-0.59 for cue, r=-0.85 for delay, $p<0.05$, n=21) showed that only areas that had very little cue and memory delay activity had spuriously large difference between left and right CS, resulting from random fluctuations in time-courses (recall that CS is a normalized measure that does not take into account the absolute amplitude of the responses). In contrast, human areas showed no significant correlation between %CSchange and response amplitude (r=-0.15, r=-0.13, $p>0.05$, n=16), because many areas that had robust cue and memory delay responses also exhibited a considerable difference between left and right hemisphere tuning.

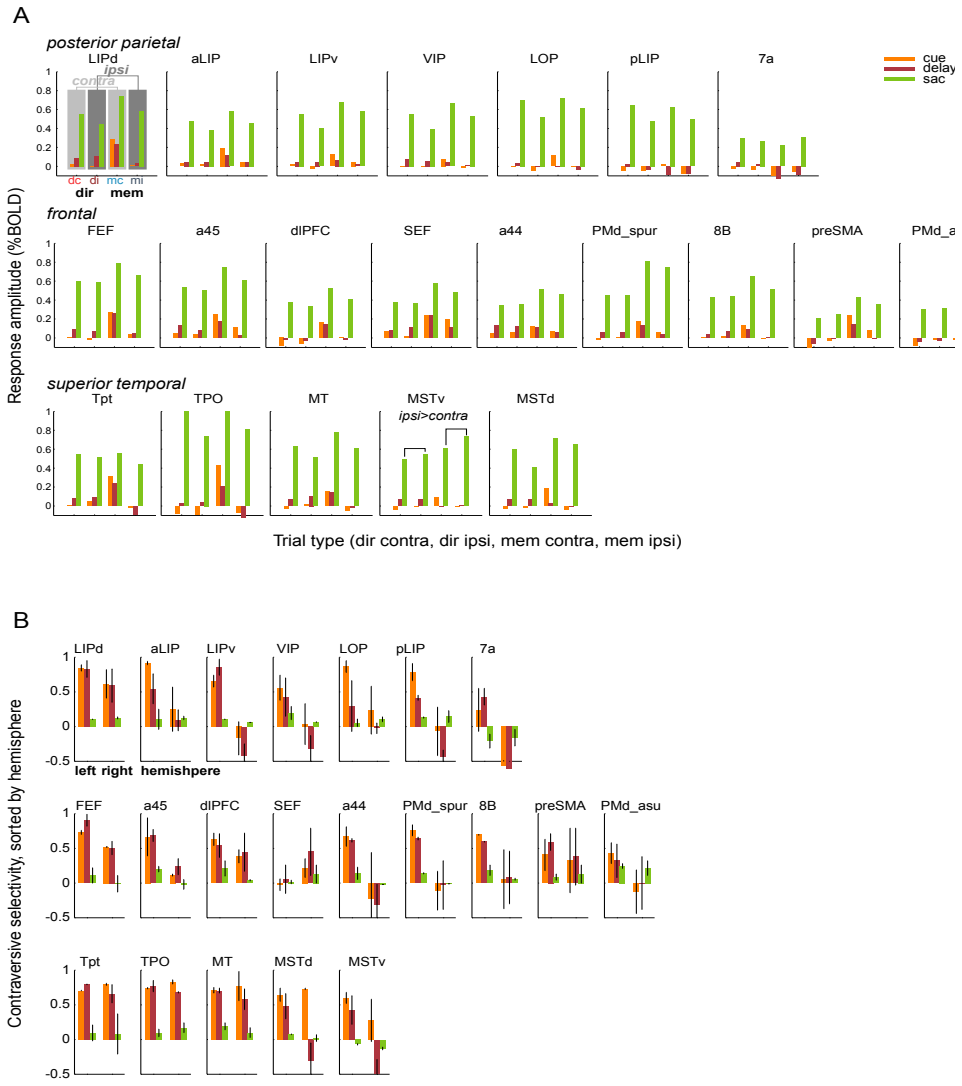

Figure 4.S5:

Mean Response Amplitude and Contraversive Selectivity by Hemisphere*(A) Mean response amplitude in monkey cortical areas. For each area, histogram plot consists of 4 bar groups: direct–contra, direct–ipsi, memory–contra, memory–ipsi, from left to right, and each group of cue, delay, and saccade response. (B) Contraversive selectivity (CS) by hemisphere. For each area, histogram plot consists of 2 bar groups: left and right hemisphere.*

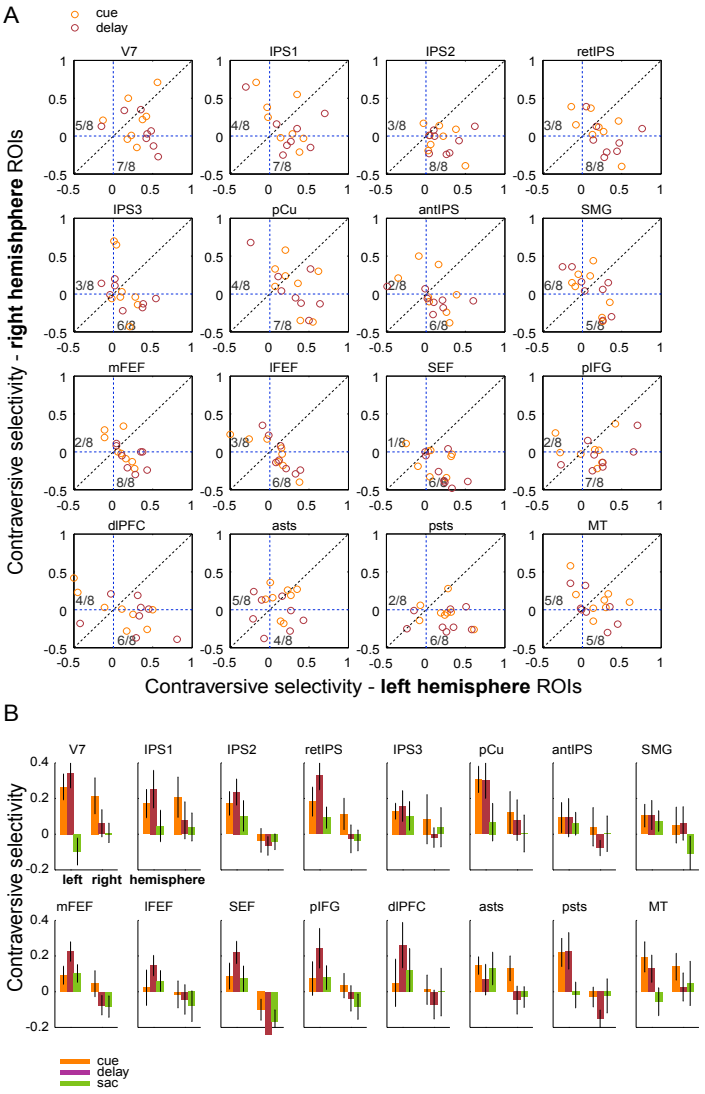

Figure 4.S6:

Contralaterality in human cortical areas in left and right hemispheres. *(A) Scatter plots showing right versus left CS for each subject and each area, for cue and memory delay. Numbers show how many subjects, out of 8, had CS>0 in each hemisphere. (B) Mean and s.e.m. of CS—each area histogram plot consists of 2 bar groups: left and right hemisphere.*

Supplemental Discussion

Previous Monkey fMRI Studies

Two previously published reports from Miyashita and colleagues employed a variant of event-related analysis that used closely spaced short trials and low (>2 s) temporal resolution, and thus were not able to resolve the dynamics of the BOLD timecourses within each trial (Koyama et al. 2004; Nakahara et al. 1999). Consequently, only a single averaged HRF timecourse that collapsed several events related to the cognitive set-shift was presented in the Nakahara et al. (2001) study; no timecourses were extracted in the Koyama et al. (2004) study.

Long Delay Periods in Monkey Electrophysiology

As stated in the main text of the paper, most monkey electrophysiology studies employed relatively short (0.5–2 s) delay periods. However, Fuster and colleagues (Fuster 1990; Quintana et al. 1988; Zhou and Fuster 1996) used delays up to 18 s in the context of delayed match-to-sample visual and somatonsensory tasks, but not in the context of spatial memory; and they also used manual responses. A seminal paper by Funahashi et al. (1989) compared 1.5, 3, and 6 s memory delays in the memory saccade task, and they found no conspicuous differences between firing timecourses during these periods in prefrontal cortex. To our knowledge, the longest memory period used for recordings during delayed oculomotor task in the parietal cortex was 3 s, in the work of Chafee and Goldman-Rakic (1998). In follow-up experiments we plan to record single units and LFP activity from frontal and parietal fMRI-identified ROIs with the same long delays used in our fMRI experiments. This will enable a more direct comparison of fMRI and neural activity timecourses.

Nature of "cue response"

We suggest that distinct time-locked activation in the early memory period that we and others refer to as the 'cue response' reflects not only initial sensory processing associated with the incoming visual input, but also subsequent higher-order cogni-

tive processes such as shift of attention to the cue, inhibition of reflexive saccades (Cornelissen et al. 2002) and memory consolidation. A direct test of this hypothesis requires comparison of responses to the same peripheral flash in the condition when it is behaviorally relevant (such as in memory trials) to a condition where it is behaviorally irrelevant (Platt and Glimcher 1997). Arguably, it is difficult to train monkeys that have previously learned saccade tasks to completely ignore distractor cues, and to ensure that monkeys do not continue to regard them as potential targets for action. In a separate set of experiments, we attempted to convey the idea of 'irrelevance' for monkeys' behavior by using larger cues in a separate task in which monkeys had to ignore the peripheral flash and to continue fixating centrally in order to get a reward; as compared to regular (smaller) targets for memory-saccade task. These two conditions were run in separate blocks (rather than interleaved trials). FEF and LIP responses to smaller but behaviorally-relevant cues tended to be stronger than responses to larger but behaviorally irrelevant distractors. Similarly, in our recent human fMRI study, we employed a control condition in which irrelevant cues were visually identical to behaviorally meaningful cues, and we observed smaller BOLD responses to the cues in the 'irrelevant' context (Lindner et al., in preparation). Together, these results provide converging evidence that the cue response comprises attentional and memory-related components, in addition to purely sensory activation (but see Brown et al. 2004 and Medendorp et al. 2006—irrelevant and relevant cues in these human fMRI studies seem to evoke very similar responses).

Response Amplitude and Contralaterality in Humans—Comparison with Other Studies

Two recent fMRI studies of delayed memory saccades also utilized long and variable delay periods, and specifically investigated spatial tuning properties of cue and delay period activity in human subjects (Schluppeck et al. 2006; Srimal and Curtis 2007). Our results generally agree with previous findings, but some quantitative differences exist. According to similarly calculated contraversive selectivity (CS) indices, we find $\sim$1.5–2 times less contralaterality in V7, IPS1, and IPS2 as compared to the study

of Schluppeck et al. Consonant with the Srimal and Curtis data (∼10% difference), we observed only small differential activation in contralateral trials. This resulted in CS_{delay} values ranging from 0.21 in V7 to 0.15 in IPS2 (and 0.24 in retIPS), as compared to 0.5–0.3 in the Schluppeck et al. data. Akin to their data, V7 had the strongest contralaterality among the three ips areas, especially for the cue response. In frontal areas, our data show more contralaterality in medial FEF, while Srimal and Curtis reported contralateral tuning for lateral FEF and not for medial FEF. Many other human fMRI studies did not observe any significant contralateral tuning (e.g., Khonsari et al. 2007), and topographic phase-mapping experiments demonstrated only weak contralateral biases (see Schluppeck et al. 2005).

Several possibilities could explain the quantitative difference between our results and the Schluppeck et al. 2006 results. Schluppeck et al. 2006 extracted timecourses from pre-selected ROIs that have already been shown to exhibit a topographic organization, but this procedure is unlikely to be a source of the discrepancy. In their study, pre-selected ROIs were quite extensive and encompassed comparable regions in our study. Trivially, the reason for the discrepancy may lie in the substantial variability of BOLD timecourses across subjects. Schluppeck et al. 2006 used only 4 subjects, so it's possible that these subjects happened to exhibit stronger contralaterality (of course, the same argument may apply to our 2 monkey subjects, although our preliminary data from a third monkey (monkey F) used in a similar memory saccade task showed similarly strong contralateral memory delay responses).

Finally, for the CS calculation we used actual %BOLD change response amplitude (see Experimental Procedures), while Schluppeck et al. used model fit predictors. This manipulation could not manufacture a contralateral bias, since the model was linear and predictor-response transformations would not affect the ratio between contra- and ipsilateral trials. However, it could explain the difference in estimates of cue-to-delay ratios between our and the Schluppeck et al. studies. In Schluppeck et al., the delay period activity predictor d was modeled as a constant level spanning the entire delay period, while cue c was modeled as an instantaneous function. Since the hemodynamic transfer function acts as a 'leaky integrator', the value of d required to

reach a similar apparent level of BOLD activation as in cue response peak would be quite low (d<<c). At the moment, it's unclear whether the assumption of constant neuronal delay activity commencing immediately after the cue is justified—for example, it could be that with such long delays, the delay period activity should be divided into early cue processing and late maintenance/preparation/recall stages. Therefore, we chose to report actual %BOLD change values that required no prior assumptions except an unbiased initial baseline period.

A recent fMRI study by Jack and colleagues (Jack et al. 2007) examined topographic and contralateral organization of human cortical areas using a variant of a time-unresolved delayed saccade task with closely spaced trials, short delay periods, and continuous presentation of cue-specific distractors. While the results of this study cannot differentiate between effects of cue, distractors, and forward-and-return saccades, they convincingly showed that under these conditions extra-occipital areas exhibited little visual topography. Instead, discrete parietal and frontal areas manifested some degree of contralateral tuning, but even in most contralateral ROIs, the ipsilateral response was approximately half as strong as the contralateral response, resulting in CS ∼0.33 (note that the 'laterality index' used by Jack at al. was calculated as L=(R_{contra}-R_{ipsi})/R_{contra}, thus L of 0.5 transforms to a CS of 0.33 in both ours and Schluppeck et al.'s formulations).

Contralaterality and Topography in Human PPC

Despite continuous attempts to characterize the organization of human PPC in terms of spatial, effector, and task specificity, and possible monkey homologies, the apparent functional and anatomical complexity of parietal areas is far from being resolved. Here we only briefly mention the spatial tuning aspect of the problem. First, several groups that used time-unresolved phase-encoding experiments reported anatomically divergent results: Sereno et al. found a discrete topographic region in medial ips while Schluppeck et al. (2005) and Silver et al. (2005) showed two larger regions, IPS1 and IPS2, tiling medial SPL along ips, dorsally and anteriorly from V7. More recently, Swisher et al. (2007) defined, in addition to IPS1/2, two more areas IPS3/4

located in the 'vicinity' of the topographic area defined by Sereno et al. Additionally, Jack et al. delineated their most contralateral medial ips area, termed 'MIPS', which corresponded reasonably well to the area of Sereno et al.; but they do not find contralateral tuning in regions that would be termed IPS1/2. Interestingly, in addition to MIPS, which also roughly corresponds to retinotopic IPS (retIPS) as defined by Medendorp and colleagues (Medendorp et al. 2006), Jack et al. reported even stronger contralaterality in anterior precuneus (pCu), in agreement with our results.

Although some differences in tasks may account for these discrepancies, the results obtained with different tasks in the same studies/labs are usually more consistent than between labs. Other possibilities include different analyses/software, SNR (due to field strength, RF coil, and resolution), statistical power, variability between subjects etc. Most importantly, these discrepancies underscore the limitations of a phase encoding approach to extra-occipital areas, both in terms of confounding different visual, motor, and cognitive components, and with respect to methodological issues (refer to Discussion in Jack et al. 2007 for extensive treatment of the latter).

References

R. A. Andersen and C. A. Buneo. Intentional maps in posterior parietal cortex. *Annu Rev Neurosci*, 25:189–220, 2002.

R. A. Andersen, G. K. Essick, and R. M. Siegel. Encoding of spatial location by posterior parietal neurons. *Science*, 230(4724):456–8, 1985.

R. A. Andersen, C. Asanuma, G. Essick, and R. M. Siegel. Corticocortical connections of anatomically and physiologically defined subdivisions within the inferior parietal lobule. *J Comp Neurol*, 296(1):65–113, 1990.

S. V. Astafiev, G. L. Shulman, C. M. Stanley, A. Z. Snyder, D. C. Van Essen, and M. Corbetta. Functional organization of human intraparietal and frontal cortex for attending, looking, and pointing. *J Neurosci*, 23(11):4689–99, 2003.

J. T. Baker, G. H. Patel, M. Corbetta, and L. H. Snyder. Distribution of activity across the monkey cerebral cortical surface, thalamus and midbrain during rapid, visually guided saccades. *Cereb Cortex*, 16(4):447–59, 2006.

S. Bakola, G. G. Gregoriou, A. K. Moschovakis, and H. E. Savaki. Functional imaging of the intraparietal cortex during saccades to visual and memorized targets. *Neuroimage*, 31(4):1637–49, 2006.

S. Bakola, G. G. Gregoriou, A. K. Moschovakis, V. Raos, and H. E. Savaki. Saccade-related information in the superior temporal motion complex: quantitative functional mapping in the monkey. *J Neurosci*, 27(9):2224–9, 2007.

S. Barash, R. M. Bracewell, L. Fogassi, J. W. Gnadt, and R. A. Andersen. Saccade-related activity in the lateral intraparietal area. i. temporal properties; comparison with area 7a. *J Neurophysiol*, 66(3):1095–108, 1991a.

S. Barash, R. M. Bracewell, L. Fogassi, J. W. Gnadt, and R. A. Andersen. Saccade-related activity in the lateral intraparietal area. ii. spatial properties. *J Neurophysiol*, 66(3):1109–24, 1991b.

S. Ben Hamed, J. R. Duhamel, F. Bremmer, and W. Graf. Representation of the visual field in the lateral intraparietal area of macaque monkeys: a quantitative receptive field analysis. *Exp Brain Res*, 140(2):127–44, 2001.

J. W. Bisley, B. S. Krishna, and M. E. Goldberg. A rapid and precise on-response in posterior parietal cortex. *J Neurosci*, 24(8):1833–8, 2004.

G. J. Blatt, R. A. Andersen, and G. R. Stoner. Visual receptive field organization and cortico-cortical connections of the lateral intraparietal area (area lip) in the macaque. *J Comp Neurol*, 299(4):421–45, 1990.

J. Bos and L. A. Benevento. Projections of the medial pulvinar to orbital cortex and frontal eye fields in the rhesus monkey (macaca mulatta). *Exp Neurol*, 49(2): 487–96, 1975.

D. Boussaoud, L. G. Ungerleider, and R. Desimone. Pathways for motion analysis: cortical connections of the medial superior temporal and fundus of the superior temporal visual areas in the macaque. *J Comp Neurol*, 296(3):462–95, 1990.

M. R. G. Brown, J. F. X. DeSouza, H. C. Goltz, K. Ford, R. S. Menon, M. A. Goodale, and S. Everling. Comparison of memory- and visually guided saccades using event-related fmri. *Journal of Neurophysiology*, 91(2):873–889, 2004.

C. Bruce, R. Desimone, and C. G. Gross. Visual properties of neurons in a polysensory area in superior temporal sulcus of the macaque. *J Neurophysiol*, 46(2):369–84, 1981.

C. J. Bruce and M. E. Goldberg. Primate frontal eye fields .1. single neurons discharging before saccades. *Journal of Neurophysiology*, 53(3):603–635, 1985.

R. B. Buxton, E. C. Wong, and L. R. Frank. Dynamics of blood flow and oxygenation changes during brain activation: the balloon model. *Magn Reson Med*, 39(6):855–64, 1998.

J. L. Calton, A. R. Dickinson, and L. H. Snyder. Non-spatial, motor-specific activation in posterior parietal cortex. *Nat Neurosci*, 5(6):580–8, 2002.

M. V. Chafee and P. S. Goldman-Rakic. Matching patterns of activity in primate prefrontal area 8a and parietal area 7ip neurons during a spatial working memory task. *J Neurophysiol*, 79(6):2919–40, 1998.

M. Cicek, D. Gitelman, R. S. Hurley, A. Nobre, and M. Mesulam. Anatomical physiology of spatial extinction. *Cereb Cortex*, 17(12):2892–8, 2007.

J. D. Connolly, M. A. Goodale, R. S. Menon, and D. P. Munoz. Human fmri evidence for the neural correlates of preparatory set. *Nat Neurosci*, 5(12):1345–52, 2002.

J. D. Connolly, R. A. Andersen, and M. A. Goodale. Fmri evidence for a 'parietal reach region' in the human brain. *Experimental Brain Research*, 153(2):140–145, 2003.

J. D. Connolly, M. A. Goodale, H. C. Goltz, and D. P. Munoz. fmri activation in the human frontal eye field is correlated with saccadic reaction time. *Journal of Neurophysiology*, 94(1):605–611, 2005.

C. Constantinidis and E. Procyk. The primate working memory networks. *Cogn Affect Behav Neurosci*, 4(4):444–65, 2004.

M. Corbetta, M. J. Kincade, C. Lewis, A. Z. Snyder, and A. Sapir. Neural basis and recovery of spatial attention deficits in spatial neglect. *Nat Neurosci*, 8(11): 1603–10, 2005.

F. W. Cornelissen, H. Kimmig, M. Schira, R. M. Rutschmann, R. P. Maguire, A. Broerse, J. A. Den Boer, and M. W. Greenlee. Event-related fmri responses in the human frontal eye fields in a randomized pro- and antisaccade task. *Exp Brain Res*, 145(2):270–4, 2002.

S. M. Courtney, L. Petit, J. M. Maisog, L. G. Ungerleider, and J. V. Haxby. An area specialized for spatial working memory in human frontal cortex. *Science*, 279 (5355):1347–1351, 1998.

H. Cui and R. A. Andersen. Posterior parietal cortex encodes autonomously selected motor plans. *Neuron*, 56(3):552–9, 2007.

C. E. Curtis and M. D'Esposito. Persistent activity in the prefrontal cortex during working memory. *Trends Cogn Sci*, 7(9):415–423, 2003.

C. E. Curtis and M. D'Esposito. Selection and maintenance of saccade goals in the human frontal eye fields. *Journal of Neurophysiology*, 95(6):3923–3927, 2006.

C. E. Curtis, V. Y. Rao, and M. D'Esposito. Maintenance of spatial and motor codes during oculomotor delayed response tasks. *Journal of Neuroscience*, 24(16): 3944–3952, 2004.

C. E. Curtis, F. T. Sun, L. M. Miller, and M. D'Esposito. Coherence between fmri time-series distinguishes two spatial working memory networks. *Neuroimage*, 26 (1):177–83, 2005.

H. L. Dean, J. C. Crowley, and M. L. Platt. Visual and saccade-related activity in macaque posterior cingulate cortex. *J Neurophysiol*, 92(5):3056–68, 2004.

K. Denys, W. Vanduffel, D. Fize, K. Nelissen, H. Peuskens, D. Van Essen, and G. A. Orban. The processing of visual shape in the cerebral cortex of human and non-human primates: a functional magnetic resonance imaging study. *J Neurosci*, 24 (10):2551–65, 2004.

J. F. DeSouza, R. S. Menon, and S. Everling. Preparatory set associated with pro-saccades and anti-saccades in humans investigated with event-related fmri. *J Neurophysiol*, 89(2):1016–23, 2003.

A. R. Dickinson, J. L. Calton, and L. H. Snyder. Nonspatial saccade-specific activation in area lip of monkey parietal cortex. *J Neurophysiol*, 90(4):2460–4, 2003.

D. J. Dubowitz, D. Y. Chen, D. J. Atkinson, K. L. Grieve, B. Gillikin, Jr. Bradley, W. G., and R. A. Andersen. Functional magnetic resonance imaging in macaque cortex. *Neuroreport*, 9(10):2213–8, 1998.

D. J. Dubowitz, D. Y. Chen, D. J. Atkinson, M. Scadeng, A. Martinez, M. B. Andersen, R. A. Andersen, and Wg Jr Bradley. Direct comparison of visual cortex activation in human and non-human primates using functional magnetic resonance imaging. *J Neurosci Methods*, 107(1-2):71–80, 2001.

J. B. Durand, K. Nelissen, O. Joly, C. Wardak, J. T. Todd, J. F. Norman, P. Janssen, W. Vanduffel, and G. A. Orban. Anterior regions of monkey parietal cortex process visual 3d shape. *Neuron*, 55(3):493–505, 2007.

M. P. Eckstein, B. R. Beutter, B. T. Pham, S. S. Shimozaki, and L. S. Stone. Similar neural representations of the target for saccades and perception during search. *J Neurosci*, 27(6):1266–70, 2007.

S. Everling and D. P. Munoz. Neuronal correlates for preparatory set associated with pro-saccades and anti-saccades in the primate frontal eye field. *J Neurosci*, 20(1): 387–400, 2000.

D. J. Felleman and D. C. Van Essen. Distributed hierarchical processing in the primate cerebral cortex. *Cereb Cortex*, 1(1):1–47, 1991.

K. A. Ford, H. C. Goltz, M. R. Brown, and S. Everling. Neural processes associated with antisaccade task performance investigated with event-related fmri. *J Neurophysiol*, 94(1):429–40, 2005.

S. Funahashi, C. J. Bruce, and P. S. Goldman-Rakic. Mnemonic coding of visual space in the monkey's dorsolateral prefrontal cortex. *J Neurophysiol*, 61:331–349, 1989.

J. M. Fuster. Inferotemporal units in selective visual attention and short-term memory. *J Neurophysiol*, 64(3):681–97, 1990.

D. Gaffan and J. Hornak. Visual neglect in the monkey. representation and disconnection. *Brain*, 120 (Pt 9):1647–57, 1997.

J. W. Gnadt and R. A. Andersen. Memory related motor planning activity in posterior parietal cortex of macaque. *Experimental Brain Research*, 70:216–220, 1988.

J. W. Gnadt, R. M. Bracewell, and R. A. Andersen. Sensorimotor transformation during eye movements to remembered visual targets. *Vision Res*, 31(4):693–715, 1991.

M. E. Goldberg, J. Bisley, K. D. Powell, J. Gottlieb, and M. Kusunoki. The role of the lateral intraparietal area of the monkey in the generation of saccades and visuospatial attention. *Ann N Y Acad Sci*, 956:205–15, 2002.

Jr. Hagler, D. J., L. Riecke, and M. I. Sereno. Parietal and superior frontal visuospatial maps activated by pointing and saccades. *Neuroimage*, 35(4):1562–77, 2007.

O. Hikosaka and R. H. Wurtz. Visual and oculomotor functions of monkey substantia nigra pars reticulata. iii. memory-contingent visual and saccade responses. *J Neurophysiol*, 49(5):1268–84., 1983.

M. Inoue, A. Mikami, I. Ando, and H. Tsukada. Functional brain mapping of the macaque related to spatial working memory as revealed by pet. *Cereb Cortex*, 14 (1):106–19, 2004.

S. Ito, V. Stuphorn, J. W. Brown, and J. D. Schall. Performance monitoring by the anterior cingulate cortex during saccade countermanding. *Science*, 302(5642): 120–2, 2003.

A. I. Jack, G. H. Patel, S. V. Astafiev, A. Z. Snyder, E. Akbudak, G. L. Shulman, and M. Corbetta. Changing human visual field organization from early visual to extra-occipital cortex. *PLoS ONE*, 2(5):e452, 2007.

H. O. Karnath, S. Ferber, and M. Himmelbach. Spatial awareness is a function of the temporal not the posterior parietal lobe. *Nature*, 411(6840):950–3, 2001.

S. Kastner, K. DeSimone, C. S. Konen, S. M. Szczepanski, K. S. Weiner, and K. A. Schneider. Topographic maps in human frontal cortex revealed in memory-guided saccade and spatial working-memory tasks. *J Neurophysiol*, 97(5):3494–507, 2007.

C. Kayser, M. Kim, K. Ugurbil, D. S. Kim, and P. Konig. A comparison of hemodynamic and neural responses in cat visual cortex using complex stimuli. *Cerebral Cortex*, 14(8):881–891, 2004.

R. H. Khonsari, E. Lobel, D. Milea, S. Lehericy, C. Pierrot-Deseilligny, and A. Berthoz. Lateralized parietal activity during decision and preparation of saccades. *Neuroreport*, 18(17):1797–800, 2007.

H. Komatsu and R. H. Wurtz. Relation of cortical areas mt and mst to pursuit eye movements. i. localization and visual properties of neurons. *J Neurophysiol*, 60(2): 580–603, 1988a.

H. Komatsu and R. H. Wurtz. Relation of cortical areas mt and mst to pursuit eye movements. iii. interaction with full-field visual stimulation. *J Neurophysiol*, 60(2): 621–44, 1988b.

M. Koyama, I. Hasegawa, T. Osada, Y. Adachi, K. Nakahara, and Y. Miyashita. Functional magnetic resonance imaging of macaque monkeys performing visually guided saccade tasks: comparison of cortical eye fields with humans. *Neuron*, 41 (5):795–807, 2004.

B. M. Lawrence and L. H. Snyder. Comparison of effector-specific signals in frontal and parietal cortices. *J Neurophysiol*, 96(3):1393–400, 2006.

J. W. Lewis and D. C. Van Essen. Corticocortical connections of visual, sensorimotor, and multimodal processing areas in the parietal lobe of the macaque monkey. *J Comp Neurol*, 428(1):112–37, 2000a.

J. W. Lewis and D. C. Van Essen. Mapping of architectonic subdivisions in the macaque monkey, with emphasis on parieto-occipital cortex. *J Comp Neurol*, 428 (1):79–111, 2000b.

D. J. Logan and C. J. Duffy. Cortical area mstd combines visual cues to represent 3-d self-movement. *Cereb Cortex*, 16(10):1494–507, 2006.

N. K. Logothetis, J. Pauls, M. Augath, T. Trinath, and A. Oeltermann. Neurophysiological investigation of the basis of the fmri signal. *Nature*, 412(6843):150–157, 2001.

K. E. Luh, C. M. Butter, and H. A. Buchtel. Impairments in orienting to visual stimuli in monkeys following unilateral lesions of the superior sulcal polysensory cortex. *Neuropsychologia*, 24(4):461–70, 1986.

J. B. Mandeville, J. J. Marota, B. E. Kosofsky, J. R. Keltner, R. Weissleder, B. R. Rosen, and R. M. Weisskoff. Dynamic functional imaging of relative cerebral blood volume during rat forepaw stimulation. *Magn Reson Med*, 39(4):615–24, 1998.

P. Mazzoni, R. M. Bracewell, S. Barash, and R. A. Andersen. Motor intention activity in the macaque's lateral intraparietal area. i. dissociation of motor plan from sensory memory. *J Neurophysiol*, 76(3):1439–56, 1996.

W. P. Medendorp, H. C. Goltz, and T. Vilis. Remapping the remembered target location for anti-saccades in human posterior parietal cortex. *Journal of Neurophysiology*, 94(1):734–740, 2005.

W. P. Medendorp, H. C. Goltz, and T. Vilis. Directional selectivity of bold activity in human posterior parietal cortex for memory-guided double-step saccades. *Journal of Neurophysiology*, 95(3):1645–1655, 2006.

M. M. Mesulam. Spatial attention and neglect: parietal, frontal and cingulate contributions to the mental representation and attentional targeting of salient extrapersonal events. *Philos Trans R Soc Lond B Biol Sci*, 354(1387):1325–46, 1999.

E. K. Miller, L. Li, and R. Desimone. Activity of neurons in anterior inferior temporal cortex during a short-term memory task. *J Neurosci*, 13(4):1460–78, 1993.

K. Nakahara, M. Ohbayashi, H. Tomita, and Y. Miyashita. The neuronal basis of visual memory and imagery in the primate: a neurophysiological approach. *Adv Biophys*, 35:103–19, 1998.

K. Nakahara, T. Hayashi, S. Konishi, and Y. Miyashita. Functional mri of macaque monkeys performing a cognitive set-shifting task. *Science*, 295(5559):1532–6, 2002.

K. Nelissen, W. Vanduffel, and G. A. Orban. Charting the lower superior temporal region, a new motion-sensitive region in monkey superior temporal sulcus. *J Neurosci*, 26(22):5929–47, 2006.

W. T. Newsome, R. H. Wurtz, and H. Komatsu. Relation of cortical areas mt and mst to pursuit eye movements. ii. differentiation of retinal from extraretinal inputs. *J Neurophysiol*, 60(2):604–20, 1988.

G. A. Orban, D. Van Essen, and W. Vanduffel. Comparative mapping of higher visual areas in monkeys and humans. *Trends Cogn Sci*, 8(7):315–24, 2004.

J. Padberg, B. Seltzer, and C. G. Cusick. Architectonics and cortical connections of the upper bank of the superior temporal sulcus in the rhesus monkey: an analysis in the tangential plane. *J Comp Neurol*, 467(3):418–34, 2003.

M. Pare and R. H. Wurtz. Monkey posterior parietal cortex neurons antidromically activated from superior colliculus. *J Neurophysiol*, 78(6):3493–7, 1997.

M. A. Pinsk, K. DeSimone, T. Moore, C. G. Gross, and S. Kastner. Representations of faces and body parts in macaque temporal cortex: a functional mri study. *Proc Natl Acad Sci U S A*, 102(19):6996–7001, 2005.

M. L. Platt and P. W. Glimcher. Responses of intraparietal neurons to saccadic targets and visual distractors. *J Neurophysiol*, 78(3):1574–89, 1997.

J. Quintana, J. Yajeya, and J. M. Fuster. Prefrontal representation of stimulus attributes during delay tasks. i. unit activity in cross-temporal integration of sensory and sensory-motor information. *Brain Res*, 474(2):211–21, 1988.

J. B. Rowe, I. Toni, O. Josephs, R. S. J. Frackowiak, and R. E. Passingham. The prefrontal cortex: Response selection or maintenance within working memory? *Science*, 288(5471):1656–1660, 2000.

K. Saleem and N. K. Logothetis. *A Combined MRI and Histology Atlas of the Rhesus Monkey Brain*. Academic Press, New York, 2006.

H. Sawamura, S. Georgieva, R. Vogels, W. Vanduffel, and G. A. Orban. Using functional magnetic resonance imaging to assess adaptation and size invariance of shape processing by humans and monkeys. *J Neurosci*, 25(17):4294–306, 2005.

H. Sawamura, G. A. Orban, and R. Vogels. Selectivity of neuronal adaptation does not match response selectivity: a single-cell study of the fmri adaptation paradigm. *Neuron*, 49(2):307–18, 2006.

S. P. Scalaidhe, T. D. Albright, H. R. Rodman, and C. G. Gross. Effects of superior temporal polysensory area lesions on eye movements in the macaque monkey. *J Neurophysiol*, 73(1):1–19, 1995.

J. D. Schall. Neuronal activity related to visually guided saccades in the frontal eye fields of rhesus monkeys: comparison with supplementary eye fields. *J Neurophysiol*, 66(2):559–79, 1991.

D. Schluppeck, P. Glimcher, and D. J. Heeger. Topographic organization for delayed saccades in human posterior parietal cortex. *J Neurophysiol*, 94(2):1372–84, 2005.

D. Schluppeck, C. E. Curtis, P. W. Glimcher, and D. J. Heeger. Sustained activity

in topographic areas of human posterior parietal cortex during memory-guided saccades. *Journal of Neuroscience*, 26(19):5098–5108, 2006.

M. I. Sereno, S. Pitzalis, and A. Martinez. Mapping of contralateral space in retinotopic coordinates by a parietal cortical area in humans. *Science*, 294(5545):1350–4, 2001.

M. A. Silver, D. Ress, and D. J. Heeger. Topographic maps of visual spatial attention in human parietal cortex. *J Neurophysiol*, 94(2):1358–71, 2005.

T. Siman-Tov, A. Mendelsohn, T. Schonberg, G. Avidan, I. Podlipsky, L. Pessoa, N. Gadoth, L. G. Ungerleider, and T. Hendler. Bihemispheric leftward bias in a visuospatial attention-related network. *J Neurosci*, 27(42):11271–8, 2007.

L. H. Snyder, A. P. Batista, and R. A. Andersen. Coding of intention in the posterior parietal cortex. *Nature*, 386(6621):167–70., 1997.

L. H. Snyder, A. P. Batista, and R. A. Andersen. Intention-related activity in the posterior parietal cortex: a review. *Vision Res*, 40(10-12):1433–41, 2000.

R. Srimal and C. E. Curtis. Persistent neural activity during the maintenance of spatial position in working memory. *Neuroimage*, 39(1):455–68, 2008.

J. D. Swisher, M. A. Halko, L. B. Merabet, S. A. McMains, and D. C. Somers. Visual topography of human intraparietal sulcus. *J Neurosci*, 27(20):5326–37, 2007.

J. Talairach and P. Tournoux. *Co-planar Stereotaxic Atlas of the Human Brain: 3-Dimensional Proportinal System - an Approach to Cerebral Imaging.* Thieme Medical Publishers, New York, 1988.

K. Tanaka and H. Saito. Analysis of motion of the visual field by direction, expansion/contraction, and rotation cells clustered in the dorsal part of the medial superior temporal area of the macaque monkey. *J Neurophysiol*, 62(3):626–41, 1989.

K. Tanaka, Y. Sugita, M. Moriya, and H. Saito. Analysis of object motion in the ventral part of the medial superior temporal area of the macaque visual cortex. *J Neurophysiol*, 69(1):128–42, 1993.

P. Thier and R. A. Andersen. Electrical microstimulation distinguishes distinct saccade-related areas in the posterior parietal cortex. *J Neurophysiol*, 80(4):1713–35, 1998.

D. Y. Tsao, W. A. Freiwald, T. A. Knutsen, J. B. Mandeville, and R. B. Tootell. Faces and objects in macaque cerebral cortex. *Nat Neurosci*, 6(9):989–95, 2003.

D. Y. Tsao, W. A. Freiwald, R. B. Tootell, and M. S. Livingstone. A cortical region consisting entirely of face-selective cells. *Science*, 311(5761):670–4, 2006.

L. G. Ungerleider. Functional brain imaging studies of cortical mechanisms for memory. *Science*, 270(5237):769–75, 1995.

L. G. Ungerleider and J. V. Haxby. 'what' and 'where' in the human brain. *Curr Opin Neurobiol*, 4(2):157–65, 1994.

D. C. Van Essen. Surface-based approaches to spatial localization and registration in primate cerebral cortex. *Neuroimage*, 23 Suppl 1:S97–107, 2004.

W. Vanduffel, D. Fize, H. Peuskens, K. Denys, S. Sunaert, J. T. Todd, and G. A. Orban. Extracting 3d from motion: differences in human and monkey intraparietal cortex. *Science*, 298(5592):413–5, 2002.

M. Vesia, J. A. Monteon, L. E. Sergio, and J. D. Crawford. Hemispheric asymmetry in memory-guided pointing during single-pulse transcranial magnetic stimulation of human parietal cortex. *J Neurophysiol*, 96(6):3016–27, 2006.

R. T. Watson, E. Valenstein, A. Day, and K. M. Heilman. Posterior neocortical systems subserving awareness and neglect. neglect associated with superior temporal sulcus but not area 7 lesions. *Arch Neurol*, 51(10):1014–21, 1994.

Y. D. Zhou and J. M. Fuster. Mnemonic neuronal activity in somatosensory cortex. *Proc Natl Acad Sci U S A*, 93(19):10533–7, 1996.

Chapter 5

Conclusion

Goal-directed behavior requires the planning and preparation of actions in order to respond flexibly and dynamically to environmental stimuli. The existence of these planning processes has long been expounded by psychologists, who recognized that the manner in which a movement was initiated already reflected the pre-specified information about the movement and the intended objective of the movement (Rosenbaum 1980; Jeannerod 1981).

Delayed-response tasks, which temporally separate instructive information from the execution of contingent motor responses, have been ubiquitously used to disentangle neural activity related to processing the contextual/sensory instructive information, performing the movement, and the intervening 'planning the movement'. However, the debate has long ensued as to the nature of the activity probed during this 'delay' period. This delay-period activity, bridging the cue and the motor response, may correspond to a retrospective sensory memory of, or attention to, the contextual information previously cued; it may also incorporate prospective planning of upcoming actions. In studying these processes, human imaging studies generally purport a retrospective role related to attention or working memory in posterior parietal regions, and one more biased towards prospective motor planning in frontal (precentral) areas (see Chapter 2). These studies though did not adequately distinguish between working memory and a 'default set' of potential movements; nor between the preparation to perform a movement and the preparation to inhibit a movement (see Chapter 2). While controlling for these issues, we designed a time-resolved fMRI

experiment that permitted isolation of preparatory fMRI activity, specifically related to the planning and the inhibition of right index finger reaches towards memorized target locations. In so doing, preparatory fMRI activity was most robustly demonstrated in the left superior parietal lobule, though also present in other regions within the posterior parietal and premotor cortex. Additionally, the activity of these regions encoded both movements to be performed and those to be inhibited. In essence, then, action planning areas reflect both types of action goals relevant for behavior—those to be acquired and those to be avoided.

We utilized a variant of this delayed-response task to investigate the representation of multiple motor plans (not discussed in depth in this thesis, but see Discussions in Chapter 2 and 3). In this task, trials either instructed one sequence of movements (key presses); or presented two potential movement sequences, one of which would be cued at the end of the delay period. Preliminary results show that both PPC and premotor cortex activation graded with the number of possible movement sequences during the delay phase, even in conditions in which only one of these sequences would ultimately be performed (Lindner A., Kagan I., Iyer A. and Andersen, R.A. 2008 Prospective coding of alternative actions in human parietal and premotor cortex. 6th FENS Forum of European Neuroscience). These observations suggest that competing action plans are simultaneously encoded in these regions.

If multiple potential actions are represented concurrently, some mechanism must exist by which to determine an appropriate, or optimal, one to perform, i.e., the one that is likely to yield the best outcome. This determination then is presumably predicated upon an appraisal of the possible consequences of the available behavioral responses. We therefore assessed whether action-planning regions additionally incorporated such information into the action plans they encode. To do so, human subjects were scanned while performing a motor planning task, with monetary gains and losses imposed for correct or incorrect trial completion. Though previous studies have investigated the encoding of action contingencies (see Chapter 3), our experiment differed in a few respects: (1) the task was sufficiently challenging to produce a non-trivial probability of incorrect trial completion and (2) the consequence of un-

successful trial completion was not mere absence of reward, but overt punishment. Hence, both the monetary gains and the losses were viable consequences to be considered. Reward structures responded to the contextual cue indicating the gain-loss contingencies for the movement, and reflected its expected value, based on subjects' actual performance (their probability of success). In contrast, frontoparietal motor planning regions were more active during the delay period in conditions of both high expected gains and high expected losses. Furthermore, this pattern of activity depended more strongly on whether subjects believed they would attain a gain or loss than on whether they were actually more likely to attain a gain or loss. These findings suggest that subjective beliefs and biases may significantly modulate the neural representation of action plans.

The impact of cognitive biases on behavior has been the subject of much discussion (see Discussion, Ch. 3). However, their influence on neural activity in the frontoparietal network, in the experimental context of a single instructed movement sequence where subjects receive trial-by-trial (though no cumulative) feedback was surprising, and deserves further scrutiny. To probe this effect more meticulously, future experiments designed to manipulate and control subject's perceptions of their performance and track their on-going perceptions throughout the experimental session are needed. Additionally, an interesting question would be to explore how these factors affect behavior in an experimental paradigm where many response alternatives exist. Such a context of response selection would allow us to assess the respective contributions of neural activity in frontoparietal regions and in ventromedial striatal subregions (which appear to track expected outcomes more veridically) in the process of decision-making.

The human imaging studies presented in this thesis, amongst a plethora of others, have sought to unravel the multifarious nature of delay-period activity during the planning of goal-directed actions. The imaging approach proffers the advantage of glimpsing the entire brain at once, revealing the involvement and dynamics of large networks of cortical and subcortical regions. Yet its ability to elucidate neural processes underlying activations in these tasks is limited. Providing complementary

information, monkey electrophysiological studies using similar delayed-response tasks can illuminate single-unit neural firing patterns with much finer temporal resolution. However, direct generalizations and inferences between these two bodies of literature are impeded by differences in species, techniques, and trial durations. For instance, frontoparietal regions recruited by saccade planning exhibit less BOLD contralaterality in humans than would be expected based on single-unit studies in monkeys. Given that contralaterality is a major principle of organization in sensory and motor systems, this discrepancy is surprising, but whether it stems from methodological or species dissimilarities is unclear. To address such issues, fMRI in monkeys, completing the same tasks as humans, constitutes the necessary link to relate and reconcile reported findings. We therefore directly compared fMRI activation in monkeys and humans under identical experimental task requirements: delayed visually and memory-guided saccades. In addition, we successfully developed an event-related approach for the analysis of BOLD signals in alert behaving monkeys, enabling us to segregate responses from different trial epochs. In monkeys frontal, parietal and temporal areas, BOLD signals revealed spatially specific, strongly contralateral cue and memory/planning activity, as well as non-specific movement preparation during the delay period. These patterns resonated with BOLD profiles in putative human functional homologs; however, contralaterality was considerably more robust and the time-course of hemodynamic responses less sluggish in monkeys, suggesting genuine disparities between the two species.

This characterization of BOLD activity distribution, dynamics, and relative differences in human and macaque frontoparietal networks additionally serves as an indispensable foundation for our current and future studies of action planning and response selection in the two species. As choosing a target of an action is clearly an important variable in ultimately specifying a behavioral response, areas that encode object-reward associations are also relevant in guiding action planning. To map areas encoding reward associations, without the confound of neural processes related to movement, monkeys were scanned while making eye movements, either instructed or freely chosen, to differentially rewarded targets. After the saccade, reward delivery

was deferred, and activation during the expectation period was monitored. Pilot results show that the striatum, a putative reward structure, and inferotemporal regions, thought to subserve aspects of object vision, both encode stimulus-reward associations. Furthermore, when stimulus-reward associations alter, both regions reflect the new reward contingencies, though the striatum appears to play a leading role in this process.

Finally, we are conducting a free-decision variant of the delayed memory-guided saccade task, in which monkeys can make an eye movement to acquire one of two equally rewarded targets. Preliminary data demonstrate that during the delay period, between presentation of target options and the deferred saccade, BOLD signals in frontal and parietal areas reflect the choice process. In addition, the dynamics of these signals imply that regions thought to specifically mediate the planning of eye movements, namely areas LIP and FEF in the posterior parietal and frontal cortices respectively, evince the monkey's choice earlier than other subregions in these cortical areas.

In conclusion, the body of this work has provided insight into the neural substrates of action planning in humans, defining cortical regions which prospectively encode motor intentions and the consequences of those intentions. In addition, it has provided fMRI characterizations of homologous reward-encoding and action-planning structures in humans and macaques. Predicated on these findings, we look ahead to studying how the expected and experienced outcomes of actions impinge upon action-planning and decision-making in both species. In addition to conducting these future imaging experiments in humans and in monkeys, electrophysiological recordings of the same monkeys performing these same tasks forms the critical next step. With this last nexus, we can synthesize information about whole brain population dynamics and the neural computations underlying them, furnishing a greater understanding of the cortical circuits subserving the selection and planning of goal-directed actions.

Appendix 1—Expected Reward Modulation of Dorsal and Ventral Stream Activity in a Goal-Directed Oculomotor Task

A1.1 Summary

In a constantly changing environment, the ability to associate stimuli with rewards, and update this association as necessary, crucially underlies flexible goal-directed behavior. To investigate areas involved in encoding and updating these stimulus-reward associations, monkeys were scanned while making eye movements, either instructed or freely chosen, to acquire different visual targets. Expectedly, action-planning areas involving regions in frontal and posterior parietal cortices exhibited activity at the time of the eye movement that reflected the reward associated with the saccade target. In addition, reward structures such as the striatum, and areas in the temporal cortex thought to underlie object representations, displayed activity after the movement was executed in expectation of the reward; further, this activity graded with magnitude of the reward expected. When stimulus-reward associations were reversed, the activity in these regions came to reflect the new associations, albeit with differing temporal profiles. While BOLD activity in temporal cortex regions changed in step with behavior, striatal activity represented the updated associations earlier, preceding even behavioral changes. These findings suggest dissociable roles of object-representation areas and reward structures in learning and encoding the rewards associated with stimuli.

A1.2 Introduction

The selection of goals to guide action is strongly determined by the expected utilities affiliated with environmental stimuli. In a dynamic environment, this selection process fundamentally relies on the capability to associate a stimulus with a reward, and to flexibly update this association.

Studies in humans, nonhuman primates, and rodents have implicated putative cortical and subcortical reward structures in learning and representing the values or expected outcomes tied to stimuli. Electrophysiological recordings have demonstrated that orbitofrontal cortex (OFC) may denote the relative value of available rewards and objects (Tremblay et al. 1999; Schultz et al. 2000), and OFC lesions often lead to impairments in learning stimulus-reward associations (Schoenbaum et al. 2002; Bechara et al. 1994, 2000). Similarly, the striatum is thought to play a key role in both the selection of previously reinforced goals and in learning through positive reinforcement (Schultz et al. 2000; Tremblay et al. 2000; Hikosaka et al. 1991). Ablations and pathologies of basal ganglia structures also hamper the acquisition of new stimulus-reward associations (Swainson et al. 2000; Ragozzino 2007). Moreover, single-unit recordings suggest that striatal firing rates quickly reflect changes in and update stimulus-reward contingencies (Pasupathy and Miller 2005).

Cortical networks involved in the control of action also encode reward information about stimuli. Numerous studies document variables related to expected utility that influence activity in dorsal stream areas. As 'where' areas processing sensory and spatial information for the guidance of behavior, these cortical regions presumably incorporate the importance of the stimulus as a target for action, rather than the value of the object per se (Goodale et al. 1998; Glimcher 2003).

In addition to frontostriatal reward circuitry and action-planning networks, brain areas involved in visual object representation and recognition would be hypothesized to reflect reward associations, since information about the value of an object derived from past experience is critical for the facilitation of effective and rapid goal-directed behavior. As information regarding the value of objects is accumulated, such infor-

mation is likely incorporated into long-term neural representations of objects. The ventral visual or 'what' pathway (Goodale et al. 1998), including the inferotemporal (IT) cortex, is thought to subserve visual object discrimination and recognition, and its activity may thus reflect reward associations.

Prior work however has not provided a definitive account of reward encoding in the ventral visual stream. IT cortical lesions can result in the inability to form object-reward associations; this inability though could conceivably derive from IT's role in object recognition. Previous electrophysiological studies in macaques suggest that polymodal subregions such as perirhinal cortex may encode reward information. Findings about unimodal visual object areas such as TE remain equivocal, while reward-related modulation of activity in other parts of the inferotemporal cortex has not been specifically explored. Thus, whether the temporal lobe further contributes to coupling of object and reward information is still unclear.

The objective of the current study is to delineate those regions underlying visual object-reward associations, with a particular focus on the ventral object-vision stream. Specifically, we aimed to map areas that represent and update object-related reward expectancy signals using fMRI. To do so, monkeys were scanned while performing instructed- and free-choice saccade tasks where eye movements were made to acquire either a small-reward target or large-reward target. We found that areas in the temporal cortex along the superior temporal sulcus, as well as in the striatum, showed sustained activity reflecting the expectation of a delayed reward. These expectancy signals were graded with the magnitude of the reward, as long as the reward-predicting target (and/or color of target) was visible.

To ensure these responses stemmed from reward associations and not other properties of the targets, target-reward associations were reversed after the initial associations were well learned. Preliminary findings from the days immediately following reversals offer insight into how these areas dynamically update object-reward representations. The first brain area to reflect the new object-reward associations was the striatum, even preceding changes in the monkey's behavior. However, once the new associations were evident behaviorally, both striatal and temporal cortical activity

reflected the updated target-reward associations.

In addition, in reliably mapping brain substrates encoding reward information, this study serves as an important prerequisite for future reward-based decision-making studies in the macaque.

A1.3 Results

The experimental paradigm primarily demanded that monkeys saccade to peripherally presented targets to acquire a reward, described in Phase I (Fig. A1.1). Two variants were conducted chiefly as controls, explained further in Phases II and III (Fig. A1.2).

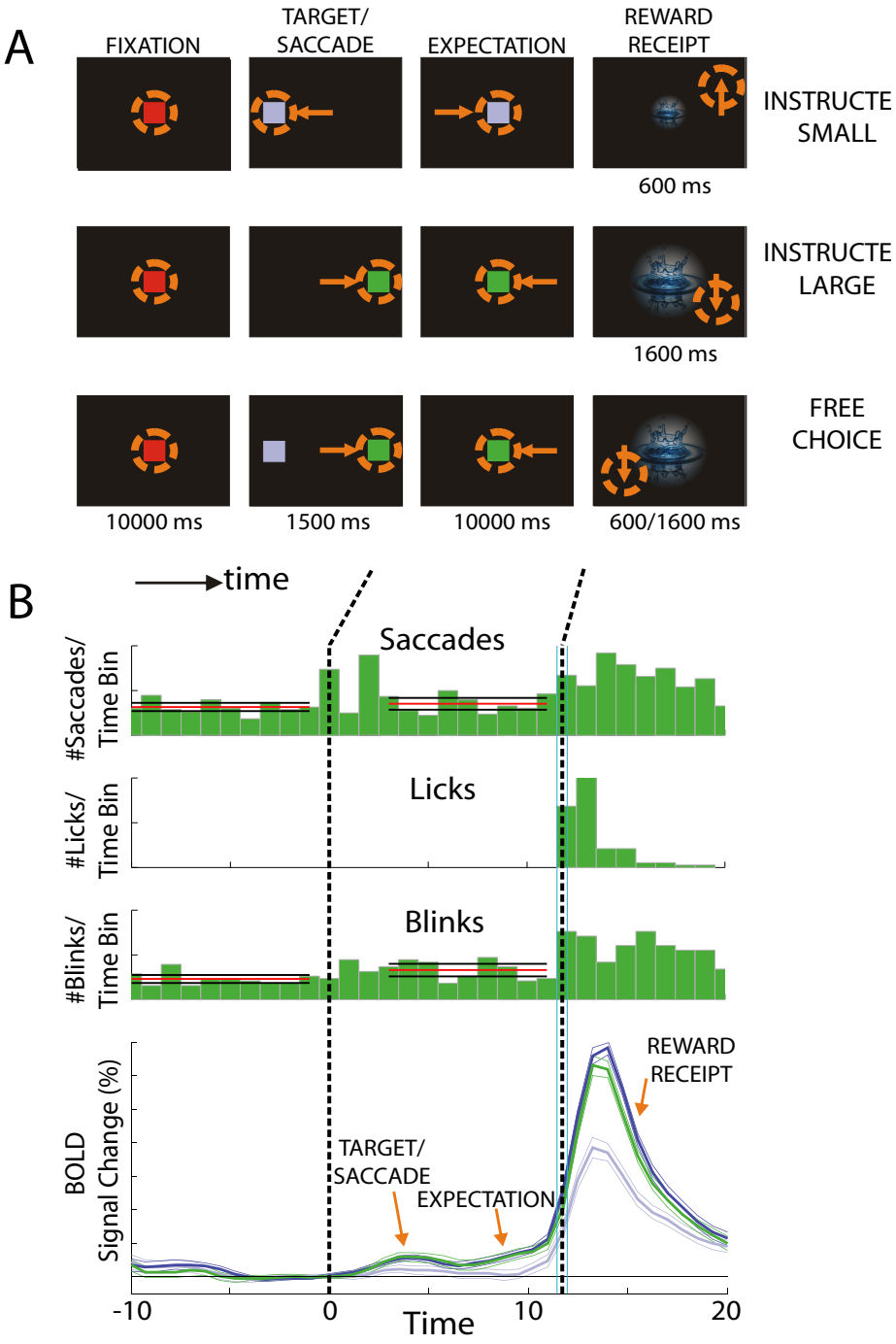
A
FIXATION
TARGET/
SACCADE
EXPECTATION
REWARD
RECEIPT
INSTRUCTE
SMALL
600 ms
INSTRUCTE
LARGE
1600 ms
FREE
CHOICE
10000 ms
1500 ms
10000 ms
600/1600 ms
B
time
Saccades
#Saccades/
Time Bin
Licks
#Licks/
Time Bin
Blinks
#Blinks/
Time Bin
REWARD
RECEIPT
TARGET/
SACCADE
EXPECTATION
BOLD
Signal Change (%)
-10
0
10
20
Time

Figure A1.1:

Experimental task and timing. *(a) Phase I: Monkeys fixated on a central red square. In 'Instructed Small' reward trials (top row), a blue target was presented either 15^o to the right or left of the fixation spot. The monkey immediately saccaded to the target, then returned to the central fixation for 10 seconds, during which time the fixation square was blue. The monkey then received 0.5 mls of water. In 'Instructed Large' reward trials (second row), the same sequence occured, but the peripheral target (and subsequent fixation square) was green. The monkey received 1.5 mls for successful completion. In 'Free choice' trials, blue and green targets were both presented (randomized right versus left). The monkey could saccade to either, and received the corresponding amount of water if he successfully completed the trial. (b) Behavior recorded throughout trials. Saccades, licks, and blinks are portrayed, above a representative timecourse that exhibits BOLD responses to all task events. For behavior, horizontal lines in task epochs indicate mean number of saccades/blinks (red), with 95% confidence interval (black lines).*

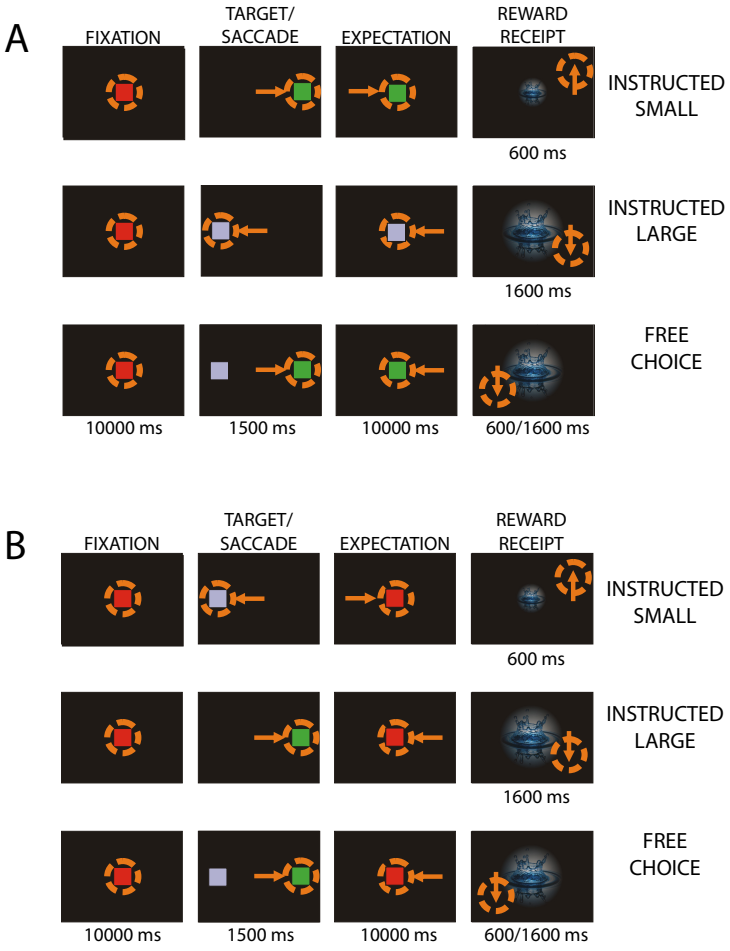

Figure A1.2:

Phase II and III *(A) Phase II: Experimental structure and timing were the same as in Phase I, but blue targets were now associated with the large fluid reward, and green targets with the small fluid reward. (B) Phase III: Again, the experimental structure, timing, and stimuli/color-reward contingencies were the same as in Phase I. After monkeys saccaded and returned to central fixation, the fixation square remained red, rather than indicating the color of the saccade-acquired target.*

Phase I: Reward Magnitude

Three monkeys were scanned while performing saccade tasks, either making an eye movement that was (1) instructed to one presented target, or (2) a free choice to one of two presented targets. The amount of reward associated with each target was indicated by the color of the target: blue denoted a small amount of fluid; and green, a large amount. Monkeys saccaded to the target at the time of target presentation, then subsequently returned to central fixation for ten seconds, after which they received the reward associated with the saccade target (Fig. A1.1A). The color of the fixation point during this expectation period prior to reward receipt signified the upcoming reward (i.e., the fixation point turned the same color as the instructed or chosen target for that trial). The long expectation period permitted disambiguation of: (1) activity due to sensory and motor processes during the target presentation and immediate saccade execution (Target/Saccade epoch), (2) signals deriving solely from expectation of the reward, the amount of which was determined by the stimulus acquired by the saccade (Expectation epoch), and (3) signals due to reward consumption and related motion artifacts produced by this consumption (Receipt epoch).

Given the confounds of the target/saccade and receipt epochs, the imaging findings for these events will be only briefly discussed, summarized in Phase I. Regions predicted to be recruited during the target/saccade period were considerably distorted in one monkey (monkey FLO). An additional monkey was therefore scanned for Part I of the experiment.

Behavioral Findings

Behavioral performance measures attest that all three monkeys grasped the stimulus-reward associations. Monkeys almost exclusively chose the high-reward target in free choice trials. In addition, they successfully completed a significantly higher percentage of instructed large-reward trials as compared to small-reward trials ($p<0.05$) (Fig. A1.3A–C, lowest rows). Reaction time latencies revealed similar inclinations. Two

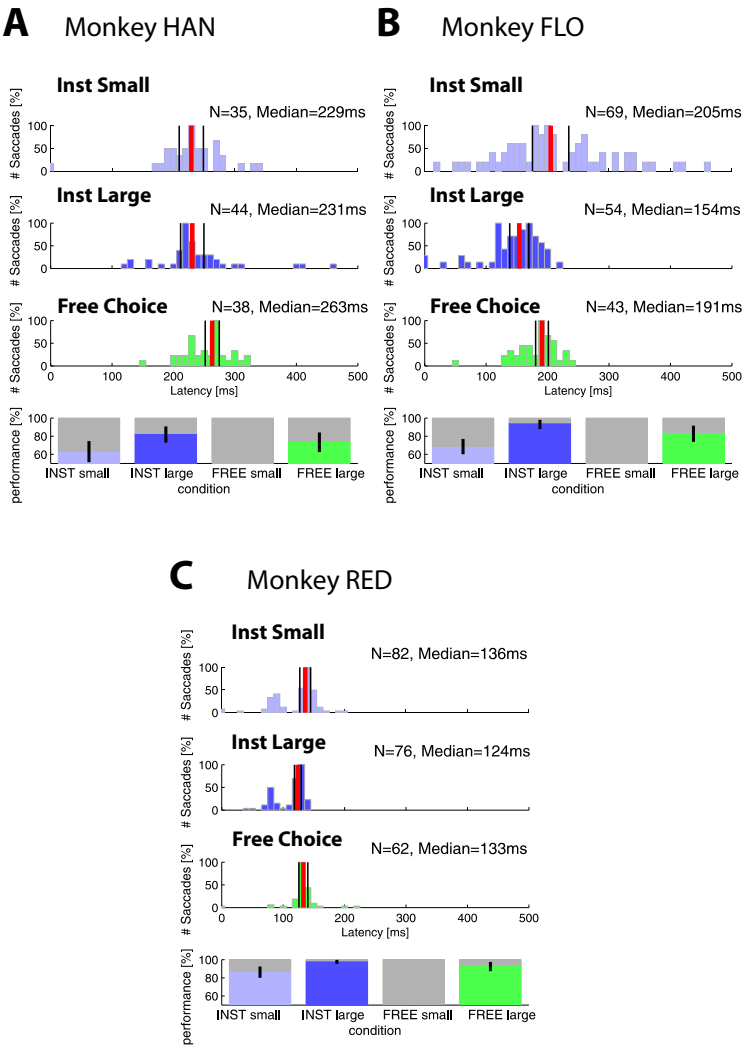

Figure A1.3:

Behavioral findings for Phase I. *(A) Monkey HAN (B) Monkey FLO (C) Monkey RED. For all monkeys—Top Row: Distribution of saccadic latencies in Instructed Small Trials. Second Row: Distribution of saccadic latencies in Instructed Large Trials. Third Row: Distribution of saccadic latencies in Free Choice Trials. Bottom Row: Mean performance (percentage of successfully completed trials) per trial type. The left column represents behavioral data from monkey HAN; the middle column, monkey FLO; and the right column, monkey RED.*

of three monkeys saccaded to instructed large reward targets with shorter laten-

cies than to instructed small-reward targets (significant in monkeys FLO and RED, $p<0.05$) (Fig. A1.3A–C, top two rows). In addition, monkeys showed a slightly increased latency when saccading to the large-reward target in free-choice trials as compared to the large reward target in instructed trials (significant in two monkeys FLO and HAN, $p<0.05$) (Fig. A1.3A–C, second and third rows). This latency difference may suggest additional processing, such as the comparison of two targets, or some hesitation in free-choice trials.

Imaging Findings

Target Presentation and/or Saccade Execution. To elucidate areas with significant reward-related modulation during the target presentation/saccade execution epoch, a contrast between instructed large reward and instructed small reward trials was implemented, The contrast did not specifically assay choice trials, as additional choice-related activity may be occurring and visual load is unbalanced as compared to instructed trials (two versus one target at time of presentation). By this contrast, the target presentation/saccade execution epoch produced significant activations bilaterally in frontal, parietal, and temporal cortical regions (voxel level $p(FWE)<0.05$ for the instructed large>instructed small contrast) (Fig. A1.4A).

Voxels in the arcuate sulcus (FEF/PMd) and in the intraparietal sulcus (IPS) displayed similar patterns of activity. However, these frontal and parietal regions could not be reliably detected in all monkeys. Distortions in monkey HAN impeded accurate characterization and localization of BOLD activity in posterior aspects of IPS; whereas inhomogeneities and distortions did not permit reliable mapping of frontal areas/FEF in monkey FLO. These distortions are likely due to proximity to the monkeys' headposts. For the monkeys in which reasonable images could be generated for these regions, the statistical maps are presented in Fig. A1.4A.

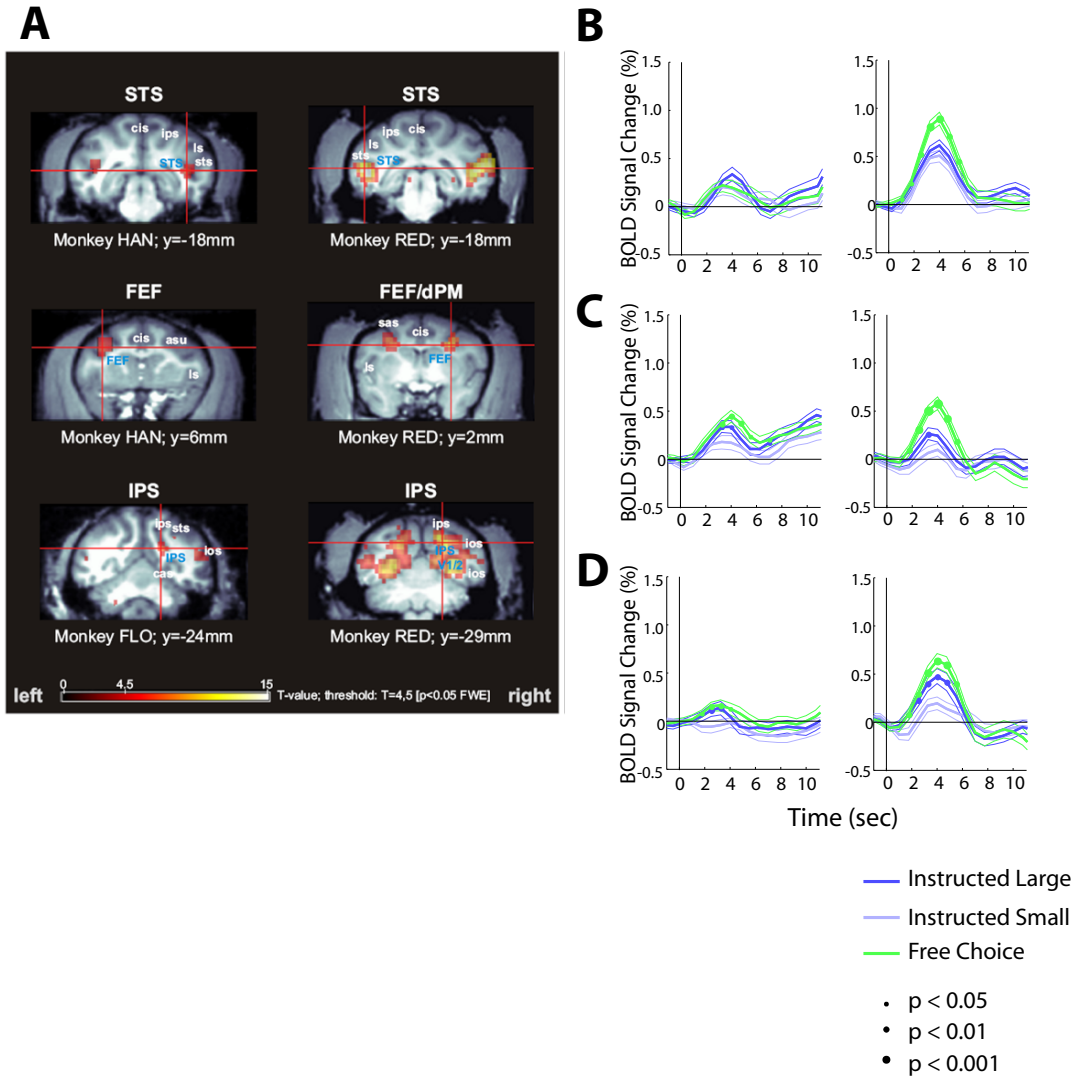

Figure A1.4:

Statistical map and timecourses: Target presentation/saccade execution epoch*(A) Statistical map for Instructed Large Reward Trial > Instructed Small Reward Trial, p(FWE)<0.05. Coronal sections to best exemplify regions in temporal, frontal, and parietal regions are shown. (B) BOLD timecourses extracted from superior temporal sulcus (sts), corresponding to the two monkeys whose maps are presented. (C) BOLD timecourses extracted from arcuate sulcus (i.e., voxels in frontal eye fields and dorsal premotor cortex), corresponding to the two monkeys whose maps are presented. (D) BOLD timecourses extracted from intraparietal sulcus (ips), corresponding to the two monkeys whose maps are presented. In all timecourse plots, signals in Instructed Large and Free Choice trials are both compared to Instructed Small trials with a two-sample t-test, at each 1 second interval. Times at which either instructed large or free choice signals are significantly different than instructed small signals are indicated with a dot.*

The BOLD signal amplitude in instructed large trials and free choice trials were both compared to the signal amplitude in instructed small reward trials at 1-second intervals (time bins) throughout the trial, using a two-sample t-test. Times at which the signal amplitudes significantly differed are indicated by a dot. (This convention is used throughout this chapter.) The BOLD timecourses extracted from frontal and parietal ROIs (Fig. A1.4C,D) demonstrate that the target/saccade event elicited a peak of activation, modulated by trial type: instructed large and free-choice trials (in which the large reward was persistently chosen) produced a significantly larger BOLD signal than did instructed small-reward trials ($p<0.05$, at most time bins between 2–6 seconds after target/saccade epoch onset).

Voxels in the banks and fundus of the superior temporal sulcus (sts) also exhibited a robust target/saccade response under this contrast. However, timecourses reveal less robust modulation of this response due to trial type and/or expected reward (Fig. A1.4B). While significant voxels lay in several subregions along the banks of sts, peak activation was in the dorsoposterior section along the sulcus, and corresponded to areas FST/TPO (Fig. A1.4A, top row).

Expectation. Temporal regions along sts and aspects of the ventromedial striatum displayed prolonged activation between saccadic acquisition of the target and receipt of reward. The statistical map presents the contrast of instructed large reward greater than instructed small reward activation during the expectation period (voxel level $p(FWE)<0.05$) (Fig. A1.5A). For this contrast, the peak of activation along sts was even further posterior along the sulcus than voxels exhibiting reward-modulated target/saccade activation, and on the lower bank of the sulcus, in areas FST/TEO.

Timecourses of BOLD activity in these regions (Fig. A1.5B,C) show significant modulation due to reward magnitude, with instructed large-reward and free-choice trials eliciting an increased signal amplitude over small-reward trials as early as the target/saccade response.

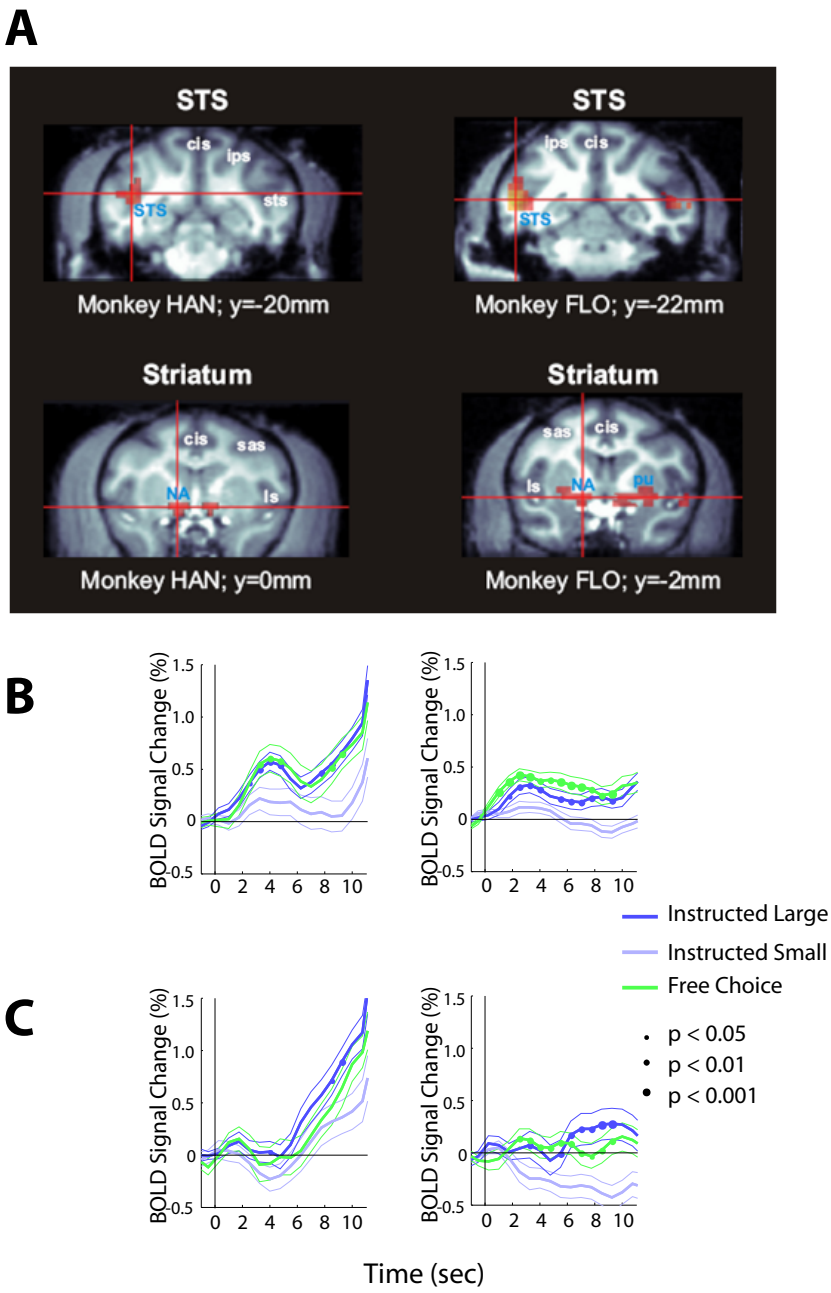

Figure A1.5:

Statistical map and timecourses: Expectation delay epoch. *(A) Statistical map for for Instructed Large Reward Trial > Instructed Small Reward Trial, p(FWE)<0.05. (B) BOLD timecourses extracted from superior temporal sulcus (sts), corresponding to the two monkeys whose maps are presented. (C) BOLD timecourses extracted from the striatum, corresponding to the two monkeys whose maps are presented. Times during the trial at which either instructed large or free choice signals were significantly different than instructed small signals are indicated with a dot (two-sample t-test).*

Receipt of Reward. While several subcortical and cortical regions should generate a response to receipt of reward, this task epoch lies particularly susceptible to distortion in brain images. As the monkeys lick and swallow fluid at the time of receipt, jaw and tongue motion produce substantial artifacts, particularly throughout the inferior aspects of the brain (i.e., subcortical regions, orbitofrontal cortex, etc.). More dorsal areas less affected by motion-induced distortions exhibited some robust and reproducible activity. Most notably, areas in the banks of the central sulcus (voxel level $p(FWE)<0.05$) showed a significant reward-related response (Fig. A1.6A). This signal amplitude scaled with reward amount, higher with large amounts of fluid received and lower for small amounts of fluid received (Fig. A1.6B). Activation in the central sulcus comprised somatosensory cortex in both monkeys, and extended slightly into M1 motor cortex in one monkey, ostensibly corresponding to motor and sensory stimulation due to drinking the fluid reward. However, even in one of these monkeys (monkey HAN, Fig. A1.6B, left panel), the reward-related response appears more motion- than hemodynamic-related: (1) the BOLD signal amplitude is suspiciously large, and (2) onset of signal rise occurs immediately at time of receipt (10 sec) rather than occurring with the characteristic hemodynamic delay. Thus, considerable caution is required in interpreting activation during the receipt epoch in this task.

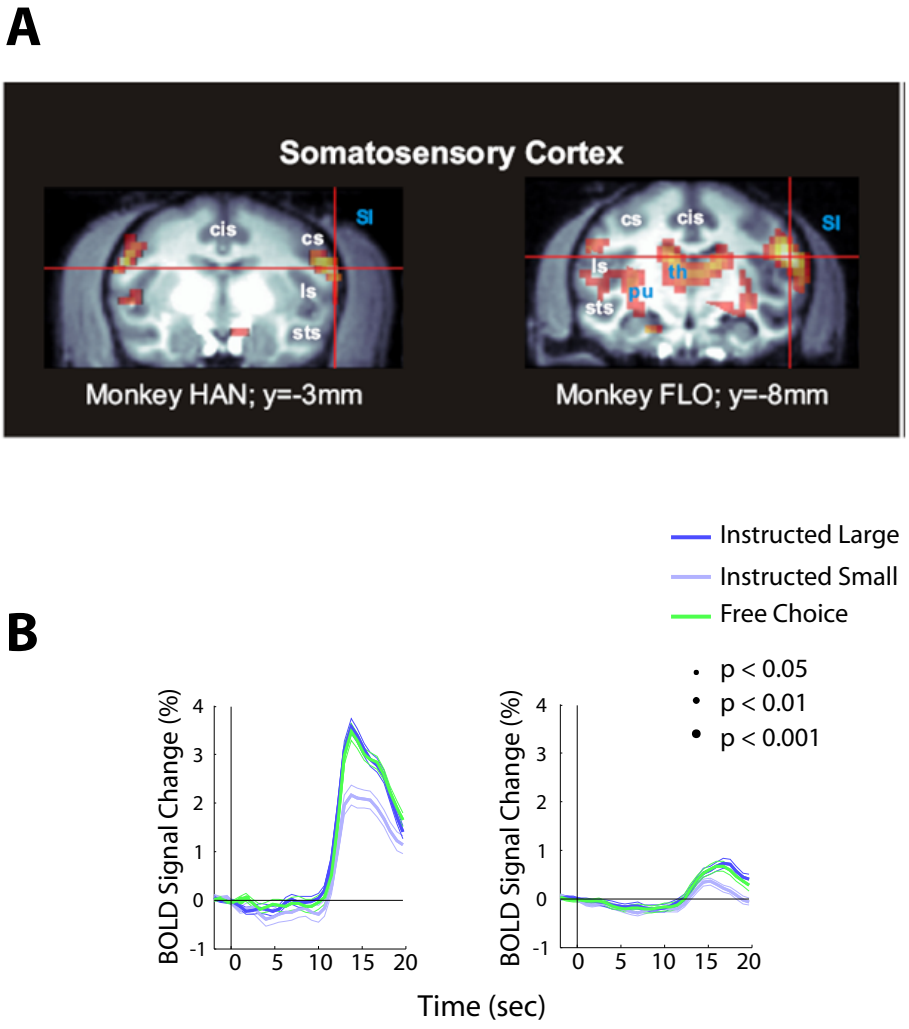

Figure A1.6:

Statistical map and timecourses: Reward receipt epoch. *(A) Statistical map for +Receipt of reward Epoch. p(FWE)<0.05. Coronal sections to best exemplify regions in S1. (B) BOLD timecourses extracted from S1, corresponding to the two monkeys whose maps are presented. Times during the trial at which either instructed large or free choice signals significantly differed from instructed small signals are indicated with a dot (two-sample t-test).*

Phase II: Reward Magnitude Reversal

The modulation of BOLD responses observed in Part I can conceivably be explained by differential visual characteristics of the targets, e.g., the color or luminance of the target. To ensure that such basic visual properties did not give rise to the previous findings, the stimulus-reward contingencies were reversed. This reversal additionally provided a window in which to discern areas engaged in learning and updating object-reward associations.

The color previously indicating a large reward now denoted a small reward (green now produced the smaller reward), and the previous small reward color (blue) now indicated a larger reward (Fig. A1.2A). Two monkeys participated in this phase of the experiment (At this time, multiple reversals have been imposed upon only on one monkey; both monkeys will be scanned doing more reversals in the future). For these scanned reversals, no training occurred beforehand, i.e., monkeys were scanned beginning with the first day of reversed contingencies.

Behavioral Findings

Fig. A1.7A depicts choice behavior of monkeys after stimulus color-reward associations were reversed. Day 0 denotes the day immediately prior to reversal, when the old associations were well established and monkeys constantly saccaded to the large-reward target. On the first day of reversed reward associations (Day 1), they persistently chose the previously large-, now small-, reward target. By the second day (Day 2) after reversal, monkeys began to explore the other (now large-reward) target for the period of a few trials, and then regularly selected the large-reward target. Finally, by Day 3, monkeys reliably identified and chose the large-reward target.

Trends in performance rates over days post-reversal corresponded to choice behavior (Fig. A1.7B). Both monkeys successfully completed a greater percentage of large-reward than small-reward trials on Day 0. Following reversal, on Days 1 and 2, performance for the instructed, now-small-reward trials equaled if not exceeded performance in large-reward trials. On Day 3, when monkeys chose the new large-

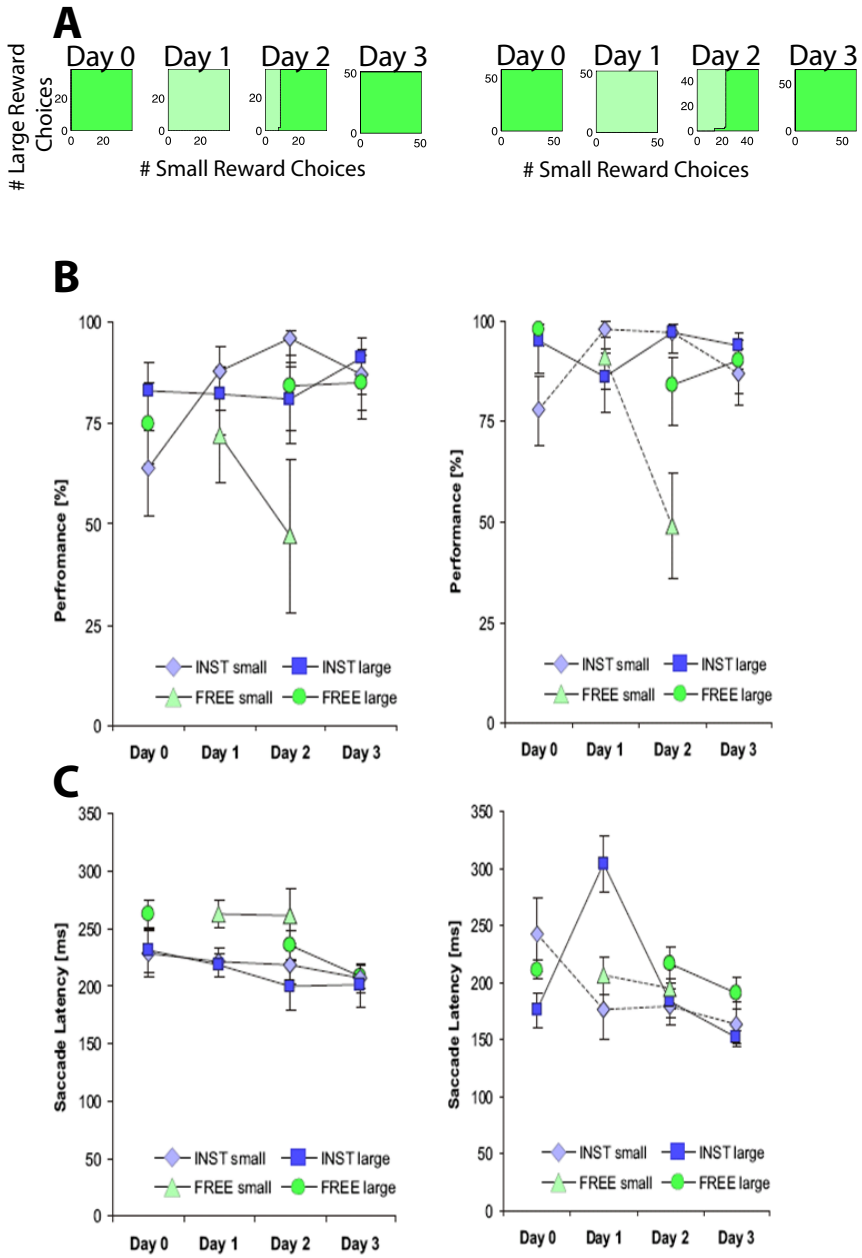

Figure A1.7:

Behavioral findings for Phase II. *(A) Cumulative choices, as a function of day relative to reversal (where Day 0 denotes day before reversal, and Day 3 the third day of reversed reward contingencies). On Days 0 and 3, both monkeys exclusively choose the large-reward target. On Day 1, they perseverate and choose the small (previously large) reward target. On Day 2, they begin choosing the now-large-reward target. (B) Performance (% successful trial completion) for each trial type as a function of day (Day 0–3) (C) Saccadic latencies for each trial type as a function of day (Day 0-3). The left column represents behavioral data from monkey HAN; the right column, monkey FLO.*

reward target, performance in instructed large-reward trials once again surpassed performance in small-reward trials.

Finally, saccadic latencies (in monkey FLO) on Day 0 were shorter for large-reward trials than for small-reward trials ($p<0.05$); on Day 1, saccades to small-reward (previous large-reward) targets were now faster ($p<0.05$), a tendency which diminished by Day 2 (Fig. A1.7C, right panel). In monkey HAN no significant changes in reaction time patterns for instructed trials transpired in the days after reversal (Fig. A1.7C, left panel); however, for this monkey, no significant latency differences for large- versus small-reward targets were observed with well-established stimulus-reward associations (as can be observed on Day 0, or in Phase I).

Imaging Findings

As the reversal phase of the task specifically probed aspects of stimulus-reward encoding, neural activity during the expectancy period, without motor confounds, was the principal focus. Thus, the striatum and regions in the sts (mapped in part I) constituted our regions of interest. Both monkeys showed similar signal dynamics in these ROIs. BOLD timecourses separated by monkey, ROI, and day post-reversal are plotted in Fig. A1.8.

As frontoparietal regions displayed significant modulation in Phase I, elucidating the effects of reversed contingencies on BOLD activity in this network forms an important goal of this work. However, severe distortions in these regions in the monkeys thus far scanned for this phase of the experiment (HAN and FLO) provide only one reliable sample (monkey) per region. We are currently scanning an additional monkey, in order to better speculate on BOLD trends in these areas.

Expectation. On Day 0, both striatal and sts areas exhibited expectancy signals scaling with the magnitude of anticipated reward, i.e., instructed large and free-choice trials generated higher signal amplitudes than did instructed small trials (Fig. A1.8A–D, leftmost panels). On Day 3, by which time choice behavior of both monkeys indicated that the new stimulus-reward associations had been learned, expectancy-related activity in both areas again correlated with the magnitude of reward denoted

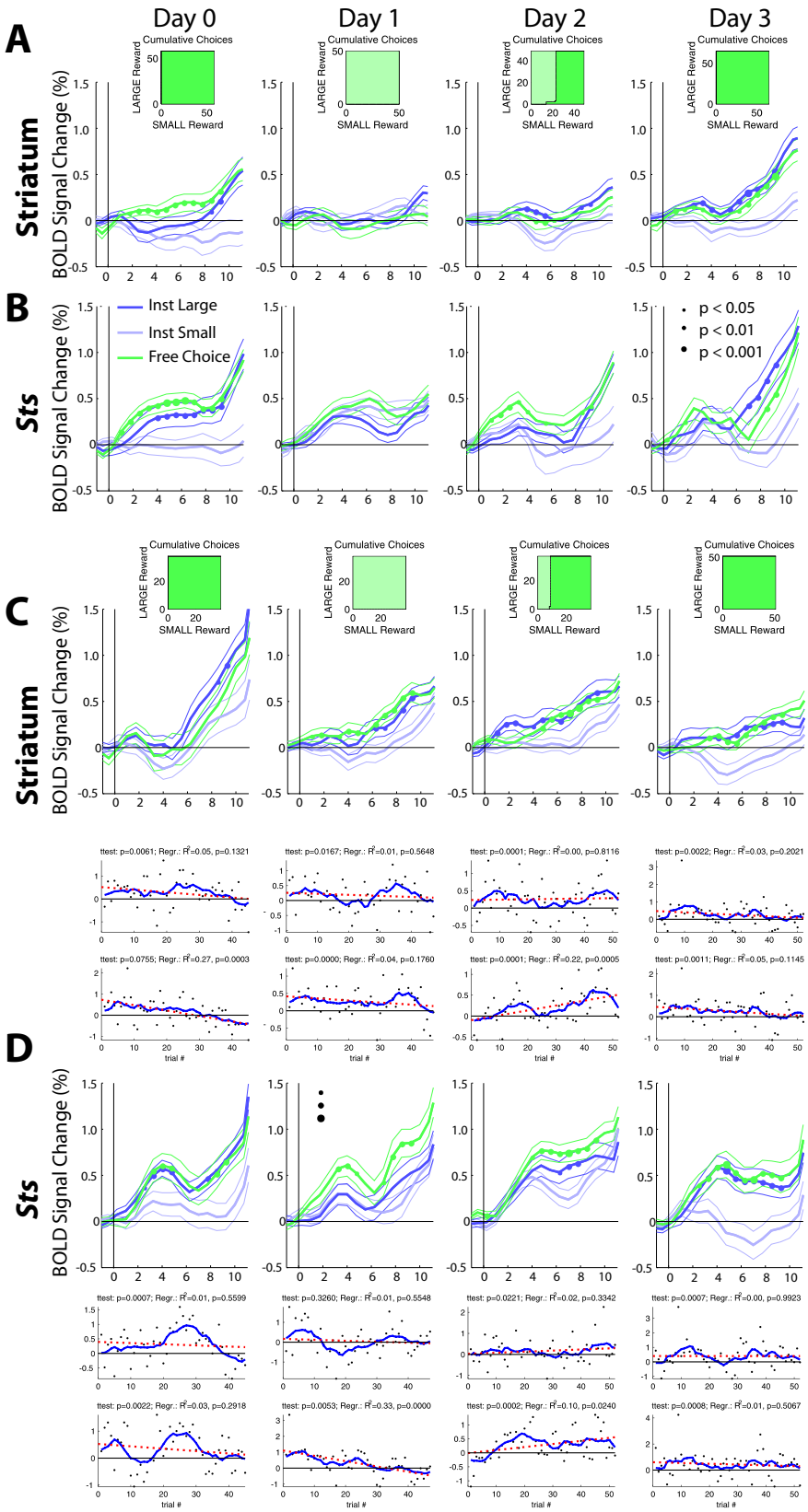
A
Day 0
Day 1
Day 2
Day 3
Striatum
BOLD Signal Change (%)
Cumulative Choices
LARGE Reward
SMALL Reward
B
Sts
Inst Large
Inst Small
Free Choice
p < 0.05
p < 0.01
p < 0.001
C
Striatum
D
Sts
trial #

Figure A1.8:

BOLD timecourses separated by day relative to reversal. *Choice behavior is plotted above each day for reference. In both monkeys, striatal signals reflected updated reward contingencies a session earlier than did sts signals. From monkey FLO: (A) extracted from the striatum and (B) sts. From monkey HAN: (C) extracted from the striatum and (D) sts. For monkey HAN mean percent signal change (PSC) for the expectation period was further quantified. For each day from Day 0–3, the differences in mean PSC between trial types (i.e, for Instructed Large minus Instructed Small, and Free Choice minus Instructed Small) were assessed. Significance of this difference is indicated above each plot (first p-value). Second, the difference in mean PSC between Instructed Large and Instructed Small, and between Free Choice and Instructed Small, is plotted as a function of trial number within each day's session (each sequential occurrence of each trial type are compared, i.e., the first Instructed Large versus the first Instructed Small; the second Instructed Large versus the second Instructed Small trial, and so forth). A linear regression is plotted to extract trends within each day's session; the R^2 and p-value for the regression are stated above each plot (see Experimental Procedures). Times during the trial at which either instructed large or free choice signals significantly differed from instructed small signals are indicated with a dot (two-sample t-test).*

by the stimuli (Fig. A1.8A–D, rightmost panels). Thus BOLD activation in these regions tracked the reward amount rather than other characteristics associated with the stimuli.

Before Day 3, however, activity in striatal and temporal areas evolved asynchronously. Since the monkey's assessment of and cognitive processes in free-choice trials can less clearly be interpreted, the difference between instructed large and small trials, which perhaps better reflects the evolving valuation of the targets, will primarily be discussed. In monkey FLO, striatal responses were higher for large reward compared to small reward targets on Day 2 (Fig. A1.8B, third panel); however, sts responses still did not reflect this magnitude difference until Day 3 (Fig. A1.8A, fourth panel).

Monkey HAN, who began selecting the new large-reward target before monkey FLO, revealed similar reward-dependent BOLD modulation, but changes manifested earlier. To better observe trends in neural activity following reversal, mean BOLD signal amplitude for the expectation epoch is plotted underneath timecourses; differences between expectation periods in different trial types is assessed across days and within days (see Experimental Procedures). In sts, the difference between instructed large and instructed small is not significant on Day 1 of the reversal ($p=0.32$). On Day 2 (Fig. A1.8D, third panel), during which choice behavior alters, the difference between instructed large and small trials reaches significance ($p<0.05$), and the difference between free choice trials (where the monkey starts choosing the large reward) and small trials significantly increases over the course of the day ($R^2=0.1$, $p<0.05$). Dynamics of sts activity appear to correspond to choice behavior.

Conversely, striatal activity in instructed large and free choice significantly exceeded that for small rewards already on Day 1 ($p<0.05$) (Fig. A1.8C, second panel). Subsequently (on Day 2), these differences escalated (in terms of signal amplitude difference and significance); the difference between free choice and instructed small trials significantly increased over the course of the session ($R^2=0.22$,$p<0.05$?). In both monkeys, BOLD signal profiles in the striatum revealed evidence of updated reward-stimulus associations before behavior manifested these new reward contingen-

cies; and striatal activity significantly differentiated between instructed large- and small- reward trials earlier than parallel changes manifested in sts activation.

On Day 0, the striatal signal difference between free choice and instructed small trials (and less significantly, between instructed large and instructed small trials) decreased over time, prior to any stimulus-reward reversal or behavioral changes. This may reflect motivation or subjective value of the reward to the monkey, as he becomes progressively more sated and less thirsty during the course of the session. This decrease within the session on Day 0 may constitute a truer baseline for trends within following days.

Phase III: No Post-Saccadic Color Context

Phase III of the experiment investigated the dependence of reward-modulated expectancy signals on the presence of the reward-associated visual object/feature. The task structure and stimulus-reward associations were identical to that in Phase I. However, Phase III digressed from Phase I in that the color of the fixation spot during the expectation period remained red (the initial color of the fixation point), rather than assuming the color of and thereby resembling the saccade target. The same two monkeys were scanned in this phase of the experiment as in Phase II; thus frontoparietal regions and target/saccade epoch responses will not be discussed, until more data is collected.

Behavioral Findings

In free choice trials, monkeys recurrently saccaded to the large-reward target (Fig.A1.9A). Saccadic latency patterns of monkeys mostly concurred with those from Phase I. However, as compared to Phase I, monkeys exhibited shorter latencies for free choice trials relative to instructed large or small trials (Fig.A1.9B–D). Performance rates increased for all trial types (except free choice-small, as small reward targets were still never chosen) (Fig.A1.9E). Given this increase in successful trial completion across all conditions, relative differences between performance rates per trial type

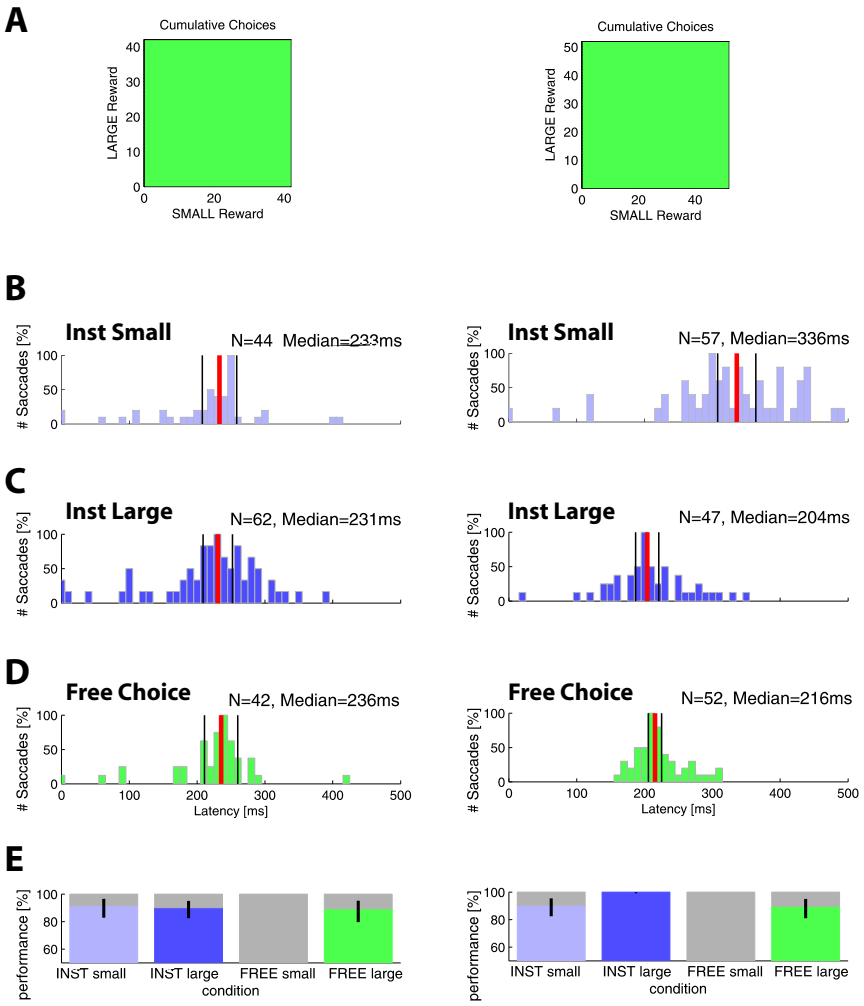

Figure A1.9:

Behavioral Findings for Phase III, with No Post-Saccadic Color Context. *(A) Cumulative choices, indicating exclusively large-reward targets were chosen. (B) Distribution of saccadic latencies in Instructed Large Trials. (C) Distribution of saccadic latencies in Instructed Small Trials. (D) Distribution of saccadic latencies in Free Choice Trials. (E) Mean performance (percentage of successfully completed trials) per trial type. The left column represents behavioral data from monkey HAN; the right column, monkey FLO. Behavioral trends for both monkeys are similar to Phase I, though performance rates are higher.*

were less robust than in Phase I. This improved performance and shorter reaction times may reflect a greater duration/degree of training on the task prior to scanning, as compared to Phase I.

Imaging Findings

Expectation. Instructed large compared to instructed small reward trials during the expectation period (instructed large > instructed small contrast, p(FWE)<0.05) yielded no significant clusters (Fig. A1.10A). For comparison, timecourses from those regions in the striatum and sts exhibiting expectation-related activation in Phase I are shown (Fig. A1.10B,C). These regions did not display any modulation of BOLD signals during this epoch, i.e., free choice or instructed large reward trials did not produce a significantly greater signal amplitude than did instructed small reward trials, demonstrating a lack of reward-magnitude-related effects when the fixation spot no longer denotes the reward amount. With the current task design, whether reward-related modulation requires the object indicating reward (e.g, green square) or solely the color (e.g. green) to be present cannot be determined.

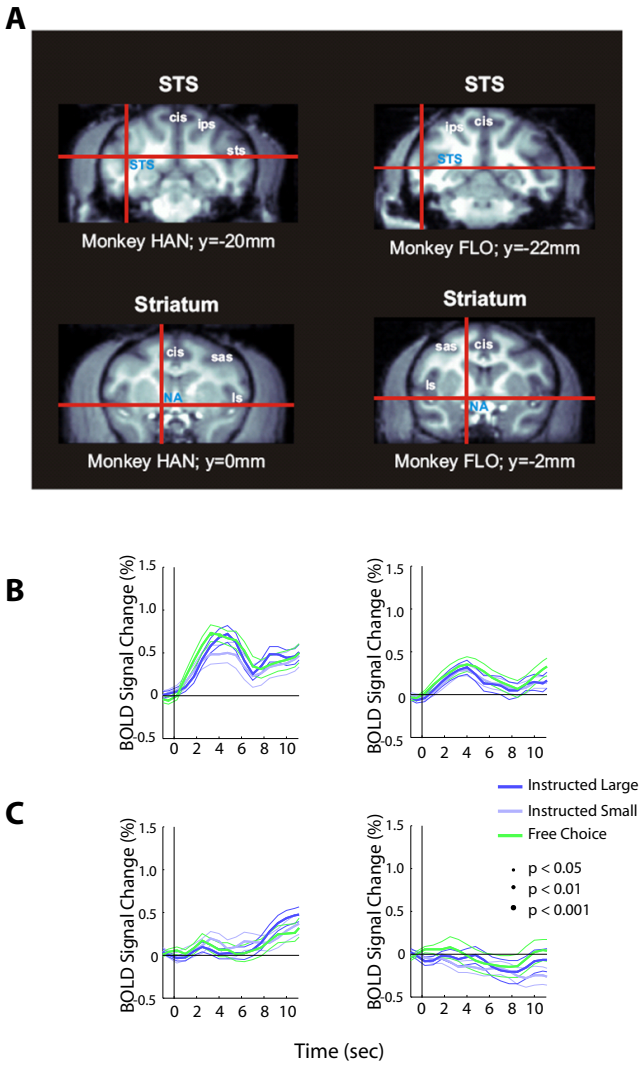

Figure A1.10:

Profile of activity in ROIs exhibiting a modulation of activity during the expectation period in Phase I. *(A) Statistical map for for Instructed Large Reward trial > Instructed Small Reward trial: Expectation delay epoch. p(FWE)<0.05. Coronal sections are chosen to exemplify ROIs from Phase I. (B) BOLD timecourses extracted from superior temporal sulcus (sts) corresponding to the two monkeys whose maps are presented. (C) BOLD timecourses extracted from the striatum, corresponding to the two monkeys whose maps are presented. Times during the trial at which either instructed large or free choice signals significantly differed from instructed small signals are indicated with a dot (two-sample t-test).*

A1.4 Discussion

In order to identify areas which encode and revise stimulus-reward associations, we conducted an fMRI investigation of monkeys performing saccades, either instructed or freely chosen, to differentially rewarded stimuli. Behavioral measures intimate that monkeys comprehended the stimuli-reward contingencies: in 'free choice' trials, they consistently made saccades to the target predicting the larger reward; in 'instructed' trials, they successfully completed a higher percentage of large-reward trials, with shorter reaction time latencies, as compared to small-reward trials. Thus, the monkeys expended more effort in trials in which they could garner more reward.

BOLD activity in the ventral and dorsal cortical streams exhibited greater response amplitudes during target presentation and/or saccade execution in the large-reward trials. Furthermore, ventral stream areas (specifically, areas along the superior temporal sulcus) and the ventromedial striatum revealed sustained activation throughout the expectation period before reward delivery. The level of this sustained activity varied with reward magnitude, but only when the reward-predicting stimulus/feature was visible during this period.

After reversal of stimuli-reward contingencies, monkeys initially perseverated and chose the incorrect (previously correct) stimulus. The first brain area to 'learn' the new reward magnitude being indicated by the stimuli was the striatum. Only later (in the next experimental session) did this new reward association become apparent in monkeys' behavioral patterns (i.e., choice preference, saccadic latencies, and performance rates) and in BOLD activity changes in inferotemporal cortex. These findings suggest dissociable contributions of the basal ganglia and inferotemporal object-vision areas in the representation of object-reward associations.

Differences between Ventral and Dorsal Stream Task Involvement

Dorsal (frontal and parietal) and ventral (inferotemporal) stream areas exhibited different patterns of activity throughout this task. First, dorsal stream areas showed significantly stronger reward-related modulation during the target/saccade epoch than did ventral stream regions: instructed large reward and free-choice trials (in which the large reward was consistently chosen) generated larger signal amplitudes than did instructed small-reward trials. In addition, dorsal stream and ventral stream areas evinced different patterns in the expectation period prior to receipt of reward, during which parietal and frontal regions did not exhibit sustained activity, while temporal regions did. The purported function of the dorsal cortical 'where' pathway in spatial and sensorimotor processes preceding movement potentially explicates both these disparities: (1) first, while visual, motor, preparatory, and mnemonic processes cannot be disambiguated in this paradigm, the target/saccade signal observed in IPS and FEF may reflect saccade-preparatory activity in addition to cue-related processing. Given the role of frontoparietal areas in subserving motor preparation, they likely are strongly recruited during this epoch; and as rewarding consequences have been speculated to bias action planning activity in these regions (Glimcher 2004; Platt and Glimcher 1999), different rewards associated with saccades possibly leads to enhanced reward-modulated BOLD signals, as compared to temporal regions in response the target/saccade event. (2) The observed lack of significant activity during the expectation period in these action-planning areas would be forecasted, since the action has already been executed and the monkey is simply waiting for reward delivery.

In addition to frontal and posterior parietal cortices, regions along the banks and in the fundus (namely, FST/TPO) of the superior temporal sulcus, sts, displayed robust target/saccade-related activity. Anatomical examinations of area FST in the macaque document its connections to parietal cortex and feedforward projections to the frontal eye fields; the region is thus often functionally classified as more related

to dorsal stream areas, with a role in visual motion analysis (Boussaud et al. 1990). Similarly, area TPO derives inputs from both the dorsal and ventral pathway (Seltzer and Pandya 1978), and has been strongly implicated in the control of visually guided saccades (Scalaidhe et al. 1995; Bakola et al. 2007). These activations then are still consistent with the recruitment of 'dorsal stream' regions for saccadic preparation and execution.

Voxels in sts demonstrating peak activation during the reward expectation phase were posteriorly located along the sulcus, on its lower bank. Given the spatial resolution of the images, these voxels corresponded most closely to area TEO (ventral stream area), but possibly may have been area FST (dorsal stream area). To ascertain the nature of expectation-related activations, a localizer control was conducted, where monkeys were scanned while viewing motion stimuli which drive areas FST and MT. Activation for motion stimuli neighbored, but did not co-localize, with reward expectation signals (data not shown). Thus, sts activations for the expectation epoch in the current study are taken to be TEO, or ventral stream.

Ventral Stream Functions in Encoding Stimulus-Reward Associations

The role of IT cortex in visual object representations has long been recognized: Single-cell recordings in nonhuman primates have consistently revealed differential tuning of individual neurons in temporal cortex to faces, whole objects, and complex object form features (Gross et al. 1972; Tanaka 1996; Logothetis and Sheinberg 1996); analogously, fMRI studies of the ventral object-vision pathway have demonstrated differential patterns of responses to a variety of categories of objects in the ventral temporal cortex (Kanwisher et al. 1997; McCarthy et al. 1996; Aguirre et al. 1998; Gauthier et al. 1999). However, the additional contribution of IT cortex to the encoding of visual object-reward associations has remained nebulous.

In the current paradigm, regions in inferotemporal (IT) cortex demonstrated reward magnitude-modulated expectancy signals. Additionally, after the reward magnitude contingencies for stimuli were reversed, signal modulations in IT reflected the updated reward magnitudes of the presented stimuli. This confirmed that these

BOLD representations tracked the value, rather than other visual attributes, associated with the targets. Furthermore, reward-related modulation of signals abated when the fixation square/object during the expectation period was no longer presented in color, the attribute which dictated the reward association. This finding suggests that IT signals during this period reflected specifically object/feature-reward associations, rather than a generalized anticipation of reward. Nonetheless, the possibility that the diminished signal differences may arise from mnemonic factors cannot be ruled out, as such long delays prior to reward receipt may impair monkeys' ability to remember the upcoming reward.

The principal region in the inferotemporal cortex demonstrating reward-modulated expectancy signals was TEO, though significant voxels displaying comparable patterns of activity were found along sts. Studies of the connectivity of TEO depict the area as an important link in the occipitotemporal pathway for object recognition, sending visual information forward from V1 and prestriate relays in V2–V4 to anterior inferior temporal area TE (Distler et al. 1993; Seltzer and Pandya 1978). Previous studies addressing the question of ventral stream object-reward encoding have generally focused on two subregions in IT, namely the perirhinal cortex and area TE. As a polymodal region receiving converging inputs from various sensory modalities, limbic and reward-related areas, the perirhinal cortex is well situated to signify the value of objects; macaque single-unit studies corroborate that perirhinal neuronal activity reflects the reward associated with stimuli (Mogami et al. 2006; Liu et al. 2000). Findings regarding TE, the final unimodal visual stage in the occipitotemporal pathway, are more ambiguous: while responses reveal considerable stimulus-selectivity, their modulation due to reward is less certain (Mogami et al. 2006; Liu et al. 2000). Unfortunately these IT subregions, particularly the perirhinal cortex, could not be accurately examined in our images due to their location more ventrally in the inferior temporal cortex, an area particularly prone to distortions and signal drop-outs. In future experiments, imaging geometry and sequences may be specifically adapted to optimize IT coverage.

Inferotemporal Regions in Learning Stimulus-Reward Associations

Unilateral inferior temporal lesions have been clearly shown to cause deficits in visual association learning in simple visual-reward association tasks (Parker and Gaffan 1998). These deficits may stem from compromised capabilities for visual identification and memory processes, including storage of visual representations (Cowey et al. 1970; Meunier et al. 1996; Buffalo et al. 1999) and associations with reward (Daum et al. 1991; Owen et al. 1991). Alternatively, these impairments could derive from a specific role in learning associations.

The evolution of activity in IT regions (such as TEO) after reversal of stimulus-reward contingencies in this experiment sheds some light on the involvement of this region, and possibly those downstream, in learning object-reward associations. Preliminary findings imply that while IT region TEO updated its expectancy-related signals to reflect the reversed reward associations, this activity changed concomitantly with behavior. An area engaged in learning may be predicted to reflect the new contingencies prior to changes in behavioral measures. If so, then the temporal profile of observable IT voxels insinuates that this region did not play a principal role in learning new stimulus-reward associations. This interpretation concurs with previous studies which suggest that IT appears to make a noncrucial contribution to reversal learning and attentional set-shifting (Daum et al. 1991; Owen et al. 1991). However, the possibility remains that IT does underlie some stage of learning, but its BOLD activity changes at a similar rate as, or imperceptibly before, behavior alters.

Striatal and Orbitofrontal Cortex Involvement

In both 'instructed' and 'free choice' trials, the striatum exhibited sustained activation during the expectation period between saccade execution and receipt of reward. Moreover, instructed large-reward and free choice trials (on which the monkey chose the large-reward target almost 100% of the time) generated expectancy signals of higher magnitude than the instructed small-reward trials. This finding is consistent with previous studies that demonstrated reward-modulated firing rates in these ar-

eas in anticipation of reward, after a movement was completed (Schultz et al. 2000; Hollerman et al. 2000; Simmons et al. 2008).

In our paradigm, reward-modulated striatal neural activity required the presence of the reward-predicting stimuli/color during the expectation period. Human fMRI and monkey recording findings have previously shown that anticipatory signals in the striatum reflect the expected value of the upcoming reward, even when the outcome was not definitively specified during the anticipation period (Dillon et al. 2008; Knutson et al. 2001; Ernst et al. 2004). However, our results can only be tenuously assessed with respect to these reports. Expectation periods employed in most other experimental paradigms are considerably shorter. The dynamics of BOLD and/or neural signals as well as the mnemonic abilities and strategies used across these dissimilar timescales may differ, impeding direct comparison of results. Additionally, the task variant with the uninformative fixation spot was presented to the monkeys after a period of extensive overtraining with the original task (with the fixation point indicating the reward); the monkeys may have therefore experienced some degree of confusion or uncertainty during the reward expectation period in the new, 'uninformative' condition. As the monkeys were scanned immediately upon switching to this task, assessing activation patterns after more training may better clarify the basis of striatal responses in this paradigm.

After reward contingencies were reversed, monkeys learned the new associations within a few sessions. Striatal activity accordingly reflected the new value predicted by the stimuli: BOLD responses to previously learned associations rapidly extinguished, and acquisition of specific responses to the new stimuli-reward association soon emerged. Interestingly, these trends in striatal activity following reversal preceded behavioral changes. These findings resonate with prior electrophysiological studies of monkeys learning visual stimulus-reward contingencies, in which striatal neural activity reflected changes in preferred stimuli, before corresponding behavioral alterations or prefrontal changes in neuronal selectivity became evident (Pasupathy and Miller 2005). Our data advances the notion that the striatum may rapidly link object representations with potential reward, and thus aid in adapting existing re-

ward expectations and behaviors to novel or changing environmental conditions. Such a general role in reward-based acquisition of stimulus-stimulus or stimulus-response associations may account for the array of deficits observed with basal ganglia lesions. As opposed to OFC and PFC lesions, dysfunction of basal ganglia structures lead to regressive errors in a broad range of tasks involving behavioral shifts and learning from feedback, where patients explore but do not appear to learn contingencies as quickly as normal subjects (Knowlton et al. 1996; Swainson et al. 2000). However, the delay between striatal changes and behavioral changes may also imply the existence of another link or stage between them, i.e. that the reward associations may need to be processed or become embedded elsewhere to trigger behavioral changes.

In addition to the striatum, regions in the OFC are typically recruited in visually guided reward schedule tasks. As single-unit reports have claimed that larger neural subpopulations in OFC encode cue-reward contingencies during reward anticipation than in the striatum, we would expect to see significant OFC activation in our paradigm. However, distortions in the ventral frontal lobes due to the proximity of the eyes and sinuses hindered our ability to reliably detect OFC activity. With EPI sequences optimized for this region, we may better be able to characterize OFC involvement in this task in the future.

In summary, we demonstrated the ability to map areas underlying cortical representations of both visual action goals and action plans, documented in ventral 'what' and dorsal 'where' pathways, respectively. Both cortical pathways evinced reward-related modulation, Furthermore, these results propose a leading role for the striatum in stimulus-outcome learning. The use of fMRI in the macaque in this experimental paradigm enabled a unique opportunity to probe for whole-brain patterns and dynamics of neural activity during the encoding and learning of stimulus-reward associations, and to relate these findings to a larger body of macaque electrophysiological and lesion studies pertaining to this subject.

A1.5 Experimental Procedures

Experimental preparation (surgery, training, and scanning) of monkeys, MR imaging parameters, stimulus presentation, task online behavioral control, and data acquisition are the same as those described in Chapter 4. In addition to the monitoring of body and eye movements described previously, an additional infrared camera (same as used for motion detection) was utilized to monitor the monkeys' licking. All trials in which monkeys licked before the receipt of reward (i.e., during the expectation period or earlier) were aborted. Lick detection and contingent trial abortion were introduced for two reasons: (1) to minimize the motion-related artifacts before the receipt of reward period, and (2) some indication existed that monkeys licked more in anticipation of larger than smaller rewards. In not permitting any licking during the trial (except receipt), BOLD responses due to differential licking rather than reward expectation can be ruled out. Fig. A1.1B shows behavior recorded throughout trials (saccades, licks, blinks).

Experimental Task

As Fig. A1.1 portrays, monkeys began each trial by fixation on a central fixation 'point', drawn as a red square. After 10 seconds of fixation, a peripheral cue was flashed for 200ms. In one-third of trials, a blue square target was presented, indicating a small (0.5ml) reward (Instructed Small-Reward Trials). In one-third of trials, a green square target was presented, indicating a large (1.5ml) reward (Instructed Large-Reward Trials). In the last third of trials, both a blue square and a green square were shown, providing monkeys with a choice of which target to acquire (Free Choice Trials). All targets were located at 15^o on the horizontal meridian (i.e., 15^o to the right or left of the fixation point; and in free choice trials, one was presented to the left and one presented to the right). Once monkeys made a saccade to a target, they immediately returned to central fixation for 10 more seconds. During this period, the central fixation square assumed the color of the target that the monkey had just acquired, thus reminding the monkey throughout of the upcoming reward

amount. Finally, the monkey received water at the end of this period.

In Phase II (Fig. A1.2), the experimental timing and structure were identical, except that the reward contingencies were reversed: blue targets now denoted a large amount (1.5ml) of fluid reward, and green targets a smaller (0.5ml) reward. For subsequent reversals, the color-fluid amount relationships were exchanged.

In Phase III (Fig. A1.2B), the experiment proceeded as in Phase I (including the same reward contingencies). However, after monkeys returned to central fixation, the fixation point during the expectation period (delay between saccade and reward) continued to be presented in red, rather than in the color of the saccade-acquired target.

Data Analysis

Functional data were analyzed in SPM and MATLAB. The first 5 EPI volumes were always excluded from functional analyses to remove transient effects of magnetic saturation, but were used for co-registration, since they provide better contrast for anatomical landmarks. Anatomical T1-weighted scans were processed in SPM. EPI sequences for each run were preprocessed using slice time correction, linear trend removal and a high-pass temporal filter with 3 cycles per 20 min run cut-off, and 6DOF 3D-aligned to a first volume of the last run in the session, which was always followed by the in-plane anatomical T1-weighted scan. The in-plane anatomical scan for each separate session was co-registered to the high-resolution structural scan in the AC-PC plane, and then EPI runs were aligned to the AC-PC-registered anatomical scan using automated alignment procedures (involving rigid body transformations). No spatial smoothing was applied to the data.

All trial events (except baseline initial fixation period)—target/saccade, delay before reward receipt (expectation period), and reward receipt—were extracted and used as predictors for general linear model (GLM) after convolution with hemodynamic response function (HRF) (defined for monkeys, see Chapter 4). Each session was analyzed separately to check the consistency of the results, and final statistical

maps were generated using multi-session GLM.

For the BOLD timecourse event-related averaging (ERA), only successful trials were accumulated. Importantly, the epochs of the run affected by body or limb motions were automatically detected and eliminated from ERA analysis. ERA timecourses were constructed using individual baseline estimates for each single trial: mean activity in the last 4 seconds of the initial fixation period. To assess significance of BOLD signals, a two-sample t-test was used to compare the means of signal amplitude (percent signal change) of a given two trial types at each second time bin. The trial types being compared are specified in each figure.

To better quantify the evolution of neural activity following reversal, two analyses were conducted. First, to track changes in neural activity across days, activity during the expectancy period in different trial types was determined as a function of day. For each day from Day 0–3, the differences in mean percentage signal change (PSC) between trial types (i.e, for instructed large minus instructed small, and free-choice minus instructed small) were assessed. Second, mean PSC during the expectancy period was plotted for each trial throughout the experimental session for Days 0 to 3. The difference in mean PSC between instructed large and instructed small, and between free choice and instructed small, is plotted as a function of trial number during the day's session (each sequential occurrence of each trial type are compared, i.e., the first Instructed Large versus the first Instructed Small; the second Instructed Large versus the second Instructed Small trial, and so forth). A linear regression is plotted to extract trends within each day's session (see Experimental Procedures). As an initial attempt to characterize trends in BOLD timecourses, this analysis has as of now been performed on only one monkey. After more reversal sessions have been scanned, the complete analysis will be conducted across both monkeys.

References

G. K. Aguirre, E. Zarahn, and M. D'Esposito. Neural components of topographical representation. *Proc Natl Acad Sci U S A*, 95(3):839–46, 1998.

S. Bakola, G. G. Gregoriou, A. K. Moschovakis, V. Raos, and H. E. Savaki. Saccade-related information in the superior temporal motion complex: quantitative functional mapping in the monkey. *J Neurosci*, 27(9):2224–9, 2007.

H. M. Bayer and P. W. Glimcher. Midbrain dopamine neurons encode a quantitative reward prediction error signal. *Neuron*, 47(1):129–41, 2005.

A. Bechara, A. R. Damasio, H. Damasio, and S. W. Anderson. Insensitivity to future consequences following damage to human prefrontal cortex. *Cognition*, 50(1-3): 7–15, 1994.

A. Bechara, H. Damasio, and A. R. Damasio. Emotion, decision making and the orbitofrontal cortex. *Cereb Cortex*, 10(3):295–307, 2000a.

A. Bechara, D. Tranel, and H. Damasio. Characterization of the decision-making deficit of patients with ventromedial prefrontal cortex lesions. *Brain*, 123 (Pt 11): 2189–202, 2000b.

D. Boussaoud, L. G. Ungerleider, and R. Desimone. Pathways for motion analysis: cortical connections of the medial superior temporal and fundus of the superior temporal visual areas in the macaque. *J Comp Neurol*, 296(3):462–95, 1990.

D. Boussaoud, R. Desimone, and L. G. Ungerleider. Visual topography of area teo in the macaque. *J Comp Neurol*, 306(4):554–75, 1991.

E. A. Buffalo, S. J. Ramus, R. E. Clark, E. Teng, L. R. Squire, and S. M. Zola. Dissociation between the effects of damage to perirhinal cortex and area te. *Learn Mem*, 6(6):572–99, 1999.

A. Cowey and C. G. Gross. Effects of foveal prestriate and inferotemporal lesions on visual discrimination by rhesus monkeys. *Exp Brain Res*, 11(2):128–44, 1970.

I. Daum, M. M. Schugens, S. Channon, C. E. Polkey, and J. A. Gray. T-maze discrimination and reversal learning after unilateral temporal or frontal lobe lesions in man. *Cortex*, 27(4):613–22, 1991.

D. G. Dillon, A. J. Holmes, A. L. Jahn, R. Bogdan, L. L. Wald, and D. A. Pizzagalli. Dissociation of neural regions associated with anticipatory versus consummatory phases of incentive processing. *Psychophysiology*, 45(1):36–49, 2008.

C. Distler, D. Boussaoud, R. Desimone, and L. G. Ungerleider. Cortical connections of inferior temporal area teo in macaque monkeys. *J Comp Neurol*, 334(1):125–50, 1993.

M. C. Dorris and P. W. Glimcher. Activity in posterior parietal cortex is correlated with the relative subjective desirability of action. *Neuron*, 44(2):365–78, 2004.

M. J. Eacott, D. Gaffan, and E. A. Murray. Preserved recognition memory for small sets, and impaired stimulus identification for large sets, following rhinal cortex ablations in monkeys. *Eur J Neurosci*, 6(9):1466–78, 1994.

M. Ernst, E. E. Nelson, E. B. McClure, C. S. Monk, S. Munson, N. Eshel, E. Zarahn, E. Leibenluft, A. Zametkin, K. Towbin, J. Blair, D. Charney, and D. S. Pine. Choice selection and reward anticipation: an fmri study. *Neuropsychologia*, 42(12): 1585–97, 2004.

D. Gaffan. Dissociated effects of perirhinal cortex ablation, fornix transection and amygdalectomy: evidence for multiple memory systems in the primate temporal lobe. *Exp Brain Res*, 99(3):411–22, 1994.

D. Gaffan and S. Harrison. Inferotemporal-frontal disconnection and fornix transection in visuomotor conditional learning by monkeys. *Behav Brain Res*, 31(2): 149–63, 1988.

D. Gaffan, A. Easton, and A. Parker. Interaction of inferior temporal cortex with frontal cortex and basal forebrain: double dissociation in strategy implementation and associative learning. *J Neurosci*, 22(16):7288–96, 2002.

E. A. Gaffan, M. J. Eacott, and E. L. Simpson. Perirhinal cortex ablation in rats selectively impairs object identification in a simultaneous visual comparison task. *Behav Neurosci*, 114(1):18–31, 2000.

I. Gauthier, M. J. Tarr, A. W. Anderson, P. Skudlarski, and J. C. Gore. Activation of the middle fusiform 'face area' increases with expertise in recognizing novel objects. *Nat Neurosci*, 2(6):568–73, 1999.

P. W. Glimcher. The neurobiology of visual-saccadic decision making. *Annu Rev Neurosci*, 26:133–79, 2003.

P. W. Glimcher and A. Rustichini. Neuroeconomics: the consilience of brain and decision. *Science*, 306(5695):447–52, 2004.

M. A. Goodale and A. Haffenden. Frames of reference for perception and action in the human visual system. *Neurosci Biobehav Rev*, 22(2):161–72, 1998.

C. G. Gross, C. E. Rocha-Miranda, and D. B. Bender. Visual properties of neurons in inferotemporal cortex of the macaque. *J Neurophysiol*, 35(1):96–111, 1972.

O. Hikosaka. Basal ganglia–possible role in motor coordination and learning. *Curr Opin Neurobiol*, 1(4):638–43, 1991.

O. Hikosaka, M. Sakamoto, and S. Usui. Functional properties of monkey caudate neurons. iii. activities related to expectation of target and reward. *J Neurophysiol*, 61(4):814–32, 1989.

O. Hikosaka, M. K. Rand, S. Miyachi, and K. Miyashita. Learning of sequential movements in the monkey: process of learning and retention of memory. *J Neurophysiol*, 74(4):1652–61, 1995.

O. Hikosaka, K. Sakai, S. Miyauchi, R. Takino, Y. Sasaki, and B. Putz. Brain activation during learning of sequential procedures. *Electroencephalogr Clin Neurophysiol Suppl*, 47:245–52, 1996.

O. Hikosaka, Y. Takikawa, and R. Kawagoe. Role of the basal ganglia in the control of purposive saccadic eye movements. *Physiol Rev*, 80(3):953–78, 2000.

J. R. Hollerman, L. Tremblay, and W. Schultz. Influence of reward expectation on behavior-related neuronal activity in primate striatum. *J Neurophysiol*, 80(2):947–63, 1998.

J. R. Hollerman, L. Tremblay, and W. Schultz. Involvement of basal ganglia and orbitofrontal cortex in goal-directed behavior. *Prog Brain Res*, 126:193–215, 2000.

J. W. Kable and P. W. Glimcher. The neural correlates of subjective value during intertemporal choice. *Nat Neurosci*, 10(12):1625–33, 2007.

N. Kanwisher, M. M. Chun, J. McDermott, and P. J. Ledden. Functional imaging of human visual recognition. *Brain Res Cogn Brain Res*, 5(1-2):55–67, 1996.

N. Kanwisher, J. McDermott, and M. M. Chun. The fusiform face area: a module in human extrastriate cortex specialized for face perception. *J Neurosci*, 17(11): 4302–11, 1997.

B. J. Knowlton, J. A. Mangels, and L. R. Squire. A neostriatal habit learning system in humans. *Science*, 273(5280):1399–402, 1996.

B. Knutson, C. M. Adams, G. W. Fong, and D. Hommer. Anticipation of increasing monetary reward selectively recruits nucleus accumbens. *J Neurosci*, 21(16):RC159, 2001a.

B. Knutson, G. W. Fong, C. M. Adams, J. L. Varner, and D. Hommer. Dissociation of reward anticipation and outcome with event-related fmri. *Neuroreport*, 12(17): 3683–7, 2001b.

B. Lau and P. W. Glimcher. Action and outcome encoding in the primate caudate nucleus. *J Neurosci*, 27(52):14502–14, 2007.

Z. Liu and B. J. Richmond. Response differences in monkey te and perirhinal cortex: stimulus association related to reward schedules. *J Neurophysiol*, 83(3):1677–92, 2000.

N. K. Logothetis and D. L. Sheinberg. Visual object recognition. *Annu Rev Neurosci*, 19:577–621, 1996.

R. A. McCarthy, J. J. Evans, and J. R. Hodges. Topographic amnesia: spatial memory disorder, perceptual dysfunction, or category specific semantic memory impairment? *J Neurol Neurosurg Psychiatry*, 60(3):318–25, 1996.

M. Meunier, W. Hadfield, J. Bachevalier, and E. A. Murray. Effects of rhinal cortex lesions combined with hippocampectomy on visual recognition memory in rhesus monkeys. *J Neurophysiol*, 75(3):1190–205, 1996.

S. Miyachi, O. Hikosaka, K. Miyashita, Z. Karadi, and M. K. Rand. Differential roles of monkey striatum in learning of sequential hand movement. *Exp Brain Res*, 115 (1):1–5, 1997.

T. Mogami and K. Tanaka. Reward association affects neuronal responses to visual stimuli in macaque te and perirhinal cortices. *J Neurosci*, 26(25):6761–70, 2006.

H. Nakahara, K. Doya, and O. Hikosaka. Parallel cortico-basal ganglia mechanisms for acquisition and execution of visuomotor sequences - a computational approach. *J Cogn Neurosci*, 13(5):626–47, 2001.

A. M. Owen, A. C. Roberts, C. E. Polkey, B. J. Sahakian, and T. W. Robbins. Extra-dimensional versus intra-dimensional set shifting performance following frontal lobe

excisions, temporal lobe excisions or amygdalo-hippocampectomy in man. *Neuropsychologia*, 29(10):993–1006, 1991.

A. Parker and D. Gaffan. Memory after frontal/temporal disconnection in monkeys: conditional and non-conditional tasks, unilateral and bilateral frontal lesions. *Neuropsychologia*, 36(3):259–71, 1998.

A. Pasupathy and E. K. Miller. Different time courses of learning-related activity in the prefrontal cortex and striatum. *Nature*, 433(7028):873–6, 2005.

M. L. Platt and P. W. Glimcher. Neural correlates of decision variables in parietal cortex. *Nature*, 400(6741):233–8, 1999.

M. E. Ragozzino. The contribution of the medial prefrontal cortex, orbitofrontal cortex, and dorsomedial striatum to behavioral flexibility. *Ann N Y Acad Sci*, 1121:355–75, 2007.

M. R. Roesch and C. R. Olson. Impact of expected reward on neuronal activity in prefrontal cortex, frontal and supplementary eye fields and premotor cortex. *J Neurophysiol*, 90(3):1766–89, 2003.

M. R. Roesch and C. R. Olson. Neuronal activity related to reward value and motivation in primate frontal cortex. *Science*, 304(5668):307–10, 2004.

M. R. Roesch and C. R. Olson. Neuronal activity related to anticipated reward in frontal cortex: does it represent value or reflect motivation? *Ann N Y Acad Sci*, 1121:431–46, 2007.

S. P. Scalaidhe, T. D. Albright, H. R. Rodman, and C. G. Gross. Effects of superior temporal polysensory area lesions on eye movements in the macaque monkey. *J Neurophysiol*, 73(1):1–19, 1995.

G. Schoenbaum, S. L. Nugent, M. P. Saddoris, and B. Setlow. Orbitofrontal lesions in rats impair reversal but not acquisition of go, no-go odor discriminations. *Neuroreport*, 13(6):885–90, 2002.

G. Schoenbaum, B. Setlow, S. L. Nugent, M. P. Saddoris, and M. Gallagher. Lesions of orbitofrontal cortex and basolateral amygdala complex disrupt acquisition of odor-guided discriminations and reversals. *Learn Mem*, 10(2):129–40, 2003.

W. Schultz, L. Tremblay, and J. R. Hollerman. Reward prediction in primate basal ganglia and frontal cortex. *Neuropharmacology*, 37(4-5):421–9, 1998.

W. Schultz, L. Tremblay, and J. R. Hollerman. Reward processing in primate orbitofrontal cortex and basal ganglia. *Cereb Cortex*, 10(3):272–84, 2000.

W. Schultz, L. Tremblay, and J. R. Hollerman. Changes in behavior-related neuronal activity in the striatum during learning. *Trends Neurosci*, 26(6):321–8, 2003.

B. Seltzer and D. N. Pandya. Afferent cortical connections and architectonics of the superior temporal sulcus and surrounding cortex in the rhesus monkey. *Brain Res*, 149(1):1–24, 1978.

M. N. Shadlen and W. T. Newsome. Neural basis of a perceptual decision in the parietal cortex (area lip) of the rhesus monkey. *J Neurophysiol*, 86(4):1916–36, 2001.

K. Shima and J. Tanji. Role for cingulate motor area cells in voluntary movement selection based on reward. *Science*, 282(5392):1335–8, 1998.

J. M. Simmons and B. J. Richmond. Dynamic changes in representations of preceding and upcoming reward in monkey orbitofrontal cortex. *Cereb Cortex*, 18(1):93–103, 2008.

R. Swainson, R. D. Rogers, B. J. Sahakian, B. A. Summers, C. E. Polkey, and T. W. Robbins. Probabilistic learning and reversal deficits in patients with parkinson's disease or frontal or temporal lobe lesions: possible adverse effects of dopaminergic medication. *Neuropsychologia*, 38(5):596–612, 2000.

K. Tanaka. Inferotemporal cortex and object vision. *Annu Rev Neurosci*, 19:109–39, 1996.

J. Tanji, K. Shima, and Y. Matsuzaka. Reward-based planning of motor selection in the rostral cingulate motor area. *Adv Exp Med Biol*, 508:417–23, 2002.

L. Tremblay and W. Schultz. Relative reward preference in primate orbitofrontal cortex. *Nature*, 398(6729):704–8, 1999.

L. Tremblay and W. Schultz. Reward-related neuronal activity during go-nogo task performance in primate orbitofrontal cortex. *J Neurophysiol*, 83(4):1864–76, 2000a.

L. Tremblay and W. Schultz. Modifications of reward expectation-related neuronal activity during learning in primate orbitofrontal cortex. *J Neurophysiol*, 83(4): 1877–85, 2000b.

L. Tremblay, J. R. Hollerman, and W. Schultz. Modifications of reward expectation-related neuronal activity during learning in primate striatum. *J Neurophysiol*, 80 (2):964–77, 1998.

M. Watanabe, H. C. Cromwell, L. Tremblay, J. R. Hollerman, K. Hikosaka, and W. Schultz. Behavioral reactions reflecting differential reward expectations in monkeys. *Exp Brain Res*, 140(4):511–8, 2001.

Appendix 2—Frontoparietal Timecourses Reflect Decision in a Free-Choice Oculomotor Task

A2.1 Summary

In everyday life, we are usually free to make decisions among several options available to us. When external cues do not explicitly signify the 'best' option, we generally rely on internal biases to make a decision and plan a corresponding behavioral response. In this study, we sought to investigate neural correlates of such internally generated choices. To do so, monkeys were scanned while they performed a variant of a delayed response task, in which they made memory-guided saccades, either to one instructed previously cued target, or to one freely chosen among two previously cued targets. While results are still tentative, our findings thus far demonstrate no areas preferentially recruited during choice as compared to instructed trials. However, putative saccadic planning frontoparietal areas, which were recruited during the delay period before the saccade, showed an evolution of directional selectivity during the delay corresponding to upcoming choice. In addition, regions in frontal and parietal cortices evinced this 'choice' at different times, suggesting dissociable contributions of these areas in the selection and planning of impeding actions.

A2.2 Introduction

Explorations of decision-making typically focus upon and characterize externally guided choices. In these paradigms, the variables governing choice behavior, such as sensory/perceptual information, conditional rules, and reward reinforcement, are externally determined; hence behavior is exogenously controlled and extremely predictable. However, in a natural milieu, internal biases and attitudes also come to bear upon the generation of behavior and selection of goal-directed actions.

A small number of studies have directly probed the neural correlates of internally generated decisions. Monkey electrophysiology experiments (Scherberger et al. 2007; Watanabe et al. 2007; Pesaran et al. 2008) have permitted monkeys to freely choose a spatial target, holding external parameters, such as expected value, reward magnitude, and visual stimulus configurations, constant. In these single-unit recordings, neural activity in dorsolateral prefrontal cortex and a subregion of posterior parietal cortex have been shown to exhibit directional selectivity prior to movement that indicated the monkey's upcoming choice. Imaging studies in humans, both PET and fMRI, have similarly allowed subjects to choose either when or where to make a movement (Jenkins et al. 2000; Milea et al. 2007; Khonsari et al. 2007). These imaging findings have generally emphasized a preferential engagement of dorsolateral prefrontal cortex, posterior parietal cortex, and supplementary motor areas in free choice as opposed to instructed conditions.

These previous experiments, however, face limitations in characterizing the involvement and relative contributions of areas engaged in free-decision tasks. Mostly, single-unit recordings have as of yet not elucidated the relative dynamics of a distributed network of task-relevant regions, focusing instead on one or two cortical regions (but see Coe et al. 2002). While human imaging studies can address this drawback, prior studies have not employed event-related analysis, making it difficult to unequivocally ascribe activation to specific cognitive processes related to decision-making, or to track temporal evolution of activity that may correspond to choice.

We therefore sought to investigate the neural substrates of voluntary decision-

making, response selection, and motor planning with a delayed saccade task, using high-field fmri in awake behaving monkeys. The goals of this study were to dissociate visual cue events from subsequent selection and planning of motor response, and then to investigate dynamics of multiple brain areas involved in saccade selection. To do so, monkeys performed delayed eye movements either to an instructed target, or to one of two possible targets. Though monkeys did exhibit spatial biases in target choice behavior, they did not perseverate, but rather picked both targets throughout the experimental sessions. Pilot data indicate that the frontoparietal network traditionally recruited in delayed-response tasks showed increasing directional selectivity of BOLD signals in the delay period of choice trials, reflecting the monkey's upcoming choice. Furthermore, the dynamics of this choice-related activity suggests that LIP and FEF may exert a leading role in oculomotor decision-making. Currently, we are conducting this study on additional monkeys to confirm these preliminary results, and will soon begin testing humans on the same task to better generalize our findings.

A2.3 Results

To investigate regions either specifically recruited for choice processes or whose activity mirrors the monkey's evolving decision, monkeys were scanned while performing a variant of a delayed-oculomotor response task.

In 'instructed' trial types, one peripheral target was flashed, and after a delay, monkeys saccaded to its remembered location. In 'free-choice' trial types, two targets were presented symmetrically (left-right) around the fixation point. After a delay, the monkey saccaded to one of the previously indicated targets. Targets were identical, with respect to visual properties and associated fluid reward, differing only in their location; in addition, they were placed equidistantly from the fixation point.

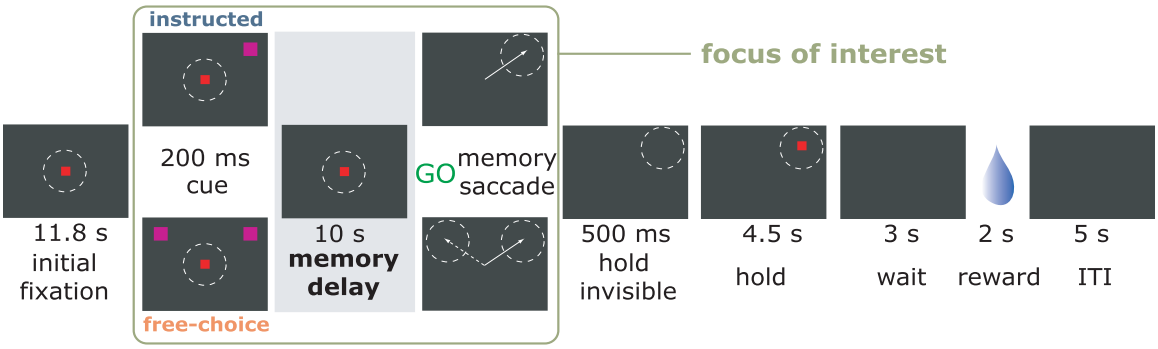

Figure A2.1:

Task structure and timing. *After a period of central fixation, peripheral cues were flashed: one in 'instructed' trials, and two in 'choice' trials. After a delay, monkeys executed a saccade (either to the instructed cue, or to either of the choice cues). After an additional waiting period, they were provided fluid reward for successful trial completion.*

Behavioral Findings

When presented with two left-right symmetric targets, monkeys chose both targets, but with unequal frequency. Fig. A2.2A plots number of choices at each spatial location, depicting a proclivity for right target selection amongst most pairs of targets for both monkeys. Fig. A2.2B,C segregate targets into right (9 targets) or left (9 targets), and shows cumulative choice history of both monkeys over all scanned sessions. The deviation from the unity/diagonal in choice history (Fig. A2.2B) more clearly demon-

strates that both monkeys, but particularly monkey G (bottom panel), saccaded with a consistent rightward bias. However, unlike previous studies (Scherberger and Andersen 2007; Coe et al. 2002), cues were not experimentally manipulated, e.g. with different reward schedules or onset times, to promote equitable selection of both left and right targets. Thus, choice ratios can be more cleanly be attributed to internal factors.

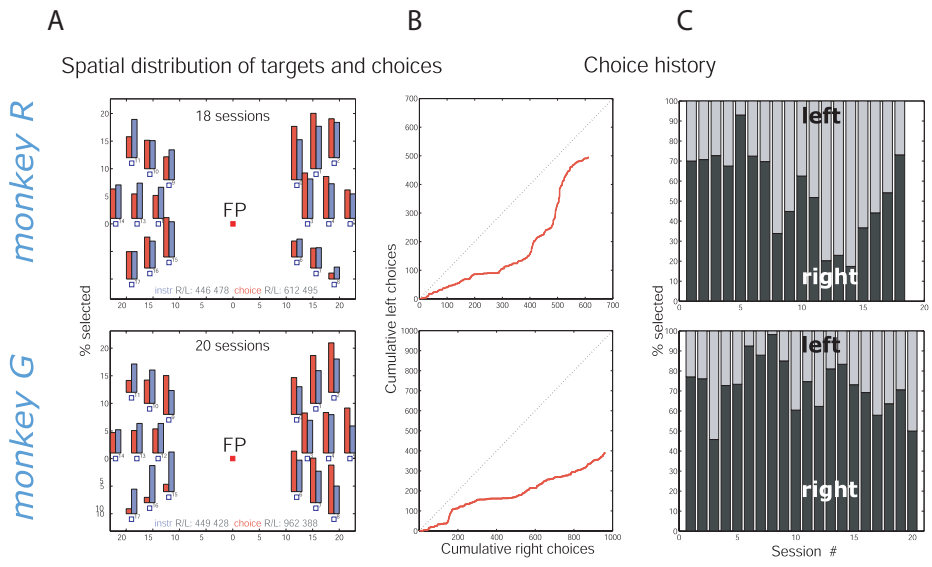

Figure A2.2:

Choice behavior of both monkeys. *(A) For all target locations, the number of saccades made is presented, divided by instructed or choice trial types. Collapsing all targets by hemisphere (i.e., right or left), a cumulative history of choices made to both hemifields is presented (B) as a function of trial number and (C) within each experimental session. Upper row: monkey R; Lower row: monkey G*

Instructed and free choice trials prompted similar saccadic reaction times. However, slightly longer latencies were consistently observed in choice trials, on the order of 5ms in monkey R and 10ms in monkey G slower than in instructed trials. Though small, these differences in reaction times reached significance ($p<0.05$) in both monkeys (Fig. A2.3).

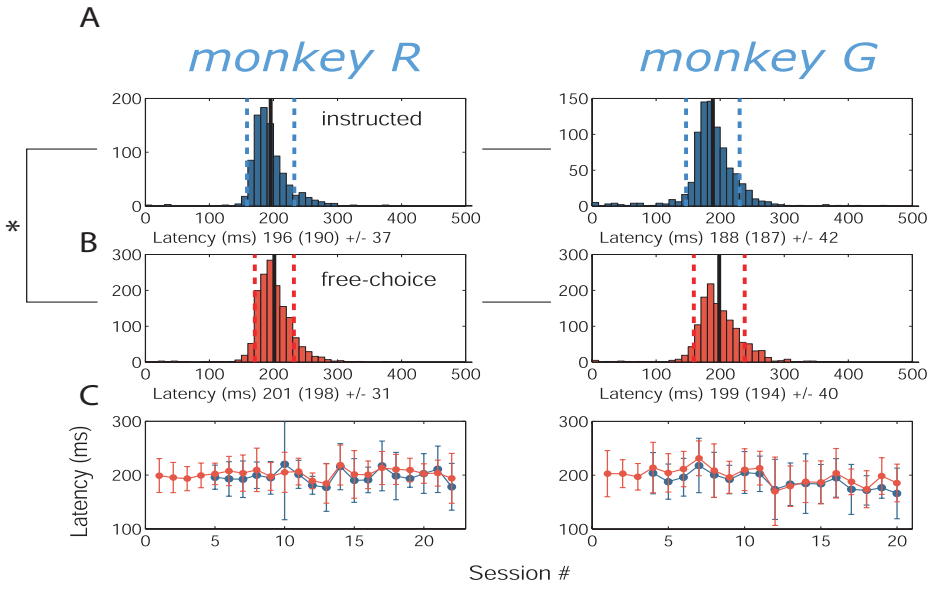

Figure A2.3:

Reaction times for Instructed and Choice trials. *(A) Distribution of reaction times for instructed trials. (B) Distribution of reaction times for choice trials. (C) Mean reaction time for instructed trials (blue) and choice trials (red), as a function of experimental session. Left column: monkey R; Right column: monkey G*

Neuroimaging Findings

As neural correlates of the evolving decision-process is our interest, the focus of this analysis lies upon the delay period: the interval between presentation of the targets, and the saccade indicating the decision made. The cue epoch receives only brief description.

Choice versus Instructed Activation

Two methods were adopted to examine choice-related BOLD responses. The first approach probed for all areas preferentially engaged by decision trials over instructed trials. In this contrast (Choice > Instructed), no regions demonstrated significant activation, either for the cue epoch or for the delay period.

Neural Activity during the Delay Period

The second approach exploited the contralateral nature of responses in many areas recruited during the delay period, characterized in Chapter 3. Specifically, contralateral action-planning/delay period activity should differentiate between a saccade planned to a left or right target in choice trials. As contralaterality is necessary to observe choice-related activity in this paradigm, regions of interest (ROIs) were delineated as those areas manifesting significant contralateral delay period activations, in the instructed trial type. In accordance with prior findings (see Chapter 4, delay period activation in the macaque), this contrast elucidated significant voxels along the arcuate sulcus (e.g. frontal eye fields, dorsal premotor areas), the intraparietal sulcus, and dorsolateral prefrontal cortex (Fig. 4.3), contrast delay period right > left, for both monkeys).

To examine the BOLD signal profiles from these ROIs, timecourses were extracted bilaterally (from left and right hemispheres) for a given region, sorted by trial type and direction (left or right) of saccade (as an example, see Fig. A2.4E). For presentation, timecourses were then collapsed across hemispheres, and shown sorted both by trial type, and by contra- versus ipsilaterality of saccade. Fig. A2.4 depicts BOLD

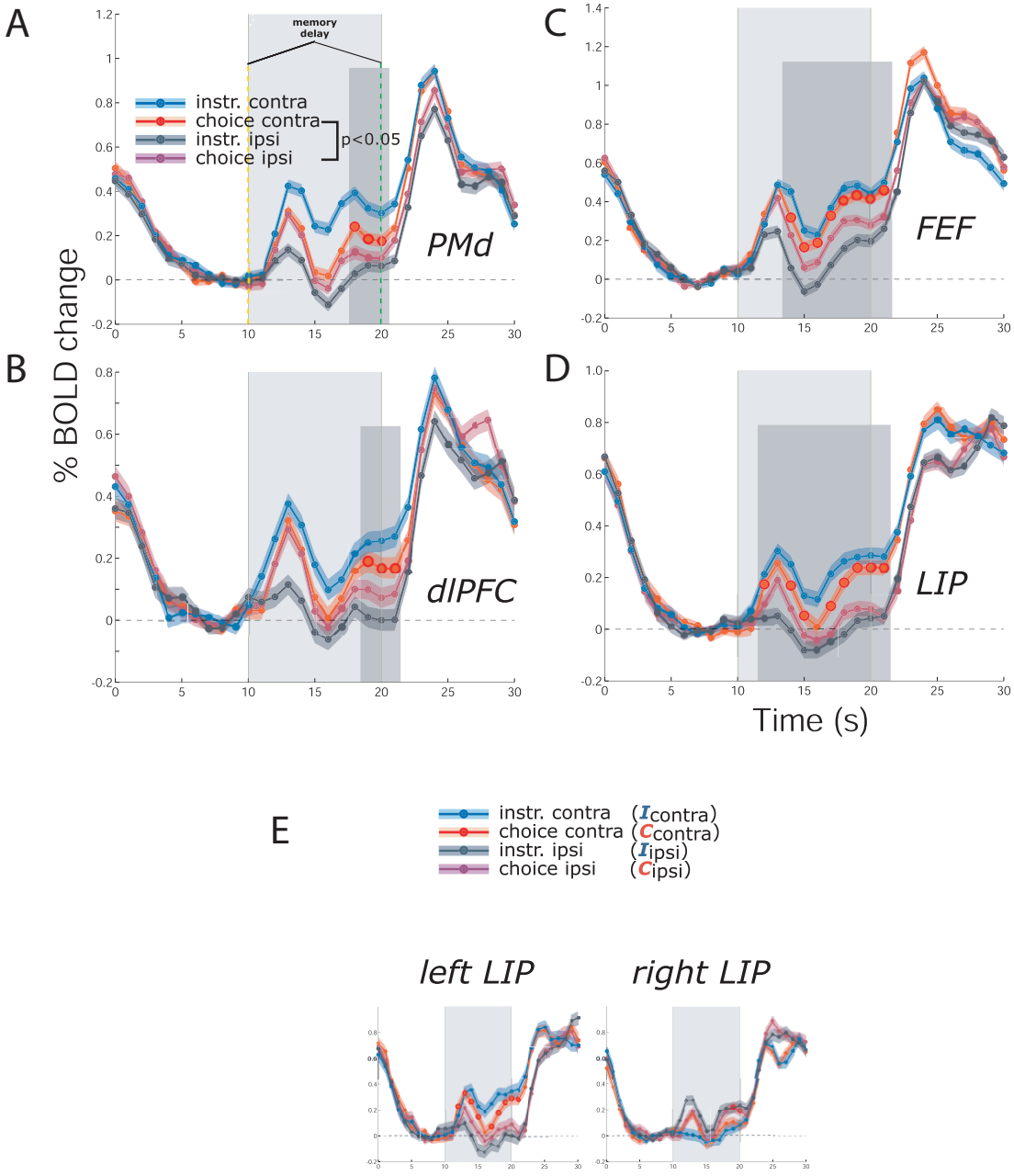

Figure A2.4:

BOLD timecourses from monkey R for delay-period ROIs exhibiting contralaterality. *All trials are grouped by direction (ipsilateral and contralateral) and trial type (instructed or choice), collapsed over both hemispheres for each ROI. (A) Dorsal premotor cortex, (B) Dorsolateral prefrontal cortex, (C) Frontal eye fields, (D) Lateral intraparietal area (LIP). In (E), representative BOLD timecourses are separated by right and left hemisphere for LIP.*

timecourses from monkey R for (A) dorsal premotor cortex, (B) dorsolateral prefrontal, (C) frontal eye fields, and (D) lateral intraparietal area (along intraparietal sulcus). In all regions, signal amplitude in instructed contralateral trials was significantly higher than in instructed ipsilateral trials, as expected given the criteria for defining ROIs.

Timecourses for contralateral and ipsilateral choice trials were coincident at the start of the delay period, immediately after cue presentation. Directional selectivity evolved, with signals diverging and contralateral choice trials displaying higher signal amplitudes than ipsilateral choice trials. This increased contralateral activity during the delay period implies that a choice was made before the go signal.

Activation in choice trials lay intermediate to instructed trials: contralateral choice trials generated a smaller BOLD signal than contralateral instructed trials, while ipsilateral choice trials produced a larger signal than did ipsilateral instructed trials. That contralateral activity remained lower than in instructed trials insinuates potential competition between targets in opposite hemifields. The increased ipsilateral choice activity (as compared to instructed) may additionally suggest that two potential motor plans are present though the end of the delay period.

The BOLD signal amplitude in contralateral choice trials was compared to the signal amplitude in ipsilateral choice trials at 1second intervals (time bins) throughout the trial, using a two-sample t-test. Times at which the signal amplitudes significantly differed are indicated by a dot. By this assessment, the point at which activity diverges in free choice trials varies by ROI. In both dorsolateral prefrontal cortex and dorsal premotor cortex (Fig. A2.4A,B), significant directional selectivity manifests only in the last few seconds of the delay period. In contrast, in areas LIP and FEF (Fig. A2.4C,D), signal timecourses in contralateral and ipsilateral choice trials deviated earlier in the delay period, within the first half of the delay period, and within the first few seconds in LIP. These regions may reflect the evolving choice sooner than other frontal and parietal subregions.

In the second monkey, BOLD patterns disclosed a similar, but not quite as lucid, trend. Areas LIP and FEF, where significant directional selectivity evolved, showed

similar patterns as in monkey R. Ipsilateral choice trials again generated a higher amplitude signal than did ipsilateral instructed trials; and contralateral choice produced signals equal to or less than those in contralateral instructed. Divergence

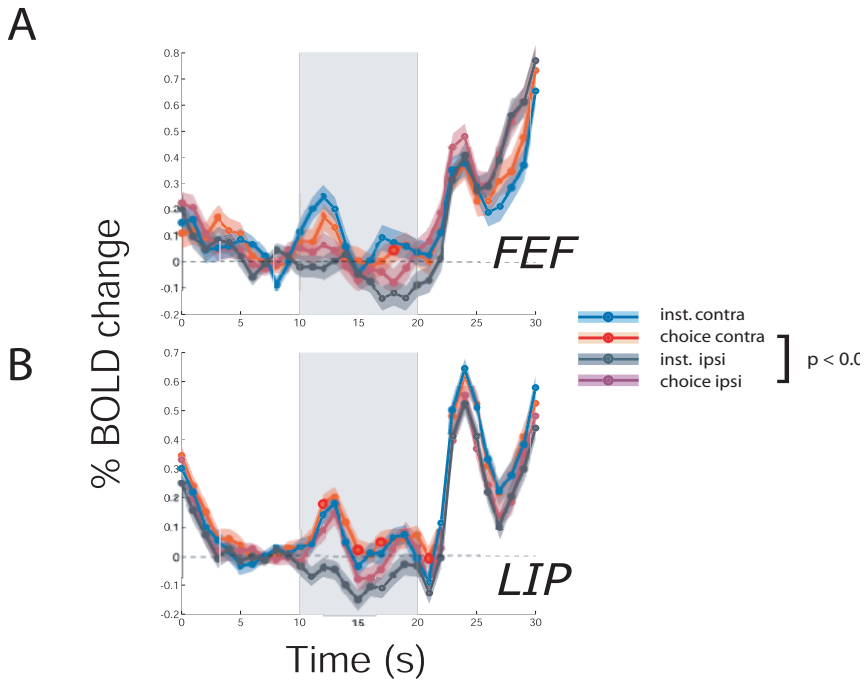

Figure A2.5:

BOLD timecourses from monkey G for delay-period ROIs exhibiting contralaterality. *All trials are grouped by direction (ipsilateral and contralateral) and trial type (instructed or choice), collapsed over both hemispheres for each ROI. (A) Frontal eye fields, (B) Lateral intraparietal area (LIP). Dorsolateral prefrontal and dorsal premotor ROIs did not show significant divergence in choice trials; see Results for further discussion of these regions.*

in choice trials again occurred later in FEF than in LIP (Fig. A2.5A,B). However, in dorsal premotor cortex (PMd), no divergence was apparent in choice trials. As this region in monkey R only demonstrated directional selectivity towards the end of the delay period, PMd may only weakly reflect the evolving oculomotor decision.

Dorsolateral prefrontal cortex, even in instructed trials, exhibited weak contralaterality (Fig. 4.3), diminishing the divergence that could be discerned in choice trials altogether.

Responses During the Cue Period

As the cue epoch represents possible options to be encoded, and decision processes may already commence, it in principle constitues an interesting epoch to be analyzed. However, the cue presentation conflates sensory, mnemonic, and possibly decision processes; additionally, as the number of cues presented varied between instructed and free choice conditions, sensory and attentional demands presumably differ between these conditions. Therefore, comparisons will be briefly made within choices of contra- and ipsiversive trials.

Regions of interest were defined as those areas exhibiting a significant contralateral response during the cue period in instructed trials. This assessment yielded significant voxels in areas FST and TPO in the temporal cortex, along the superior temporal sulcus (but only in monkey R; see Fig. 4.3). Choice trials demonstrated significant directional selectivity early, as soon as the cue response onset (at 2–3 seconds after cue presentation) (Fig. A2.6A,B). However, as with most responses in frontal and parietal regions, signal amplitudes in choice trials were intermediate to those observed in instructed trials, with contralateral responses again less in choice as compared to instructed trials. This further corroborates the notion that some competition or mutual inhibition between simultanously presented cues may be transpiring.

These preliminary findings across two monkeys show some consistent tendencies. However, more sessions are required to clarify response patterns. An additional monkey, where contralaterality through these frontal and parietal regions is robust, would help confirm trends noted thus far. In addition, a greater number of trials in each monkey would allow left and right hemispheres to be analyzed separately with adequate statistical power. For example, Fig. A2.4E proposes the possibility that left and right LIP may evince contralaterality at different times. Independent examination of these regions would potentially reduce noise in the signals, and constitute the most

conservative approach to characterizing signal dynamics.

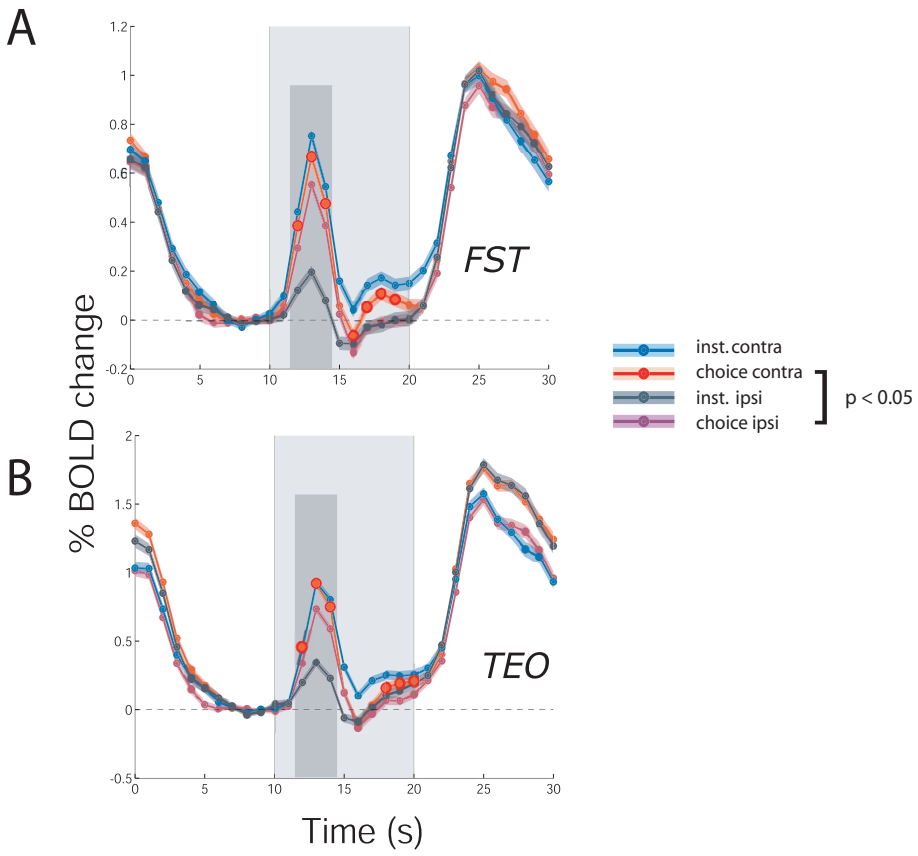

Figure A2.6:

BOLD timecourses from monkey R for ROIs exhibiting contralaterality during the cue as well as the delay period. *All trials are grouped by direction (ipsilateral and contralateral) and trial type (instructed or choice), collapsed over both hemispheres for each ROI. Areas (A) FST, and (B) TEO, along the superior temporal sulcus*

A2.4 Discussion

In the present study, we examined neural regions that may be engaged by the oculomotor decision process of selecting where to look. To do so, we assessed profiles of BOLD activation in free-choice delayed-saccade tasks. Variables such as sensory characteristics, visuomotor associations, and reward schedule were not varied externally. Instead, monkeys were provided identical visual stimuli/cues, and all choices were equally valid. Under these conditions (i.e, the absence of external choice cues and equal expected value for all choices in a given trial), differential BOLD activity reflected an internal selection bias and/or the consequent choice. In the current experiment, no regions exhibited greater delay period activation in free-choice as compared to instructed trials. However, during the delay period in choice trials, regions in frontal and parietal cortices showed a gradual increase in directional selectivity (i.e., contralaterality), reflecting the evolving decision and associated motor planning. Activity in choice trials was intermediate to instructed contralateral and ipsilateral trials, suggesting either competition between presented targets and/or co-existence of two potential motor plans. Finally, the dynamics of contralateral BOLD activity in these regions suggest that frontal and parietal subregions may play distinct roles in the spatial goal-directed decision process.

fMRI Activity for Chosen versus Instructed Movements

The analysis in this study utilized an event-related approach, focusing primarily on the delay period to minimize confounds of cognitive processes occurring during cue presentation or movement execution. While human imaging reports of free-choice tasks have not employed a comparable analysis, neurophysiological studies in monkeys have adopted experimental approaches similar to the current study. Recordings from the dorsolateral prefrontal cortex (dlPFC), though over a much shorter delay period, reported that saccades to receptive field targets produced more spiking activity when the saccade was instructed rather than chosen; however, instructed saccades to non-receptive field targets generated less activity than chosen eye movements to the

same targets (Watanabe et al. 2007). These firing rate patterns concur with trends observed here: all ROIs, including dlPFC, reveal levels of BOLD activation for chosen trials intermediate to instructed contraversive and ipsiversive trials. These findings raise the possibility that simultaneous competing plans may be maintained in conditions where multiple options exist. Evidence of simultaneous neural representations of multiple motor plans has been documented in our earlier work (Lindner A., Kagan I., Iyer A. and Andersen, R.A. 2008 Prospective coding of alternative actions in human Parietal and Premotor cortex. 6th FENS Forum of European Neuroscience). However, these motor plans coexisted during trial epochs when more than one movement option was cued and valid, before one was externally instructed as the appropriate response. Here, potential competing plans are still represented, even after selection of one of them has become apparent. Alternatively, neural activity for one option may be completely suppressed after the activity for the other reaches some decision 'threshold,' as competition models of response selection have contended (see Introduction, Chapter 1). However, with variability in decision times or uncertainty during the delay period, BOLD timecourses for ipsilateral targets averaged over all choice trials may remain higher than the signal amplitudes observed in ipsilateral instructed trials.

During both the cue and delay period, no areas demonstrated significantly higher activity in choice over instructed trials. Conversely, previous fMRI and PET analyses (Jenkins et al. 2000; Khonsari et al. 2007; Milea et al. 2007) have disclosed greater BOLD activation for chosen versus instructed movements in an array of motor association/planning areas. Particularly, Khonsari et al. and Milea et al. utilized an experimental task closely resembling the one employed here, and reported a specific recruitment of dorsolateral prefrontal cortex (dlPFC) and posterior parietal cortex in choice trials. However, the inconsistencies between their findings and those presented here may stem from the differences at the time of cue presentation. In these human imaging studies, visual load/stimulation was balanced during presentation of cues; however, in the present study, to easily convey trial type demands to the monkey, only one peripheral target was presented in instructed trials, whereas two were

presented in choice trials. Inhibitory competition between the two simultaneously presented cues may have lowered the net signal observed in choice versus instructed trials. Currently, we are conducting similar experiments in which visual stimulation is held constant across trial types, both in monkeys and in humans. These studies will permit more direct comparison and hopefully reconciliation of these disparate findings.

Evolution of Decisions in Action Plans

This study extends our previous work, in which cortical regions recruited by saccade-planning/memory tasks were identified and characterized (described in Chapter 4). In particular, these regions comprised a frontoparietal network traditionally implicated in oculomotor and mnemonic processes, including FEF, area 8, dlPFC, LIP, and other voxels along the intraparietal sulcus, as well as a few areas along the superior temporal sulcus. Importantly, in monkeys, these areas all exhibited some degree of contraversive selectivity, with each hemisphere yielding greater delay period activity for saccades directed to the contralateral side. Our current analysis exploited this feature to probe activity related to saccade selection in the oculomotor network. In free choice trials, the divergence in signal for contraversive versus ipsiversive saccades served as an indicator, marking when the animal's saccade decision manifested in a given region.

Results thus far suggest significant directionally selective divergence in activity occurs earlier in LIP and FEF, areas specifically involved in the planning and generation of eye movements, as compared to PMd and dlPFC. In addition, LIP signals demonstrated a significant difference between contraversive and ipsiversive free-choice trials before FEF activity did in both monkeys. Thus, the BOLD signal timecourses extracted from these ROIs provided some evidence of dissociable roles between task-relevant regions. The finding that directional selectivity evolved later in choice trials in all regions may again reflect uncertainty and variability in decision times.

An electrophysiological study conducted by Coe et al. (2002) explicitly considered

the question of which oculomotor planning regions first demonstrated decision-related activity. In monkeys performing a decision-making task, firing rates for receptive field and non-receptive field targets deviated at approximately the same time in both areas LIP and FEF. Therefore, Coe et al. concluded that these areas reflected 'choice' concomitantly, doing so later than other regions such as SEF, which the authors speculated played a leading role in the decision-making process. In addition, firing rate patterns deviated for receptive field and non-receptive field targets before the targets were presented, leading to their supposition that anticipatory activity in these areas may play a role in biasing the monkeys' later decision; in contrast, no anticipatory activity emerged in BOLD patterns in the current study. The discrepancies between our results and those of Coe et al. may arise from a few factors. First, while cue locations were randomized in this study, Coe et al. repetitively placed targets in and diametrically opposed to the cell's receptive field. This predictability may have produced greater anticipatory activity than observed here Secondly, the onset of differential activity in SEF cannot readily be assessed in our paradigm. Given the level of distortion/noise, the spatial resolution afforded by our images, and the medial/midline location of SEF, contralaterality cannot reliably be observed, precluding accurate delineation of contra- vs. ipsi- time of divergence. Thirdly, with respect to relative FEF and LIP activity, methodological differences may lead to disparities. FEF cells (as well as posterior parietal subregions) tend to display a rather heterogeneous set of responses to task events in delayed- or memory-saccade tasks (Wurtz et al 2001); the net population activity translating into a BOLD signal may not echo the firing rate pattern of a smaller sample of neurons. In addition, complicated reward-adjusting algorithms in Coe et al.'s task may have engendered more processing to understand and predict task contingencies. Depending on the nature of these processes and the regions subserving them, the dynamics of activity in a distributed network may shift relative to those gleaned in our experiment.

Cue Responses and Choice

Temporal subregions, such as FST and TEO, showed robust BOLD activation during the cue epoch. Peaks of cue activity in these subregions exposed a contralateral bias in instructed trials. Additionally, cue responses displayed directional selectivity in free choice trials. In our previous work, signals in areas FST and TEO scaled with the exogenously determined value or reward of saccade targets. These rewards, in turn, biased the monkey's decision in trials where they were allowed to choose between targets (See Appendix 5). Correspondingly, the same areas differentiated between visually identical cues, contingent upon selection as a saccadic target based on internal biases. These findings bolster the conception that the neural representations of objects incorporate the behavioral relevance of objects, whether that relevance is internally or externally endowed.

In summary, studies currently being conducted, controlling for confounds of unbalanced visual stimulation and target load, will better probe for regions specifically engaged by the choice process. However, preliminary findings already indicate that the choice of a behavioral response, and the attendant planning of that response, can clearly be discerned from patterns of activity in the frontoparietal action-planning network. With more data collected from more monkeys, we hope to better assess the differential roles that these areas may play in the representation and evolution of saccadic choice-related acitivity.

A2.5 Experimental Procedures

Experimental preparation (surgery, training, and scanning) of monkeys; MR imaging parameters; stimulus presentation, task online behavioral control and data acquisition are the same as those described in Chapter 4. In addition to the monitoring of body and eye movements described previously, an additional infrared camera (same as used for motion detection) was utilized to monitor the monkeys' licking. All trials in which monkeys licked before the receipt of reward (i.e., during the expectation period or

earlier) were aborted. Lick detection and contingent trial abortion were introduced for two reasons: (1) to minimize the motion-related artifacts before the receipt of reward period, and (2) some indication existed that monkeys licked more in anticipation of larger than smaller rewards. In not permitting any licking during the trial (except receipt), BOLD responses due to differential licking rather than reward expectation can be ruled out.

Experimental Task

Initial central fixation lasted for 10 seconds, after which time cues were presented for 200msec. In 'instructed trials' (top row), one peripheral cue was flashed. In 'choice' trials (bottom row), two peripheral cues were flashed, left-right symmetric with respect to the fixation point. Monkeys were required to maintain fixation during cue presentation. After a 10s delay, the fixation point extinguished, serving as a 'go' signal. For successful trial completion in 'instructed' trials, monkeys were required to saccade to the previously indicated cue; for 'choice' trials, they were permitted to saccade to either of the previously flashed targets. However, in both trial types, only 500ms was allowed for saccade execution, prompting advance decision and planning of the response. Monkeys maintained fixation at the cue location for 500ms, at which time the cue reappeared to serve as confirmation of correct trial completion. The cue remained on-screen for 4.5 secs (requiring continued fixation), then disappeared; after an additional; 5secs, reward was delivered.

A spatial configuration of 18 possible targets was used; see Experimental Procedures, Chapter 4, for detailed description.

Data Analysis

Functional data were analyzed in BrainVoyager QX and MATLAB running on a Fedora Core 5 (64 bit) Linux platform. The first 5 EPI volumes were always excluded from functional analyses to remove transient effects of magnetic saturation, but were used for co-registration, since they provide better contrast for anatomical landmarks.

Anatomical T1-weighted scans were processed in BrainVoyager QX and MIPAV. In monkey experiments, EPI sequences for each run were preprocessed using slice time correction, linear trend removal, and a high-pass temporal filter with 3 cycles per 20 min run cut-off, and 6DOF 3D-aligned to a first volume of the last run in the session, which was always followed by the in-plane anatomical T1-weighted scan. The in-plane anatomical scan for each separate session was co-registered to the high-resolution structural scan in the AC-PC plane, and then EPI runs were aligned to the AC-PC-registered anatomical scan using rigid body transformations. Automated alignment procedures were followed by careful visual inspection and manual fine-tuning based on anatomical landmarks. Using these transformations, 3D volume time-courses were computed in AC-PC space using 2×2×2 voxel size and 1000 unit image intensity threshold (mean image intensity within the brain ranged from 4000 to 6000 units).

All trial events (except baseline initial fixation period)—instruced/choice cue, instruced/choice delay, instructed/choice saccades, target fixation, and reward delivery—were extracted and used as predictors for general linear model (GLM) after convolution with hemodynamic response function (HRF). Events from all trials (successful and failed) were modeled to account for the overall variance. Fixational saccades and blinks were also detected, but not used as GLM predictors for final results, since their inclusion to GLM did not bring about any significant effect. Each session was analyzed separately to check the consistency of the results, and final statistical maps were generated using multi-session GLM. The faster 'monkey' HRF was used for GLM analysis (described in Fig. 4.S2).

For the BOLD time-course event-related averaging (ERA), only successful trials were accumulated; the epochs of the run affected by body or limb motions were automatically detected and eliminated from ERA analysis (see Supplementary Data, Fig. 4.S1 for more detail). ERA time-courses were constructed using individual baseline estimates for each single trial: mean activity in the last 3 or 4 s of the initial fixation period. To assess significance of BOLD signals, a two-sample t-test was used to compare the means of signal amplitude (percent signal change) of a given two trial

types at each second time bin. The trial types being compared are specified in each figure.

References

B. Coe, K. Tomihara, M. Matsuzawa, and O. Hikosaka. Visual and anticipatory bias in three cortical eye fields of the monkey during an adaptive decision-making task. *J Neurosci*, 22(12):5081–90, 2002. 1529-2401 (Electronic) Journal Article Research Support, Non-U.S. Gov't.

I. H. Jenkins, M. Jahanshahi, M. Jueptner, R. E. Passingham, and D. J. Brooks. Self-initiated versus externally triggered movements. ii. the effect of movement predictability on regional cerebral blood flow. *Brain*, 123 (Pt 6):1216–28, 2000. 0006-8950 (Print) Comparative Study Journal Article Research Support, Non-U.S. Gov't.

R. H. Khonsari, E. Lobel, D. Milea, S. Lehericy, C. Pierrot-Deseilligny, and A. Berthoz. Lateralized parietal activity during decision and preparation of saccades. *Neuroreport*, 18(17):1797–800, 2007. 0959-4965 (Print) Journal Article Research Support, Non-U.S. Gov't.

D. Milea, E. Lobel, S. Lehericy, P. Leboucher, J. B. Pochon, C. Pierrot-Deseilligny, and A. Berthoz. Prefrontal cortex is involved in internal decision of forthcoming saccades. *Neuroreport*, 18(12):1221–4, 2007. 0959-4965 (Print) Journal Article Research Support, Non-U.S. Gov't.

B. Pesaran, M. J. Nelson, and R. A. Andersen. Free choice activates a decision circuit between frontal and parietal cortex. *Nature*, 453(7193):406–9, 2008. 1476-4687 (Electronic) Journal Article Research Support, N.I.H., Extramural Research Support, Non-U.S. Gov't Research Support, U.S. Gov't, Non-P.H.S.

H. Scherberger and R. A. Andersen. Target selection signals for arm reaching in the posterior parietal cortex. *J Neurosci*, 27(8):2001–12, 2007. 1529-2401 (Electronic) Journal Article Research Support, N.I.H., Extramural Research Support, Non-U.S. Gov't Research Support, U.S. Gov't, Non-P.H.S.

K. Watanabe and S. Funahashi. Prefrontal delay-period activity reflects the decision process of a saccade direction during a free-choice odr task. *Cereb Cortex*, 17 Suppl 1:i88–100, 2007. 1047-3211 (Print) Journal Article Research Support, Non-U.S. Gov't.

R. H. Wurtz, M. A. Sommer, M. Pare, and S. Ferraina. Signal transformations from cerebral cortex to superior colliculus for the generation of saccades. *Vision Res*, 41 (25-26):3399–412, 2001. 0042-6989 (Print) Journal Article.

Appendix 3—Published Work

A3.1 Components of bottom-up gaze allocation in natural images

Abstract

Recent research [Parkhurst D., Law K., and Niebur E., 2002. Modeling the role of salience in the allocation of overt visual attention. Vision Research 42 (1) (2002) 107-123] showed that a model of bottom-up visual attention can account in part for the spatial locations fixated by humans while free-viewing complex natural and artificial scenes. That study used a definition of salience based on local detectors with coarse global surround inhibition. Here, we use a similar framework to investigate the roles of several types of non-linear interactions known to exist in visual cortex, and of eccentricity-dependent processing. For each of these, we added a component to the salience model, including richer interactions among orientation-tuned units, both at spatial short range (for clutter reduction) and long range (for contour facilitation), and a detailed model of eccentricity-dependent changes in visual processing. Subjects free-viewed naturalistic and artificial images while their eye movements were recorded, and the resulting fixation locations were compared with the models' predicted salience maps. We found that the proposed interactions indeed play a significant role in the spatiotemporal deployment of attention in natural scenes; about half of the observed inter-subject variance can be explained by these different models. This suggests that attentional guidance does not depend solely on local visual features, but must also include the effects of interactions among features. As models of these interactions be-

come more accurate in predicting behaviorally-relevant salient locations, they become useful to a range of applications in computer vision and human-machine interface design.

Vision Research 45(18):2397-416.

http://www.sciencedirect.com/science?_ob=ArticleURL&_udi=B6T0W-4G9GN35-1&_user=10&_rdoc=1&_fmt=&_orig=search&_sort=d&view=c&_acct=C000050221&_version=1&_urlVersion=0&_userid=10&md5=66169a408bec4c11a4c1d41d52346c89

Acknowledgements: This work was done in collaboration with Robert Peters. R. Peters incorporated interactions between orientation-tuned units into the saliency model, while I implemented eccentricity-dependent predictions.

A3.2 What do we perceive in a glance of a real-world scene?

Abstract

What do we see when we glance at a natural scene and how does it change as the glance becomes longer? We asked naive subjects to report in a free-form format what they saw when looking at briefly presented real-life photographs. Our subjects received no specific information as to the content of each stimulus. Thus, our paradigm differs from previous studies where subjects were cued before a picture was presented and/or were probed with multiple-choice questions. In the first stage, 90 novel grayscale photographs were foveally shown to a group of 22 native-English-speaking subjects. The presentation time was chosen at random from a set of seven possible times (from 27 to 500 ms). A perceptual mask followed each photograph immediately. After each presentation, subjects reported what they had just seen as completely and truthfully as possible. In the second stage, another group of naive individuals was instructed to score each of the descriptions produced by the subjects in the first stage. Individual scores were assigned to more than a hundred different attributes. We show that within a single glance, much object- and scene-level information is perceived by human subjects. The richness of our perception, though, seems asymmetrical. Subjects tend to have a propensity toward perceiving natural scenes as being outdoor rather than indoor. The reporting of sensory- or feature-level information of a scene (such as shading and shape) consistently precedes the reporting of the semantic-level information. But once subjects recognize more semantic-level components of a scene, there is little evidence suggesting any bias toward either scene-level or object-level recognition.

Journal of Vision 7(1):10.

http://journalofvision.org//7/1/10/

Acknowledgements: Li Fei-fei and I contributed equally to this work. Li Fei-fei designed the initial stimuli, and ran the first set of psychophysical experiments. I designed and conducted the second phase of psychophysical experiments, and performed all data analysis.